

**THE EFFECT OF INTERACTIONS BETWEEN PROTOCOLS AND
PHYSICAL TOPOLOGIES ON THE LIFETIME OF WIRELESS SENSOR
NETWORKS**

by

Debdhanit Yupho

B.E. in Electrical Engineering, Thammasat University, Thailand, 1999

M.S. in Interdisciplinary Telecommunications, University of

Colorado at Boulder, 2000

Submitted to the Graduate Faculty of
The School of Information Sciences in partial fulfillment
of the requirements for the degree of
Doctor of Philosophy

UNIVERSITY OF PITTSBURGH
SCHOOL OF INFORMATION SCIENCES

This dissertation was presented

by

Debdhanit Yupho

It was defended on

April 2, 2007

and approved by

Dr. Richard Thompson, Director and Professor, DIST

Dr. Prashant Krishnamurthy, Associate Professor, DIST

Dr. Vladimir Zadorozhny, Assistant Professor, DIST

Dr. Rohit Negi, Associate Professor, ECE

Dissertation Advisor: Dr. Joseph Kabara, Assistant Professor, DIST

Copyright © by Debdhanit Yupho

2007

THE EFFECT OF INTERACTIONS BETWEEN PROTOCOLS AND PHYSICAL TOPOLOGIES ON THE LIFETIME OF WIRELESS SENSOR NETWORKS

Debdhanit Yupho, PhD

University of Pittsburgh, 2007

Wireless sensor networks enable monitoring and control applications such as weather sensing, target tracking, medical monitoring, road monitoring, and airport lighting. Additionally, these applications require long term and robust sensing, and therefore require sensor networks to have long system lifetime. However, sensor devices are typically battery operated. The design of long lifetime networks requires efficient sensor node circuits, architectures, algorithms, and protocols. In this research, we observed that most protocols turn on sensor radios to listen or receive data then make a decision whether or not to relay it. To conserve energy, sensor nodes should consider not listening or receiving the data when not necessary by turning off the radio. We employ a cross layer scheme to target at the network layer issues. We propose a simple, scalable, and energy efficient forwarding scheme, which is called *Gossip-based Sleep Protocol* (GSP). Our proposed GSP protocol is designed for large low-cost wireless sensor networks with low complexity to reduce the energy cost for every node as much as possible. The analysis shows that allowing some nodes to remain in sleep mode improves energy efficiency and extends network lifetime without data loss in the topologies such as square grid, rectangular grid, random grid, lattice topology, and star topology. Additionally, GSP distributes energy consumption over the entire network because the nodes go to sleep in a fully random fashion and the traffic forwarding continuously via the same path can be avoided.

TABLE OF CONTENTS

PREFACE.....	XXIV
1.0 INTRODUCTION.....	1
1.1 CHALLENGES.....	2
1.2 REQUIREMENTS	3
1.3 NETWORK LIFETIME.....	5
1.4 SUMMARY AND PROBLEM STATEMENT	6
2.0 BACKGROUND	7
2.1 PHYSICAL LAYER.....	8
2.1.1 Radio Model	9
2.1.2 Modulation/Demodulation Schemes.....	13
2.1.3 Power Modes for the Sensor Node	14
2.2 DATA LINK LAYER.....	16
2.2.1 CSMA-Based Medium Access	17
2.2.2 Synchronous TDMA/FDMA-Based	19
2.2.3 SMACS and EAR Algorithm.....	20
2.2.4 Error Control	22
2.3 NETWORK LAYER.....	23
2.3.1 Proactive vs. Reactive Routing Protocol.....	24

2.3.2	Energy-Efficient Routes	25
2.3.3	Data Aggregation and Backoff-based Cost Field Scheme.....	26
2.3.3.1	Data Aggregation Technique	26
2.3.3.2	Backoff-based Cost Field Establishment Scheme	27
2.4	PROPAGATION MODELS	29
2.4.1	Rayleigh Fading Link Model	30
2.5	SUMMARY	32
3.0	ROUTING AND ENERGY BALANCING TECHNIQUES.....	34
3.1	EXISTING ROUTING PROTOCOLS.....	35
3.1.1	Clustering Routing Protocols.....	35
3.1.1.1	Low Energy adaptive Clustering Hierarchy (LEACH)	35
3.1.1.2	Threshold sensitive Energy Efficient Sensor Network protocol (TEEN)	36
3.1.1.3	Adaptive Period Threshold sensitive Energy Efficient Sensor Network protocol (APTEEN)	37
3.1.1.4	Power-Efficient Gathering in Sensor Information Systems (PEGASIS).....	38
3.1.1.5	Two-Tier Data Dissemination Model (TTDD).....	39
3.1.2	Flat Routing Protocols.....	40
3.1.2.1	Directed Diffusion.....	40
3.1.2.2	Sensor Protocols for Information via Negotiation (SPIN)	41
3.1.2.3	Energy Aware Routing (EAR).....	42
3.1.2.4	Minimum Cost Forwarding Algorithm (MCFA).....	42

3.1.2.5	Routing Protocols with Random Walks	43
3.1.2.6	Rumor Routing	44
3.1.2.7	Geographical and Energy-Aware Routing (GEAR).....	44
3.2	ENERGY BALANCING.....	45
3.2.1	Energy Balancing Strategy.....	46
3.2.2	Energy Balanced Routing.....	48
3.3	TOPOLOGY CONTROL	51
3.4	SUMMARY	53
4.0	PRELIMINARY RESEARCH	56
4.1	GOALS AND CONTRIBUTIONS.....	57
4.2	GOSSIP-BASED SLEEP PROTOCOL (GSP).....	58
4.2.1	Gossip-based Ad Hoc Routing and Percolation Theory.....	58
4.2.2	Gossip-based Sleep Protocol (GSP).....	59
4.3	PRELIMINARY ANALYSIS OF GSP.....	61
4.3.1	Radio Model	61
4.3.2	GSP Theoretical Performance	62
4.3.3	Simulation Model	64
4.3.4	Simulation Results	67
4.3.5	Continued Theoretical Analysis.....	68
4.3.6	Analysis at Frame Level	70
4.4	GSP FOR WIRELESS AD HOC NETWORKS.....	71
4.5	SUMMARY	73
5.0	INTEGRATING ROUTING AND TOPOLOGY MANAGEMENT.....	74

5.1	SQUARE GRIDS	74
5.1.1	Simulation Model to Determine Gossip Sleep Probability (p)	74
5.1.2	Simulation Model to Determine Network Lifetime	75
6.0	ANALYSIS IN INCREASING TRANSMISSION POWER/RADIUS	89
6.1	PRELIMINARY ANALYSIS	89
6.1.1	Continued Analysis of Increasing Transmission Power/Radius in GSP	93
6.2	NETWORK LIFETIME ANALYSIS WHEN INCREASING TRANSMISSION POWER/RADIUS.....	95
6.2.1	Square Grids.....	95
7.0	NETWORK TOPOLOGIES.....	99
7.1	PERFORMANCE EVALUATION.....	100
7.1.1	Energy Consumption Model	100
7.1.2	Simulation Parameters	100
7.2	TOPOLOGY	109
7.2.1	Square Grids.....	109
7.2.1.1	Transmission Power/Radius d in the Square Grids.....	109
7.2.1.2	Transmission Power/Radius $2d$ in the Square Grids.....	117
7.2.2	Rectangular Grids.....	126
7.2.2.1	Transmission Power/Radius d in the Rectangular Grids.....	126
7.2.2.2	Transmission Power/Radius $2d$ in the Rectangular Grids.....	134
7.2.3	Random Grid Topology.....	144
7.2.3.1	Transmission Power/Radius d in the Random Grid Topology.....	144
7.2.3.2	Transmission Power/Radius $2d$ in the Random Grid Topology.....	155

7.2.4	Lattice Topology.....	161
7.2.4.1	Transmission Power/Radius d in the Lattice Topology.....	163
7.2.4.2	Transmission Power/Radius $2d$ in the Lattice Topology.....	168
7.2.5	Star Topology	174
7.2.5.1	Transmission Power/Radius d in the Star Topology	177
7.2.5.2	Transmission Power/Radius $2d$ in the Star Topology	182
8.0	CONCLUSIONS AND FUTURE WORK	189
	BIBLIOGRAPHY.....	194

LIST OF TABLES

Table 1: Radio characteristics.....	10
Table 2: Crossbow TinyOS Mica2 mote measured energy consumption in Watts	11
Table 3: Crossbow TinyOS Mica2 mote measured energy consumption in Joules/bit	12
Table 4: Useful sleep states for the sensor node.....	15
Table 5: The classic radio model.....	61
Table 6: Energy consumption model for Lucent IEEE 802.11 WaveLAN PC CARD with 2 Mbps.....	71
Table 7: Energy consumption model.....	76
Table 8: Simulation parameters and energy consumption model when using transmission power/radius d	110
Table 9: Simulation parameters and energy consumption model when using transmission power/radius $2d$	117

LIST OF FIGURES

Figure 1: Distributed sensor network: physical topology.....	2
Figure 2: Simple radio model	9
Figure 3: Radio model.	11
Figure 4: Multiple access methods.	19
Figure 5: The energy-efficiency of the routes.....	26
Figure 6: Negotiation and aggregation steps.	27
Figure 7: a) Forwarding along the minimum energy path; b) An example for Backoff-based Optimal Cost Field Establishment.	29
Figure 8: Clustering communication in wireless sensor network.....	35
Figure 9: Timeline for the operation of a) TEEN and b) APTEEN.....	38
Figure 10: Token passing approach.	38
Figure 11: An example of directed diffusion.....	40
Figure 12: A one dimensional chain of sensor nodes.	46
Figure 13: Sketch of percolation probability.	58
Figure 14: a) Central area of the grid topology used by the simulation. b) An example of GSP network with $N = 16$, and $p = 0.25$	64
Figure 15: Flowcharts to determine a) average path length (L_{GSP}) and b) average number of disconnected nodes.	65

Figure 16: Probability of sleeping nodes vs. average path length (L_{GSP}) for connected nodes with 95% c.i.	66
Figure 17: Probability of sleeping nodes vs. ratio of nodes disconnected from the sink.	66
Figure 18: Network size vs. ratio of average extra path length (α) when $p = 0.3$, with a 95% c.i.	67
Figure 19: Network size vs. ratio of nodes disconnected from the sink when $p = 0.3$ with a 95% c.i.	68
Figure 20: Energy difference (E_{diff}) between $E_{GSP-saved}$ and $E_{GSP-extra}$ vs. traffic load (B) in bits when $p = 0.3$, $N = 100$, $L_{min} = 5$ and $\alpha = 0.1092$	69
Figure 21: Network size N (nodes) vs. traffic load B (bits) when $p = 0.3$, $\alpha = 0.315$ and $E_{diff} = 0$	70
Figure 22: A flowchart of the Known Path (KP) scheme simulation.	77
Figure 23: A flowchart of packet processing algorithm in the Known Path (KP) scheme.	78
Figure 24: A flowchart of GSP/Flooding simulation in the Unknown Path (UKP) scheme.	79
Figure 25: A flowchart of GSP/Flooding algorithm in the Unknown Path (UKP) scheme.	80
Figure 26: Average number of gossip periods (G_p) until network termination vs. Network size.	81
Figure 27: Change in network lifetime for both Known and Unknown path schemes when using GSP with $p = 0.3$ compared to $p = 0$ (non-GSP).	81
Figure 28: Average remaining energy (ARE) vs. network size.	82
Figure 29: Average energy consumed per gossip period vs. network size.	83
Figure 30: ARE for the Known path scheme in 100 nodes square grid network with $p = 0$	84
Figure 31: ARE for the Known path scheme in 100 nodes square grid network with $p = 0.3$	84
Figure 32: ARE for the Known path scheme in 900 nodes square grid network with $p = 0$	85

Figure 33: ARE for the Known path scheme in 900 nodes square grid network with $p = 0.3$	85
Figure 34: ARE for the Unknown path scheme in 100 nodes square grid network with $p = 0$	86
Figure 35: ARE for the Unknown path scheme in 100 nodes square grid network with $p = 0.3$.	86
Figure 36: ARE for the Unknown path scheme in 900 nodes square grid network with $p = 0$	87
Figure 37: ARE for the Unknown path scheme in 900 nodes square grid network with $p = 0.3$.	87
Figure 38: The grid topology to represent the transmission radius d , $1.414 d$, and $2d$	90
Figure 39: Probability of sleeping nodes vs. average path length when transmission radius = d , $1.414 d$ and $2d$ for 100 node square grid network with 95% c.i.....	91
Figure 40: Probability of sleeping nodes vs. ratio of nodes disconnected when transmission radius = d , $1.414 d$ and $2d$ for 100 node square grid network with 95% c.i.....	91
Figure 41: Probability of sleeping nodes vs. changes in average number of disconnected nodes.	92
Figure 42: Probability of sleeping nodes vs. average path length for connected nodes in square grids with $2d$ transmission power/radius.	95
Figure 43: Probability of sleeping nodes vs. ratio of nodes disconnected in square grids with $2d$ transmission power/radius.	96
Figure 44: Average number of gossip periods vs. network size in square grids with 95% c.i.	96
Figure 45: Average remaining energy (ARE) vs. network size in square grids with 95 % c.i.	97
Figure 46: Average energy consumed per gossip period vs. network size.....	98
Figure 47: Experimental design.....	101
Figure 48: A flowchart of the simulation.....	106
Figure 49: A flowchart of a threading method with packet processing in the simulation.	107
Figure 50: A flowchart of a threading method with packet processing in the simulation	

(Continue)	108
Figure 51: Average number of gossip periods vs. network size for the square grids with transmission power/distance d , $G_p = 30$ and 360 seconds.	111
Figure 52: The changes in network lifetime on the different sizes of the square grids with transmission power/radius d when using GSP with $p = 0.3$ compared to Non-GSP, $G_p = 30$ and 360 seconds.	111
Figure 53: Simulated network lifetime vs. network size for the square grids with transmission power/radius d , $G_p = 30$ and 360 seconds.	112
Figure 54: Average remaining energy (ARE) vs. network size for the square grids with transmission power/radius d , $G_p = 30$ and 360 seconds.	113
Figure 55: Average energy consumed per gossip period vs. network sizes for the square grids with transmission power/radius d , $G_p = 30$ and 360 seconds.	113
Figure 56: Packet loss ratio vs. network size for the square grids with transmission power/radius d , $G_p = 30$ and 360.	114
Figure 57: ARE for 10x10 (100 nodes) square grid Non-GSP network ($p = 0$) with transmission power/radius d	115
Figure 58: ARE for 10x10 (100 nodes) square grid GSP network ($p = 0.3$) with transmission power/radius d	115
Figure 59: ARE for 30x30 (900 nodes) square grid Non-GSP network ($p = 0$) with transmission power/radius d	116
Figure 60: ARE for 30x30 (900 nodes) square grid GSP network ($p = 0.3$) with transmission power/radius d	117
Figure 61: Average number of gossip periods vs. network size for the square grids with	

transmission power/distance $2d$, $G_p = 30$ and 360 seconds.	118
Figure 62: The changes in network lifetime on the different sizes of the square grids with transmission power/radius $2d$ when using GSP with $p = 0.6$ compared to Non-GSP, $G_p = 30$ and 360 seconds.	119
Figure 63: Simulated network lifetime vs. network size for the square grids with transmission power/distance $2d$, $G_p = 30$ and 360 seconds.	120
Figure 64: Average remaining energy (ARE) vs. network size for the square grids with transmission power/radius $2d$, $G_p = 30$ and 360 seconds.	120
Figure 65: Average energy consumed per gossip period vs. network size for the square grids with transmission power/radius $2d$, $G_p = 30$ and 360 seconds.	121
Figure 66: Packet loss ratio vs. network size for the square grids with transmission power/radius $2d$, $G_p = 30$ and 360 seconds.	122
Figure 67: The changes of the average number of gossip periods and AREs in the square grids when using GSP_{2d} compared to GSP_d with $G_p = 30$ and 360 seconds.	122
Figure 68: ARE for 10×10 (100 nodes) square grid Non-GSP network ($p = 0$) with transmission power/radius $2d$	123
Figure 69: ARE for 10×10 (100 nodes) square grid GSP network ($p = 0.6$) with transmission power/radius $2d$	124
Figure 70: ARE for 30×30 (900 nodes) square grid Non-GSP network ($p = 0$) with transmission power/radius $2d$	124
Figure 71: ARE for 30×30 (900 nodes) square grid GSP network ($p = 0.6$) with transmission power/radius $2d$	125
Figure 72: Probability of sleeping nodes vs. average path length for connected nodes in	

rectangular grids.....	127
Figure 73: Probability of sleeping nodes vs. ratio of nodes disconnected in rectangular grids..	127
Figure 74: Average number of gossip periods vs. network size for the rectangular grids with transmission power/distance d , $G_p = 30$ and 360 seconds.	128
Figure 75: The changes in network lifetime on the different sizes of the rectangular grids with transmission power/radius d when using GSP compared to Non-GSP, $G_p = 30$ and 360 seconds.	129
Figure 76: Simulated network lifetime vs. network size for the rectangular grids with transmission power/distance d , $G_p = 30$ and 360 seconds.	129
Figure 77: Average remaining energy (ARE) vs. network size for the rectangular grids with transmission power/radius d , $G_p = 30$ and 360 seconds.	130
Figure 78: Average energy consumed per gossip period vs. network size for the rectangular grids with transmission power/distance d , $G_p = 30$ and 360 seconds.	131
Figure 79: Packet loss ratio vs. network size for the rectangular grids with transmission power/radius d , $G_p = 30$ and 360 seconds.....	131
Figure 80: ARE for 5x20 (100 nodes) rectangular grid Non-GSP network ($p = 0$) with transmission power/radius d	132
Figure 81: ARE for 5x20 (100 nodes) rectangular grid GSP network ($p = 0.25$) with transmission power/radius d	133
Figure 82: ARE for 5x200 (1000 nodes) rectangular grid Non-GSP network ($p = 0$) with transmission power/radius d	133
Figure 83: ARE for 5x200 (1000 nodes) rectangular grid GSP network ($p = 0.15$) with transmission power/radius d	134

Figure 84: Probability of sleeping nodes vs. average path length for connected nodes in rectangular grids with $2d$ transmission power/radius.	135
Figure 85: Probability of sleeping nodes vs. ratio of nodes disconnected in rectangular grids with $2d$ transmission power/radius.	135
Figure 86: Average number of gossip periods vs. network size for the rectangular grids with transmission power/distance $2d$, $G_p = 30$ and 360 seconds.	136
Figure 87: The changes in network lifetime on the different sizes of the rectangular grids with transmission power/radius $2d$ when using GSP compared to Non-GSP, $G_p = 30$ and 360 seconds.	137
Figure 88: Simulated network lifetime vs. network size for the rectangular grid topologies with transmission power/distance $2d$, $G_p = 30$ and 360 seconds.	137
Figure 89: Average remaining energy (ARE) vs. network size for the rectangular grids with transmission power/radius $2d$, $G_p = 30$ and 360 seconds.	138
Figure 90: Average energy consumed per gossip period vs. network size for the rectangular grids with transmission power/distance $2d$, $G_p = 30$ and 360 seconds.	139
Figure 91: Packet loss ratio vs. network size for the rectangular grids with transmission power/radius $2d$, $G_p = 30$ and 360 seconds.	139
Figure 92: The changes of the average number of gossip periods and AREs in the rectangular grids when using GSP_{2d} compared to GSP_d with $G_p = 30$ and 360 seconds.	140
Figure 93: ARE for 5×20 (100 nodes) rectangular grid Non-GSP network ($p = 0$) with transmission power/radius $2d$	141
Figure 94: ARE for 5×20 (100 nodes) rectangular grid GSP network ($p = 0.55$) with transmission power/radius $2d$	141

Figure 95: ARE for 5x200 (1000 nodes) rectangular grid Non-GSP network ($p = 0$) with transmission power/radius $2d$.	142
Figure 96: ARE for 5x200 (1000 nodes) rectangular grid GSP network ($p = 0.4$) with transmission power/radius $2d$.	142
Figure 97: A random $10d \times 10d$ grid topology with one node in a $d \times d$ grid.	144
Figure 98: A random $10d \times 10d$ grid topology with two nodes in a $d \times d$ grid.	145
Figure 99: A random $10d \times 10d$ grid topology with three nodes in a $d \times d$ grid.	145
Figure 100: A plot to represent average number of disconnected nodes when a node, two nodes, and three nodes placed in a $d \times d$ grid with d transmission power/radius.	147
Figure 101: Probability of sleeping nodes vs. average path length for connected nodes in the selected random grids with transmission power/radius d .	147
Figure 102: Probability of sleeping nodes vs. ratio of nodes disconnected in the selected random grids with transmission power/radius d .	148
Figure 103: A selected 20x20 random grid topology (800 nodes) using in the network lifetime analysis.	149
Figure 104: A selected 25x25 random grid topology (1250 nodes) using in the network lifetime analysis.	150
Figure 105: Average number of gossip period vs. network size for the random grids with transmission power/radius d , $G_p = 30$ and 360 seconds.	151
Figure 106: The changes in network lifetime on the different sizes of the random grids with transmission power/radius d when using GSP compared to Non-GSP, $G_p = 30$ and 360 seconds.	151
Figure 107: Simulated network lifetime vs. network size for the random grids with transmission	

power/radius d , $G_p = 30$ and 360 seconds.....	152
Figure 108: Average remaining energy (ARE) vs. network size for the random grids with transmission power/radius d , $G_p = 30$ and 360 seconds.	153
Figure 109: Average energy consumed per gossip period vs. network size for the random grids with transmission power/radius d , $G_p = 30$ and 360 seconds.	153
Figure 110: Packet loss ratio vs. network size for the random grids with transmission power/radius d , $G_p = 30$ and 360 seconds.....	154
Figure 111: Probability of sleeping nodes vs. average path length for connected nodes in the selected random grids with transmission power/radius $2d$	155
Figure 112: Probability of sleeping nodes vs. ratio of nodes disconnected in the selected random grids with transmission power/radius $2d$	156
Figure 113: Average number of gossip periods vs. network size for the random grids with transmission power/radius $2d$, $G_p = 30$ and 360 seconds.	156
Figure 114: The changes in network lifetime on the different sizes of the random grids with transmission power/radius $2d$ when using GSP compared to Non-GSP, $G_p = 30$ and 360 seconds.	157
Figure 115: Simulated network lifetime vs. network size for the random grids with transmission power/radius $2d$, $G_p = 30$ and 360 seconds.....	158
Figure 116: Average remaining energy (ARE) vs. network size for the random grids with transmission power/radius $2d$, $G_p = 30$ and 360 seconds.	158
Figure 117: Average energy consumed per gossip period vs. network size for the random grids with transmission power/radius $2d$, $G_p = 30$ and 360 seconds.	159
Figure 118: Packet loss ratio vs. network size for the random grids with transmission	

power/radius $2d$, $G_p = 30$ and 360 seconds.....	160
Figure 119: The changes of the average number of gossip periods and AREs in the random grids when using GSP_{2d} compared to GSP_d with $G_p = 30$ and 360 seconds.....	160
Figure 120: A small lattice topology with 240 nodes.....	161
Figure 121: A medium lattice topology with 656 nodes.....	162
Figure 122: A large lattice topology with 1136 nodes.....	162
Figure 123: Probability of sleeping nodes vs. average path length for connected nodes in lattice topologies with transmission power/radius d	163
Figure 124: Probability of sleeping nodes vs. ratio of nodes disconnected in lattice topologies with transmission power/radius d	164
Figure 125: Average number of gossip periods vs. network size for the lattice topologies with transmission power/radius d , $G_p = 30$ and 360 seconds.	164
Figure 126: The changes in network lifetime on the different sizes of the lattice topologies with transmission power/radius d when using GSP compared to Non-GSP, $G_p = 30$ and 360 seconds.	165
Figure 127: Simulated network lifetime vs. network size for the lattice topologies with transmission power/radius d , $G_p = 30$ and 360 seconds.	166
Figure 128: Average remaining energy (ARE) vs. network size for the lattice topologies with transmission power/radius d , $G_p = 30$ and 360 seconds.	166
Figure 129: Average energy consumed per gossip period vs. network size for lattice topologies with transmission power/radius d , $G_p = 30$ and 360 seconds.	167
Figure 130: Packet loss ratio vs. network size for the lattice topologies with transmission power/radius d , $G_p = 30$ and 360 seconds.....	168

Figure 131: Probability of sleeping nodes vs. average path length for connected nodes in lattice topologies with transmission power/radius $2d$	169
Figure 132: Probability of sleeping nodes vs. ratio of nodes disconnected in lattice topologies with transmission power/radius $2d$	169
Figure 133: Average number of gossip periods vs. network size for lattice topologies with transmission power/radius $2d$, $G_p = 30$ and 360 seconds.	170
Figure 134: The changes in network lifetime on the different sizes of lattice topologies with transmission power/radius $2d$ when using GSP compared to Non-GSP, $G_p = 30$ and 360 seconds.	170
Figure 135: Simulated network lifetime vs. network size for lattice topologies with transmission power/radius $2d$, $G_p = 30$ and 360 seconds.....	171
Figure 136: Average remaining energy (ARE) vs. network sizes for lattice topologies with transmission power/radius $2d$, $G_p = 30$ and 360 seconds.	172
Figure 137: Average energy consumed per gossip period vs. network size for the lattice topologies with transmission power/radius $2d$, $G_p = 30$ and 360 seconds.....	172
Figure 138: Packet loss ratio vs. network size for lattice topologies with transmission power/radius $2d$, $G_p = 30$ and 360 seconds.....	173
Figure 139: The changes of the average number of gossip periods and AREs in lattice topologies when using GSP_{2d} compared to GSP_d with $G_p = 30$ and 360 seconds.....	174
Figure 140: An example of 5 nodes and 6 lines star topology with a sink at the center.	175
Figure 141: A small star topology with 320 nodes.....	175
Figure 142: A medium star topology with 720 nodes.	176
Figure 143: A large star topology with 1280 nodes.....	176

Figure 144: Probability of sleeping nodes vs. average path length for connected nodes in star topologies with transmission power/radius d	177
Figure 145: Probability of sleeping nodes vs. ratio of nodes disconnected in star topologies with transmission power/radius d	178
Figure 146: Average number of gossip periods vs. network size for star topologies with transmission power/radius d , $G_p = 30$ and 360 seconds.....	178
Figure 147: The changes in network lifetime on the different sizes of the star topologies with transmission power/radius d when using GSP compared to Non-GSP, $G_p = 30$ and 360 seconds.....	179
Figure 148: Simulated network lifetime vs. network size for star topologies with transmission power/radius d , $G_p = 30$ and 360 seconds.....	180
Figure 149: Average remaining energy (ARE) vs. network size for star topologies with transmission power/radius d , $G_p = 30$ and 360 seconds.....	180
Figure 150: Average energy consumed per gossip period vs. network size for star topologies with transmission power/radius d , $G_p = 30$ and 360 seconds.....	181
Figure 151: Packet loss ratio vs. network size for star topologies with transmission power/radius d , $G_p = 30$ and 360 seconds.....	182
Figure 152: Probability of sleeping nodes vs. average path length for connected nodes in star topologies with transmission power/radius $2d$	183
Figure 153: Probability of sleeping nodes vs. ratio of nodes disconnected in star topologies with transmission power/radius $2d$	183
Figure 154: Average number of gossip periods vs. network size for star topologies with transmission power/radius $2d$, $G_p = 30$ and 360 seconds.....	184

Figure 155: The changes in network lifetime on the different sizes of the star topologies with transmission power/radius $2d$ when using GSP compared to Non-GSP, $G_p = 30$ and 360 seconds. 185

Figure 156: Simulated network lifetime vs. network size for star topologies with transmission power/radius $2d$, $G_p = 30$ and 360 seconds..... 185

Figure 157: Average remaining energy (ARE) vs. network size for star topologies with transmission power/radius $2d$, $G_p = 30$ and 360 seconds. 186

Figure 158: Average energy consumed per gossip period vs. network size for star topologies with transmission power/radius $2d$, $G_p = 30$ and 360 seconds. 186

Figure 159: Packet loss ratio vs. network size for star topologies with transmission power/radius $2d$, $G_p = 30$ and 360 seconds..... 187

Figure 160: The changes of the average number of gossip periods and AREs in star topologies when using GSP_{2d} compared to GSP_d with $G_p = 30$ and 360 seconds..... 188

PREFACE

I would like to give heartfelt thanks to my advisor, Dr. Joseph Kabara, who has not only been a wonderful patient teacher, but who also constantly inspires and guides me to delve deeper into my research. His intelligence, knowledge and kindness have motivated me all these years. I would also like to express my gratitude to my committee including Dr. Richard Thompson, Dr. Prashant Krishnamurthy, Dr. Vladimir Zadorozhny, and Dr. Rohit Negi for all valuable guidance and suggestions on my dissertation.

I would like to give a special thanks to my organization, Aeronautical Radio of Thailand, for supporting me financially during my graduate study at the University of Pittsburgh. Also, I would like to thank my SiNE research group, Natthapol, Maria, and Yuttasart, for their helpful comments and thoughts all these years.

Most importantly, I would like to thank my father and mother, Kitti and Sumana, who always give me unconditional love, support and inspiration. Without their love, I cannot be who I am today. I would also like to thank my sister for being such a wonderful friend, who I can always rely on. Lastly, I would like to thank my wife, Supak, for her continual love, support and understanding. Without all the love from my family, the world seems hard work. You all are pieces of my success today.

1.0 INTRODUCTION

Networked microsensor technology is a key technology for the future [1]. Large number of smart devices with multiple onboard sensors, networked through wireless links and the Internet, provide unique opportunities for controlling homes, cities and the environment [2]. Smart disposable sensors can be deployed on the ground, in the air, under water, in vehicles, and inside buildings. A system of sensor network can detect threats and used for weapon targeting and are denial. Each sensor nodes will have embedded processing capability operating such as in the acoustic, infrared, and magnetic modes. Current applications of sensor networks are military sensing, physical security, traffic surveillance, air traffic control, industrial and manufacturing automation, disaster management, environment monitoring, airport lighting, and road monitoring. In these applications, the sensors can be small or large. Typically, wireless sensor networks contain hundreds or thousands of these sensor nodes, and these sensors have the ability to communicate either among each other or directly to one or more sinks. A large number of sensors allows for sensing over large geographical regions with greater accuracy. Sensor nodes are usually scattered in a sensor field, which is an area of where the sensor nodes are deployed. Sensor nodes coordinated among themselves to produce information about the physical environment. Each sensor nodes bases its decisions on its mission, the information it currently has, and its knowledge of its computing, communication, and energy resources [3]. Each sensor has the capability to collect and route data either to other sensors or back to a sink. A sink may be fixed or mobile node capable of connecting the sensor network to an existing communications infrastructure or to the Internet where a user can access to the information.

The development of wireless sensor networks requires technologies from three different research areas, which are sensing, communication, and computing including hardware, software, and algorithms. In recent years, intensive research that addresses the potential of collaboration among

sensors in data gathering and processing, and coordination and management of the sensing activity was conducted. Sensor nodes are constrained in energy supply in most application. Therefore, techniques to provide energy efficiency that prolong the lifetime of the network are required. This poses many challenges to the design of wireless sensor networks at all layers of the networking protocol stack.

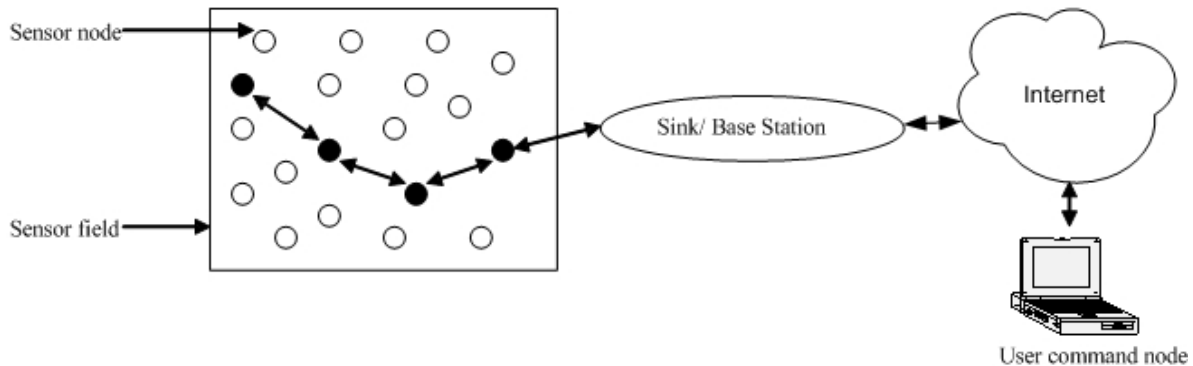


Figure 1: Distributed sensor network: physical topology.

1.1 CHALLENGES

In spite of diverse applications, wireless sensor networks pose unique technical challenges due to the following factors [2]-[4].

- *Deployment:* The deployment of sensor nodes in the physical environment may take several forms. Most sensor nodes are deployed in areas which have no infrastructure at all. Nodes may be deployed at random, e.g., by dropping them from the aircraft or installed at chosen spots [4]. In such a situation, it is up to the node to identify its connectivity and distribution. Deployment may be a one-time activity, where the installation and use of a sensor network are strictly separate activities. However, deployment may also be a continuous process, with more nodes being deployed at anytime during the use of the network.

- *Operation*: In most cases, once deployed, the networks do not have human intervention. Thus, the nodes themselves are responsible for reconfiguration in case of any changes.
- *Energy constrained*: Since the sensor nodes usually are not connected to any energy source, their energy and other resources are limited by size and cost constraints. Varying size and cost constraints directly result in corresponding varying limits on the energy available, i.e., size, cost, and energy density of batteries, as well as on computing, storage and communication resources. Power may be either stored, e.g., in batteries, or scavenged from the environment, e.g., by solar cells. There is an only finite source of energy that must be optimally used for processing and communication. Section 2.1.1 shows that communication dominates processing in energy consumption. As a result, to make optimal used of energy, communication should be minimized as possible.
- *Dynamic changes*: It requires that a network system can adapt to changing connectivity, e.g., due to nodes failure, and addition nodes as well as changing environmental stimuli.

Therefore, unlike traditional networks, where the focus is on maximizing channel throughput or minimizing node deployment, the major consideration in a wireless sensor network is to extend the system lifetime as well as the system robustness.

1.2 REQUIREMENTS

These requirements are important because they serve as a guideline to design a protocol or an algorithm for wireless sensor networks. Chapter 3 shows that most protocols follow these requirements in designing their schemes. Thus, this section addresses those requirements for wireless sensor networks as the following.

- *Long battery life*: In many applications, sensors are placed in locations that are not conveniently accessible. In addition, if the batteries must be replaced often, not only will the primary benefit of wireless networks be lost, but also many remote sensing applications may become impractical [5]. Thus, long battery life is necessary in wireless

sensor networks.

- *Size of device*: To embed in their operating environment, sensor devices need to be small. This requirement affects the choice of the batteries, e.g., AA battery and coin battery.
- *Large number of sensors*: To make use of the cheap small-sized sensors, sensor networks may contain thousands of nodes. Thus, the major issue focuses on scalability and managing these large numbers of sensors.
- *Low cost*: Since most applications employ large number of sensor nodes, the cost of individual node must be minimal.
- *Efficient use of the small memory*: When building sensor networks, issues such as routing tables, data replication, security and such should be considered to fit the small size of memory in the sensor nodes.
- *Low data rate*: Since the sampling rate, e.g., rate of temperature sensing, is usually small, the number of bits transmitted per second is low.
- *Centralized architecture*: Most of these applications consist of one or more sophisticated central nodes called sinks. This node is usually responsible to collect all data from or send query to the network [5].
- *Data aggregation*: The huge number of sensing nodes may congest the network with information. One way to solve this problem is to aggregate the duplicated data. In cluster-based routing scheme, cluster-heads are responsible to aggregate the data by doing some computational, e.g., average, summation, and highest [6]. Then they will broadcast the summarized new information.
- *Network self-organization*: Given the large number of nodes and their potential placement in hostile locations, it is essential that the network be able to self-organize itself. In addition, nodes may fail either from the lack of energy or from physical destruction. Also, new nodes may join the network. Thus, the network must be able to periodically reconfigure itself so that it can continue to function. Individual nodes may become disconnected from the rest of the network, but a high degree of connectivity overall must be maintained.
- *Robustness*: Robustness is the ability of the network to withstand unexpected failures. For example, sensor nodes on airport runway must be able to withstand jet blasts or bad weather otherwise they may die before their batteries run out.

- *Balanced energy consumption*: Some mechanisms strive to balance the energy consumption among the sensors. One common argument for doing this is that if the energy of certain nodes is depleted before the others, holes may appear in the sensing coverage or the sensor network may become disconnected [7]. Even if those nodes die prematurely, there should still be some redundant nodes that can be turned on at or near those locations.
- *Simplicity*: Current sensors have very limited memory space for storing programs, e.g. MICA2 mote has only 8KB of memory for this purpose. Moreover, they usually have limited computational power. Thus, simpler mechanisms are more likely to be deployed in sensor networks.

1.3 NETWORK LIFETIME

Network lifetime is considered as an important metric since sensor network has limited energy capacity, which requires protocols that use this energy efficiently. With efficient management of energy usage, system lifetime is lengthened. The two common examples that define the network lifetime of a system are as the following.

- Definition 1: The system lifetime for a sensor network is the shortest lifetime of any participating node in the network [8]. In applications, any sensor node may be responsible to perform functions. Thus, one dead node can provide the lost of important system information. It is possible that some redundant nodes are added to the network.
- Definition 2: The end of system lifetime is when the network is partitioned. Since some dead nodes will divide network, the network may become disconnected. When network partition occurs, some data will be lost because they can not pass through the network from any partition nodes to the sink.

1.4 SUMMARY AND PROBLEM STATEMENT

A sensor network is energy constrained network, the protocols must be designed to be *Energy Efficiency*. Although many protocols exist for both topology management and routing, each has overhead for organizing the network. A question emerges of how much overhead is necessary to improve the energy performance and how much improvement could be made with less overhead. Therefore, Gossip-based Sleep Protocol (GSP) was proposed as a zero overhead protocol to investigate how much could be done with zero overhead. GSP emerges from the observation that flat routing protocols try to reduce the routing overhead as much as possible. However, these flat routing protocols have no explicit sleep mechanisms and require all the nodes in the network to be awake (i.e. in receive or idle mode), which consumes a significant amount of energy. Thus, GSP was created as a tool to investigate energy efficiency with zero protocol overhead. However, the original version of GSP [9] may be sensitive to the energy consumption model, the radio propagation model, sleep/awake cycle synchronization and physical topology of the nodes used in simulating its performance. Additionally, initial research shows a decreased rate of energy consumption, but has not shown how this translates into increased network lifetime.

Chapter 2 provides background on the first three layers in wireless sensor networks, which are the physical layer, data link layer, and network layer. Chapter 3 reviews other energy efficient-routing protocols for wireless sensor networks to study the advantages and disadvantages of each. Chapter 4 presents analyses on energy consumption then reviews the original Gossip-based sleep protocol. Chapter 5 discusses GSP in terms of both routing and topology management. Chapter 6 analyzes the effects of increasing transmission power/radius. Chapter 7 tests GSP performances on five different topologies. Chapter 8 summarizes the dissertation.

2.0 BACKGROUND

To introduce the energy-efficient protocols in wireless sensor networks, the first three layers of protocol stack are discussed in this chapter. First, the *Physical Layer* is responsible for radio transmission, modulation, and power modes. The equations of radio model are set up to measure the energy consumption of the radio transmission. In addition, the modulation and demodulation schemes of sensor networks must be studied since it is another important factor that can impact the energy consumption of the node. Extending a sensor node's operating life requires multiple power modes. A sensor node senses the environment periodically; however, a continuously operating transceiver will deplete the node's energy. Thus, a sensor node should be able to turn off its transceiver (sleep state) when it has no data to send.

Second, the *Data Link Layer* protocol must conserve the battery power in sensor nodes. CSMA-based MAC is suitable in sensor networks because of the simple and scalability characteristics. Using this scheme, the network can be extended to a large network. On the other hand, a collision-free Synchronous TDMA/FDMA-based MAC may require network to be divided into clusters. Each cluster has a cluster-head node that responsible for assigning TDMA timeslot to every member nodes of its cluster after the cluster setup period. Since each node is assigned a unique timeslot, it is easy to implement the sleep mode. A problem in cluster-based TDMA MAC protocol is how to determine the cluster memberships and cluster-heads such that the entire network is covered while the nodes move. Therefore, one of the flat-topology algorithms is discussed in section 2.2.3. The advantage of this algorithm is that it enables nodes to discover their neighbor and establish transmission and reception schedules for communicating with them without the need for any local or global master nodes. The *Network Layer* protocol must also be energy efficient in routing the information/data from the source node to the sink node. Thus, the energy-efficient routes are discussed in section 2.3.2 in term of minimum energy path, minimum

hop path, and maximum available path. Minimum-transmission-energy routing and direct transmission routing are not always optimal because the nodes, which are closest to the base station, will be used to route a large number of data messages to the base station. Therefore, these nodes will die out quickly, resulting in increasing in energy requirements for the remaining nodes. Using a direct routing protocol, each sensor node sends its data directly to the base station. If the base station is far away from the nodes, direct communication will require a large transmit power from each node, which will quickly drain the battery of the nodes and reduce the system lifetime. One mechanism to prolong the network's lifetime is to organize the network into clusters. Each cluster has a cluster-head node that communicates directly to base station. The cluster-head node will change every refresh time to avoid using the same node all the time. In chapter 3, the clustering and flat existing routing protocols will be discussed in detail. Also, since sensor networks are usually dense networks, a node with multiple neighbors may receive many identical sensor reading. Overcoming this overlap requires routing protocols in wireless sensor networks to also perform data aggregation. Moreover, the data aggregation technique allows sensor node to efficiently distribute data given limited energy supply. If a flooding network protocol is used, a node broadcasts immediately after obtaining a lower cost path, no matter whether the cost is optimum or not. A backoff cost field establishment scheme will reduce the number of broadcast messages when the network is set up. This backoff scheme will defer the time that each node will broadcast message. It will wait until each node receives the optimum cost. As a result, it will reduce number of broadcast messages and energy consumption.

2.1 PHYSICAL LAYER

Understanding power efficiency at the physical layer requires understanding radio models, modulation and their relationship to power efficiency. In specific examples, the 915 MHz Industrial, Scientific, and Medical (ISM) is used. Long distance wireless communication can be expensive in terms of both energy and implementation complexity. Energy minimization assumes significant importance in relation to the propagation and fading effects while designing the physical layer for sensor networks. Generally, the minimum output power required to

transmit a signal over a distance d is proportional to d^α , where $2 \leq \alpha \leq 4$ [10]. Most applications employ low-lying antenna and near-ground channels, which the exponent α is closer to four, as is typical in sensor network communication [11].

2.1.1 Radio Model

Although this paper will not discuss radio circuit design, it must account for energy consumption in radio communication. A simple radio transceiver can sometimes be used in cluster-based routing protocols [12] (Figure 2).

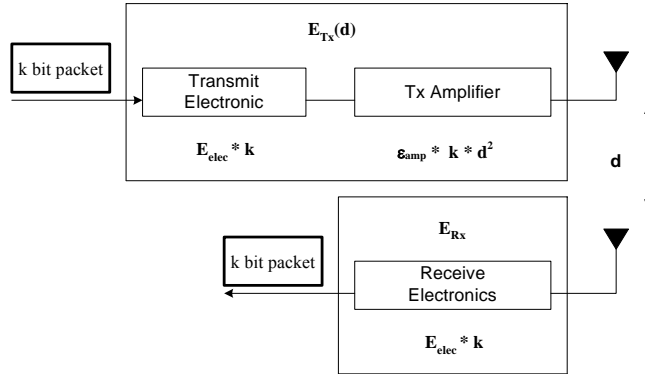


Figure 2: Simple radio model

In Table 1, transmitting ($E_{Tx-elec}$) and receiving ($E_{Rx-elec}$) data will consume $50nJ/bit$ (E_{elec}). The transmitter amplifier (ϵ_{amp}) uses $100nJ/bit/m^2$. Therefore, transmitting a k -bit message over a distance d , the energy consumption can be calculated as the following.

$$E_{Tx}(k, d) = E_{Tx-elec}(k) + E_{Tx-amp}(k, d) \quad (2.1)$$

$$E_{Tx}(k, d) = E_{elec} * k + \epsilon_{amp} * k * d^2 \quad (2.2)$$

Receiving this message, the energy consumed is as the following.

$$E_{Rx}(k) = E_{Rx-elec}(k) \quad (2.3)$$

$$E_{Rx}(k) = E_{elec} * k \quad (2.4)$$

Minimizing energy consumption for the network requires the protocols to minimize not only the transmit distances, but also the number of transmit and receive operations for each message.

Table 1: Radio characteristics.

<i>Operation</i>	<i>Energy Dissipated</i>
Transmitter Electronics ($E_{Tx-elec}$) Receiver Electronics ($E_{Rx-elec}$) ($E_{Tx-elec} = E_{Rx-elec} = E_{elec}$)	50nJ / bit
Transmit Amplifier (\mathcal{E}_{amp})	100pJ / bit / m ²

However, the simple radio model does not account for energy consumption as a function of data rate and startup time. Startup time (T_{st}) is the time when the transceiver is changes from the off state to the on. $N_{tx/rx}$ is the average number of times per second that the transmitter/receiver is used. $P_{tx/rx}$ is the power consumption of the transmitter/receiver [13]. The output transmit power (P_{out}) is the power consumed by the amplifier. The transmit/receive on-time ($T_{on-tx/rx}$) is the actual data transmission/reception time. Note that $T_{on-tx/rx} = L / R$, where L is the packet size in bits and R is the data rate in bits per second. The proposed energy consumption in [13] is calculated by:

$$P_{radio} = N_{tx} * [P_{tx} * (T_{on-tx} + T_{st}) + P_{out} * T_{on-tx}] + N_{rx} * [P_{rx} * (T_{on-rx} + T_{st})] \quad (2.5)$$

This model improves the accuracy of energy consumption, but a consequence is that when designing the system, it must now account for how often sensor turns the radio on and off. The elements of radio model are shown in Figure 3. The model has two main circuit parts, which are

transmission circuit and reception circuit. In order to overcome the path loss attenuation, the modulated signal will be amplified by amplifier before sending to antenna. The purpose of the mixer stage is to up-convert and down-convert the outgoing and incoming radio frequencies respectively to intermediate frequencies [14]. This is accomplished by mixing the RF signals with the local oscillator frequency.

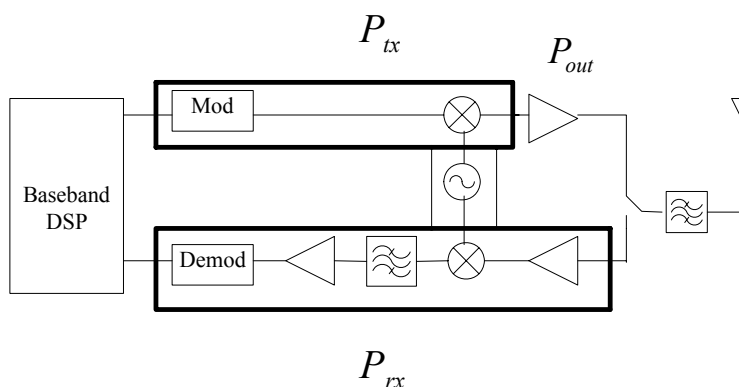


Figure 3: Radio model.

Tables 2 and 3 present an energy consumption model for TinyOS Mica2 mote [15]. By measuring energy consumption in Mica2 motes, this model shows that the energy consumption in transmission and reception should be higher than values in the classic radio model (see Table 3). Thus, this analysis will use this energy consumption model values. Analysis in chapter 5 employed 5 dBm transmission power as the power necessary to communicate over a distance of length d . However, to conduct the network lifetime experiments, the analysis in chapter 6 requires two transmission power values for d and $2d$ transmission power/radius.

Table 2: Crossbow TinyOS Mica2 mote measured energy consumption in Watts

	<i>5 dBm</i>	<i>0 dBm</i>	<i>-20 dBm</i>
<i>Transmit</i>	82.33 mW	59.03 mW	45.23 mW
<i>Receive</i>	45.35 mW	42.41 mW	45.23 mW
<i>Sleep</i>	17.23 mW	16.69 mW	16.69 mW

Table 3: Crossbow TinyOS Mica2 mote measured energy consumption in Joules/bit

	<i>5 dBm</i>	<i>0 dBm</i>	<i>-20 dBm</i>
<i>Transmit</i>	4.28 μ Joules/bit	3.07 μ Joules/bit	2.35 μ Joules/bit
<i>Receive</i>	2.36 μ Joules/bit	2.21 μ Joules/bit	2.35 μ Joules/bit
<i>Sleep</i>	0.9 μ Joules/bit	0.87 μ Joules/bit	0.87 μ Joules/bit

The energy consumption model in [15] did not determine the transmission range of the TinyOS Mica2 mote. However, by knowing the transmission power, the free space propagation model can approximate the Mica2 mote's transmission range.

Consider a simple case where there is a direct path between the transmitter and receiver, where d is the distance between them. Assuming the transmitter and receiver gains are equal to 1, the received power (P_r) is expressed as the following [16].

$$P_r(d) = \frac{P_t \lambda^2}{(4\pi)^2 d^2 L} \quad (6.1)$$

The transmitted power is P_t in mWatts. The free space loss, L_{free} , given by

$$L_{free} = -20 \log_{10} \left(\frac{\lambda}{4\pi d} \right) \quad dB \quad (6.2)$$

$$L_{free} = -20 \log_{10} \left(\frac{c/f}{4\pi d} \right) \quad dB \quad (6.3)$$

Where d is in km, and c is the free-space velocity, which is equal to 3×10^8 m/s. f is the frequency in MHz. L_{free} can be expressed as the following.

$$L_{free} = 32.44 + 20 \log_{10}(f) + 20 \log_{10}(d) \quad (6.4)$$

Thus, the received power is described as below.

$$P_{receive} (dBm) = P_{transmit} (dBm) - L_{free} (dB) \quad (6.5)$$

Assume a free space propagation model with $f = 903$ MHz, -98 dBm receiver sensitivity applies to equation 6.5 [17], the Mica2 mote can transmit with the range of 3.7 km and 2.1 km by using transmitted powers 5 dBm and 0 dBm respectively. The transmission range of 5 dBm transmitted power is approximately double the transmission range of 0 dBm. Thus, these values are employed in simulations to determine the network lifetime when increase transmission power/radius from d to $2d$.

2.1.2 Modulation/Demodulation Schemes

The modulation scheme used by the radio is another important factor that strongly impacts the energy consumption of the sensor node. The choice of a good modulation scheme is critical for reliable communication in a sensor network. One way to increase the energy efficiency of communication is to reduce transmission on time of the radio. This can be accomplished by sending multiple bits per symbol, that is, by using M-ary modulation. In M-ary modulation, each transmitted symbol comes from a set of M rather than 2 as in binary. This means that $\log_2 M$ bits are sent per symbol [18]. However, using M-ary modulation will increase the circuit complexity and power consumption of the radio. Moreover, when M-ary modulation is used, the efficiency of the power amplifier is reduced. Under startup power dominant conditions, a binary modulation scheme is more energy-efficient than M-ary modulation scheme [19].

In contrast to most current systems, sensor networks require low data rates, short range, and low power consumption to operate for long period of time on batteries [20]. These requirements drive the design to reduce power consumption and radio complexity. A coherent demodulator achieves the highest Signal-to-Noise Ratio (SNR) at the receiver for a given transmit power. However, it is costly in terms of complexity due to the need for phase and frequency tracking. On the other hand, a non-coherent demodulator is substantially less complex and consumes less power, but it has a degraded SNR performance. For example, at 900 MHz frequency, 1 mW transmit power, bit rate of 10 kbps, the path loss exponential model in [21] as a function of distance d is shown in

equation 2.6.

$$L(d) = \left\{ \begin{array}{ll} d^2, & 1 < d < 10m \\ \frac{d^3}{10}, & 10 < d < 20m \\ \frac{d^6}{6.572}, & 20 < d < 40m \\ \frac{d^{12}}{10^{10.912}}, & d > 40m \end{array} \right\} \quad (2.6)$$

Analysis in [21] shows that at a BER of 0.001, the link margin at 30 meters is 50 dB which is sufficient to absorb the losses in SNR due to non-coherent demodulation as well as fading effects. Although, the SNR loss due to non-coherent demodulation can usually be tolerated at short transmission ranges, it is still vulnerable to frequency offsets. To accommodate large frequency offsets, in contrast to traditional encoding and decoding which are applied to data symbols, the differential encoding and decoding of direct sequence spread spectrum (DSSS) chips is employed. The SNR degradation frequency offset Δf over a period of T is approximately $20 \log |\pi T \Delta f / \sin(\pi T \Delta f)|$. As an example a transmitted waveform with a chipping rate of 1 Mchips/sec, 127-chip spreading sequence, and 50-ppm crystals, the frequency offset is approximately 100 ppm of 900 MHz or 90 kHz. Since the chip duration is much shorter than the data symbol, the phase change due to a given frequency offset is small enough to achieve a sufficiently low SNR loss at the output of the demodulator.

Enabling the radio receiver at all times consumes energy even when data is not being received. However, if the radio is to be turned off, we must use a radio model that accounts for energy consumed in turning the radio on and off. The next section will discuss power modes for sensor nodes.

2.1.3 Power Modes for the Sensor Node

A sensor's energy consumption can also be controlled through device power management

modes: active, idle, and sleep mode [22]. However, the energy consumption on each mode is not provided. Each operating mode corresponds to a particular combination of component power modes. In general, if there are n components labeled $(0, 1, 2, \dots, n-1)$, each with k_i number of sleep states, the total number of node-sleep states is $\prod_{i=0}^{n-1} k_i$. However, every component power mode is associated with latency overhead for transitioning to that mode. Therefore, each mode is characterized by power consumption and latency overhead, and therefore, not all the states are useful. The component power modes corresponding to five different useful energy modes for sensor nodes are shown in Table 4. Each node consists of embedded sensor, microprocessor, and the RF circuits.

Table 4: Useful sleep states for the sensor node.

State	Microprocessor/ Data Processing	Sensor	Radio
Active	On	On	Tx/Rx
Ready	Idle	On	Rx
Monitor	Off	On	Rx
Observe	Off	On	Off
Sleep	Off	Off	Off

Each of these node-sleep modes corresponds to an increasingly deeper state, characterized by increasing latency and decreasing power consumption. *Active* is the only state and in which data processing can only occur. In the *Ready* state, the microprocessor is idle, and the sensor device is on. The microprocessor is turned off in the *Monitor* state, but the sensor device and radio are still operating. The radio will be turned-off in the *Observe* state (no communication with other nodes), but the sensor device is still on. In the *Sleep* state, the microprocessor, sensor device, and RF radio are turned-off. The sleep states are differentiated by the power consumed and the wakeup time. It can be said that the deeper the sleep state, the lower the power consumption and the longer the wakeup time.

Another method to assign different power modes to sensor node is to organize network into clusters. Every cluster has a central node/ base station that is responsible for the mission-oriented organization of the sensors by determining the set of sensors that will be responsible for sensing the environment. Sensor nodes are assumed to be capable of operating in an active mode or a low-power stand-by mode. The sensing and processing circuits can be powered on and off. Moreover, both radio transmitter and receiver can be turned on and off independently and the transmission power can be programmed based on the required range. Sensor nodes in clusters can be in one of four main states: sensing only, relaying only, sensing-relaying, and inactive [23]. In the sensing state, the node's sensing circuitry is on, and it sends data to the central node/ base station in a constant rate. In the relaying state, the node does not sense the environment, but its communication circuitry is on to relay the data from other active nodes. A node is in the sensing-relaying state when a sensor node is in both sensing the environment and relaying messages from other nodes. In the inactive state, a node turns off its sensing and communication circuitry.

2.2 DATA LINK LAYER

The data link layer protocol multiplexes data streams, performs data frame detection, medium access, and error control. The data link layer ensures the reliability of point-to-point and point-to-multipoint connections in a communication network. In this section, the medium access and error control strategies for sensor networks are discussed. Being an effective data link layer protocol in a wireless multi-hop sensor network, the MAC must achieve two goals. First, the creation of the network infrastructure must be achieved. This activity establishes the basic infrastructure needed for wireless communication hop by hop and gives the sensor network self-organizing ability. Second, sensor nodes must fairly and efficiently share communication resources.

To illustrate the reasons why existing MAC protocols cannot be used in sensor network scenario, MAC schemes in other wireless networks are analyzed. The first scenario is Mobile Ad hoc NETWORK (MANET). The MAC protocol's goal in the MANET is the provision of high QoS

under mobile conditions because it has the duty to form the network infrastructure and maintaining it in the face of mobility. Power consumption is of secondary importance in this scenario since nodes can be replaced by the user; although, the nodes are portable battery-powered devices [24]. The sensor network, in contrast to MANET, may have much larger number of nodes. The transmission power (~ 0 dBm) and radio range of a sensor node is much less than those of MANET [24]. In a sensor network, topology changes more frequently often because of node failure. Also, the mobility rate can be expected to be much lower than in the MANET since most sensor nodes are fixed and normally placed in the specific environment without moving. Second, in a Cellular system, the base stations form a wired backbone and a mobile node is only a single hop away from the nearest base station [25]. However, in sensor network, this access scheme is impractical since there is no central controlling agent like the base station. Even though the sensor nodes may be organized into clusters, the cluster-head node working as a control agent is still energy constrained. In addition, energy efficiency directly influences network lifetime in a sensor network and hence is of the primary importance. In the next subsection, three types of MAC protocols for wireless sensor networks will be discussed.

2.2.1 CSMA-Based Medium Access

Traditional CSMA-based schemes implicitly assume distributed traffic and independent point-to-point flows, which may not be true for wireless sensor networks. More likely, since the sensor networks are dense, the MAC protocol for sensor networks must be able to support not only variable, but also highly correlated and dominantly periodic traffic. The *listening mechanism* and the *backoff scheme* are important components in any CSMA-based medium access scheme.

The *listening mechanism*, such as CSMA/CD, is very effective when all nodes can hear one another (no hidden nodes). However, to save energy in wireless sensor networks, the additional circuitry of collision detection is not possible to be used because adding a circuitry will increase the battery depletion in sensor node [26]. Although listening is simple, it comes with an energy cost since the radio must be on to listen. Also, it is important to shorten the length of carrier sense to conserve energy. Many protocols such as 802.11 require sensing the channel even

during the backoff period. However, CSMA for sensor networks should turn the radio off during this period. In *backoff scheme*, the idea is to restrain a node from accessing the channel for a period of time and hopefully, the channel will become free after the backoff period. In sensor networks, the traffic is often a superposition of different periodic streams, backoff scheme should not only restrain a node from sending for the backoff period, but also be applied as a phase shift to unsynchronize the sensor nodes [26]. Nodes that happen to send simultaneously will corrupt one another, however if the traffic pattern of each node is independent, this situation is not likely to repeat.

Explicit contention control schemes can be used in many MAC protocols, e.g., IEEE 802.11, requiring the use of control packets, such as Request to send (RTS), Clear to Send (CTS), and Acknowledgements (ACKs). In computer networks, these small control packets impose very little overhead when data packets are large. On the other hand, in sensor networks where data packet size is small, these control packets can increase overhead load and result in an energy inefficient network. Thus, a contention control scheme for sensor networks should use a minimum number of control packets. Since the DATA-ACK control packets would constitute a large overhead to network, the most basic types of control packets are only RTS and CTS. To conserve energy, an RTS/CTS handshake may be employed when the amount of traffic is high while a simple CSMA scheme is actually adequate for low traffic since the probability of corruption due to collision is very small. The communication starts when a node, which wishes to transmit a packet, first sends an RTS packet to its central/control node and waits for a CTS reply. The sensor node will enter backoff with an exponential increasing backoff window if no CTS is received for a timeout period. It will also backoff if it overhear a CTS not destined to it. To avoid infinite CTS retries, the transmission will be dropped after a fix number of retries. Moreover, if a node hears a CTS before any of its own transmission, it will defer transmission for one packet time to avoid a collision.

Although the CSMA-based scheme is simple and has high scalability, the energy consumption in idle mode is high. Therefore, the collision-free synchronous TDMA/FDMA-based scheme is introduced in the next subsection to provide no collisions and allow sensor nodes to sleep when

they are not scheduled to send data.

2.2.2 Synchronous TDMA/FDMA-Based

In a TDMA scheme, which is introduced by [13], the full bandwidth of the channel is dedicated to a single sensor node for communication purposes. Therefore, the signal bandwidth per sensor is equal to the available bandwidth. Also, sensors can transmit at the highest data rate. T_{on-tx} is minimized in TDMA scheme since the transmit on time (T_{on-tx}) of the radio model described in equation 2.5 is inversely proportional to the signal bandwidth. On the contrary, in FDMA scheme, the total signal bandwidth is divided by the number of sensor nodes. As a result, the T_{on-tx} is at its maximum [13].

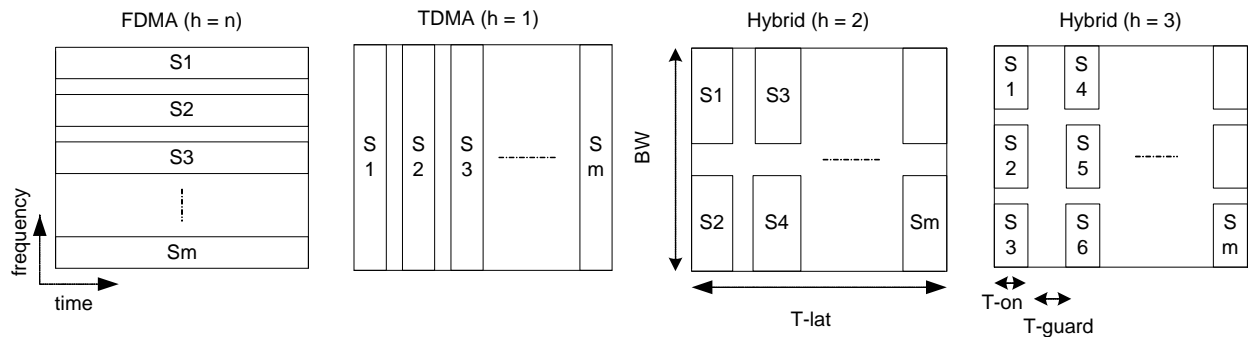


Figure 4: Multiple access methods.

A hybrid scheme involving both TDMA and FDMA (TDM-FDM) divides both time and frequency into available transmission timeslots (Figure 4). Note that a downlink from the base station/control node to the sensor nodes is required to maintain time synchronization among the nodes in the network. The base station/control node must send out synchronization packets (SYNCs) to avoid collisions among transmitted packets. To receive the SYNC signals, the receiver circuitry of each node must be activated periodically, resulting in energy inefficiency, since that the receiver consumes more power than the transmitter. The number of times the receiver needs to be active (N_{rx}) will depend on T_{guard} , the minimum time difference between

two time slots in the same frequency band, as shown in Figure 4. A larger guard time will decrease not only the probability of packet collisions, but also the average number of times that the receiver is used (N_{rx}). However, in [13], how the transmitters and receivers know the time-slots or frequency-band were not addressed.

Simulation results demonstrate that the average power reaches a minimum value when a hybrid TDM-FDM scheme is used [13]. The variation in power consumption for different h (the number of channels in the given bandwidth) grows smaller when T_{st} (start up time) is increased since the overall power consumption is dominated by the start up time. Although a TDMA scheme will have the minimum transmission on time (T_{on-tx}), it does not achieve the lowest power. In fact, as the number of channels (h) is reduced, the guard time decreases. Thus, more synchronization packets are needed. As a result, the receiver power starts consuming a large portion of the total power.

One possible mechanism for improving energy efficiency is to eliminate the control node assigning timeslots in the network, and use an algorithm so that the sensors self-organize and establish transmission/reception schedules for communication without the need of local or global master nodes.

2.2.3 SMACS and EAR Algorithm

Establishing transmission/reception schedules for communication without the need of local or global master nodes requires sensor nodes to find each other to setup the network. After a link is established, a node knows when to turn on its transceiver ahead of time to communicate with another node. It will turn off when no communication is scheduled. As a result, the protocol is energy-efficient without requiring accumulation of global connectivity information. *Self-Organizing Medium Access Control for Sensor Networks (SMACS) Algorithm* is a distributed infrastructure-building protocol that forms a flat topology and enables nodes to discover their neighbors [27]. The neighbor discovery and channel assignment phases are combined in

SMACS, so after a node hears from all neighbors, they can form a connected network.

To illustrate the methods how the nodes find each other and how the network is set up, the node A, B, and C are given as examples. These nodes wake up at random times. Upon waking up, each node will listen to the channel for some random time duration. However, the number of frequency bands was not suggested in [27]. If a node has not heard any invitations from other nodes, it will decide to transmit an invitation by the end of initial listening time. Node A first broadcasts invitation or TYPE1 message. The awake neighboring node B and C hear this message and response with TYPE2 message. Node A will respond to a TYPE2 message that either arrives first or has higher received signal level (depending on selection criteria) with a TYPE3 message. This message is to notify all respondents which node was chosen to turn on its transceiver. The node that was not chosen will turn off its transceiver for some time and then start the search procedure. The TYPE3 message also contains transmission schedule and the start time of the next T_{frame} of node A. T_{frame} is the length of the super frame in SMACS, and it is fixed for all nodes. The chosen neighbor node will send the location of these timeslots along with the randomly selected frequency band of operation to node A in a TYPE4 message. The frequency band is chosen at random from large possible choices when the links are formed [27]. Once a pair of short test messages is successfully exchanged between the two nodes using the newly assigned slots, the link is added to the nodes' schedules permanently. The transmission and reception will be repeated periodically every T_{frame} .

To offer continuous service to mobile nodes, the *Eavesdrop-And-Register (EAR) Algorithm* is introduced. The mobile nodes assume full control of the connection process and decide when to drop connections. A stationary node transmits an invitation message to surrounding neighbors. A mobile node eavesdrops on these control messages but does not respond. Keeping a constant record of neighboring activity, the mobile node will form a registry of neighbors. This registry will be used to hold the information for forming, maintaining, and disconnecting. A stationary node will also maintain a registry of mobile sensors that have formed connections and remove them when the links are broken. Thus, four types of messages are used for making and breaking connections. The stationary node invites other nodes to join by using *Broadcast Invite (BI)* message. The mobile node responds to BI to request a connection using *Mobile Invite (MI)*

message. The *Mobile Response* (MR) message is used by stationary node to accept the MI request. To disconnect, mobile node informs the stationary node using *Mobile Disconnect* (MD) message.

In summary, these three MAC protocols have characteristics that suit different applications. In power conservation, SMACS and EAR algorithm propose a random wake up sensor nodes during setup and turning radio off during idle period. While CSMA-based medium access proposed a mechanism that minimizes overhead by using only RTS and CTS handshake. On the other hand, Synchronous TDMA/FDMA-based protocol uses hardware-based approach for system energy minimization. The optimum number of channels in this scheme will be calculated for minimum system energy.

2.2.4 Error Control

Error control of transmission data is another important function of the data link layer in sensor networks. Forward error correction (FEC) and automatic repeat request (ARQ) are two methods of error control in communication networks. The additional retransmission cost and overhead will limit the usefulness of ARQ in multi-hop sensor network environments. On the other hand, FEC has a greater complexity because error correction capabilities must be built in. As a result, simple error control codes with low-complexity encoding and decoding will present the best solutions for sensor networks [19].

Convolutional codes often used for FEC require the additional processing energy, E_{dsp} , to encode and decode the data. Additional energy cost will be incurred during the communication since encoding a bit stream will increase the size of the packet by approximately $1/R_c$. As a result, it will increase the radio energy required to transmit a packet. However, in this proposed research, we did not take encode and decode into account in the energy model. We can derive the average energy to transmit, receive, encode, and decode each information bit using equation 2.7 where E_{dsp}^e is the energy to encode data and E_{dsp}^d is the energy to decode data.

$$E = P_{tx}(T_{on-tx} + T_{st}) + P_{out}T_{on-tx} + E_{dsp}^e + P_{rx}(T_{on-rx} + T_{st}) + E_{dsp}^d \quad (2.7)$$

Let R_c be the code rate, e.g., 1/2 and 1/3-rate of convolutional codes and L is the packet length transmitted. Then the number of information bits is $L' \approx LR_c$. Thus, the energy per bit is $E_b = E / L'$.

Simulation results show that when the desired probability of error (P_b) is decreased the average energy consumption per bit of no coding shows an exponential increase [13]. Due to the transceiver power ($P_{tx/rx}$) is dominant at high P_b desired at the receiver, no coding is recommended. Using coding will increase the overall energy per bit because coding the data will increase the on time (T_{on}) of the transceiver. However, since the energy of the power amplifier (P_{out}) will begin to dominate at low probability of error (P_b), codes with greater redundancy will have better performance.

The energy-efficient medium access control protocols and the error control coding in sensor networks are presented in this section. CSMA-based protocols are simpler and highly scalable while the synchronous TDMA/FDMA-based is more complex since it requires synchronization. The advantage of TDMA/FDMA is that it is easy to assign a sleep state to sensor nodes to save energy. It is also recommended to use hybrid TDMA-FDMA scheme to reach the minimum value of the average power consumption. Since coding will increase the overall energy per bit, error control coding is not recommended when the high probability of error is required. To further increase the energy-efficiency in the network, the next section introduces efficient routing schemes.

2.3 NETWORK LAYER

A specific routing protocol for wireless sensor networks is required in the network layer since traditional routing protocols for wireless ad-hoc networks may not be directly applicable to

sensor networks due to the severe constraints on power. Additionally, sensor networks can be characterized as data centric networks, where data is not always requested from a specific node, but requested based on certain attributes. Sensor networks are also application-specific in that the network's requirements change with the applications. As an example, in some applications, the sensor nodes are fixed, but other networks are a combination of fixed and mobile nodes, thus requiring mobility support. Adjacent nodes might have similar data; therefore, sensor networks should aggregate similar data to reduce unnecessary transmissions and save energy. Assigning unique IDs may not be suitable in sensor networks because these networks are data centric—routing to and from specific node is not required. In addition, the large number of nodes will require large IDs, making addressing overhead large compared to data being transmitted. Therefore, routing protocols in sensor networks must optimize energy consumption, and be application specific, data centric, and capable of aggregation data.

Routing schemes in wireless sensor networks can be categorized into two types, i.e., cluster-based and non-cluster-based (flat), which will be reviewed in chapter 3. The *Network layer* section begins by reviewing traditional ad-hoc proactive and reactive routing protocols to provide a background.

2.3.1 Proactive vs. Reactive Routing Protocol

To help understand the routing protocols in wireless sensor networks, we review how various traditional routing protocols have been applied to ad-hoc packet radio networks. *Proactive routing protocols* attempt to maintain consistent up-to-date routing information from each node to every other node in the network. Every node maintains one or more routing tables that store the routing information. The network view remains steady since the topology changes are propagated throughout the network as updates. The protocols vary in the number of routing tables maintained and the method by which the routing updates are propagated. Two examples of proactive routing protocol are Destination-Sequenced Distance-Vector Routing Protocol (DSDV) and Link-state Routing [24]. DSDV is based on the Bellman-Ford algorithm for the shortest paths and ensures that there is no loop in the routing tables. Every node in the network maintains

distance information and the next hop to every other node in the network. To maintain table consistency, routing table updates are periodically transmitted throughout the network. In Link-state routing protocols, each node floods the cost of all the links to which it is connected throughout the network, each node works out a least cost path to every other node.

Reactive routing protocols, in contrast to proactive routing protocols, create routes only when needed. An explicit route discovery process creates routes, and it is initiated only on as-needed basis. It can be either source-initiated or destination-initiated. Source-initiated routing means the source node begins the discovery process. Once a route has been established, and the route discovery process ends, a maintenance procedure maintains that route until it is no longer needed. An example of reactive routing protocol is Dynamic Source Routing (DSR). DSR is a source-initiated reactive protocol, and based on the concept of source routing [24]. The source node will specify the entire route to be taken by a packet, rather than just a next hop. If the source node does not have a route, it floods the network with a Route Request (RREQ). Any node that has a path to the destination can reply with the Route Reply (RREP) to the source node. This reply contains the entire path recorded in the RREQ packet. However, these existing routing algorithms are not sensitive to energy constraints.

2.3.2 Energy-Efficient Routes

The decisions required for selecting the energy-efficient routes between a source node and a sink node in wireless sensor network is based on minimum energy path, minimum hop path, and maximum available power. Energy-efficient paths are chosen based on the energy required (α) for the transmission in the links along the paths and the available power (β) in the nodes. The source node senses the environment and is ready to transmit sensed data to the sink node (Figure 5). However, there are three possible paths to communicate with the sink. An energy-efficient path can be chosen by any of the following approaches.

- *Minimum energy (α) path*: The minimum energy path is the path that consumes minimum energy (α) to transmit data packets between the sink and the source.
- *Minimum hop path*: This path has the minimum hops from source node to reach the sink

node. In Figure 5, the minimum hop path is Path 2 (Sink-C-Source). Note that the minimum hop path is not always the minimum energy path.

- *Maximum available power (β) path*: The path that has the maximum total available power (β) will be selected in this approach. However, this approach may not be able to handle the unbalanced available power of nodes along the path, i.e., there can be some nodes with no power and others with a lot of power.

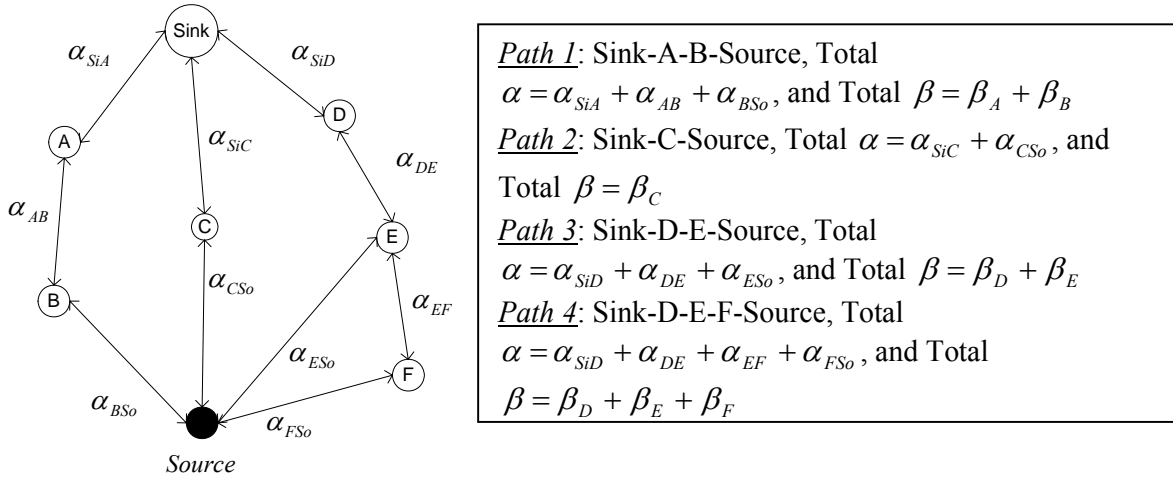


Figure 5: The energy-efficiency of the routes.

2.3.3 Data Aggregation and Backoff-based Cost Field Scheme

Recently, the routing schemes in wireless sensor networks have been proposed to maximize the network lifetime. The proposed data aggregation technique and backoff-based cost field establishment scheme are discussed in this section.

2.3.3.1 Data Aggregation Technique

Achieving energy efficiency requires the routing protocols in wireless sensor networks to perform data aggregation. The idea of data aggregation is to combine the data coming from different sources to eliminate redundancy, minimize the number of transmissions and thus, save energy [28]. One method is for a sink to request data from sensor nodes instead of sensor nodes

periodically reporting the condition of the phenomena. The same data coming from multiple sensor nodes are aggregated when they arrive the same routing node.

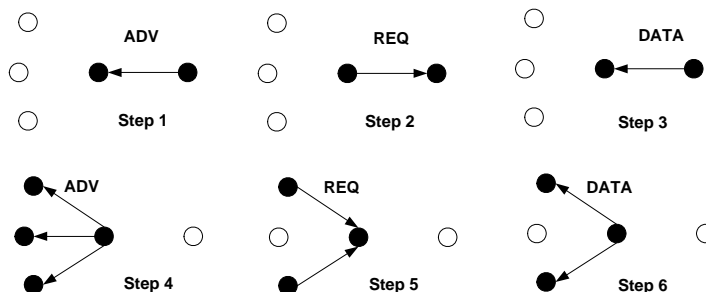


Figure 6: Negotiation and aggregation steps.

The three types of data, which are advertisement message (ADV), request message (REQ), and data message (DATA) will be used to address the deficiencies of classic flooding (e.g. implosion and overlap problems) by negotiation [29]. Figure 6 demonstrates how the negotiation and aggregation work. In step 1, before sending DATA, the sensor node broadcasts an ADV containing a descriptor called meta-data. This meta-data is used for negotiation to eliminate the transmission of redundant data throughout the network. The neighbors who are interested in the data will send a REQ message for the data as in step 2. In step 3, the data will be sent to this neighbor sensor node. The neighbor sensor node then repeats this process (step 4, 5 and 6). Thus, only nodes that are interested in the data will receive a copy. In step 3, it can be observed that if a neighbor node has its own data, it can aggregate this with the data received from the source node. Also, nodes are not required to respond to every message. This aggregation technique is employed by SPIN (Sensor Protocols for Information via Negotiation) protocol. It allows the sensor to efficiently distribute data given limited energy supply.

2.3.3.2 Backoff-based Cost Field Establishment Scheme

As a flooding network, the reason that a node broadcasts message more than once is that it broadcasts immediately after obtaining a lower cost path, no matter whether the cost is optimum or not. If node can defer the broadcast to the time after it has heard the message leading to the

minimum cost, the node may broadcast only once, carrying its optimum cost. Thus, how long the node defers its broadcast becomes critical.

Backoff-based cost field establishment scheme can be illustrated by the *Minimum-Cost Path Forwarding* [30]. At each node, the cost field is defined as the minimum cost from the node to the sink on the optimal path. The link cost can be any form, e.g., consumed energy or hop count or a combination. Once the cost field is established, messages may flow to the sink along the minimum cost path. When a message is sent out by the source, it carries the minimum cost from the source to the sink. This message also carries the total cost that it has consumed so far starting from the source to the current intermediate node. A neighboring node hearing the messages decides to forward the message only if the sum of the consumed cost in message header and the cost at this node matches the source's cost in the message header (Figure 7a).

Figure 7a assumes that the minimum costs OL_B , OL_C , and OL_{source} from nodes B, C and the source node to the sink are 60, 70, and 150 respectively. Suppose when A broadcasts the report message (REP), the total amount of consumed cost from the source to A is 90 (including A's broadcast cost). After B and C hear the message, both nodes determine if they are closer to the sink than sender A by comparing their costs with A's cost, which is in message header. A node with a greater cost will drop the message. Suppose both node B and C pass the comparison, they calculate the remaining cost budget as $150 - 90 = 60$. Since $OL_B = 60$, node B will forward REP message. On the other hand, node C will not forward the REP message because the remaining budget is not sufficient to reach the sink, i.e., $OL_C > 60$. This means it is not on the optimal path of the source.

Figure 7b illustrates the idea of Backoff-based cost field establishment scheme. At time T, node A broadcasts an ADV message and neighbors B and C hear this message. Assume minimum cost at A is L_A and the cost for B and C are ∞ . B sets its cost as $L_A + 3$ where 3 is the link cost between A and B after B receives the ADV from A. B will set a backoff timer that expires after $\gamma * 3$. Suppose a constant γ is set at 10, thus the backoff timer will expire at $T = 30$. Similarly, C sets its cost as $L_A + 6$ and set a backoff timer $\gamma * 6 = 60$. Without using this backoff scheme, both B and C will broadcast immediately since they have received some costs less than ∞ . At $T + 30$,

B's backoff timer expires. B finalizes its minimum cost as $L_B = L_A + 30$, and broadcasts an advertisement message containing L_B . When C receives this message, C updates its cost to $L_B + 2$, and reset its backoff timer to be $\gamma * 2 = 20$ since $L_C = L_A + 6 > L_B + 2 = L_A + 5$. When A receives advertisement message from B, it discards message since $L_B > L_A$. Finally, at $T + 50$, C's timer expires, and C finalizes its cost as $L_C = L_B + 2 = L_A + 5$. Then, it broadcasts a message with its minimum cost [30].

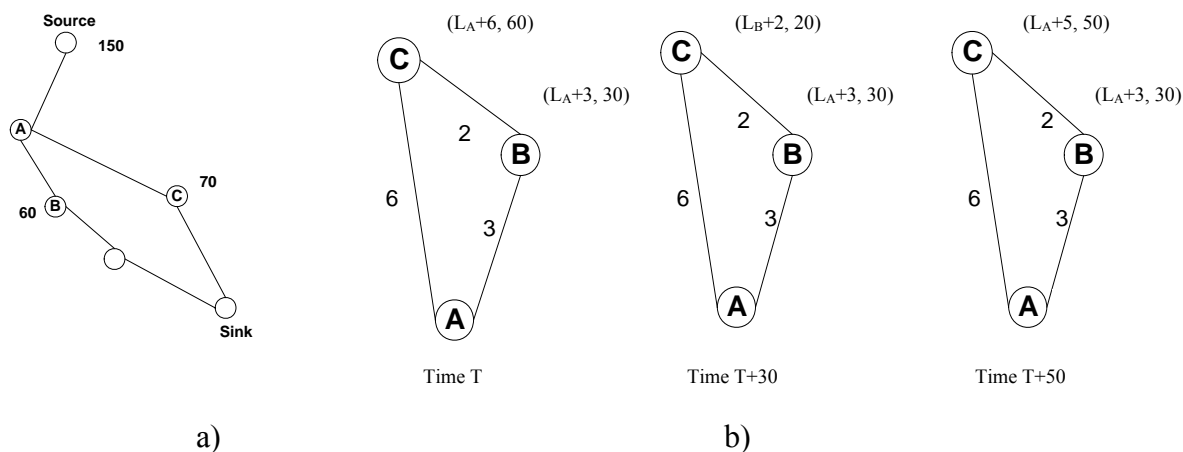


Figure 7: a) Forwarding along the minimum energy path; b) An example for Backoff-based Optimal Cost Field Establishment.

2.4 PROPAGATION MODELS

In sensor network, the highest consumer of energy is transmitter, the amount of energy required is the energy consumed by transmitter circuit and amplifier. The radio model assumes the fix distance d , called *disk model* in applying the energy consumed by amplifier. Disk model is often used for the analysis of multi-hop networks. The radius for successful transmission has a deterministic value. The signal-to-noise ratio which is a random variable is neglected. This leads to the assumption that a transmission over a multi-hop either fails completely or successful [31]. However, this assumption ignores the fact that end-to-end packet loss probabilities increase with the number of hops, except the transmit power is adjusted. As a result, this section is dedicated to

study more realistic model which is called *Threshold model*. To overcome some of the limitations of the disk model, the simple Rayleigh fading link model that relates transmit power is discussed.

2.4.1 Rayleigh Fading Link Model

The narrowband Rayleigh block fading channel is assumed. A transmission from node i to node j is successful if the signal-to-noise-and-interference ratio (SINR) β_{ij} is above a certain threshold Θ that is determined by the communication hardware, and the modulation and coding scheme, normally between 1 and 100 or 0dB and 20 dB [32]. The SINR β is a discrete random process with exponential distribution $p_\beta(x) = \frac{1}{\bar{\beta}} e^{-x/\bar{\beta}}$ with mean

$$\bar{\beta} = \frac{\bar{R}}{\sigma_z^2 + \sigma_I^2} \quad (3.1)$$

Where R is the received power, which is exponentially distributed with mean \bar{R} . σ_I^2 is the interference power affecting the transmission. It is the sum of the received power of all the undesired transmitters. Over a transmission of distance d with attenuation d^α , we will get,

$$\bar{R} = P_0 d^{-\alpha} \quad (3.2)$$

Where, P_0 is proportional to the transmit power. N denotes the noise power. I is the interference power affecting the transmission, i.e., the sum of the received power.

The following theorem is to address the independent analysis on the signal-to-noise ratio (SNR) and signal-to-interference ratio (SIR), which will be carried to the analysis on energy balancing methods in section 3.2. Using this theorem, we can state all required parameters of transmit power to transmit over a distance d .

In a Rayleigh fading network, the reception probability $P[\beta \geq \Theta]$ can be factorized into the reception probability of a zero-noise network and the reception probability of a zero-interference network [33].

The probability that the SINR is bigger than a given threshold Θ follows from the cumulative distribution $f_\beta(x) = 1 - e^{-x/\bar{\beta}}$:

$$\begin{aligned} P[\beta \geq \Theta] &= e^{-\Theta/\bar{\beta}} = e^{-\frac{\Theta}{P}(\sigma_z^2 + \sigma_I^2)} \\ &= e^{-\frac{\Theta\sigma_z^2}{P}} \cdot e^{-\frac{\Theta\sigma_I^2}{P}} \\ &= P[\beta_z \geq \Theta] \cdot P[\beta_I \geq \Theta] \end{aligned} \quad (3.3)$$

Where $\beta_z = \bar{R}/\sigma_z^2$ denotes the signal-to-noise ratio (SNR) and $\beta_I = \bar{R}/\sigma_I^2$ denotes the signal-to-interference ratio (SIR). From equation 3.3, the first term is the reception probability in a zero-interference network, as it depends only on the noise. On the other hand, the second term is the reception probability in a zero-noise network, as it depends only on the interference. Thus, the independence analysis of the effect caused by noise and the effect caused by interference is allowed. It is assumed that, for the light load or low interference probability, SIR is much greater than SNR; therefore, the noise analysis alone provides accurate results. For the high load, a separate interference analysis has to be carried out [33]. As a result, in this section only zero-interference network has been discussed.

The reception probability over a link distance d at a transmit power P_0 is given by

$$P_R = P[\beta_z \geq \Theta] = e^{-\frac{\Theta\sigma_z^2}{P_0 d^{-\alpha}}} \quad (3.4)$$

Solving for P_0 , the necessary transmit power to achieve link reliability or P_R is as follow

$$P_0 = \frac{d^\alpha \Theta \sigma_Z^2}{-\ln P_R} \quad (3.5)$$

2.5 SUMMARY

The energy constraint is an important factor in designing the protocols in wireless sensor networks. Maximizing a sensor network's lifetime requires energy-efficient sensor node circuits, algorithms, and protocols. This chapter organized the energy-efficient protocols in wireless sensor networks into three parts, Physical Layer, Data Link Layer, and Network Layer. Also, this chapter presented examples of the energy-efficient schemes that are employed in wireless sensor networks. To explain energy efficiency in physical layer, the study of radio model, modulation and demodulation schemes, and power modes of sensor nodes were discussed. The radio model equations are used to measure the energy consumption in radio communication. In addition, the M-ary and binary modulation schemes are compared. The binary modulation scheme is more energy-efficient under startup power dominant conditions. Even though coherent demodulation achieves higher SNR, a non-coherent demodulator is recommended since it is less complex and lower power. The power modes of the sensor nodes are one of the most important factors in reducing the battery depletion since the sensor node can turn-off its transceiver when it is idle or has no data to send. Three widely used media access control protocols were discussed, the collision-free synchronous TDMA-based is mostly used in cluster topology due to the need of a control node to schedule the TDMA timeslots. Energy saving in this scheme occurs because the sensor nodes that are not scheduled to send data can be in sleep mode. CSMA protocols are less complex because network synchronization is not required. However, the high-energy consumption in idle mode is a disadvantage. As we further study the network layer, energy-efficient routing schemes were discussed to further reduce energy consumption and prolong the network lifetime. Data aggregation technique and backoff-based cost field establishment scheme are useful in flooding or broadcasting communication. Data aggregation techniques reduce the data overlap and implosion problems and the number of transmissions of duplicate messages. On the other hand, the backoff-based scheme extends the network lifetime by reducing the number

of broadcast messages. Since analysis in wireless sensor networks are usually assumed a disk model, propagation model is discussed to study an alternative in designing routing protocols called a threshold model. The next chapter reviews the existing routing protocols and energy balancing strategies in wireless sensor networks. Then, chapter 4 proposes a scheme that achieves the simplicity and energy efficiency, named Gossip-based Sleep Protocol (GSP).

3.0 ROUTING AND ENERGY BALANCING TECHNIQUES

Wireless sensor networks have utility in a variety of applications such as military, industrial, and medical. Each application can be specific and employs sensor network based on its desire. Thus, it is helpful that we study several such applications and classified them based on their modes of acquiring and propagation sensor data [5]. The following three classes are the most common.

- *Periodic Sampling*: For applications where a certain condition or process needs to be monitored continuously, such as temperature in a conditioned space or runways at the airport. Sensed data is acquired from remote sensors and forwarded to a data collection center or sink on a periodical basis.
- *Event Driven*: Some applications require monitoring one or more crucial variables and transmit only when a certain thresholds is reached. Common examples include fire alarms, door or window sensors.
- *Store and Forward*: There are many cases that sensed data can be captured and stored or even processed by a remote node before it is transmitted to sink.

This chapter studies and surveys the existing routing protocols in wireless sensor networks, which can be categorized into two categories -- clustering and flat routing protocols. Even though some of the routing protocols may be already stated in the other chapters before, this chapter will discuss each of them in details. The rest of this chapter will be left for the energy balancing methods used in wireless sensor networks.

3.1 EXISTING ROUTING PROTOCOLS

3.1.1 Clustering Routing Protocols

Hierarchical or clustering based routing methods [12], [34], [35] are techniques with advantages related to scalability and efficient communication. It is also utilized to perform energy efficient routing in wireless sensor networks. The creations of clusters and assigning task to cluster-heads can contribute to scalability, energy efficient, and network lifetime. To provide energy efficient, the cluster routings employed energy balanced routing setup scheme, which will be discussed in section 3.2.2. Examples of clustering routing protocols in wireless sensor networks are discussed in this section.

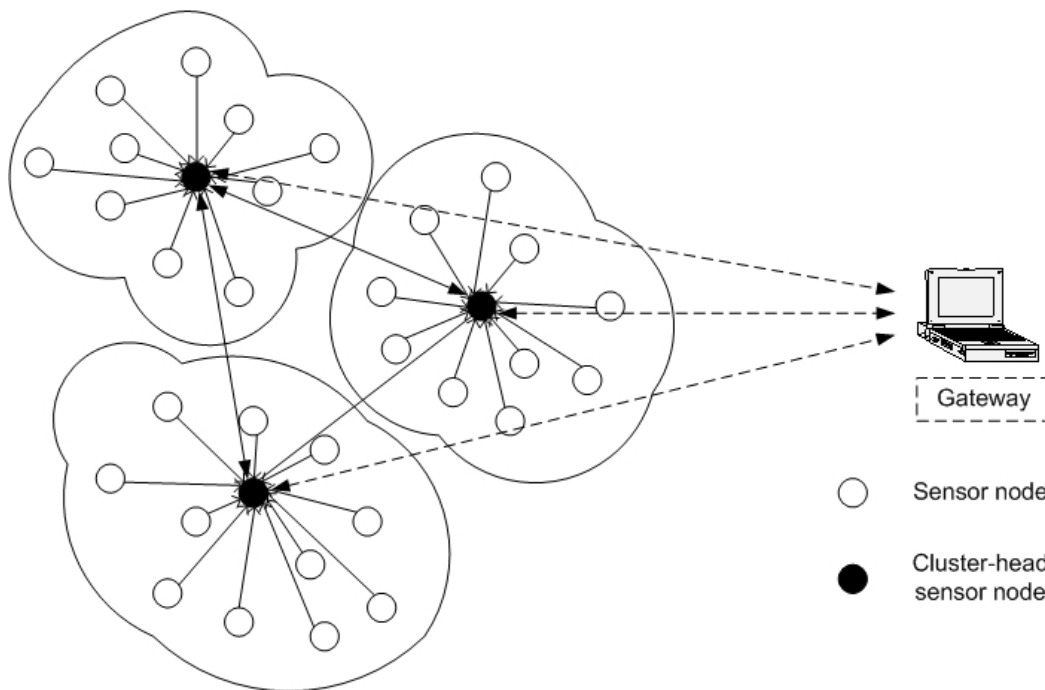


Figure 8: Clustering communication in wireless sensor network.

3.1.1.1 Low Energy adaptive Clustering Hierarchy (LEACH)

LEACH is non-energy-aware routing protocol. Unlike many other routing protocols, LEACH

does not follow a hop-by-hop routing [12]. In LEACH, the time span is divided into fixed-length rounds. The duration of each round is pre-determined for a network with specific parameters. A round contains two phases: setup phase and steady-state phase. A number of clusters are formed in the setup phase. Each cluster will select its cluster-head which will schedule the nodes in its cluster in a TDMA. During steady-state phase, cluster-heads receive data packets from their cluster nodes through direct communication. Compared to direct transmissions, LEACH improves by a factor of 8 [3]. This is because the use of clusters for transmitting data to the base station in LEACH provides small transmit distances for most nodes. LEACH requires only a few nodes to transmit far distances to the base station. Though LEACH is an efficient and self-organized algorithm, it has some disadvantages as the following.

- In setup phase, clusters formation and rotating cluster-heads require of overhead added to network.
- Since LEACH assumes that all nodes can transmit with enough power to reach the base station. It may not be applicable to networks deployed in large regions.
- It is not obvious how the number of predetermined cluster-heads probability is going to be uniform distributed through the network. Thus, there is a possibility that the elected cluster-heads will be concentrated in one part of the network. As a result, some nodes will not have any cluster-heads in their region.
- The idea of dynamic clustering brings extra overhead (advertisements, cluster-head changes, etc.), which may weaken the gain in energy consumption.

3.1.1.2 Threshold sensitive Energy Efficient Sensor Network protocol (TEEN)

TEEN is a cluster-based routing protocol based on LEACH [34]. It is targeted at reactive networks (see section 2.3.1). The unique definitions in this protocol are:

- *Hard Threshold* (H_T): The absolute value of the attribute beyond which, the node sensing this value must switch on its transmitter and report it.
- *Soft Threshold* (S_T): A change in the value of the sensed attribute which triggers the node to switch on its transmitter and report sensed data.

Some assumptions are made as follows.

- The base station (BS) has a constant power supply and can transmit with high power to all the nodes directly.
- The network is composed of a base station and sensor nodes with the same initial energy.

A node which has the sensed value determines whether to report it or not based on the values of H_T and S_T . Data are sent only when the sensed value exceeds H_T or the value's change is bigger than S_T . TEEN employs LEACH's strategy to form cluster. Some issues are unaddressed by LEACH are left unaddressed by TEEN as well. Additionally to LEACH's drawbacks; TEEN suffers from the following disadvantages. Since TEEN is based on Thresholds, timeslot is wasted if it does not have data to send. Also, there is no mechanism to distinguish a node that does not reach thresholds from the dead or fail node.

3.1.1.3 Adaptive Period Threshold sensitive Energy Efficient Sensor Network protocol (APTEEN)

Unlike TEEN, APTEEN is a hybrid protocol that changes the periodicity or threshold values used in TEEN protocol according to user needs and the application type [35]. In APTEEN, the cluster-heads broadcast the following parameters.

- *Attribute (A)* is a set of parameters that user is interested in obtaining information.
- *Thresholds* consists of the hard threshold (H_T) and soft threshold (S_T).
- *Schedule* is a TDMA schedule, assigning a slot to each node.
- *Count time (CT)* is the maximum time period between two successive reports sent by a node.

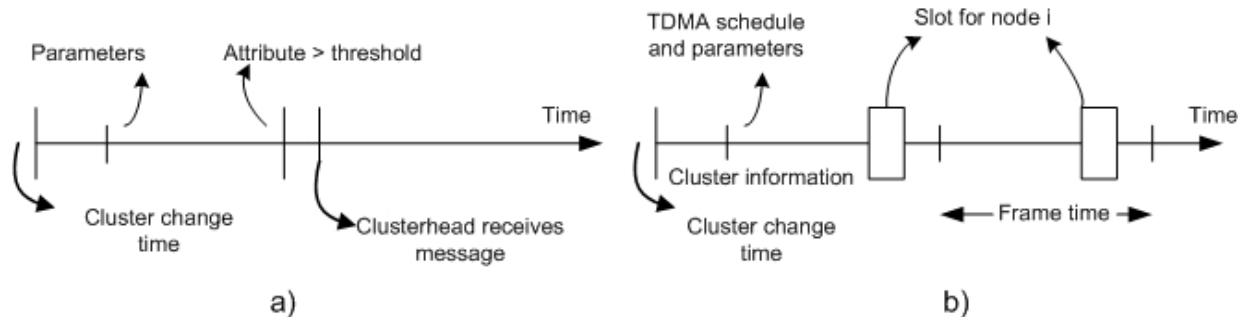


Figure 9: Timeline for the operation of a) TEEN and b) APTEEN.

Each node senses the environment continuously, and only nodes that sense a data value beyond H_T will transmit. Once a node senses a value beyond H_T , it transmits data only when the value of that attribute changes by an amount equal to or greater than S_T . If a node does not send data for a time period equal to count time (CT), it is forced to sense and retransmit the data. The main drawback of the scheme is the additional complexity required to implement the threshold functions and count time. Furthermore, the overhead and complexity associated with forming clusters are still concerned.

3.1.1.4 Power-Efficient Gathering in Sensor Information Systems (PEGASIS)

PEGASIS is a chain-based power efficient protocol based on LEACH [36]. Assumptions on this PEGASIS are as the following.

- All nodes have location information about all other nodes in order to construct the chain.
- Each node can directly transmit data to the base station.
- All nodes are fixed

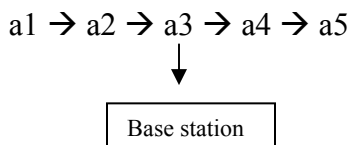


Figure 10: Token passing approach.

The chain can be created easily since each node has global knowledge of the network. This approach will distribute the energy load evenly among the sensor nodes in the network since each node takes turn to be the leader for transmission to the base station. For gathering data in each round, each node receives data from one neighbor, fuses with its own data, and transmits to the other neighbor on the chain. The leader in each round of communication is at a random position on the chain that is a key for nodes to die at random locations to make the network robust. PEGASIS outperforms LEACH by eliminating the overhead of cluster formation, limiting the transmissions, and minimizing the distances that non-cluster-head nodes have to transmit. To balance the overhead involved in communication between the leader and sink, each node in the chain takes turn to be the leader. However, there is still a disadvantage. Since PEGASIS requires global information, it may not be suitable for sensor networks where global knowledge is not easy to obtain.

3.1.1.5 Two-Tier Data Dissemination Model (TTDD)

TTDD provides scalable and efficient data delivery to multiple mobile sinks [37]. It starts data dissemination with building a grid structure that is used to disseminate data to the mobile sinks by assuming the sensor nodes are stationary and location aware. To build the grid structure, a data source chooses itself as the start crossing point of the grid, and sends a data announcement message to each of its four adjacent crossing points. It will stop when the message reaches the node closest to the crossing point. Each intermediate node stores the source information and further forwards the message to its adjacent crossing points except the one from which the messages come. With the grid available, a sink can flood its query, which will be forwarded to the nearest dissemination points in the local cell to receive data. Then the query is forwarded along other dissemination points upstream to the source. The requested data then flows down in the reverse path to the sink.

Sink mobility in TTDD brings new challenges to large-scale sensor networks. However, TTDD's design exploits the fact that sensor nodes are stationary and location-aware to construct and maintain the grid structures. TTDD assumed the availability of a very accurate positioning system that may be not yet available for wireless sensor networks. Moreover, the overhead associated with maintaining and recalculating the grid as network topology changes can be high.

3.1.2 Flat Routing Protocols

Flat wireless sensor network architecture is a homogeneous network, where all the nodes are identical in term of hardware complexity and battery energy, except for sink [38]. Sink will perform as a gateway to gather the information from all sensors then forwards them to the end user. In this section, the flat routing protocols [29], [30], [39] - [41] in wireless sensor networks are investigated.

3.1.2.1 Directed Diffusion

Directed diffusion proposed a data aggregation paradigm for wireless sensor networks [39]. Directed diffusion is a data centric and application aware paradigm in the sense that all data generated by sensor nodes is named by attribute value pairs. The idea of data centric is to combine the data coming from different sources. Also, Directed diffusion eliminates redundancy and minimizes the number of transmissions.

All communication in direct diffusion is for named data consisting of four elements:

- *Interests* are task descriptions which are named by a list of attribute value pairs that describe a task.
- *Data messages* are names using attribute value pairs.
- *Gradient* identifies both data rate and direction along which events should be sent.
- *Reinforcement* is used to select a single path from multiples paths.

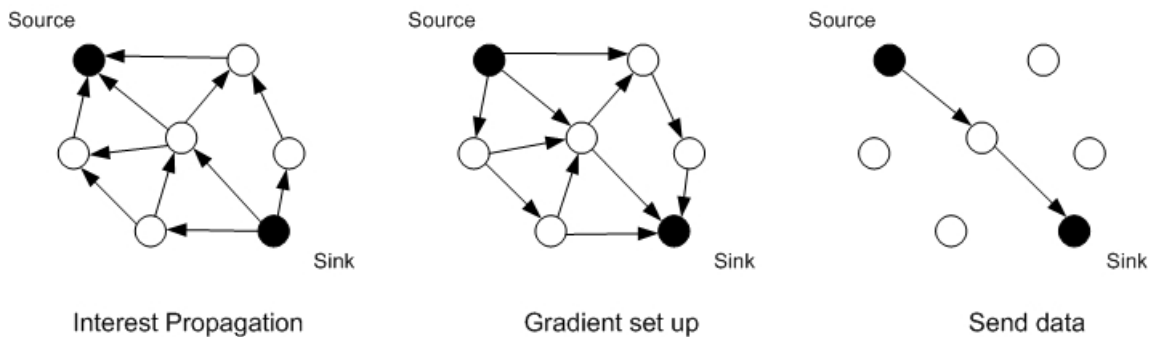


Figure 11: An example of directed diffusion.

In this protocol, a query is transformed into an interest that is diffused or flooded towards nodes in the interested region. When a sensor node in that region receives the interest, it activates sensors in interest region to observe interested events. Then, the data are transmitted back in the reverse path of the interest propagation. To make protocol more efficient, the intermediate nodes might aggregate the data based on the data's name and attribute value pairs. The propagation and aggregation procedures are based on local information. The direct diffusion protocol reaches energy saving by selecting the efficient paths empirically processing data in network. However, it has some drawbacks. Direct diffusion is the query-driven data model, which may not be applied to applications e.g., environmental monitoring that require continuous data delivery to the sink. In addition, direct diffusion employs time synchronization technique to implement data aggregation, which may be difficult in sensor networks. Also, the overhead involved in recording information in data aggregation cannot be ignored.

3.1.2.2 Sensor Protocols for Information via Negotiation (SPIN)

SPIN is a family of protocols that disseminate all the information at each node to every node in the network [29], [40]. SPIN assumes that all nodes in the network are potential base stations; therefore, it enables a user to query any node and get the required information immediately. Every node uses meta-data which is high-level data descriptors to name their data and perform metadata negotiations before any data is transmitted. SPIN uses negotiations to eliminate the redundant data transmission throughout the network. SPIN is designed to address the deficiencies of classic flooding which are implosion, overlap, and resource blindness. This is achieved by using data negotiation and resource-adaptive algorithms. SPIN is a three-stage protocol as sensor nodes use three types of messages, ADV, REQ, and DATA. ADV is used to advertise new data, and DATA is the message. When a SPIN node obtained a new data, it broadcasts an ADV message containing meta-data. If the neighbor is interested in that data, it sends a REQ message, then the data is sent to that neighbor node. The neighbor sensor node will repeat this process with its neighbors (see Figure 6). Accordingly, the entire sensor area will receive a copy of data. This assures that there is no redundant data sent throughout the network. Even though SPIN is more energy efficient than flooding, it has shown some disadvantages as the following.

- SPIN's data advertisement mechanism cannot guarantee delivery of the data. Therefore,

it will not be useful in application of intrusion detection since this application requires reliably report over periodic intervals.

- In case of nodes interested in the data are located far away from the source node, and the nodes between source and destination nodes are not interested in that data. There is no way that the data will be delivered to the destination node.
- The nodes around the sink are still critical in SPIN since they could deplete quickly if the sink interested in too many events.

3.1.2.3 Energy Aware Routing (EAR)

The energy aware routing is a destination-initiated reactive protocol [41]. Even though this routing is similar to directed diffusion, the difference between them is that the energy aware routing maintains a set of paths instead of maintaining one optimal path. These paths are chosen by certain probability. The value of this probability depends on the energy consumption or cost of each path. Paths that have a very high cost are discarded and not be added to forwarding table. The protocol basically built up the routing table by initiating a connection to localized flooding, which is used to discover all routes between a source and destination pair and their costs. Then forwarding tables are used to send data to the destination with a probability inversely proportional to the node cost. Localized flooding is performed by the destination node to keep the path alive. By having path selected at different times, the energy of any single path will not deplete quickly. As energy dissipated more equally among all nodes, it can achieve longer network lifetime. As a result, energy aware routing protocol provides an overall improvement of 21.5 percent energy saving and a 44 percent increase in network lifetime comparing to directed diffusion [40]. However, it requires gathering location information to build up routing tables and setting up the addressing mechanism for the nodes, which is complicated.

3.1.2.4 Minimum Cost Forwarding Algorithm (MCFA)

The minimum cost forwarding algorithm (MCFA) takes advantages the fact that, in sensor networks, most data flows are in a single direction, i.e. from source to sink [30]. A sensor node will need neither a unique ID nor to maintain a routing table. Instead, each node maintains the least cost estimate from itself to the base station. To forward each message, sensor node

broadcast it to its neighbors. When a sensor node receives the message, it checks if it is on the least cost path between the source sensor node and the base station. If it is, that sensor node will rebroadcast the message to its neighbors. This will be repeated until it reaches the base station.

To create cost field, each node stores its cost to the sink. It starts from the sink broadcasts an ADV message containing its own cost to its neighbors. The initially cost is 0. Then, each node receiving the message sets a back-off timer that expires after a time proportional to the difference between its old cost and new cost to the sink. The new cost is sum of the cost of its immediate previous node and the cost consumed during the previous transmission. If the new cost is less than the old one, the node will change the timer to the new one when the timer expires, and rebroadcast the ADV message containing the new cost (see Figure 7). When a source has data to send to the sink, it simply broadcasts it. Nodes will rebroadcast the data only when they have the cost that matches the difference between the cost contained in the message and the consumed cost. This protocol provides us with the flexibility by allowing the cost to be measured in terms of energy or hops. Nonetheless, this approach has the following disadvantages.

- The number of sinks should be small so that nodes do not have to store large amount of cost information related to those sinks.
- With a large network size, the time to set the cost field will be large.
- Traffic load is not balanced. Nodes with lower cost to the sink will deplete energy soon.
- It will add more complexity to the algorithm if we consider delays, channel errors, and node failures.

3.1.2.5 Routing Protocols with Random Walks

The goal of random walks based routing technique is to achieve load balancing by making use of multi-path routing in wireless sensor networks [42]. It considers only large scale networks. Sensor nodes can be turned on or off at random times, however, once nodes are deployed, their mobility is very limited. No location information is needed since each node has a unique identifier. To find the route from source to sink, location information is obtained by computing distances between nodes using Bellman-Ford algorithm. For each intermediate node, it selects

one of its neighbors which are closer to the destination according to computed probability as next hop. Some kind of load balancing is assured if the probability is well computed. Although this protocol is simple as nodes are required to maintain little state information, it has a drawback which is the topology of the network may not be practical.

3.1.2.6 Rumor Routing

The motivation of Rumor routing is discovering the arbitrary paths instead of shortest paths from an event source to the sink [43]. It combined query flooding and event flooding protocols in a random way. The main idea is to route the queries to the nodes that have observed a particular event rather than flooding the entire network. In order to flood events through the network, the rumor routing algorithm employs packets called agents. A node will add event to its local table called an event table when it detects an event. Some assumptions are made as follows.

- The network is consisted of densely distributed nodes.
- Only short distance transmissions are allowed.
- Nodes are fixed (no mobility).

Each node maintains a list of neighbors and an event table with forwarding information for all the events it is aware of. When a node detects an event, it generates an agent and lets it travel on a random path. Then, the visited nodes form a gradient to the event. A node routes the query just as the source does, when it needs to initiate a query. The agent will aggregate event info stored in the nodes on the random path. The visited nodes will update their event information if better routes are found. Rumor routing is attractive only when the number of queries is larger than a threshold and the number of events is smaller than another threshold. For other situations, query flooding or event flooding could be more efficient.

3.1.2.7 Geographical and Energy-Aware Routing (GEAR)

GEAR employs the use of geographic information while disseminating queries to approximate regions since data queries often include geographic attributes [44]. It uses energy-aware and geographically informed neighbor selection to route a packet toward the destination region. The

main idea is to limit the number of interests in directed diffusion by only considering a certain region rather than sending them to the whole network. As a result, GEAR can conserve more energy than directed diffusion.

It follows the query-response model. This routing protocol assumes that each node knows its location, energy level, and its neighbors' locations and energy levels. There are two phases in the algorithm. In the first phase, upon receiving a packet, a node checks its neighbors to see if there is one neighbor that is closer to the target region than itself. If there is more than one, the nearest neighbor to the target region is chosen as the next hop. In the second phase, the packet can be diffused in the region by either recursive geographic forwarding or restricted flooding. Restricted flooding is useful low density sensor networks. On the other hand, in high density networks, recursive geographic forwarding is more energy efficient than restricted flooding. Since GEAR is a location-based routing, each sensor node will require localization hardware, such as GPS (Global Positioning System).

3.2 ENERGY BALANCING

Since the wireless sensor network is energy constrained network, the methods to distribute energy consumption through the network needs to be investigated. The main objective of the energy balancing methods is to avoid using the same route or path all the time in order to provide energy efficient and prolong the network lifetime. Also, this idea inspires in designing our proposed protocol, GSP. In wireless sensor networks, all traffics will be gathered at the sink. Nodes around the sink are often used to relay those traffics; therefore, they die quickly. By applying the energy balancing methods, the reduction of using those nodes can be achieved. This section provides the idea how the energy balancing methods can be employed in wireless sensor networks

3.2.1 Energy Balancing Strategy

This method is called Energy Balancing Strategy [32]. It assumes that every sensor nodes generate an equal amount of traffic that is relayed to the sink along the shortest path. The energy strategy can be restricted to one dimensional chain of nodes. In grid topologies, we can assume the simple scheme that has equal node distances d with equal link reception probabilities P_R , and utilizes closet neighbors routing, i.e., node j transmits to node $j + 1$ and so on.

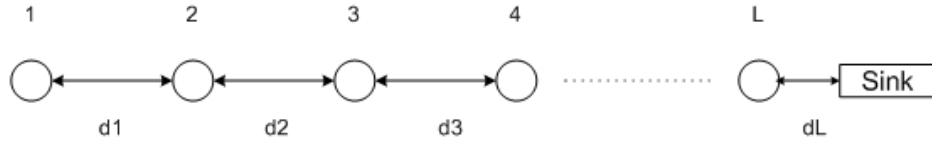


Figure 12: A one dimensional chain of sensor nodes.

In the simple strategy, the total energy consumption for one dimensional chain in Figure 12 is as the following.

$$\begin{aligned}
 E_{total} &= (1 + 2 + 3 + \dots + L) \frac{d^\alpha \Theta \sigma_Z^2}{-\ln P_R} \\
 &= \frac{L(L+1)}{2} \frac{d^\alpha \Theta \sigma_Z^2}{-\ln P_R}
 \end{aligned} \tag{3.6}$$

For the network lifetime, the critical node is the node closest to the sink in the chain which is node L.

$$E_{critical} = E_L = L \frac{d^\alpha \Theta \sigma_Z^2}{-\ln P_R} \tag{3.7}$$

Equation 3.7 can conclude that the closer the nodes to the sink, the sooner these nodes will be

dead. To prolong the network lifetime, we need to reduce the energy consumption or minimize the loads on the critical nodes around the sink area. Thus, one of the existing strategies that is used to spread out the load along the chain is discussed.

It is assumed that equal distance d between the nodes, but no longer restricts the network to strict nearest neighbor routing. Instead, the node x transmits the locally generated traffic to the next neighbor with probability a_x and directly to the sink with probability $b_x = 1 - a_x$. The goal of this strategy is to choose a_x to achieve energy balancing. All energies in the following derivation are normalized by $d^\alpha \Theta \sigma_z^2 / (-\ln P_R)$. The energy consumption at node x is

$$\begin{aligned} E_x &= (L - x + 1)^\alpha b_x + \sum_{y=1}^x a_y \\ &= x + ((L - x + 1)^\alpha - 1)b_x - \sum_{y=1}^{x-1} b_y \end{aligned} \quad (3.8)$$

As node L always transmits directly to the sink, $b_L = 0$.

$E_L = L - b_1 - b_2 - b_3 - \dots - b_{L-1} = a_1 + a_2 + a_3 + \dots + a_L$. Thus, $N-1$ unknowns can be determined by matrix solving.

By employing this energy balancing strategy, the simulation results show the 0.5% increasing in network lifetime for $\alpha = 5$ and 14% for $\alpha = 2$, which may not be a significant improvement. However, as some packets are routed to the sink in a single hop, the total energy consumption is higher than in the simple strategy. For $L = 10$, the additional energy consumption is between 60% in $\alpha = 2$ and 80% in $\alpha = 5$ [32]. By looking at the numbers, there is still a doubt about advantages on this strategy. For the huge number of nodes in the network, the total additional energy consumption will be very high and the gain in lifetime will be disappeared. In addition, the energy will be depleted very fast when the radio is turned on the whole time. Thus, the proposed Gossip-based Sleep Protocol (GSP), which is getting used of sleeping nodes around the sink area that tends to extend the network lifetime will be discussed in chapter 4.

3.2.2 Energy Balanced Routing

Another way to look at the energy balancing is to look at the routing setup schemes. Several routing setup schemes containing unique characteristics are proposed to achieve energy balancing by not using the same optimum routing path all the time. Since these schemes will distribute the energy consumption throughout the network, the longer network lifetime can be achieved. This section discusses two major energy balancing routing setup schemes. The first setup scheme is employed in most cluster-based routing protocols such as LEACH [12] and TEEN [34]. The other setup scheme for flat routing protocol is an energy balanced path setup scheme that used in Energy Aware Routing (EAR) [41].

In order to achieve energy balancing, the clustering-based protocols randomly rotate the local cluster base stations (cluster-heads) to evenly distribute the energy load among the sensors in the network [12]. The operation is broken up into rounds, where each round begins with a setup phase. In the setup phase, each node decides whether or not to become a cluster-head for the current round when clusters. The decision is based on the number of times the node has been a cluster head so far and the suggested percentage of cluster-heads for the network. This decision is made by the node n choosing a random number between 0 and 1. If the number is less than a threshold $T(n)$, the node becomes a cluster-head for the current round. The threshold is set as:

$$T(n) = \begin{cases} \frac{P}{1 - P * (r \bmod \frac{1}{P})} & \text{If } n \in G \\ 0 & \text{otherwise} \end{cases}$$

Where P is the desired percentage of cluster-heads (e.g., $P = 0.05$ or 5 %), r is the current round, and G is the set of nodes that have not been cluster heads in the last $1/P$ rounds. By using this threshold, each node will be a cluster head at some point within $1/P$ rounds. During round 0 ($r = 0$), each node has a probability P of becoming a cluster-head. The nodes that are cluster-heads in round 0 cannot be cluster-heads for the next $1/P$ rounds. Therefore, the probability that the remaining nodes will be cluster-heads in the next round is increased because there are fewer

nodes eligible to become cluster-heads. After $(1 - 1/P)$ rounds, T will be equal to 1 for any nodes that have not yet been cluster-heads, and after $1/P$ rounds, all nodes are once again eligible to become cluster-heads. Each node that has elected itself a cluster-head for the current round broadcasts an advertisement message to the rest of the nodes. The non-cluster-head nodes must keep their receivers on during this phase of setup to hear the advertisements of the cluster-head nodes. Note that each non-cluster-head node can receive more than one advertisement because there is more than one cluster in the network. After the cluster-head-setup phase is completed, each non-cluster-head node decides the cluster to which it will belong for this round, based on the received signal strength of the advertisements. After this period, each node will transmit a member status to its chosen cluster-head. During this phase, all cluster-heads must keep their receiver on. After the cluster-head receives all the messages from member nodes, it creates TDMA schedule based on number of member nodes. Then it broadcasts the schedule to its member nodes in the cluster. Once the clusters are created and the TDMA schedule is fixed, data transmission can begin.

The energy-efficient path setup scheme in Energy Aware Routing (EAR) for flat routing protocol uses a setup scheme that assigns a probability of path being chosen to achieve energy balancing [41]. None of the paths is used all the time, thus preventing energy depletion. EAR is a reactive routing and destination-initiated protocol where the destination/sink node initiates the route request and maintains the route subsequently. In path setup phase, the destination/sink node initiates the connection by flooding the network in the direction of the source node. It also sets the “Cost” field to zero before sending the request, i.e., $Cost(N_D) = 0$. Every intermediate node forwards the request only to the neighbors that are closer to the source node and farther away from the destination node. Therefore, at a node N_i , the request is sent only to a neighbor N_j that satisfies $d(N_i, N_S) \geq d(N_j, N_S)$ and $d(N_i, N_D) \leq d(N_j, N_D)$ where $d(N_i, N_j)$ is the distance between N_i and N_j . On receiving the request, the energy metric for the neighbor that sent the request is computed and is added to the total cost of the path. Thus, if the request is sent from N_i to node N_j , N_j calculates the cost of the path as the following

$$C_{N_j, N_i} = Cost(N_i) + Metric(N_j, N_i) \quad (3.9)$$

Only the neighbors N_i with the low cost paths are added to the forwarding table FT_j for N_j . The number of selected low cost paths will be based on the desired threshold, e.g., 5 paths. On the other hand, paths that have a very high cost are discarded and not added to the forwarding table. Then, node N_j assigns a probability to each of the neighbors N_i in the forwarding table FT_j , with the probability inversely proportional to the cost as shown below.

$$P_{N_j, N_i} = \frac{\frac{1}{C_{N_j, N_i}}}{\sum_{i \in FT_j} \frac{1}{C_{N_j, N_k}}} \quad (3.10)$$

Thus, each node N_j has a number of neighbors through which it can route packets to the destination. Then N_j calculates the average cost of reaching the destination using the neighbors in the forwarding table is shown as below.

$$Cost(N_j) = \sum P_{N_j, N_i} C_{N_j, N_i} \quad (3.11)$$

The average cost is set in the ‘‘Cost’’ fields of the request packet and forwarded along the source node. After this setup phase, a source node can send data packets to a sink node based on assigned probability of paths in forwarding table of each intermediate node. In this scheme, the energy balancing can be achieved by using probabilistic forwarding to send traffic on different routes providing a way to use multiple paths. However, the strategy does not consider the critical nodes around the sink. Even though the energy usage will be spread out around the network, the nodes around sink are still critical. In addition, there is no sleeping strategy applies to EAR, i.e., all nodes will turn their radios on the whole time. This provides energy inefficient that will shorten the network lifetime.

3.3 TOPOLOGY CONTROL

The deployment of a dense wireless sensor network is usually to ensure sufficient coverage of an area, which nodes failures will be protected by presenting redundancy in the network. A single node usually has many neighboring nodes, which can create loads for a MAC protocol. A direct communication can be made using a high transmission power. However, a high transmission power requires high energy consumption. To overcome these problems, topology control can be employed. Topology control considers the transmission power of the set of neighboring nodes. by introducing network hierarchies or turning off some nodes. The metrics to evaluate the quality of a topology-control algorithm include connectivity, graph metrics, throughput, robustness to mobility, algorithm overhead [45]. The connectivity metric tests whether the topology control breaks a connected graph G . There should be some path in T if there is a multihop path in G between two nodes a and b . A robust topology requires a few network adaptations caused by moving nodes and changing in radio channel characteristic. With a small memory and a highly energy constraint in a sensor, the number of additional messages and computational overhead imposed by the algorithm itself should be small to reduce energy consumptions by the management protocols.

To apply the topology controlling in flat networks, the networks control the set of neighbors, which is the basic approach of power control. Topology control changes the transmission range, which is assumed to be a unit disk, and a uniform distribution of nodes in a given area [46]. This model assumption is based on the theory of geometric random graphs, which is taken by [47] to determine an expression for the probability of a graph being k -connected. It is based on the transmission range r of the nodes and the node density ρ . The result in [48] shows that as soon as the transmission power becomes large enough to ensure the small degree in the graph is at least k , a graph with a large number of nodes is k connected. Also the result is used to develop a formula for the probability of the minimum node degree in a graph as the following.

$$P(G \text{ with } k - \text{connected}) \approx \left(1 - \sum_{l=0}^{k-1} \frac{(\rho \pi r^2)^l}{l!} e^{-\rho \pi r^2} \right) \quad (3.12)$$

The k connectivity algorithm shows that the probability that a network of n nodes is at least $k + 1$ connected when the transmission radius r satisfies $n\pi r^2 \geq \ln n + (2k - 1)\ln \ln n - 2\ln k + 2\alpha$ for $k > 0$ and n is sufficient large [49]. The results were formulated as constraints on the transmission radius, which constraints the minimum number of nodes to cover a given area. The second option is to control the number of neighbors, which focuses on the area that a node's transmission radius needs to cover, but not at the number of nodes. The expected number of a node's neighbors should increase logarithmically to create network connectivity, however there are no exact numbers defining the number of neighbors [50].

Applying topology control in cluster-based networks requires the study of the existing of the cluster-heads, clusters overlapping, and communication among clusters. Since the cluster-head assignment algorithms cannot guarantee that cluster-heads will be properly formed, there might be cases that cluster-heads will concentrate in one part of the network and not cover all of the areas. Also, when forming clusters, there may be two nodes that are adjacent to two cluster-heads. One alternative is to assign both nodes to both clusters resulting in overlapping clusters [51]. A node that is adjacent to two cluster-heads can assist in the communication between two clusters called a gateway, which used for inter-cluster communication [52]. The network can be either one-hop clusters or multi-hop clusters. After the cluster-heads are assigned by an algorithm, to ensure the connectivity requires that there are at most three hops away if a cluster-head connects to all other cluster-heads [53]. However, the load balancing between gateways needs to be considered as proposed in [54].

The rotation of cluster-heads can be considered as topology control. The previous section addressed the rotating cluster-heads algorithm proposed by LEACH, which ensures that every node is serving as a cluster-head once in some round. An example of weighted clustering algorithm of a node j , is expressed as the following [55].

$$W_j = w_1|d_j - \delta| + w_2 \left(\sum_{i \in N(j)} \text{distance}(j, i) \right) + w_3 S(j) + w_4 T(j) \quad (3.13)$$

Where w_a is nonnegative weighting factors, and $N(j)$ are the neighbors of j at the maximum

power. $S(j)$ is the average speed of node j , and $T(j)$ is the cluster-head serving time since system starts. The weight clustering algorithm rotates the cluster-heads to allow sharing of loads among nodes in the network.

One way to apply the topology control is to turn off nodes on the basis of sensing coverage. The protocol assumes that nodes know their positions and sensing ranges [56]. Also, the protocol assumes that nodes are deployed redundantly requiring that nodes exchange information with their neighbors about the sensing coverage. A node eligible for sleeping will send a message to neighbors and go to sleep. The use of topology control can improve network operations such as the network lifetime, however, it is usually difficult to determine the optimal topology, and approximations are used instead.

3.4 SUMMARY

Two classes of routing were reviewed to provide a context for the Gossip-based Sleep Protocol (GSP). Wireless sensor networks can be classified as either cluster-based or flat. Cluster-based routing schemes divide the network into clusters and utilize a sleep mode to save energy and prolong the network lifetime. Flat routing schemes try to achieve energy efficiency in an indirect way by reducing the routing overhead and sometime tradeoff for other performance, such as low delay and high throughput. In cluster-based routing protocols such as LEACH [12], TEEN [34], and APTEEN [35], nodes organize into groups with one node from each group selected to be a cluster-head. A cluster-head receives data packets from its members, aggregates them and transmits to a data sink. In some cluster-based routing protocols, a cluster-head assigns TDMA slots to its members to schedule the communication and the sleep mode. Based on the number of nodes, the cluster-head creates a TDMA schedule. Nodes send data during their allocated transmission time and are in sleep mode otherwise. Although energy is conserved by a very efficient sleep/wake cycle, extra overhead is created for synchronization, which in turn consumes energy. Low-Energy Adaptive Clustering Hierarchy (LEACH) [12] is designed for proactive networks, in which the nodes periodically switch on their sensors and transmitters, sense the

environment and transmit the data. Nodes communicate with their cluster-heads directly and the task of cluster-heads is rotated among the various sensors in order to preserve the battery of a single sensor. Conversely, Threshold sensitive Energy Efficient sensor Network protocol (TEEN) [34] is designed for reactive networks, where the nodes react immediately to changes in the environment. Nodes sense the environment continuously, but send the data to cluster-heads only when a predefined threshold is reached. The Adaptive Periodic Threshold sensitive Energy Efficient sensor Network protocol (APTEEN) protocol [35] combines the features of the above two protocols by modifying TEEN so that it also transmits data periodically. The cluster-based routing protocols can arrange the sleep mode of each node to conserve energy so that only the nodes with data to send are awake. However, this incurs overhead for cluster organization and node synchronization.

Flat routing schemes, typically implement either flooding, forwarding or data-centric based routing. In flooding, every node repeats the data once by broadcasting. Flooding does not require costly topology maintenance and complex route discovery algorithms. But it has several deficiencies [19]:

- Implosion: duplicated messages are sent to the same node. A node with multiple neighbors may receive multiple copies of the same message.
- Overlap: if two sensors share the same observation region, both of them may sense the same stimuli at the same time. As a result, neighbor nodes receive duplicated messages.
- Resource blindness: flooding does not take into account the available resources, e.g. the remaining energy stored in the sensor node.

To overcome the problems of flooding, forwarding schemes utilize local information to forward messages. However, unlike the traditional routing protocols, forwarding schemes do not maintain end-to-end routes. Instead, intermediate nodes maintain neighbor information only. In a gossiping type protocol, a node only forwards data to one randomly chosen neighbor and does not maintain any routing information [57]. Best Effort Geographical Routing Protocol (BEGHR) [58] employs position information to forward data, and therefore requires GPS or other positioning service. Field based Optimal Forwarding employs cost field to forward data [30]. A

cost field is the minimum cost from a node to the sink on the optimal path. To establish the cost field, sink broadcasts the ADV (advertisement) message. The sink node is the destination of all of the data in the network. Some other routing protocols are based on data-centric approach. In data-centric based routing, an interest message is disseminated to assign the sensing tasks to the sensor nodes and data aggregation is used to solve the implosion and overlap problems [19]. There are two types of data-centric based routing based on either the sink broadcasts the attribute for data, e.g. Directed Diffusion [39], or the sensor nodes broadcast an advertisement for the available data and wait for a request, e.g. Sensor Protocols for Information via Negotiation (SPIN) [29], [40]. The flat protocols try to reduce the routing overhead as much as possible. *However, they have no explicit sleep mechanisms and require all the nodes in the network to be awake (i.e. in receive or idle mode), which consumes a significant amount of energy.*

In short, the chapter summarized the existing routing protocols used by wireless sensor networks. In cluster routing, the overhead associated in forming clusters in each round may reduce the gain in energy efficiency. Moreover, the setup phases (advertisement, cluster setup, and schedule creation) are complex. Additionally, the elected cluster-heads may be concentrated in parts of the network where they are not needed. In flat routing, protocols turn on their sensor radios to listen or receive data then make a decision whether or not to relay it. To conserve energy, sensor nodes should consider not listening or receiving the data when not necessary by turning off the radio. Energy balancing protocols extend network lifetime by not using the optimal path all the time. Thus, in the next chapter, we employ a cross layer scheme to target at the network layer issues. We proposed a simple and energy efficient scheme called *Gossip-based Sleep Protocol* (GSP).

4.0 PRELIMINARY RESEARCH

A wireless sensor network consists of a large number of densely deployed sensor nodes [19]. Due to the large area and limited transmission range of individual nodes, routing protocols are necessary for end-to-end transmission. Although many proposed routing protocols support wireless ad hoc networks [44], [59], they are not necessarily appropriate for sensor networks. Chapter 1 mentioned that wireless sensor networks normally have larger size, higher density, more limited power supply and computational capacity than nodes in mobile ad hoc networks. Additionally, sensor networks are usually assumed to be data centric networks, where users are interested in querying an attribute of the phenomenon, rather than querying an individual node [19]. Furthermore, as the requirements on the network may change with the network applications. As an example, some sensor network applications employ only fixed nodes, but other applications use a combination of fixed and mobile nodes such as mobile monitoring in the battle field, thus requiring mobility support. Also, adjacent nodes might have similar data; therefore, sensor networks should be able to aggregate similar data to reduce unnecessary transmissions and save energy [12], [29], [34], [35], [39], [40]. Lastly, assigning unique IDs may not be suitable in sensor networks because of the data centric characteristic – there may be no routing to and from a specific node. In addition, the large numbers of nodes require long IDs, creating large overhead costs, compared to the data being transmitted.

4.1 GOALS AND CONTRIBUTIONS

The *Gossip-based Sleep Protocol* (GSP) [9] was developed to test the hypothesis that energy efficiency can be improved by coupling a sensor's sleep mode, i.e. completely shut down the radio [60] and the routing protocol. The design was driven by the following four goals:

- Energy efficiency: Since a sensor network is an energy constraint network, the efficient use of energy is required.
- Simplicity: sensors have limited computing capability and memory resources. Minimized operation and information maintenance are required.
- Scalability: unlike conventional ad hoc networks, a sensor network could be composed of a great number of nodes.
- Connectivity: network connectivity can keep the path setup and transmission delay low. We try to improve those routing protocols that are delay-sensitive but not energy efficient.

GSP employs probabilistic based sleep modes – essentially, tossing a coin to decide whether or not a node should sleep for the next period. Using a particular value of gossip sleep probability (p) and under certain topology density constraints, the network remains connected. The use of sleep mode is the major mechanism by which a protocol can reduce the total energy consumption of the network and thus prolong the network lifetime [61]. The remainder of this chapter is organized as the following. Section 4.2 presents the Gossip-based Sleep Protocol (GSP) proposed and developed by Hou, Yupho and Kabara. Section 4.3 presents the preliminary analysis, simulation, and analytical results, which have been previously published. Section 4.4 discusses GSP when employing in wireless ad-hoc network. Section 4.5 summarizes this chapter.

4.2 GOSSIP-BASED SLEEP PROTOCOL (GSP)

4.2.1 Gossip-based Ad Hoc Routing and Percolation Theory

In ad hoc networks, gossiping protocols were proposed to reduce the flooding overhead [62]. Almost all ad hoc routing protocols use some kind of flooding scheme to send routing messages. With flooding, every node must forward the message once, but this is not necessary since a node with more than one neighbor receives multiple copies of that message. Gossiping reduces this by requiring some of the nodes to discard the message instead of forwarding it. A node decides whether or not to forward the message with probability p , the gossip probability. Given a sufficiently large network and a gossip probability p greater than certain threshold, almost all the nodes in the network will receive the message [62]. As an example, in a 20×50 grid topology, a value of $p = 0.72$ with the first 4 hops from the source node forwarding the message with probability 1 allows almost all the nodes to receive the message in almost all the executions of the simulation. This reduces the number of messages transmitted by about 28%.

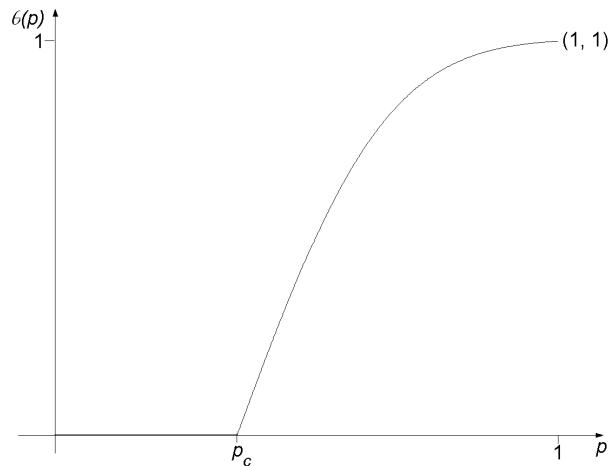


Figure 13: Sketch of percolation probability.

GSP implements concepts from percolation theory [63], [64]. In an infinite network, if every link or node is available with probability p , the network will be grouped into clusters. We are interested in the size and the shape of the clusters as p varies from 0 to 1. Percolation theory hypothesizes that there exists a critical value $p_c > 0$ such that in the *subcritical phase* (when $p < p_c$), nodes form finite clusters and in the *supercritical phase* (when $p > p_c$), a single infinite cluster will form. The probability that a given node belongs to an infinite cluster $\theta(p)$ is termed *percolation probability*, is shown in Figure 13 [64]. The fraction of nodes belonging to this infinite cluster determines the quality of the connectivity. To date, there is unfortunately no explicit expression of this fraction, nor of p_c . However, a part of our work on developing GSP, we have developed a method to obtain approximations through simulation.

4.2.2 Gossip-based Sleep Protocol (GSP)

As discussed in section 3.1.2, flat routing protocols such as directed diffusion [39], SPIN [29], [40], energy aware routing (EAR) [41], and minimum cost forwarding algorithm (MCFA) [30] require all sensors to be awake and listening for messages from neighboring nodes, thus consuming energy with no data being exchanged as shown in section 4.3. GSP tested the hypothesis that the energy consumption will reduce by placing some nodes into a sleep mode for a specified period of time. The observation is that, in the supercritical phase, not all nodes are necessary to maintain network connectivity. From the view of gossip-based ad hoc routing, if gossiping can make all the nodes receive a message, then the nodes forwarding the message are connected at least by the paths the message passes through. Therefore, with a probability p' , if gossiping protocols can make almost all nodes in the network receiving the message. Therefore, if each sensor in the network enters a sleep state with probability $p = (1 - p')$, almost all the nodes remaining awake remain connected [62]. Thus, it can be safely put a percentage (p) of the nodes in sleep mode without losing network connectivity. The p is termed as *gossip sleep probability*. Since the sleep nodes are randomly distributed throughout the network, it is assumed that this will not affect the data collection. The assumption is justified when the awake nodes provide sufficient coverage, or when the application can tolerate an additional delay. GSP is described as follows.

- At the beginning of a period, each node chooses either going to sleep with probability p or staying awake with probability $(1 - p)$ for this period
- All sleeping nodes wake up at the end of each period
- All nodes repeat the above process for every period

Fairness requires that the length of the period in GSP must be much smaller than the lifetime of the nodes in the network to prevent the condition where some nodes die in each subsequent period. Although GSP requires synchronization, the requirement is not strict and it is not necessary to maintain a synchronized clock in every node. The nodes can be synchronized by a control message at the beginning of every n^{th} period. The nodes can also wake up just prior to the end of each period to wait for the control message and the network performance will not be affected by the extra awake nodes, which are doing nothing but waiting during that short time.

Unlike other protocols using sleep mode (e.g., cluster-based schemes, LEACH, TEEN, APTEEN, SPAN and GAF), GSP is extremely simple and requires almost no information, even from immediate neighbors. The gossip sleep probability (p) is purely dependent on the network density and can be configured before the deployment of the network. GSP improves upon the energy consumption of schemes such as SPAN and GAF by not requiring nodes to transmit and receive additional network maintenance traffic. However, by allowing nodes to enter sleep state in a fully random fashion, we expect some improvement on network lifetime because traffic forwarding continuously via the same path is avoided. Therefore, GSP is more suitable to the large low-cost wireless sensor network, which seeks lower complexity to reduce the cost of every node as much as possible.

The major objective of GSP is to achieve energy efficiency by making some nodes go to sleep mode. However, the data may go through longer paths if the sleep nodes are on the optimal paths of other nodes to the sink. This requires additional forwarding time for each message and results in more energy consumption in the network-wide data transmission. Thus, it is concerned if the energy saved in sleeping by GSP is larger than the extra energy consumed by non-optimal paths. The evaluation in the next sections focuses on this problem.

4.3 PRELIMINARY ANALYSIS OF GSP

In the following analysis, only grid topologies with a single sink node are considered. One assumption is made that all calculations are based on the period of time to transmit one bit of data, i.e. *bit-time*. Transmissions are actually a frame which will be discussed in section 4.3.6. Analysis assumes the traffic load remains constant with or without GSP, i.e. the number of bits generated by the sensors in a bit time are the same. Although the actual application may generate bursty traffic, this assumption will not change in results in that the extra energy consumption GSP incurred is based on the amount of the traffic, not the fashion of the traffic.

4.3.1 Radio Model

Table 5: The classic radio model.

Radio mode	Energy Consumption
Transmitter Electronics ($E_{Tx-elec}$) Receiver Electronics ($E_{Rx-elec}$) ($E_{Tx-elec} = E_{Rx-elec} = E_{elec}$)	$50nJ / bit$
Transmit Amplifier (\mathcal{E}_{amp})	$100pJ / bit / m^2$
Idle (E_{idle})	$40nJ / bit$
Sleep	0

In this preliminary analysis, we employ the radio model in [12] and follow their notation in the simulations. Since this model includes the transmit amplifier, which analyzes the energy consumption including the transmission radius (m^2), this model is preferred on this preliminary analysis. However, chapter 7 time-based analysis will use more appropriate energy consumption model introduced in [65]. In Table 5, the radio dissipates $E_{elec} = 50 nJ/bit$ to run the transmitter or receiver circuitry and $\mathcal{E}_{amp} = 100 pJ/bit/m^2$ for the transmit amplifier to achieve an acceptable

signal to noise ratio (SNR). As in [12], it assumes a r^2 path loss model to describe the energy loss due to channel transmission. Although many other radio models and path loss models exist, it is expected that they will not change the analytic results but only the amount of final energy conserved or workable scenarios (e.g. traffic load, network size). Additionally, an idle receiver consumes $E_{idle} = 40 \text{ nJ}$ in the period of transmitting or receiving a bit. The difference between this value and the energy consumption in receive mode is relative large compared to the values for existing sensors [58] and creates a conservative estimate for the performance of GSP. For simplicity, it is assumed a sleep node does not dissipate any energy. As the protocol developed, this assumption will be addressed. The above radio characteristics are summarized in Table 5, and each node is 10 meters apart from one another.

4.3.2 GSP Theoretical Performance

In the remainder of this section and the next section, how much the energy can be saved by employing GSP in the sensor network is examined. By randomly applying sleep mode to some nodes, GSP may not be able to establish the optimal path between two nodes if some of the nodes on the path are in sleep. To achieve energy efficiency, GSP must conserve more energy by employing sleep mode than is consumed by the longer average path length incurred. Let L_{GSP} and L_{min} to represent the average path length in hops with and without GSP respectively. The average total energy consumption during a bit-time without GSP can be calculated by equation 4.1. Analysis assumes every traffic source transmits as fast as possible to keep all the intermediate nodes busy. This assumption will hurt GSP since more traffic consumes more extra energy due to the longer paths. The first term of equation 4.1 is the transmission energy consumed by all the nodes in the network that have traffic to send. The second term is the energy consumed by the rest of the nodes. Although some of them are in receive mode, for simplicity, analysis assumes all of them are in idle mode. This assumption makes us underestimate the energy consumed by the protocols without GSP, thus underestimate the performance improvement of GSP.

$$E_{non-GSP} = (E_{elec} + d^2 \times \epsilon_{amp}) \times B \times L_{min} + E_{idle} \times (N - (B \times L_{min})) \quad (4.1)$$

Where, B is the traffic load, i.e. the number of bits generated during a bit time in the entire network. d is the distance between nodes, which is 10 meters. N is the number of sensor nodes in the network. Similarly, the average total energy consumption during a bit time with GSP can be calculated by equation 4.2. The difference is the second term, since the total number of the idle nodes is reduced.

$$E_{GSP} = (E_{elec} + d^2 \times \varepsilon_{amp}) \times B \times L_{GSP} + E_{idle} \times (N \times (1 - p) - (B \times L_{GSP})) \quad (4.2)$$

If E_{diff} defines as the difference between $E_{non-GSP}$ and E_{GSP} , it is expressed as equation 4.3. If E_{diff} can be greater than zero then GSP can reduce the energy consumption of the network.

$$\begin{aligned} E_{diff} &= E_{non-GSP} - E_{GSP} \\ &= E_{idle} \times N \times p - (E_{elec} + d^2 \times \varepsilon_{amp} - E_{idle}) \times B \times (L_{GSP} - L_{min}) \end{aligned} \quad (4.3)$$

(α) is defined as the ratio of average extra path length with GSP, i.e.

$$\alpha = (L_{GSP} - L_{min}) / L_{min} \quad (4.4)$$

Thus, equation 4.3 can be expressed as the following.

$$E_{diff} = E_{idle} \times N \times p - (E_{elec} + d^2 \times \varepsilon_{amp} - E_{idle}) \times B \times L_{min} \times \alpha \quad (4.5)$$

The first term of equation 4.5 is the energy saved by GSP due to the sleep mode, and the second term is the extra energy consumed by GSP due to the longer average path. $B \times L_{min}$ is the total bits in the network at any given time and $B \times L_{min} \times \alpha$ is the extra number of bits in the network since data must travel through a longer path. In equation 4.5, more energy can be saved when a network has larger number of nodes and higher gossip sleep probability. However, high sleep probability could lead to a partitioned network. According to [62], p is dependent on different network scenarios. Also, the extra energy consumption increases when the network has higher traffic load and longer average path. The results of gossiping protocol in [62] is utilized to obtain

the gossip sleep probability p . The sensor node number N and the traffic load B depend on the specific network scenario and the application. L_{min} and α are also dependent on the sensor network scenario, but simulation can be used to obtain them for a grid topology, as used in [62] to get gossip probability. Since L_{min} is fixed for a given network, it is required to study α with respect to various topologies and values of p .

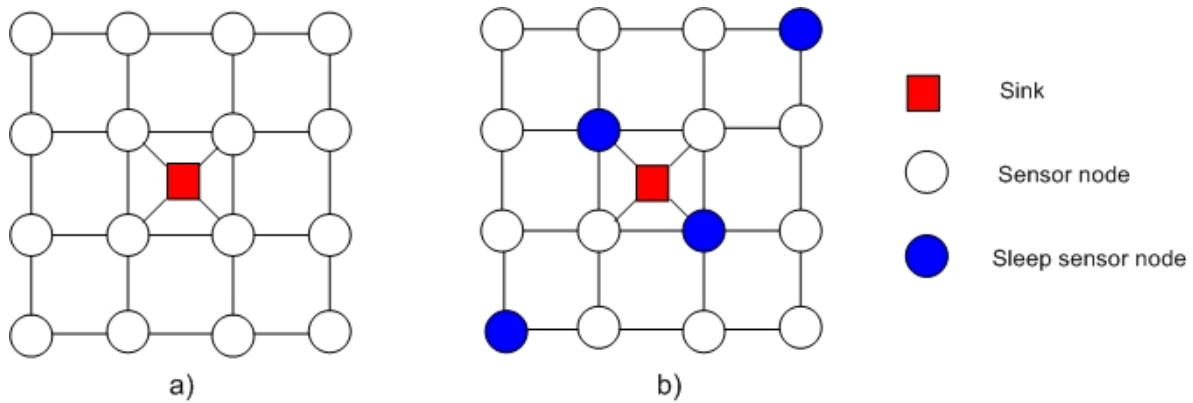


Figure 14: a) Central area of the grid topology used by the simulation. b) An example of GSP network with $N = 16$, and $p = 0.25$.

4.3.3 Simulation Model

The Java programming is utilized to study the effects of the various grid topologies by employing GSP. To study the change of average path length for different network size, five grid topologies with a single sink node in the center are used, 10x10, 15x15, 20x20, 25x25, and 30x30. There are total of 101, 226, 401, 626, and 901 nodes respectively, i.e. 100, 225, 400, 625, and 900 sensors and a sink. Figure 14 shows the central area of the topologies and an example of GSP network. Analysis assumes that the sink is not power limited. In the simulation, all nodes are awake with Non-GSP and $(1 - p)$ % of nodes are awake with GSP. Then, the length of the shortest path in hops from every sensor node to the sink is determined. Figure 15 presents the flowcharts to determine the average path length (L) and number of disconnected nodes. The gossip sleep probability in the simulation is 0.3, i.e. $p = 0.3$, approximately the highest value resulting in a connected network (see Figure 16 and 17). The simulation results are the average

of 50 runs with a 95% confidence interval.

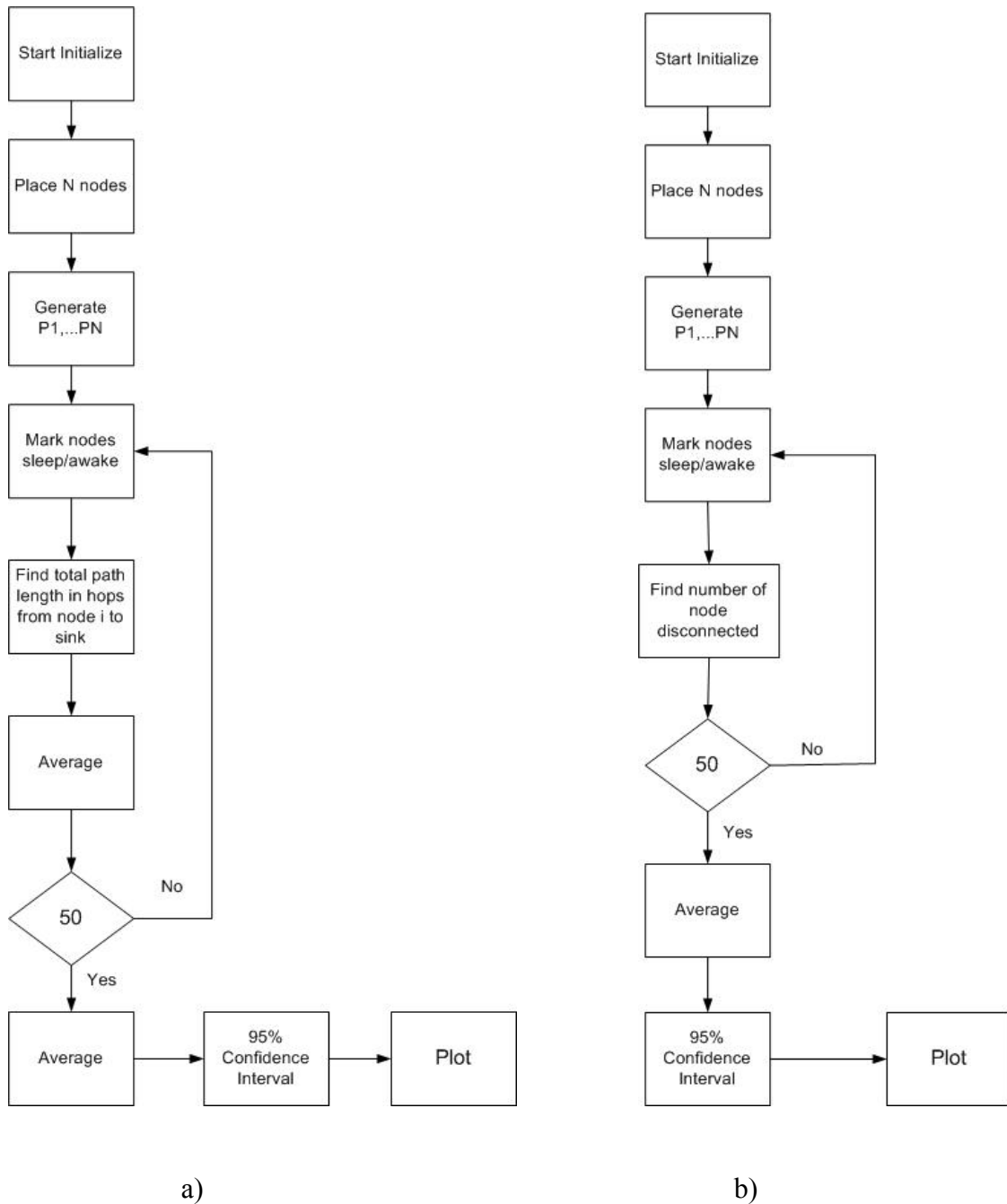


Figure 15: Flowcharts to determine a) average path length (L_{GSP}) and b) average number of disconnected nodes.

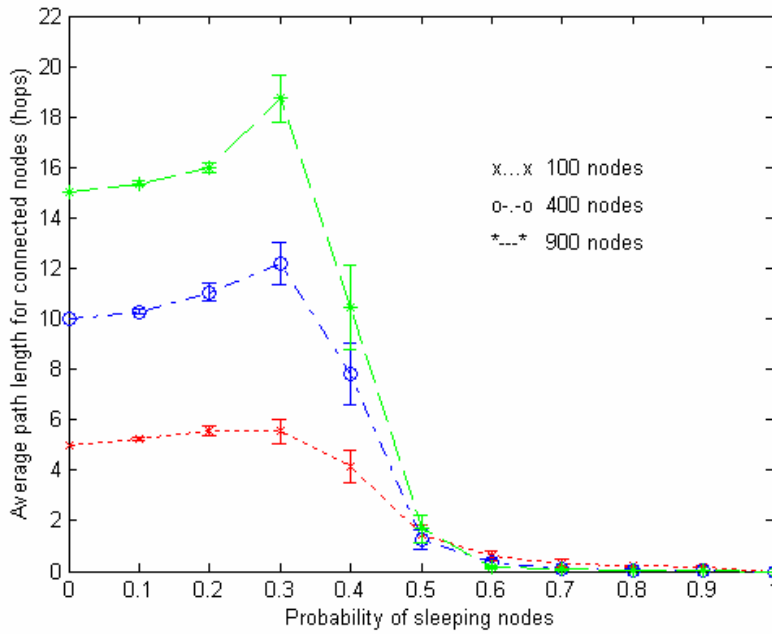


Figure 16: Probability of sleeping nodes vs. average path length (L_{GSP}) for connected nodes with 95% c.i.

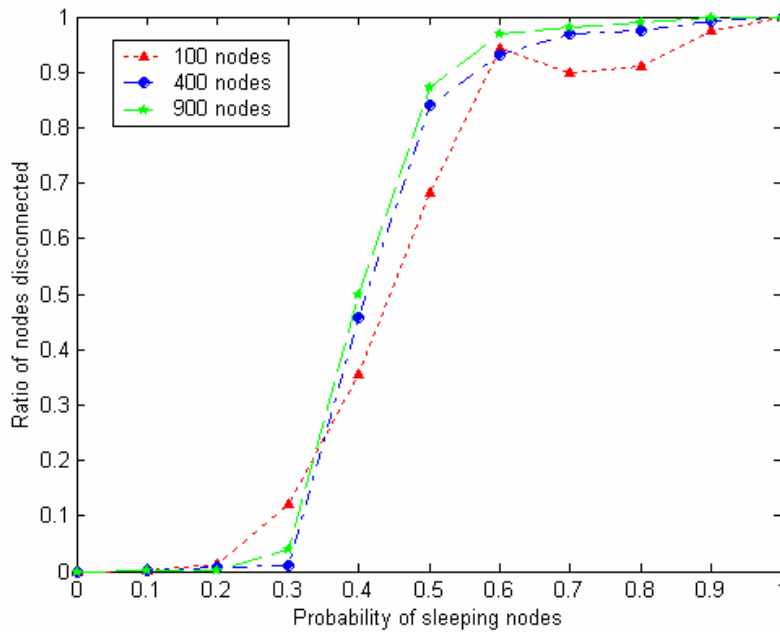


Figure 17: Probability of sleeping nodes vs. ratio of nodes disconnected from the sink.

4.3.4 Simulation Results

Figure 18 presents the simulation results. As expected from the discussion above, the average path length with GSP becomes longer than without GSP. For example, without GSP, the average path length is 5 for the 10x10 grid topology. With GSP, the value of this variable is 5.546, with a 95% confidence interval (5.0776, 6.0144). The result shows that the average path length increases by around 11%, i.e. $\alpha = (5.546 - 5)/5 = 0.1092$. Figure 18 shows that α does not vary over the tested topologies.

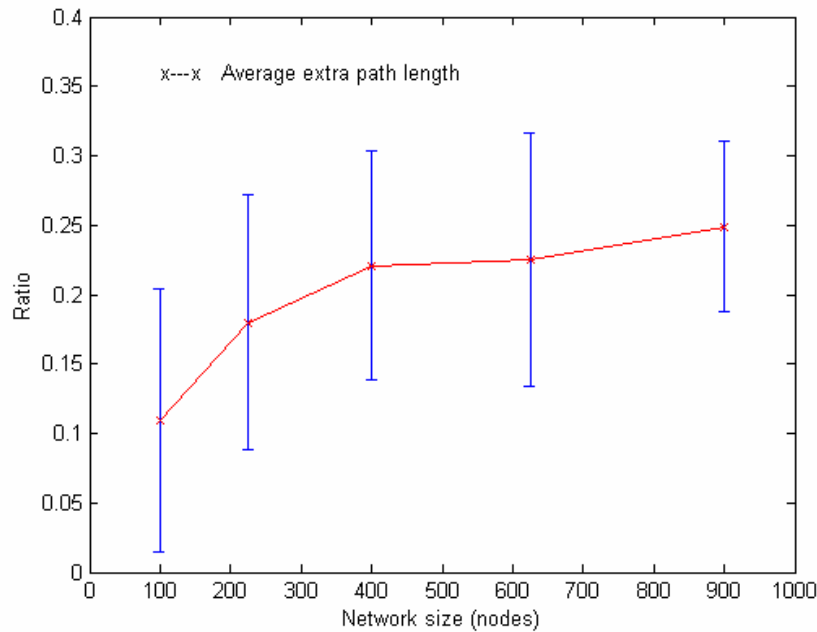


Figure 18: Network size vs. ratio of average extra path length (α) when $p = 0.3$, with a 95% c.i.

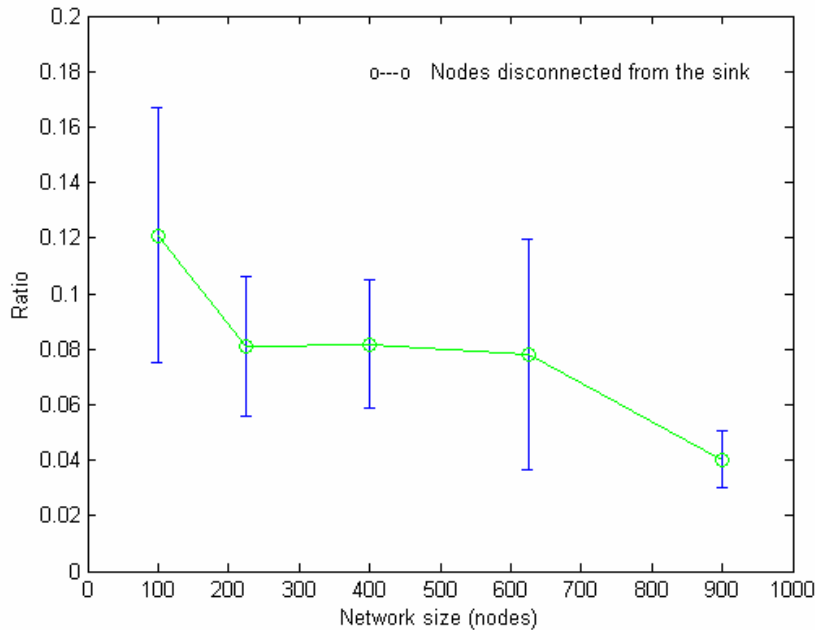


Figure 19: Network size vs. ratio of nodes disconnected from the sink when $p = 0.3$ with a 95% c.i.

In addition to simulation results, in Figure 19, GSP determines the number of disconnected nodes. For example, in the 10x10 grid topology there are 8.48 sensors on average are separated from the sink with a 95% confidence interval (5.261, 11.698). The average ratio is $8.48/70 = 0.121$. As the network grows larger, the ratio of the disconnected nodes decreases.

4.3.5 Continued Theoretical Analysis

Using the simulation results from Figure 18 in equation 4.5, GSP possibly saves the energy. Figure 20 shows the value of E_{diff} for the 10x10 grid topology (solid line) with respect to the traffic load B . With around 30% of nodes in sleep the feasible highest traffic being transmitted in the entire network during a bit time is only about 70 bits, which is equal to the number of awake nodes, so the feasible B is below.

$$B \leq 70 / L_{GSP} = 70 / (L_{min} \times (1 + \alpha)) = 12.62$$

At this point and in the area smaller than it, E_{diff} is positive. Although the area of $12.62 \leq B \leq 100 / L_{min} = 20$ is feasible to non-GSP protocols, it is not feasible to GSP. In other words, GSP should employ a smaller p when the traffic is this high. Only the worst case is considered. If analysis assumes the perfect MAC layer protocol and a node can not transmit and receive data at the same time, the feasible highest traffic load for the above two cases is only about 6.3 bits and more energy can be saved. Figure 21 shows the situations in which GSP can be employed. It is a plot of network size N respected to traffic load B when the gossip sleep probability is 0.3. The solid curve is obtained by making equation 4.5 equal to zero and assuming the ratio of average extra path length (α) is always 0.315 for different network size, which is the worst case in our simulation as shown in Figure 18. The area above this curve represents the positive energy difference (E_{diff}) that leads to energy savings when using GSP. The dotted and dash-dot curves represent the feasible highest traffic load without and with GSP respectively, i.e. N / L_{min} and $N / (L_{min} \times (1 + \alpha))$. When $\alpha = 0.02$ is used, which is the lower bound from Figure 18 and makes the two curves even lower. The areas above these two curves are feasible.

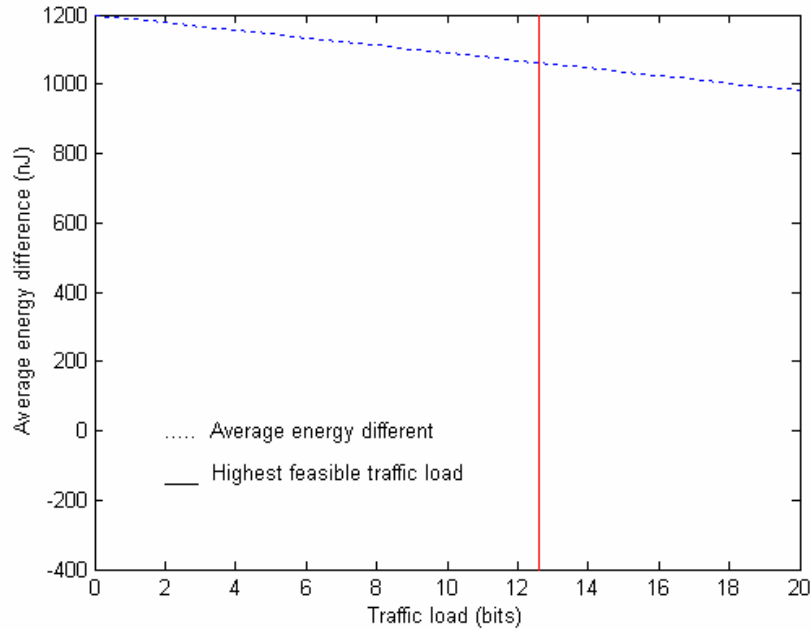


Figure 20: Energy difference (E_{diff}) between $E_{GSP-saved}$ and $E_{GSP-extra}$ vs. traffic load (B) in bits when $p = 0.3$, $N = 100$, $L_{min} = 5$ and $\alpha = 0.1092$.

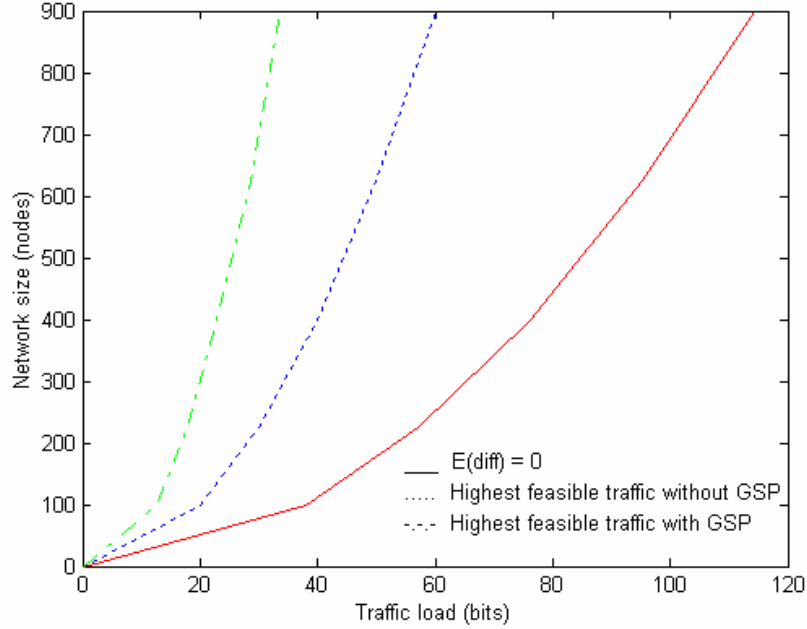


Figure 21: Network size N (nodes) vs. traffic load B (bits) when $p = 0.3$, $\alpha = 0.315$ and $E_{diff} = 0$.

4.3.6 Analysis at Frame Level

The above analysis is based on the level of bit time. In practice, data is transmitted in frames. In this subsection, analysis is extended to frames and defines the time to transmit a frame *frame-time*. At the frame level, equation 4.1, 4.2 and 4.5 are transformed as the following.

$$E'_{non-GSP} = (E_{elec} + d^2 \times \epsilon_{amp}) \times F \times L_{min} \times S + E_{idle} \times (N - F \times L_{min}) \times S \quad (4.6)$$

Where, F is the traffic load in frames, i.e. the number of frames generated during a frame time in the entire network. S is the average number of bits in a frame.

$$E'_{GSP} = (E_{elec} + d^2 \times \epsilon_{amp}) \times F \times L_{GSP} \times S + E_{idle} \times (N \times (1-p) - F \times L_{GSP}) \times S \quad (4.7)$$

and,

$$\begin{aligned}
E'_{diff} &= E'_{non-GSP} - E'_{GSP} \\
&= \left[E_{idle} \times N \times p - (E_{elec} + d^2 \times \varepsilon_{amp} - E_{idle}) \times F \times L_{min} \times \alpha \right] \times S
\end{aligned} \tag{4.8}$$

From equation 4.8, E'_{diff} is similar to E_{diff} since S is a constant. In one frame time, the number of frames being transmitted in the entire network (F) cannot be larger than the number of nodes, which is same as traffic load B at the bit level. Thus, Figures 20 and 21 also apply to E'_{diff} except the traffic load is F in term of frames.

4.4 GSP FOR WIRELESS AD HOC NETWORKS

The *Gossip-based Sleep Protocol* (GSP) was originally proposed by Hou, Yupho, and Kabara [9]. Continued research by Hou and Tipper used GSP for the energy efficient routing in wireless ad-hoc networks [66]. GSP was proposed in two versions for wireless ad-hoc network, one for synchronous networks (GSP1) and one for asynchronous networks (GSP2) [66]. In a synchronous network, it is assumed that the network is synchronized, i.e., every node decides its own mode for the next period at the same time. Although the synchronization is required, the requirement is not strict in case of low mobility (e.g., sensor networks) and it may not be necessary to maintain a synchronized clock in every node. In asynchronous network, every node independently chooses a uniformly distributed random time interval called the gossip interval. After the time expires, the node will choose another random interval immediately.

Table 6: Energy consumption model for Lucent IEEE 802.11 WaveLAN PC CARD with 2 Mbps.

Radio mode	Energy consumption (W)
Transmit	1.327
Receive	0.967
Idle	0.844
Sleep	0.066

The simulation utilized the radio model, which is similar to Lucent's WaveLAN with 2Mb/sec nominal bit rate and 250 meters radio range [67]. The energy consumption model is summarized in Table 6, which is the model of Lucent IEEE 802.11 WaveLAN PC Card.

GSP was employed as a topology management in which random sleeping nodes were used to control the paths among source and destination nodes. Since GSP requires no information from the routing algorithms and can be integrated with a number of routing protocols as a topology management. The research selected Dynamic Source Routing (DSR) to be integrated with GSP called GSP+DSR [66]. Since nodes frequently move in ad-hoc network, the simulation used the 20 m/s as a maximum speed of the nodes and each packet carries 532 bytes.

The research in [66] focused on the wireless ad-hoc network by using GSP as a topology management that integrates GSP to DSR. The energy consumption model was from the Lucent IEEE 802.11 WaveLAN, which has large bandwidth at 2 Mb/s. The network parameters concentrated on networks that assume high mobility as in ad-hoc networks. Also, the packet size is 532 bytes, which may not suitable in a sensor network that requires small information, e.g., reporting changes in room temperature. In addition, the research tested GSP in 50 – 100 node network, which is appropriate for ad-hoc network [66]. However, sensor networks usually deploy the large number of nodes, i.e., a hundreds to thousands.

The next chapter discusses GSP performance as both topology management and routing protocol. GSP a new energy consumption model is proposed based on the TinyOS Mica2 mote in Crossbow application, which also requires smaller packet size (21 bytes) and lower data rate (19.2 kbps) [65]. Chapter 6 analyzes the network lifetime when increasing transmission power/radius. To carefully evaluate GSP performance, chapter 7 studies the sensor network lifetime in which GSP performs on five different physical topologies.

4.5 SUMMARY

In this chapter, GSP was proposed as a novel sleep management approach, for wireless sensor networks. GSP reduces energy consumption in large low-cost wireless sensor networks by reducing complexity. GSP achieves simplicity by adding a timer to each sensor. When the timer expires, each sensor decides whether to sleep in the next period with the gossip sleep probability p . Nodes that choose to sleep will not receive or forward message to neighbors. The property of gossiping makes it scalable to very large networks. Network connectivity is a consequence of the gossip sleep probability p . Simulation results show that certain values of p result in connectivity between almost all the awake nodes in the network. Also, by allowing sleeping nodes, the results show that network can achieve the energy efficiency. Next chapters will carry GSP concepts and preliminary analyses with the replaced energy consumption model to perform on various network topologies. Next chapter will evaluate GSP network lifetime performance in which the rectangular grid topology will be introduced. Then chapter 6 will show that an increasing in transmission power/radius will extend network lifetime. Chapter 7 will utilize time-based simulation to test GSP on five physical topologies.

5.0 INTEGRATING ROUTING AND TOPOLOGY MANAGEMENT

GSP can be characterized either as a topology management or as a routing protocol. When GSP runs on top of routing protocols, it is considered a topology management protocol. Section 5.1 uses the concept of the Minimum Cost Forward scheme to test GSP performance on square grids. However, GSP can perform as a routing protocol itself by managing topology and using flooding, packets are constrained to a particular route. Since a wireless sensor network is energy constrained network, one of the most important constraints in designing protocols is network lifetime. Therefore, this chapter analyzes the GSP performance focusing on system lifetime [68]. When networks employ GSP, the sleeping nodes will not participate in any activities, and save energy by not transmitting or receiving the packets. Thus, this chapter shows how network lifetime can be extended by reducing overhearing of transmissions and receptions in the network.

5.1 SQUARE GRIDS

5.1.1 Simulation Model to Determine Gossip Sleep Probability (p)

In chapter 4, simulation was developed to determine the highest sleep probability, called gossip sleep probability (p) that results in almost all awake nodes receiving a message. To study the change of average path length for different network sizes, networks employ three square grid topologies with a single sink node in the center, 10x10, 20x20, and 30x30. In these experiments the sink has an unlimited energy source. The simulation compared the cases where network has all awake nodes in non-GSP, i.e., ($p = 0$) and $(1 - p)$ % awake nodes in GSP. Then, simulation determined the length of the shortest path in hops from every sensor node to the sink. Figure 15

represents the flowcharts to determine the average path length in hops and average number of awake nodes that will not receive the message called disconnected nodes. The dropping of the curves in average path length (Figure 16) and increasing of average number of disconnected nodes after $p = 0.3$ (Figure 17) demonstrate the sign of the losing network connectivity. The simulation recommends 0.3 gossip sleep probability, i.e. $p = 0.3$, as approximately the highest value resulting in a connected network. To verify this statement, Figures 16 and 17 represent the results, which are the average of 50 runs with a 95% confidence interval. In the next subsection, the simulations use this probability in the network lifetime analysis.

5.1.2 Simulation Model to Determine Network Lifetime

Network Lifetime is usually assumed to be the most critical network constraint because sensor networks have limited energy stores. In some applications, any sensor node may be responsible for performing critical functions. One dead node may create a loss of required system information. Thus, in this research, the simulation defines network lifetime when the first node has completely depleted its energy. To determine network lifetime, the simulation model utilizes C++ with multithreading method. Simulation restricted each node to transmit once in each gossip period (G_p). Network lifetime analysis determines the gossip period (G_p) and energy remaining in the network, and a high average number of gossip periods indicates longer network lifetime. Simulation parameters such as *average number of gossip periods* and *Average Remaining Energy (ARE)* in network were 50 simulation runs. Each run stopped the simulation when it found the first completely depleted node. ARE represents the energy efficiency in the way that network can continuously use the energy remaining when the network is able to reconfigure itself, or the network considers the lifetime as the multiple depleted nodes or network partitions. In square grids analysis, the simulation used the gossip sleep probability (p) that maintains network connectivity, which is 0.3 to test the GSP performance.

Table 7: Energy consumption model.

<i>Transmit</i>	4.28 μ Joules / bit
<i>Receive</i>	2.36 μ Joules / bit
<i>Sleep</i>	~ 0 Joules
<i>Initial energy stored</i>	10 Joules

Table 7 summarizes the TinyOS Mica2 mote’s measured energy consumption model for transmitting and receiving [15]. The frame size is 21 bytes and the data rate is 19.2 kbps. A node can initially store 1 joule [52] or up to 5000 Joules of energy as in [15]. However, in these studies, the analysis used 10 Joules as a convenient initial energy stored on each node. Although there are various communication schemes among source nodes and sink nodes, in this analysis, GSP performed operated using two schemes: *Known path (KP)* and *Unknown path (UKP) schemes*. In *Known path (KP) scheme*, the simulation employed minimum cost forwarding concept [30]. At the beginning of each period, $p\%$ of nodes sleep, and the simulation does not include them in the network topology. A sink broadcasts a message to setup the paths. The path setup process consumes energy at the beginning of each gossip period (G_p). To find the shortest paths, simulation employed Dijkstra’s algorithm. The simulation assumes no route maintenance mechanism performing in KP scheme. A KP scheme is useful when network has low mobility and GSP has very long gossip periods. In this case, GSP operates only to manage topology. Figures 22 and 23 present the flowchart of the simulation and packet processing algorithm in the KP scheme.

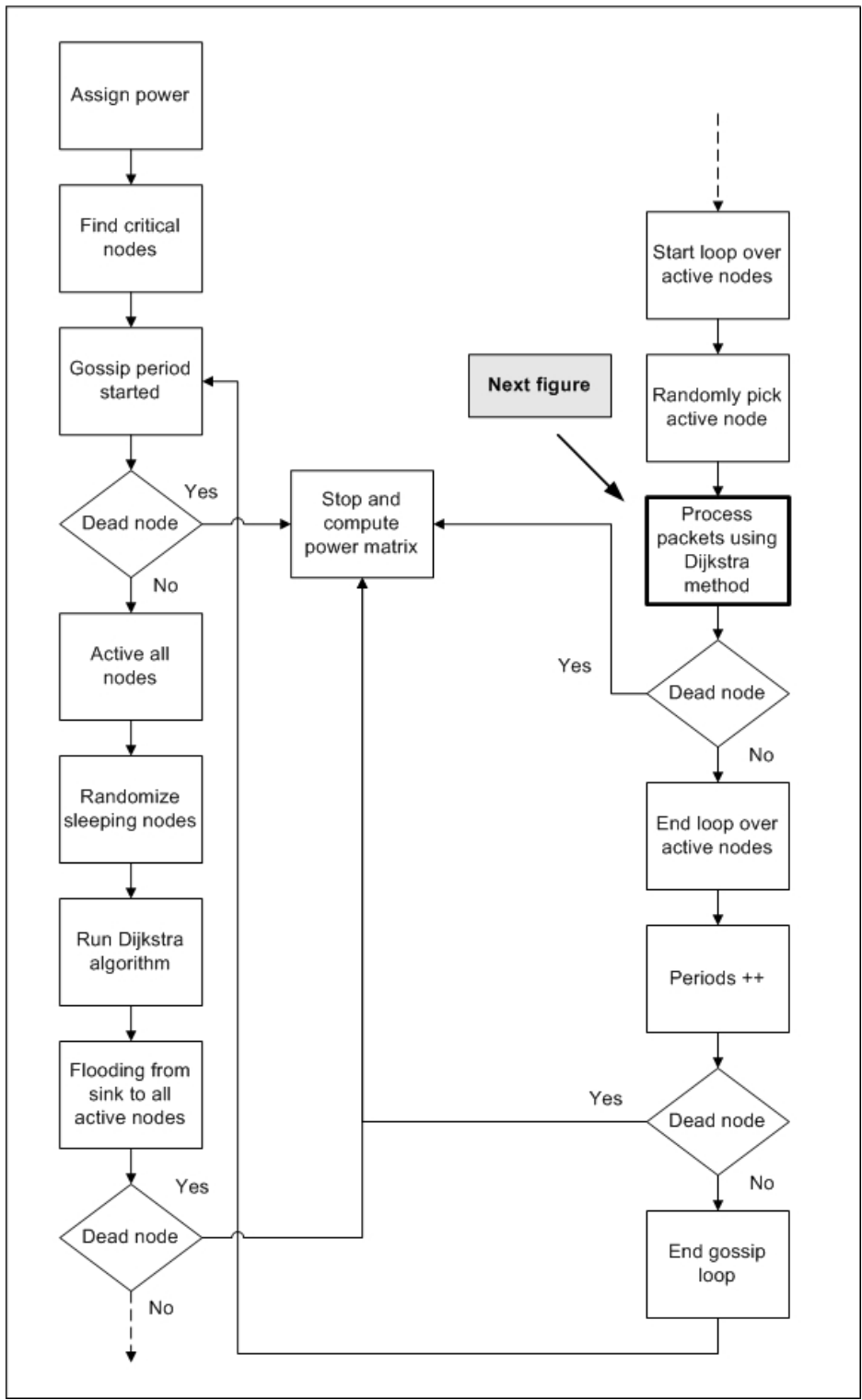


Figure 22: A flowchart of the Known Path (KP) scheme simulation.

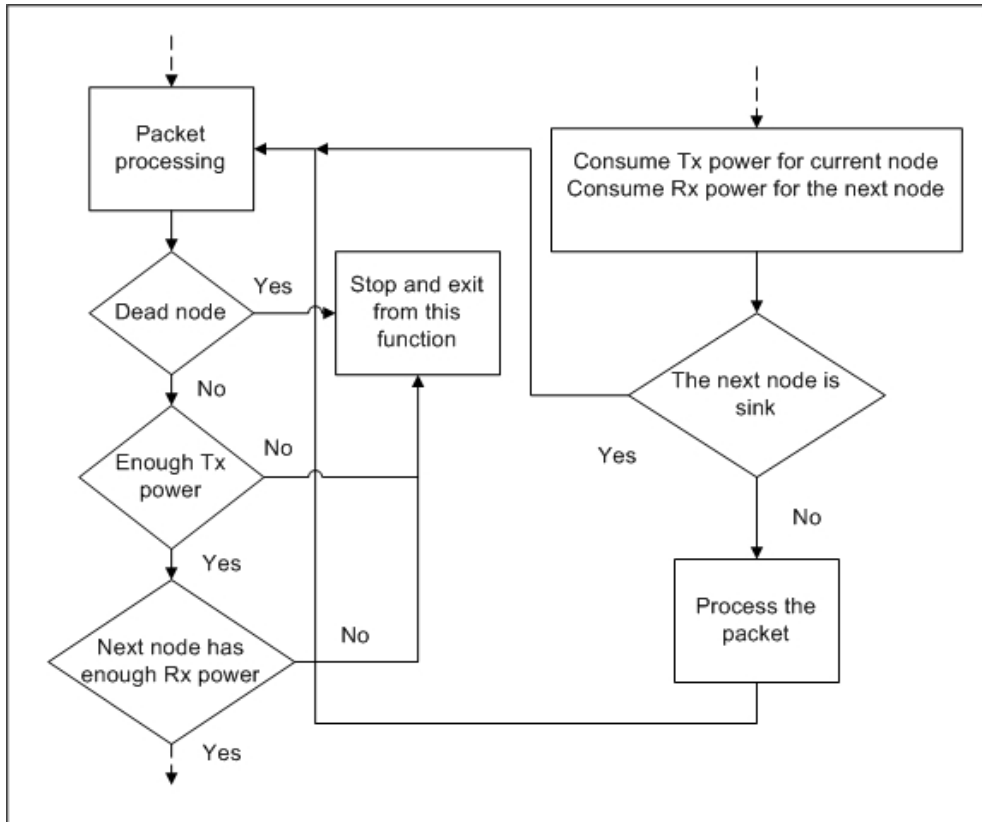


Figure 23: A flowchart of packet processing algorithm in the Known Path (KP) scheme.

An *Unknown path (UKP) scheme* may reflect a more typical use for GSP. In the UKP case, the network contains multiple sinks or sinks that enter and leave the network. In this case, managing topology manages routing as an emergent effect. By managing topology and using flooding, packets are constrained to a particular route. Nodes transmit the packets in broadcast fashion to neighbors within their transmission ranges without the knowledge of the neighbor nodes' locations. Then the awake/active neighbors or intermediate nodes will relay these packets to the sink. The process stops when the timer expires to form a new topology at the beginning of each gossip period (G_p). Sleeping nodes in each period do not participate in any activities. The simulation restricted nodes to relay the individual packet only once. When a duplicate packet arrives, it will receive that packet and discard it. An UKP scheme may be useful when the physical topology is changing quickly, or multiple sinks are part of the network. Figures 24 and 25 represent flowcharts of GSP simulation and flooding algorithm in the UKP scheme.

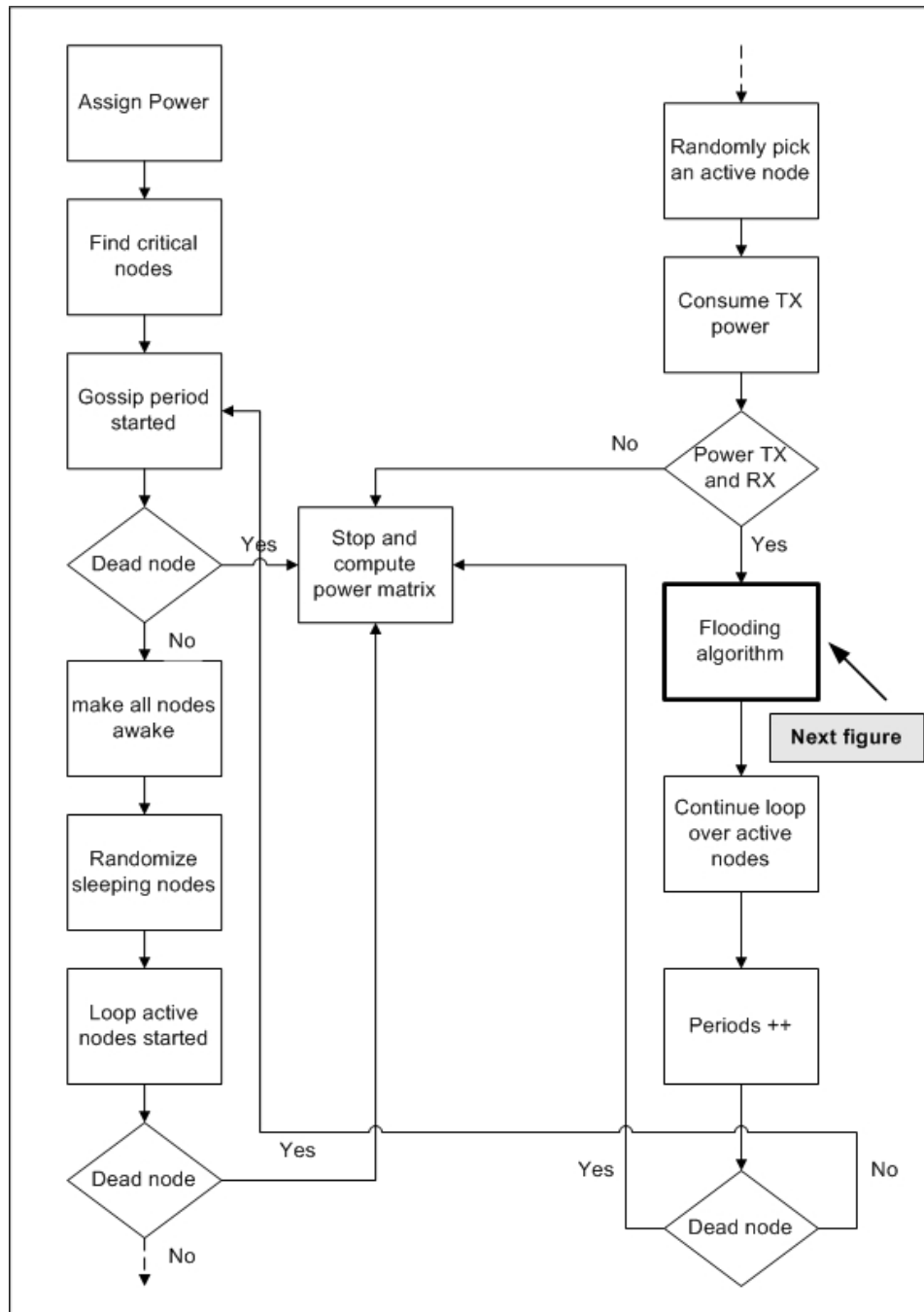


Figure 24: A flowchart of GSP/Flooding simulation in the Unknown Path (UKP) scheme.

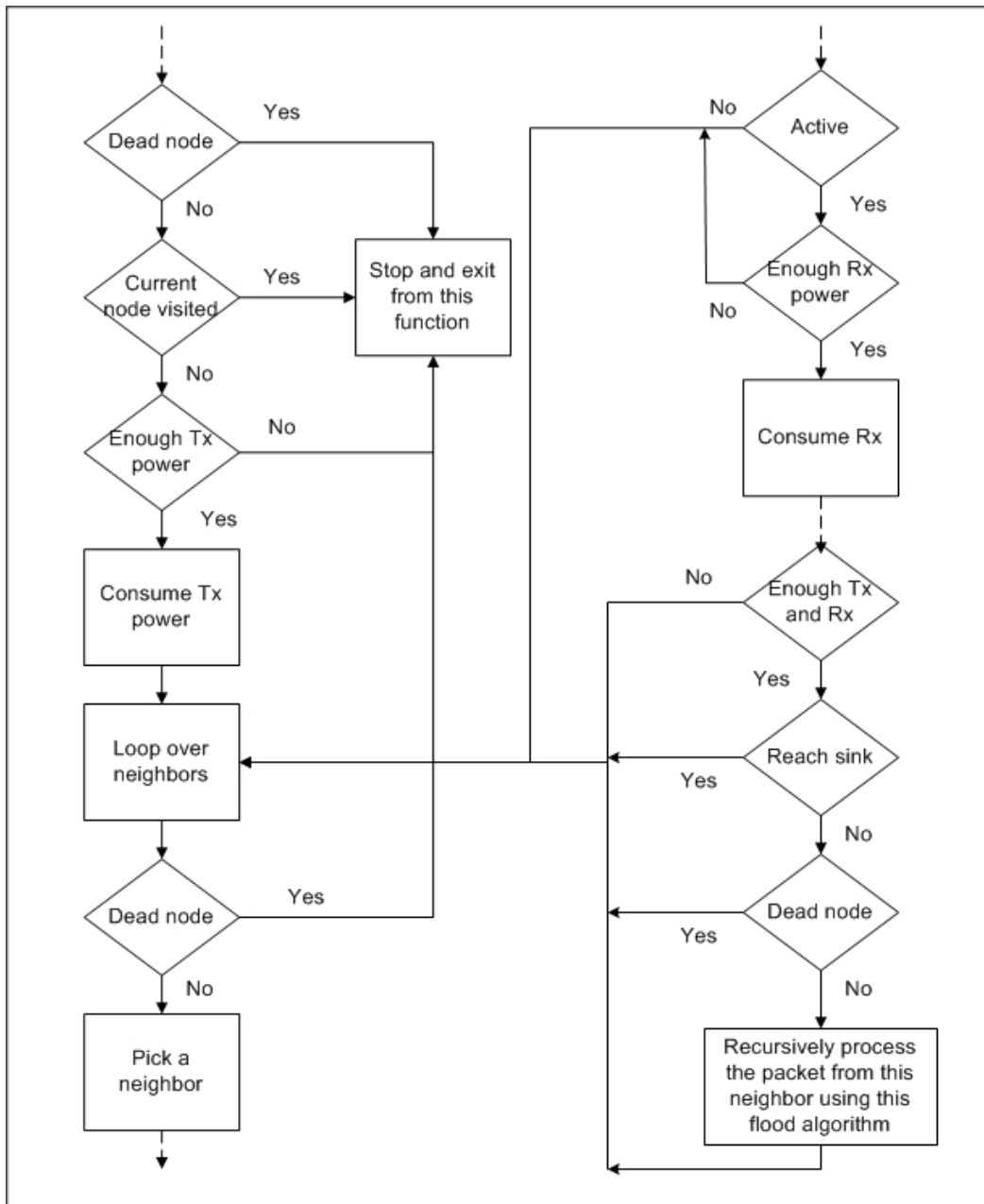


Figure 25: A flowchart of GSP/Flooding algorithm in the Unknown Path (UKP) scheme.

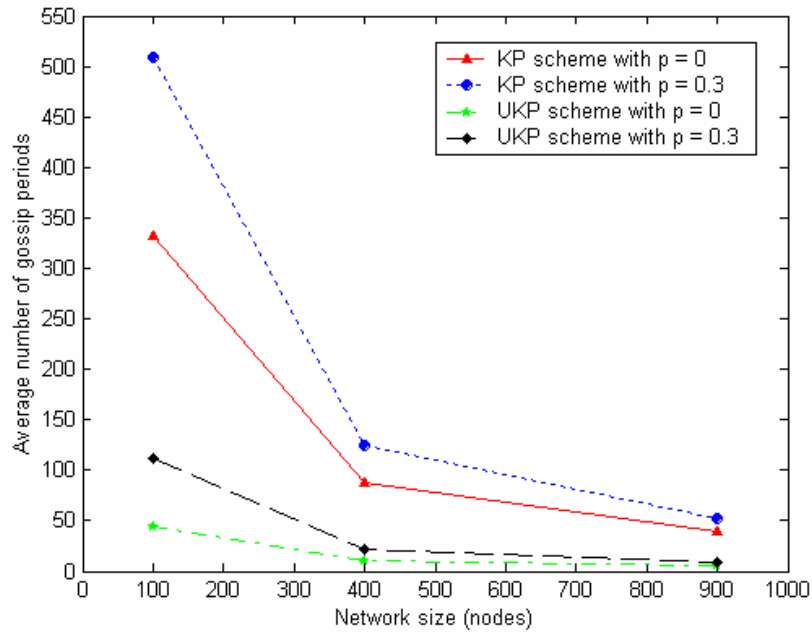


Figure 26: Average number of gossip periods (G_p) until network termination vs. Network size.

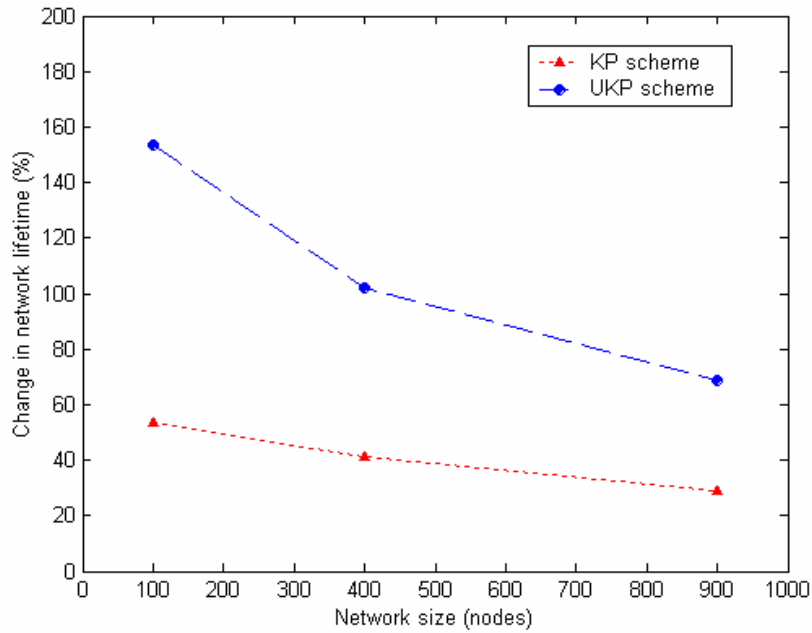


Figure 27: Change in network lifetime for both Known and Unknown path schemes when using GSP with $p = 0.3$ compared to $p = 0$ (non-GSP).

Figure 26 represents the average number of gossip periods (G_p) for different network sizes. Figure 27 shows the increase in network lifetime for both Known and Unknown path schemes when using GSP with gossip sleep probability $p = 0.3$ comparing to non-GSP ($p = 0$). By reducing the number of overhearing receptions and transmissions, simulation results show that GSP extends the network lifetime by 53, 41, and 30 percent in the KP scheme, and 150, 100, and 70 percent in UKP scheme, which performed on 100, 400, and 900 node networks respectively. However, when the network grows larger, the increasing percentage of improvement in network lifetime decreases.

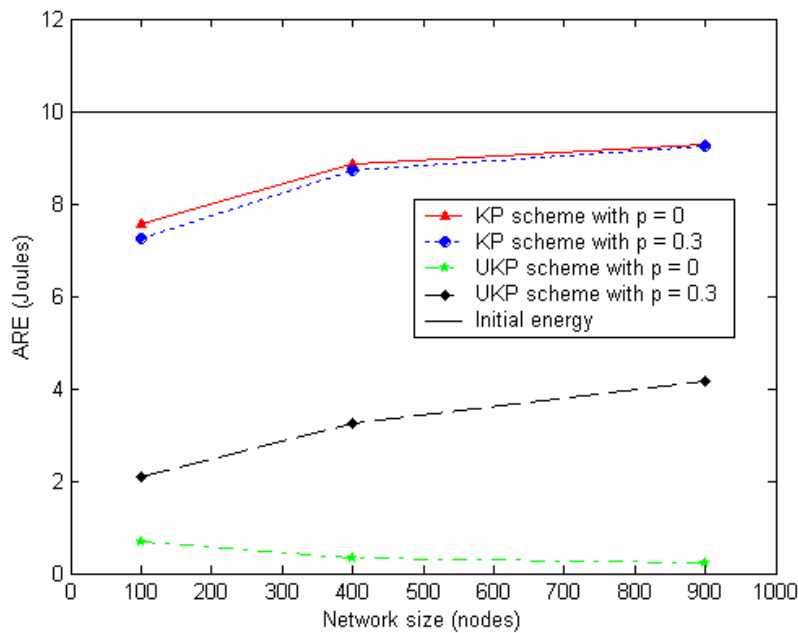


Figure 28: Average remaining energy (ARE) vs. network size.

Figure 28 illustrates the *Average Remaining Energy* (ARE) per node in the network after the simulation found the first completely depleted node at each run for the average of 50 runs. The UKP scheme consumes more energy than the KP scheme since it does not employ additional routing. As a result, UKP scheme has less ARE in the network. By comparing GSP to non-GSP, it shows little changes occurs between the KP schemes. On the other hand, because sleeping nodes reduced the overhearing of transmissions and receptions, UKP scheme using GSP with 0.3 gossip sleep probability shows a great amount of ARE comparing to non-GSP.

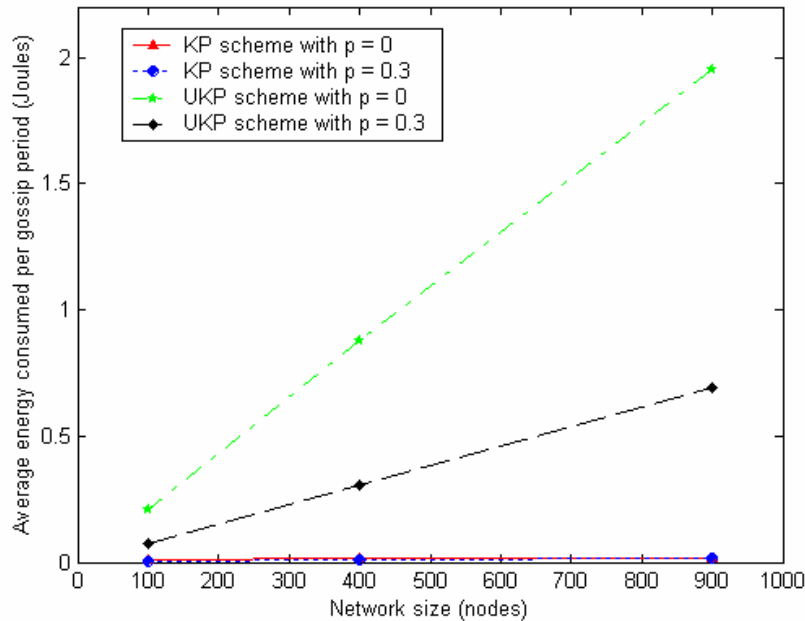


Figure 29: Average energy consumed per gossip period vs. network size.

Figure 29 shows the average energy consumed per gossip period. The largest energy consumption occurs for the UKP scheme in Non-GSP network. When networks increase in size, the average energy consumed per gossip period increases.

Figures 30 and 31 present the ARE for the KP scheme in 100 node square grid network with 0 and 0.3 sleep probabilities respectively. X and Y distances represent the coordinated nodes' locations on grid topology. By placing a sink at the center of the grid, the energy usage increases toward the sink or center of the grid. However, by using GSP with $p = 0.3$, the shape of the plot is more symmetric (see Figure 30) because the sleeping nodes were randomly distributed. The symmetry indicates the balance energy usage through the network. Thus, GSP with $p = 0.3$ provides longer network lifetime as shown in Figure 26.

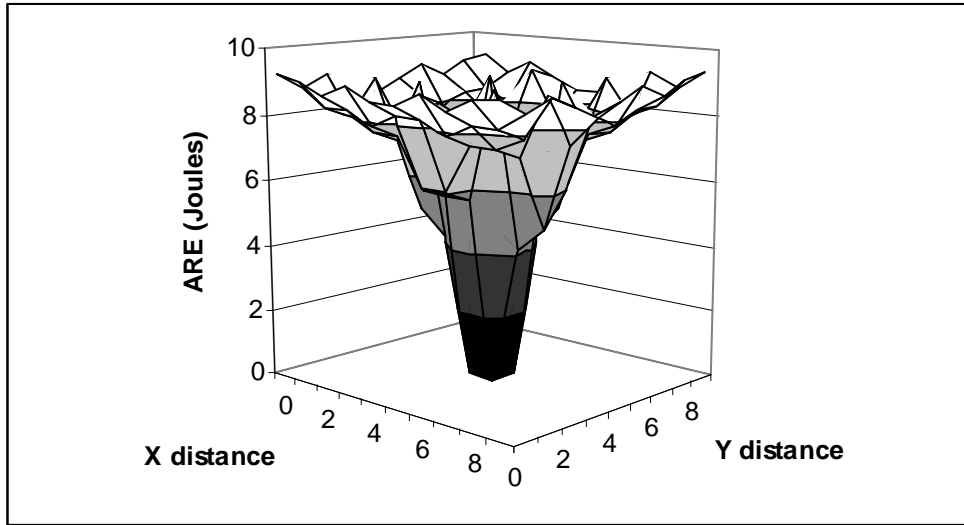


Figure 30: ARE for the Known path scheme in 100 nodes square grid network with $p = 0$.

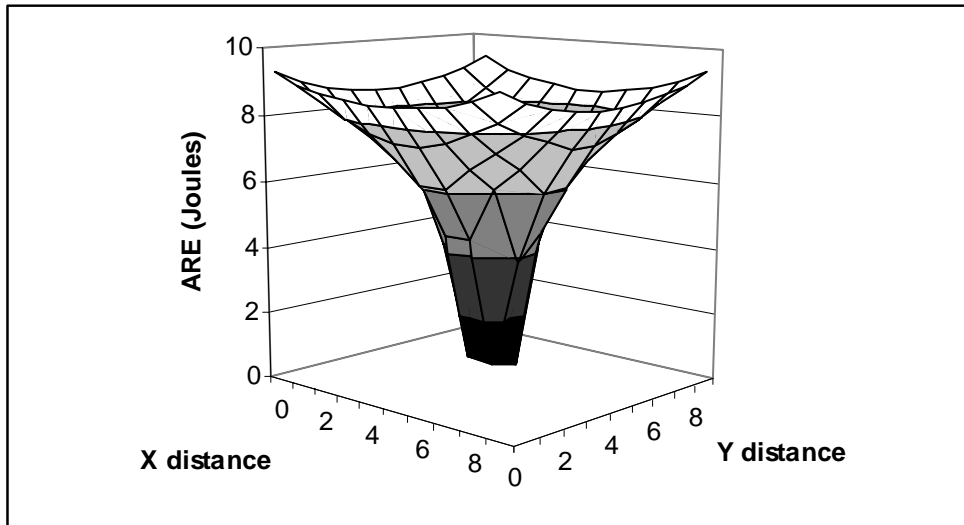


Figure 31: ARE for the Known path scheme in 100 nodes square grid network with $p = 0.3$.

Figures 32 and 33 show surface plots on ARE for KP scheme in 900 node square grid network with 0 and 0.3 sleep probabilities respectively. These two plots represent energy consumption in a large network, which sends increased traffic toward the sink because each node sends the same amount of traffic and now there are more nodes.

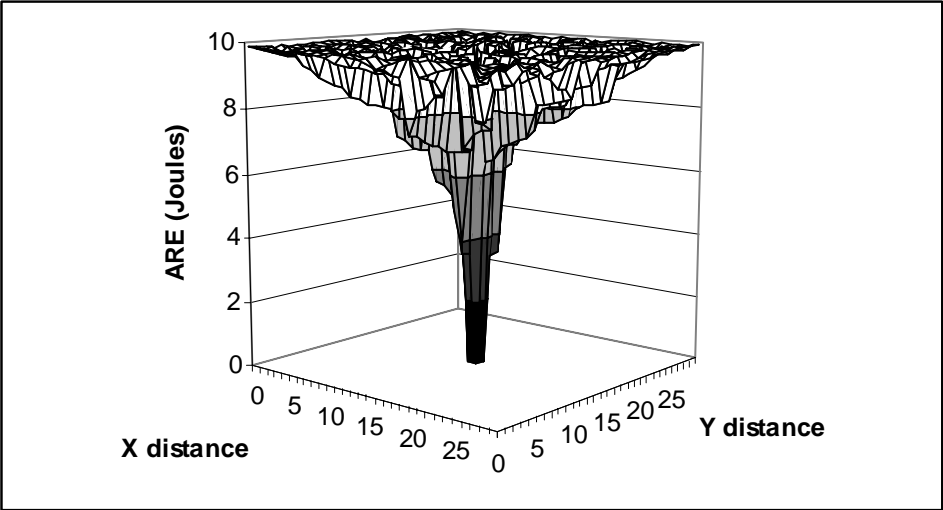


Figure 32: ARE for the Known path scheme in 900 nodes square grid network with $p = 0$.

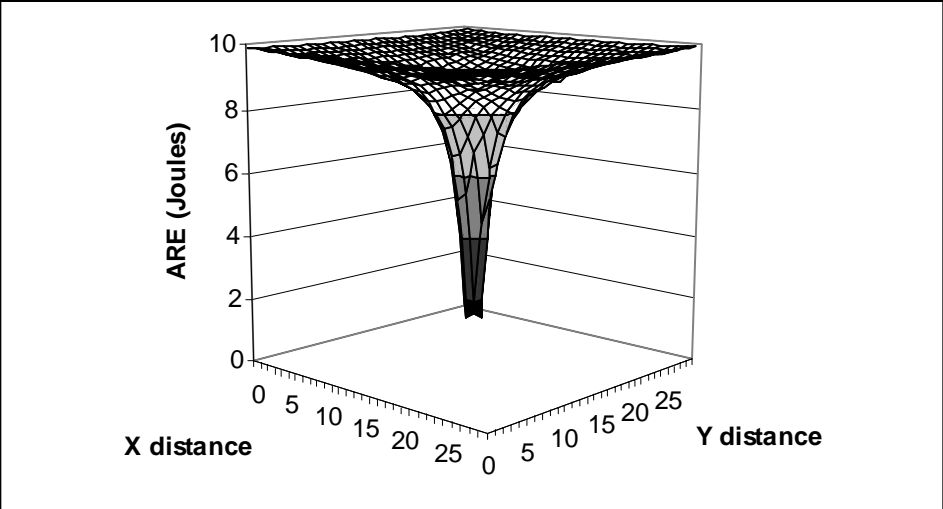


Figure 33: ARE for the Known path scheme in 900 nodes square grid network with $p = 0.3$.

Figures 34 and 35 present surface plots on ARE for UKP scheme in 100 node square grid network with 0 and 0.3 sleep probabilities respectively. Nodes deplete energy faster than in KP scheme.

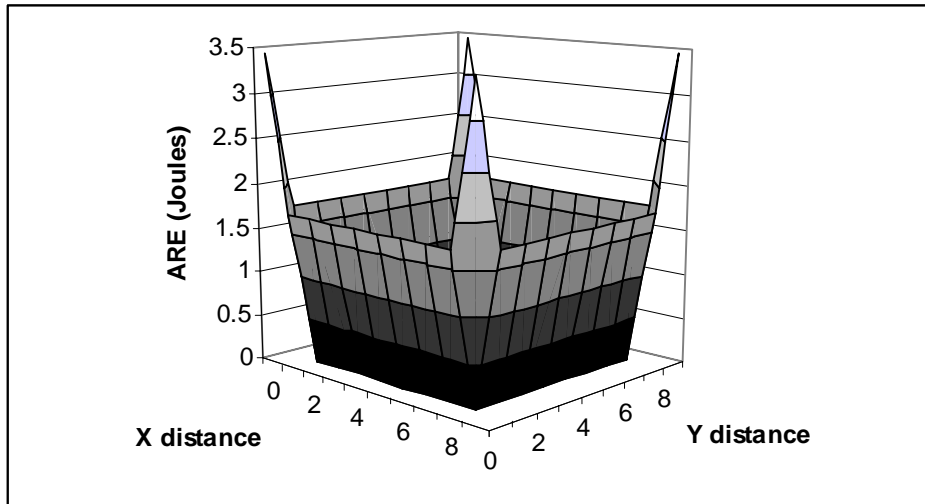


Figure 34: ARE for the Unknown path scheme in 100 nodes square grid network with $p = 0$.

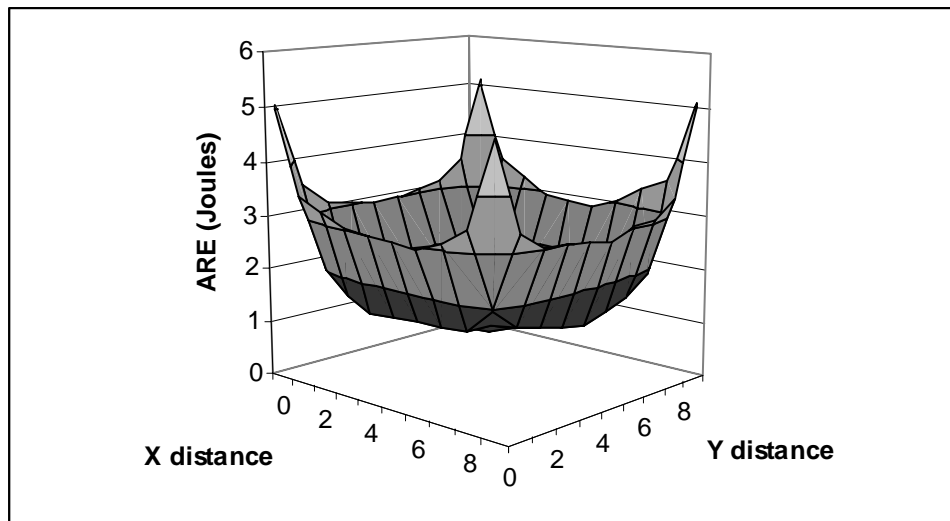


Figure 35: ARE for the Unknown path scheme in 100 nodes square grid network with $p = 0.3$.

Figures 36 and 37 plot ARE for the UKP scheme in 900 node square grid network with 0 and 0.3 sleep probabilities respectively. GSP with $p = 0.3$ for a large network as in 900 node grid has higher ARE comparing to non-GSP. GSP presents an increase on ARE at every points of the grid in larger network.

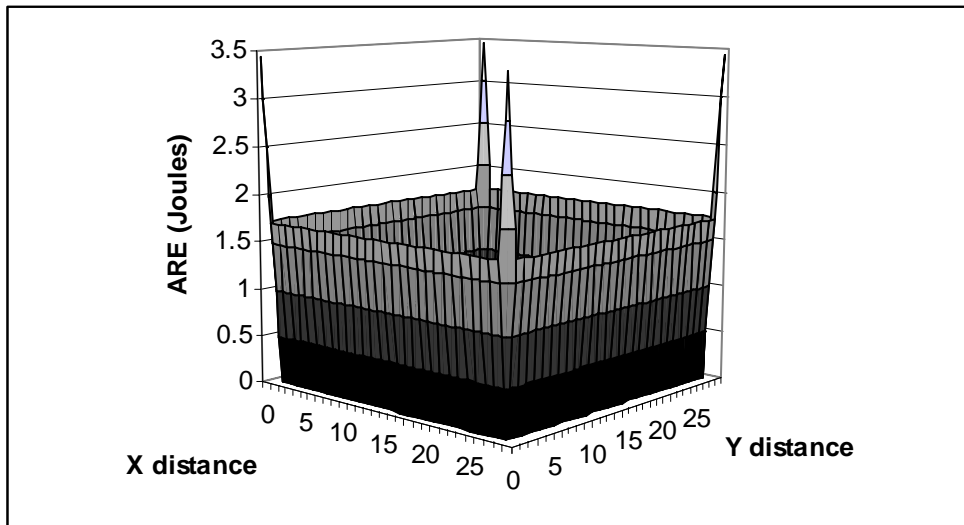


Figure 36: ARE for the Unknown path scheme in 900 nodes square grid network with $p = 0$.

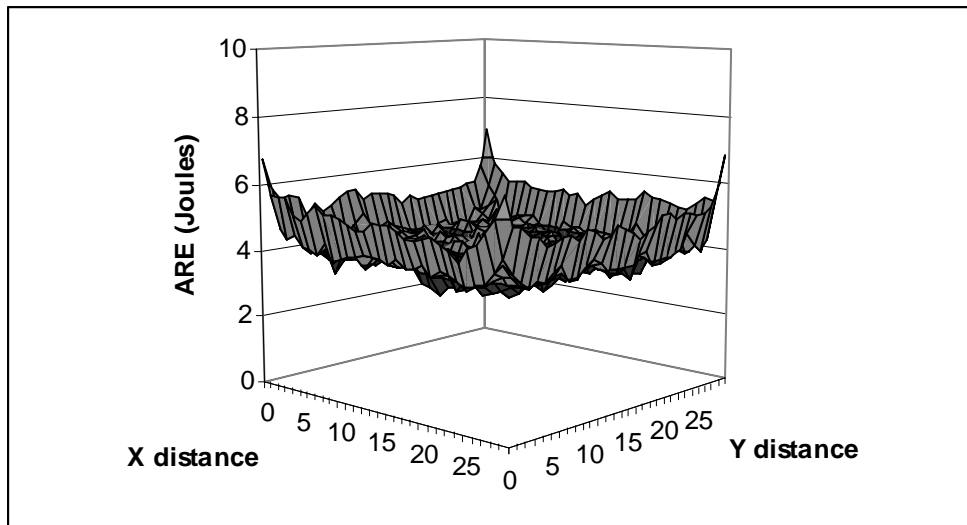


Figure 37: ARE for the Unknown path scheme in 900 nodes square grid network with $p = 0.3$.

Based on simulation results on average number of gossip periods, GSP offers longer network lifetime not only in the KP scheme but also the UKP scheme. However, only in UKP scheme that GSP shows a great amount of ARE comparing to non-GSP. In addition to UKP scheme, when network grows larger, GSP presents ARE improvement. Since GSP can integrate to other routing protocols, this ARE improvement may benefit, e.g., cluster-based protocols to use the remaining energy in network when rotating the cluster-heads or sinks. GSP was originally built upon the UKP scheme, which may reflect a more typical use for GSP. Thus, from now on, GSP simulations will consider only the UKP scheme analysis, which presents gossiping/broadcasting characteristics.

6.0 ANALYSIS IN INCREASING TRANSMISSION POWER/RADIUS

6.1 PRELIMINARY ANALYSIS

Network connectivity can also be achieved by increasing transmission power/radius when using higher gossip sleep probability (p). By increasing transmission power, a node will use higher energy when transmitting and relaying packets. However, allowing more sleeping nodes in GSP network with increase transmission power can improve overall energy efficiency. Previous chapter showed that by making network to remain connected, the highest gossip sleep probability (p) in GSP network for square grids should be 0.3. By having more sleeping nodes in the network, network would conserve more energy. However, the problem is that more sleeping nodes in the network will present less sensor nodes connected to the sink. Figure 16 shows the result of simulations on square grids of 10x10, 20x20, and 30x30 or 100, 400, and 900 nodes with transmission radius of distance d (see Figure 38), and it shows the curves of average path length in hops of all three network topologies are maximum at $p = 0.3$ or 30% of sleeping node. Beyond this point, the average path length (L_{GSP}) drops and connectivity is lost. Figure 17 shows the ratio of average number of disconnected nodes divided by awake nodes, which increases dramatically after $p = 0.3$. As examples of 100 and 400 node networks, the curves show that at $p = 0.4$ and 0.5 the number of disconnected nodes can reach 50% and 85% increasing respectively. Moreover, at $p = 0.6$, all three network topologies (10x10, 20x20, and 30x30) will have less than 5% of nodes in the network that will be able to transmit message to the sink. As a result, to maintain network connectivity by having p greater than 0.3, nodes need to increase the transmission power/radius.

To test the effect of increasing the transmission power or transmission radius, simulation tested GSP with radios having a transmission radius of distance $\sqrt{2} d$ ($1.414 d$) and $2d$.

- With transmission radius = d , the transmitting nodes can send traffic to the nodes which are located within one-hop radius.
- With transmission radius = $\sqrt{2} d$ or $1.414 d$, the transmitting nodes can send traffic to nodes which are located within about one-and-a-half-hop radius (see Figure 38).
- With transmission radius = $2d$, the transmitting nodes can send traffic to the nodes which are located within two hops radius.

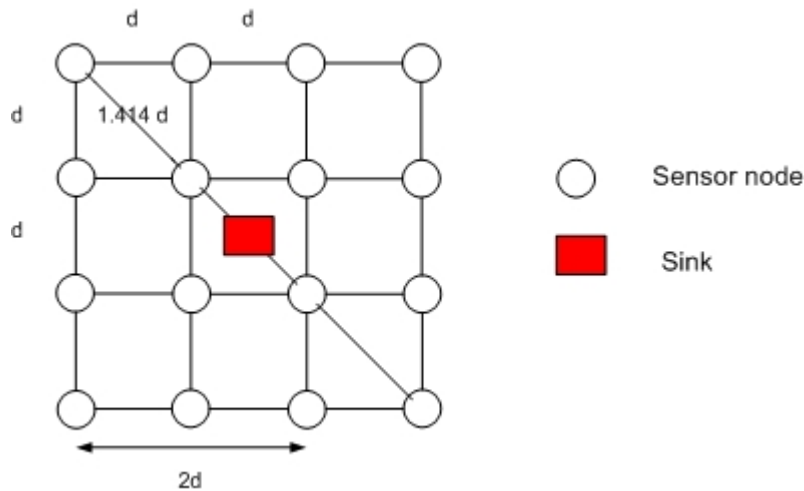


Figure 38: The grid topology to represent the transmission radius d , $1.414 d$, and $2d$.

Figure 39 shows that with $1.414 d$ transmission radius and $p = 0$, the average path length will be dropped by $(5 - 4.5) / 5 = 0.1$ or 10%. On the other hand, with $2d$ transmission radius, the average path length will be decreased by $(5 - 3.9) / 5 = 0.22$ or 22%.

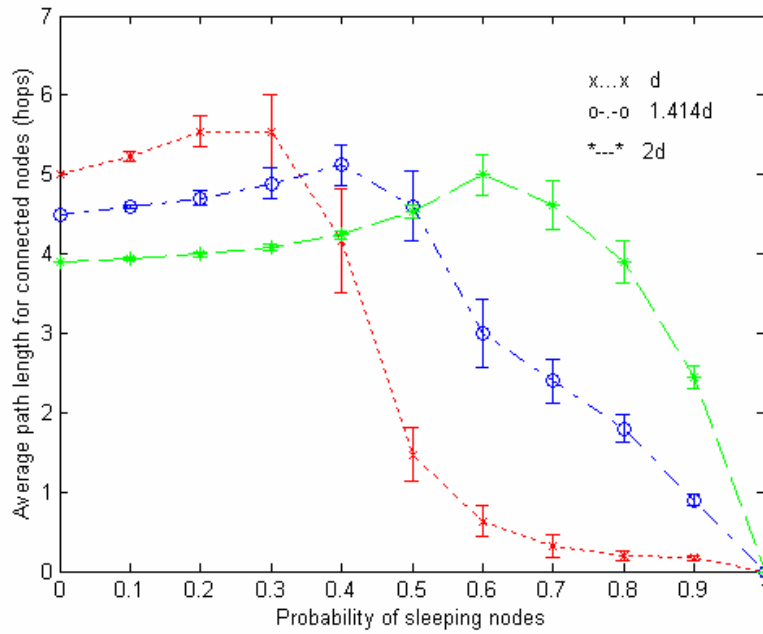


Figure 39: Probability of sleeping nodes vs. average path length when transmission radius = d , $1.414 d$ and $2d$ for 100 node square grid network with 95% c.i.

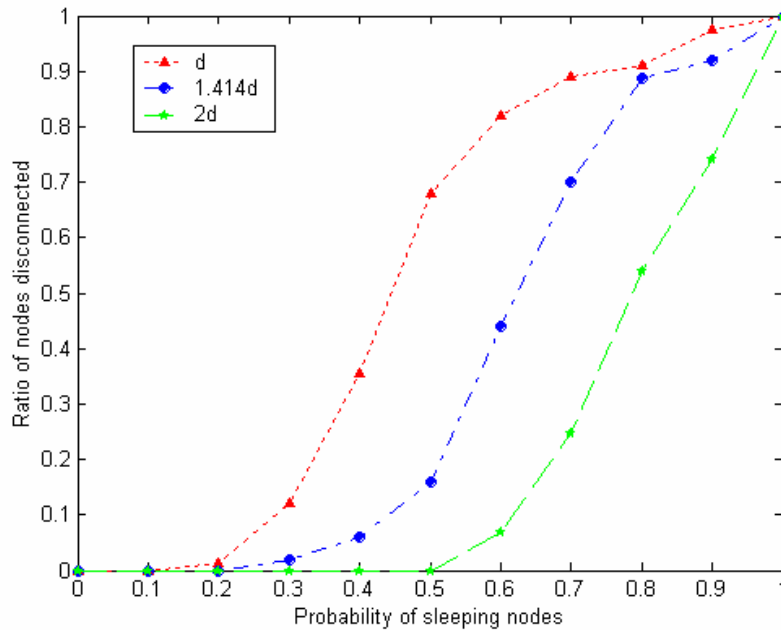


Figure 40: Probability of sleeping nodes vs. ratio of nodes disconnected when transmission radius = d , $1.414 d$ and $2d$ for 100 node square grid network with 95% c.i.

Figure 40 shows the ratio of nodes disconnected from the sink when using transmission radius of d , $1.414d$, and $2d$. It is observed that at $1.414d$ transmission radius, the network can stay connected with the $p = 0.4$. Moreover, at $2d$ transmission radius, network is able to use $p = 0.6$. This is significant in term of the energy saving when more sleep nodes apply and still having network connectivity. Figure 41 represents the improvement in disconnected node of increasing transmission radius of $1.414d$ and $2d$ comparing to transmission radius d . However, the increase in the transmission power/radius will increase the energy depletion rate. Using the r^2 path loss model, a transmission radius of $1.414d$ will require twice, and $2d$ will require four times as much energy as the d case. Even though more energy is required to transmit a packet, in some cases GSP with higher gossip sleep probability (p) resulted in a longer network lifetime. The next subsection analyzes the tradeoff between them.

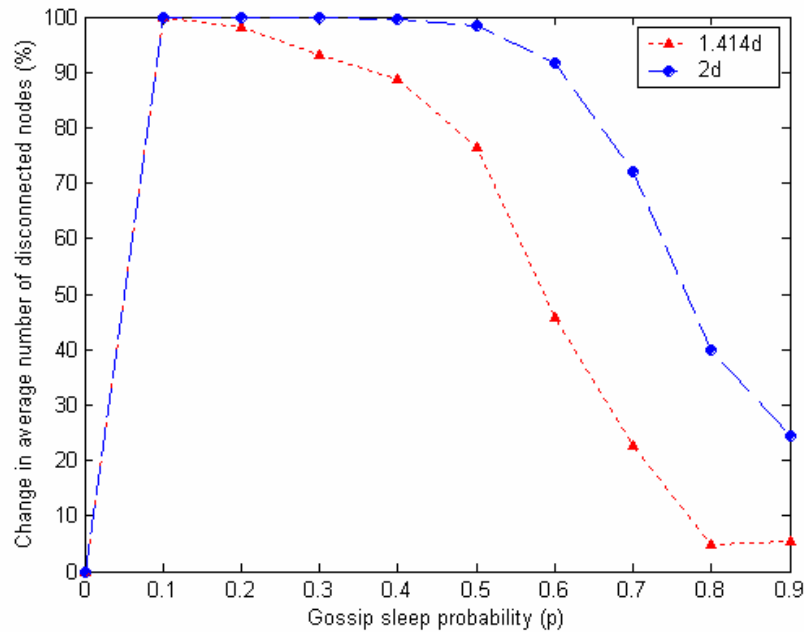


Figure 41: Probability of sleeping nodes vs. changes in average number of disconnected nodes.

6.1.1 Continued Analysis of Increasing Transmission Power/Radius in GSP

To increase the transmission power/radius, the energy will be depleted in two parts, which are transmission circuit and transmission amplifier (see Table 1). In transmission amplifier, although it consumes less energy than transmission circuit, it will consume energy by the power of 2 in increasing of transmission radius, e.g., to increase in double of the transmission radius ($2d$), the amplifier will consume energy four times more instead of double it. GSP can save energy depletion by letting some of the nodes to sleep with a certain probability. The more sleeping node can introduce more energy reserve. However, the selected number of gossip sleep probability (p) should make a connected network. This section does the analysis to see how much energy consumption is going to affect GSP when the transmission power and the gossip sleep probability increase. To make it more realistic, the comparison in mathematical analysis on transmission radiuses d , $1.414 d$, and $2d$ in 100 node square grid network is discussed. The numbers of the other parameters are acquired from simulation.

In transmission radius (d), equation 4.2 is used in this analysis. It is transformed into the following.

$$E_{GSP_d} = (E_{elec} + d^2 \times \varepsilon_{amp}) \times B_d \times L_{GSP_d} + E_{idle} \times (N \times (1 - p_d) - (B_d \times L_{GSP_d})) \quad (6.1)$$

Where $E_{elec} = 50nJ/bit$, $\varepsilon_{amp} = 100pJ/bit/m^2$, $E_{idle} = 40nJ/bit$, $d = 10$ meters, $L_{GSP_d} = 5.546$, $N = 100$. The selected probability p_d is 0.3, since it is the highest number that creates a connected network (see Figures 39 and 40). $B_d = 70/5.546 = 12.62$. By substitute all of the above into equation 6.1, the approximate total energy consumption in bit-time in network of $E_{GSP_d} = 2820nJ$.

The equation to determine the energy consumption when the transmission power/radius is increased to $1.414 d$ is the following.

$$E_{GSP_{1.414d}} = (E_{elec} + d^2 \times \varepsilon_{amp}) \times B_{1.414d} \times L_{GSP_{1.414d}} + E_{idle} (N \times (1 - p_{1.414d}) - (B_{1.414d} \times L_{GSP_{1.414d}})) \quad (6.2)$$

Where $E_{elec} = 50nJ/bit$, $\varepsilon_{amp} = 100pJ/bit/m^2$, $E_{idle} = 40nJ/bit$, $d = 14.14$ meters, $L_{GSP_{1.414d}} = 5.12$, $N = 100$. The selected probability $p_{1.414}$ is 0.4, since it is the highest number that creates a connected network (see Figures 39 and 40). $B_{1.414d} = 60/4.4 = 13.63$. By substitute all of the above into equation 6.2, the approximate total energy consumption in bit-time in network of $E_{GSP_{1.414d}} = 2430nJ$.

Now the transmission power/radius $2d$ is considered, the equation is expressed as below.

$$E_{GSP_{2d}} = (E_{elec} + d^2 \times \varepsilon_{amp}) \times B_{2d} \times L_{GSP_{2d}} + E_{idle} \times (N \times (1 - p_{2d}) - (B_{2d} \times L_{GSP_{2d}})) \quad (6.3)$$

Where $E_{elec} = 50nJ/bit$, $\varepsilon_{amp} = 100pJ/bit/m^2$, $E_{idle} = 40nJ/bit$, $d = 20$ meters, $L_{GSP_{2d}} = 4.995$, $N = 100$. The selected p_{2d} is 0.6, since it is the highest number that creates a connected network (see Figures 39 and 40). $B_{2d} = 40/3.0675 = 13.04$. By substitute all of the above into equation 6.3, the total energy consumption in bit-time in network of $E_{GSP_{2d}} = 1650nJ$.

The increase in the transmission power/radius will increase the energy depletion rate. Because of the r^2 path loss model, a transmission radius of $1.414d$ will require twice, and $2d$ will require four times as much energy as the d case. However, the results show that by increasing the transmission power/radius from d to $1.414d$ and $2d$, the network lifetimes were extended 13.8% and 41% respectively. There were two observations. First, to increase the transmission power/radius, a network can increase the number of gossip sleep probability (p). Therefore, more energy was conserved. Second, when network had less awake nodes, less traffic was transmitted. As a result, the total energy consumption by increasing transmission power/radius to $1.414d$ and $2d$ were not as much as in energy consumption when transmission power/radius was at d , which provided longer network lifetime.

6.2 NETWORK LIFETIME ANALYSIS WHEN INCREASING TRANSMISSION POWER/RADIUS

Previous analysis in this chapter simulated 5 dBm transmission power, which is the highest transmission power for TinyOS Mica2 mote [15]. However, to conduct the network lifetime experiments in this section, simulation requires two transmission power values, which are 0 dBm and 5 dBm for d and $2d$ transmission power/radius respectively (see section 2.1.1).

6.2.1 Square Grids

Before doing analysis in network lifetime, simulation determined the gossip sleep probability (p) when increase transmission power/radius to $2d$. Figures 42 and 43 suggest the gossip sleep probability equal to 0.6 for all three square grids.

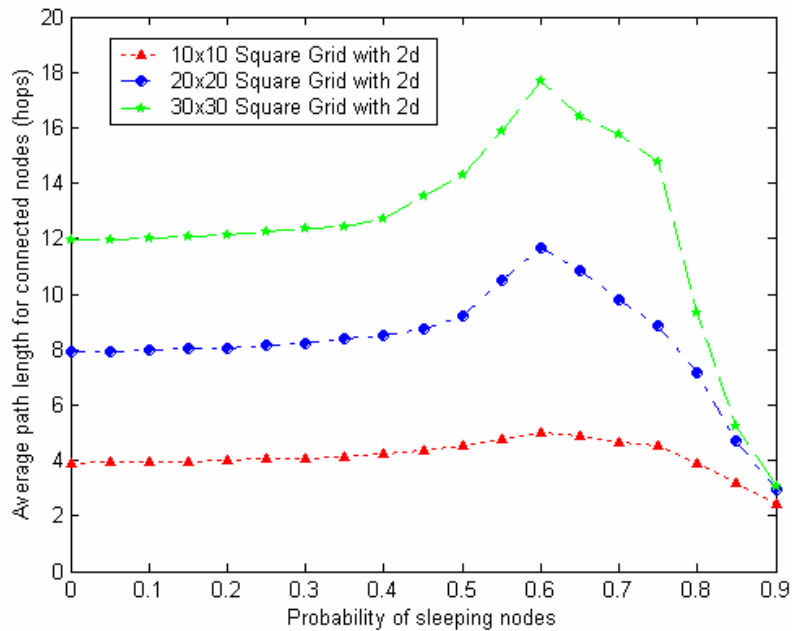


Figure 42: Probability of sleeping nodes vs. average path length for connected nodes in square grids with $2d$ transmission power/radius.

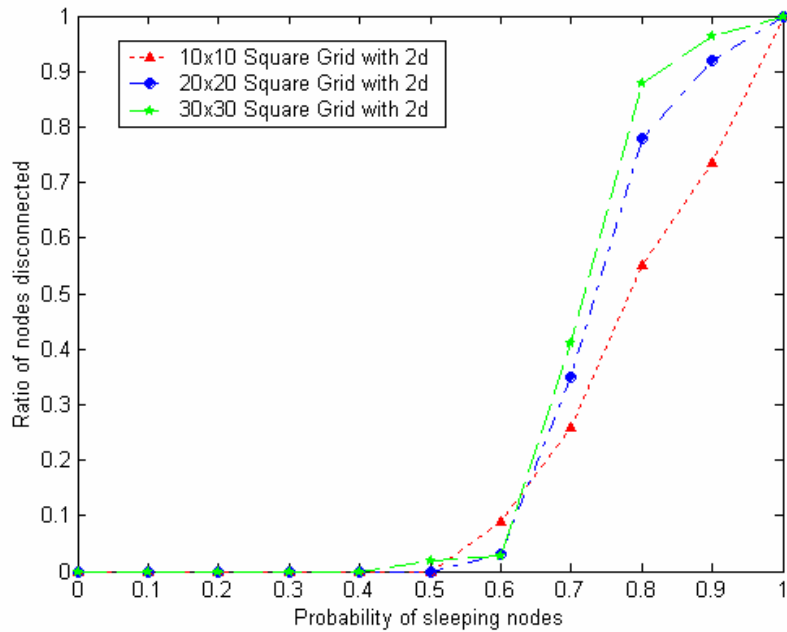


Figure 43: Probability of sleeping nodes vs. ratio of nodes disconnected in square grids with $2d$ transmission power/radius.

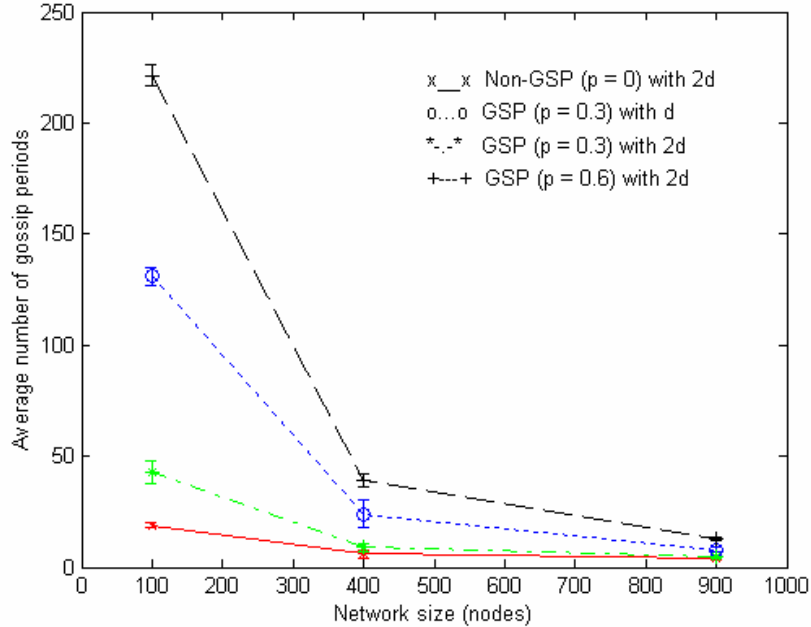


Figure 44: Average number of gossip periods vs. network size in square grids with 95% c.i.

Figure 44 compares the network lifetime in term of average number of gossip periods. The

change in network lifetime increases when using $2d$ transmission power/radius in GSP networks. However, the change decreases when using in larger networks. Also, the plot compares the average number of gossip periods of GSP_{2d} when using $p = 0.3$ to the other networks. Since GSP_{2d} with $p = 0.3$ uses high transmission power with small value of sleeping probability, it presents shorter network lifetime compared to the GSP_d with $p = 0.3$ but longer network lifetime compared to $Non-GSP_{2d}$ network.

Figure 45 shows increasing in average remaining energy (ARE) per node for $2d$ in all three sizes of square grids. When networks increase in size, the AREs increase for GSP networks. On the other hand, in Non-GSP, the ARE decrease when the network size increases.

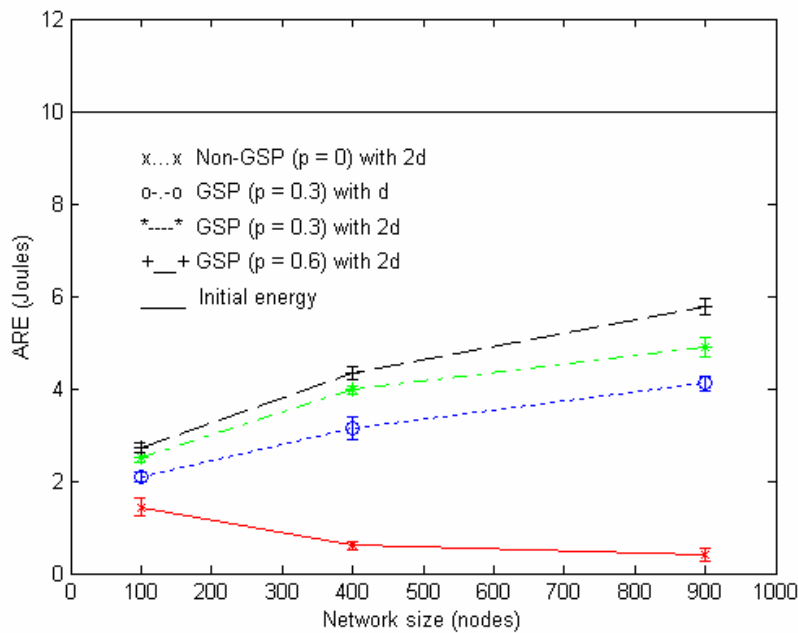


Figure 45: Average remaining energy (ARE) vs. network size in square grids with 95 % c.i.

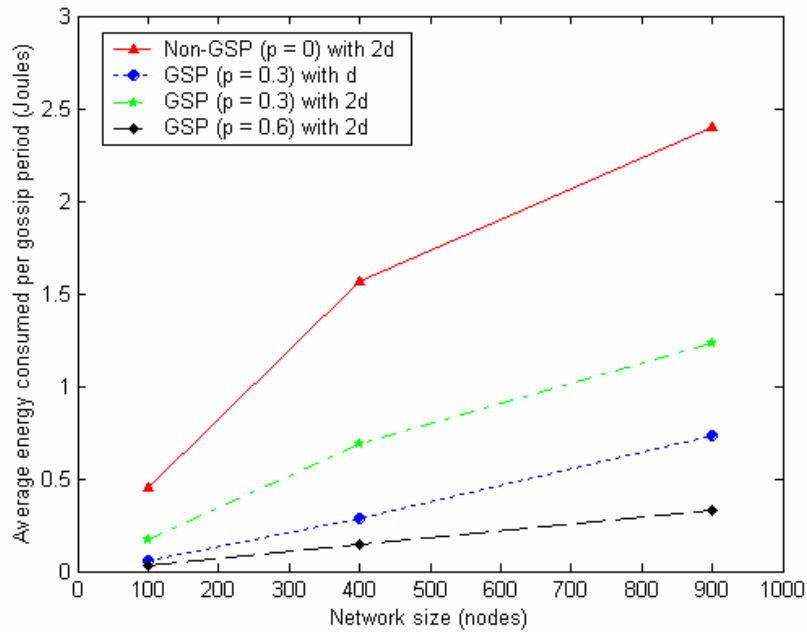


Figure 46: Average energy consumed per gossip period vs. network size.

Figure 46 shows the average energy consumed per gossip period. The Non-GSP network has higher energy consumption compared to all GSP networks. The smallest energy consumption per gossip period occurs for the GSP_{2d} with $p = 0.6$. Because of the higher traffic load in larger networks, the average energy consumed per gossip period increases when the networks increase in size.

7.0 NETWORK TOPOLOGIES

One characteristic of wireless sensor networks is that they are application specific such that one protocol may be best suited for one application but not another. GSP may be applied to networks that provide continuous sampling with fixed or mobile sinks. Some recommended applications are environmental monitoring such as airport runways, buildings, bridges, and roads monitoring [69]. Previous chapters show that GSP reducing overhearing transmissions and receptions by allowing nodes to enter sleep states can extend sensor network lifetime. However, these preliminary results have not considered the energy consumption resulting by sleep nodes in the idle and sleep periods. Nodes usually consume energy even though they are in sleep state [15]. Thus, this chapter includes a time-based simulation to evaluate GSP network lifetime performance by including energy consumption of nodes in idle and sleep states. Moreover, the simulation adjusts parameters such as gossip periods (G_p) to evaluate GSP over longer gossip periods. This chapter begins with the introduction of the energy consumption model and the simulation parameters used in the network lifetime analysis. The simulation tests the effect of increasing in transmission power/radius can improve network lifetime.

7.1 PERFORMANCE EVALUATION

7.1.1 Energy Consumption Model

The simulation used the energy consumption model as shown in Table 3. The simulation considers the energy consumption in the idle/listening and sleep periods proposed in [15].

7.1.2 Simulation Parameters

Network lifetime analysis allows simulations to consider the parameters such as the Average number of gossip periods (G_p), Average Remaining Energy (ARE), Total number of transmitted/relayed packets, Total number of dropped packets, and Packet loss ratio. Also, simulations employed the Carrier Sense Multiple Access with Collision Avoidance (CSMA/CA) as a Medium Access Control (MAC) protocol for both GSP and Non-GSP networks. The following represents the concepts of the CSMA/CA implemented in TinyOS Crossbow application, which is later implemented in the simulations.

- CSMA/CA begins with the node listening to the medium.
- If the medium is idle, the node waits during a backoff time.
- After the backoff time expires, if the medium is free, the node transmits the packet, otherwise, the node will wait for a congestion backoff time to sense the medium again.

There is no collision detection or packet acknowledgement in CSMA/CA implementation. Since there are no ACKs, the MAC protocol will not retry to send a packet. Simulations assume that a node relay a packet only once. If the duplicate packets arrive, a node will receive and discard it. As a result, the consumed energy by receiving the duplicate packets is considered in the analysis of the network lifetime.

To evaluate the network lifetime, this chapter analyses all topologies with a single sink node located at the center. All calculations assume the period of time to transmit one bit of data, i.e. *bit-time*. Also, the traffic load remains constant with or without GSP, i.e. the numbers of bits generated by the sensors in a bit time are the same.

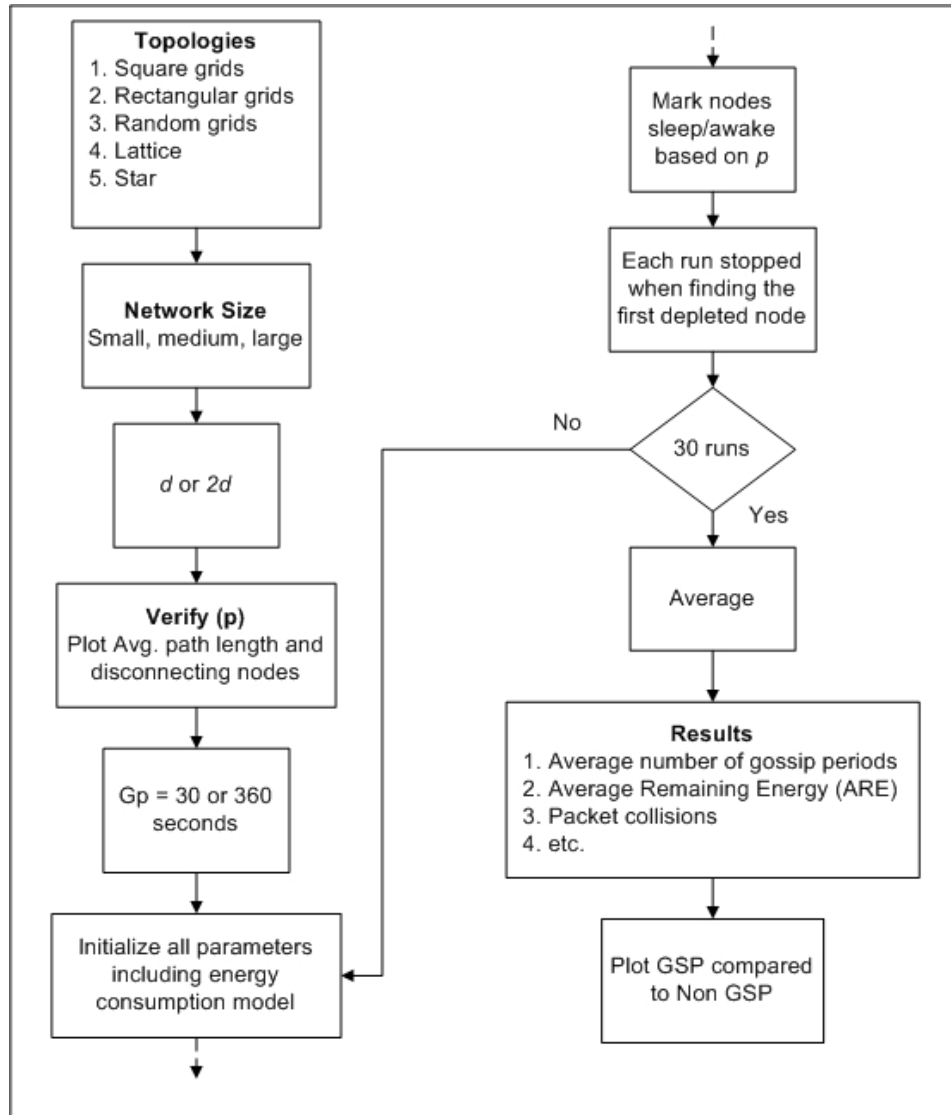


Figure 47: Experimental design.

Figure 47 illustrates the experimental design. First, a topology, network size, transmission distance, and gossip period (G_p) are chosen. The initial energy of transmission power (d and $2d$) comes from the energy consumption model. Based on topology and transmission power/radius, the program calculates the gossip sleep probability (p) that creates a connected network, which will later be used in the GSP network. Non-GSP assumes no sleeping nodes, therefore simulation uses $p = 0$ throughout the analysis. In GSP network, the simulation employs the gossip sleep probability (p) to randomly assign sleeping nodes at the beginning of each gossip period, which will be repeated until the simulation discovers the first dead node. After 30 runs, the simulation calculates the average and plots the results comparing GSP to Non-GSP network. Based on number of topologies, network size, and gossip period, the simulation analyzes GSP compared to Non-GSP with the total number of 120 experiments. The parameters used in the analysis are the following.

Average number of gossip periods: The parameter directly represents the network lifetime. The higher average number of gossip periods presents the longer network lifetime.

Average Remaining Energy (ARE): ARE demonstrates the average energy remaining of every nodes after finding the first completely depleted node. ARE represents the energy efficiency in the way that network will be able to continue using the remaining energy. ARE benefits the protocols that provide scenarios such as:

- Protocols that can reconfigure themselves after finding a dead node.
- Protocols that consider the network lifetime when the simulations discover the multiple dead nodes or consider network partitions as the lifetime of the network.
- Since GSP can be used as topology management and integrated to the other routing protocols, ARE can benefit the cluster-based routing protocols to use the remaining energy in the network when rotating the cluster-heads or sinks.

Gossip period (G_p): The simulation selected $G_p = 30$ and 360 seconds in this analysis. The shorter gossip period will force the network to change the topology faster than the longer one, which will be useful in the application such as patients' vital sign monitoring because this application requires a sensor to frequently report a patient condition [69]. The longer gossip

period can be used in the environment monitoring applications such as bridges, and airport runways monitoring since these applications require sensor to transmit the data once in a while [69]. The reason of doing two gossip periods is to study the outcome of the energy consumption when nodes turning on their transceiver in the idle/listening periods and their impacts on the packet collisions.

Transmission rate: The rate represents the number of transmitted/generated packets over the number of active nodes per second (transmitted packets / active node / second) in each gossip period. The simulation used this rate to control the traffic generated. In this research, the simulation used 0.1 packets/node/second as a transmission rate for all topologies and network sizes. As an example, in the 100 nodes network, ten out of one hundred nodes are randomly selected to transmit in a second (10 packets/second in the entire 100 node network). In the 900 nodes network, 90 nodes out of 900 nodes will transmit their packets in each second or the network generates 90 packets/second. As a reasonable comparison, the generate traffics on both GSP and Non-GSP networks are approximately the same. The 0.1 ratio will force each node to transmit approximately more than two times in each gossip period. However, the effect of the CSMA/CA backoff time probably delays the packets transmission, which can affect the total number of transmissions in each gossip period. In case of longer gossip period ($G_p = 360$ seconds), simulation assumes the same generated traffic with the short one ($G_p = 30$ seconds). Thus, to apply the same generated traffic with the 30 seconds gossip period, the generated packet rate is equal to 0.0083 packets/node/second in case of 360 seconds gossip period.

Total number of transmitted/relayed packets: The total number of transmitted and relayed packets after the simulation finds a first dead node.

Total number of dropped packets: The lost/dropped packets are the results of the packet collisions, i.e. packets arrive the same node at the time of this node is processing the other packet. In this research, simulations assume no capture effects. As a result, all packets that collide at the same receiver will be dropped.

Packet loss ratio: Ratio of the total number of lost/dropped packets over the total number of transmitted/relayed packets. The metric represents the reliability of the network.

Figures 48, 49, and 50 represent how the simulations were conducted. Figure 48 shows the steps beginning from assigning the initial energy to nodes. The simulation finds sink neighbor nodes based on the transmission power (d or $2d$) called critical nodes. Simulation assumes that at least one of these critical nodes is active to avoid losing connectivity of every node. The initial timer is set to track the gossip period before the loop over gossip periods starts. The simulation assigns sleep nodes based on the sleeping probability within the loop. Since Non-GSP network uses $p = 0$, there is no random sleeping node in the beginning of gossip period. However, to keep track and compare the number of gossip periods to the GSP network, the simulation counts the number of gossip period. After randomize sleeping nodes, the gossip period begins. Then simulation picks all active nodes one by one to start the threading process. Figure 49 and 50 demonstrates this process. The process starts with the simulation picking the first node called pCurrNode (current node). The simulation checks whether pCurrNode has enough power to transmit. Then, the simulation looks at the neighbors of this pCurrNode to check the neighbors whether they are free from CSMA lock. CSMA lock representing the node is processing a packet. If at least one of the pCurrNode neighbors is in CSMA lock, the simulation will walk through the CSMA/CA algorithm. In the CSMA/CA algorithm, the pCurrNode checks whether one of any neighbors is in CSMA lock. If not, the pCurrNode enters backoff period which the simulation randomizes between 10 – 20 milliseconds. Then, the pCurrNode listens to medium again, if no neighbor is in CSMA lock, node transmits the packet otherwise it goes through the backoff period again. When pCurrNode transmits a packet, simulation reduces the energy by one unit, which the value comes from the energy consumption model. While transmitting, the pCurrNode enters CSMA lock. The packet travels to all of the active neighbors, which is randomly picked one by one to relay this packet. The picked neighbor called pNextNode. The simulation determines whether the pNextNode is under Tx or Rx lock. If so, the collision occurs and the collision counter increases. If the pNextNode does not lock, simulation increases the counter on packet processing. The lock delay is approximately the same with the transmission time. The transmission time is about 8.75 milliseconds, which is the packet size divided by the data rate. The pNextNode consumes the receiving energy. The node releases the Tx and Rx lock. The simulation goes through the loop

over the neighbors to pick the next neighbor. The simulation continues to repeat the algorithm with pNextNode as input for pCurrNodes recursively until all node processes this packet. The simulation process continues checking for a dead node. If the simulation discovers a depleted energy node, the simulation run is stopped and the number of gossip periods, number of packet collisions, and power matrix are computed. Each experiment is run 30 times.

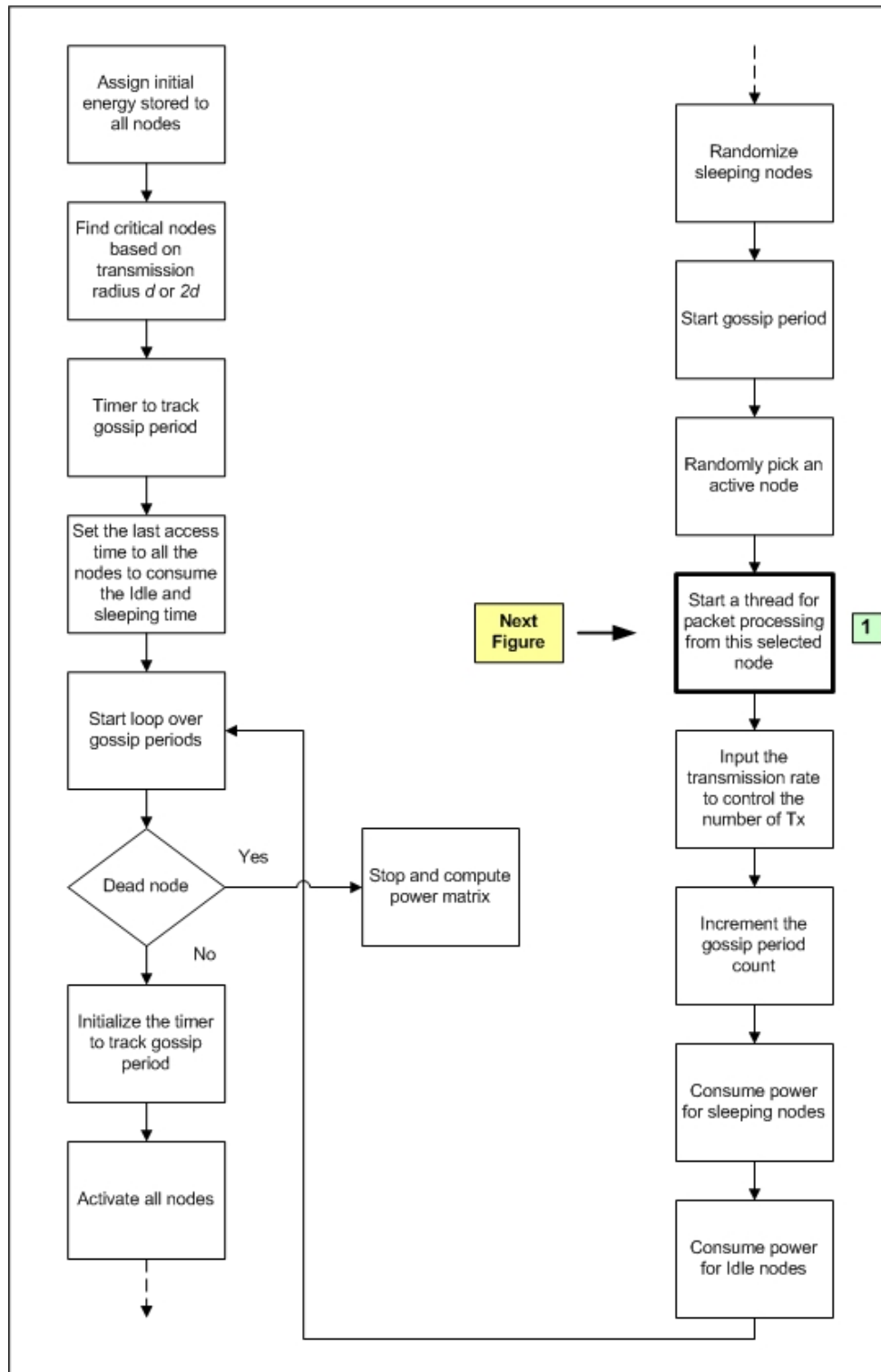


Figure 48: A flowchart of the simulation.

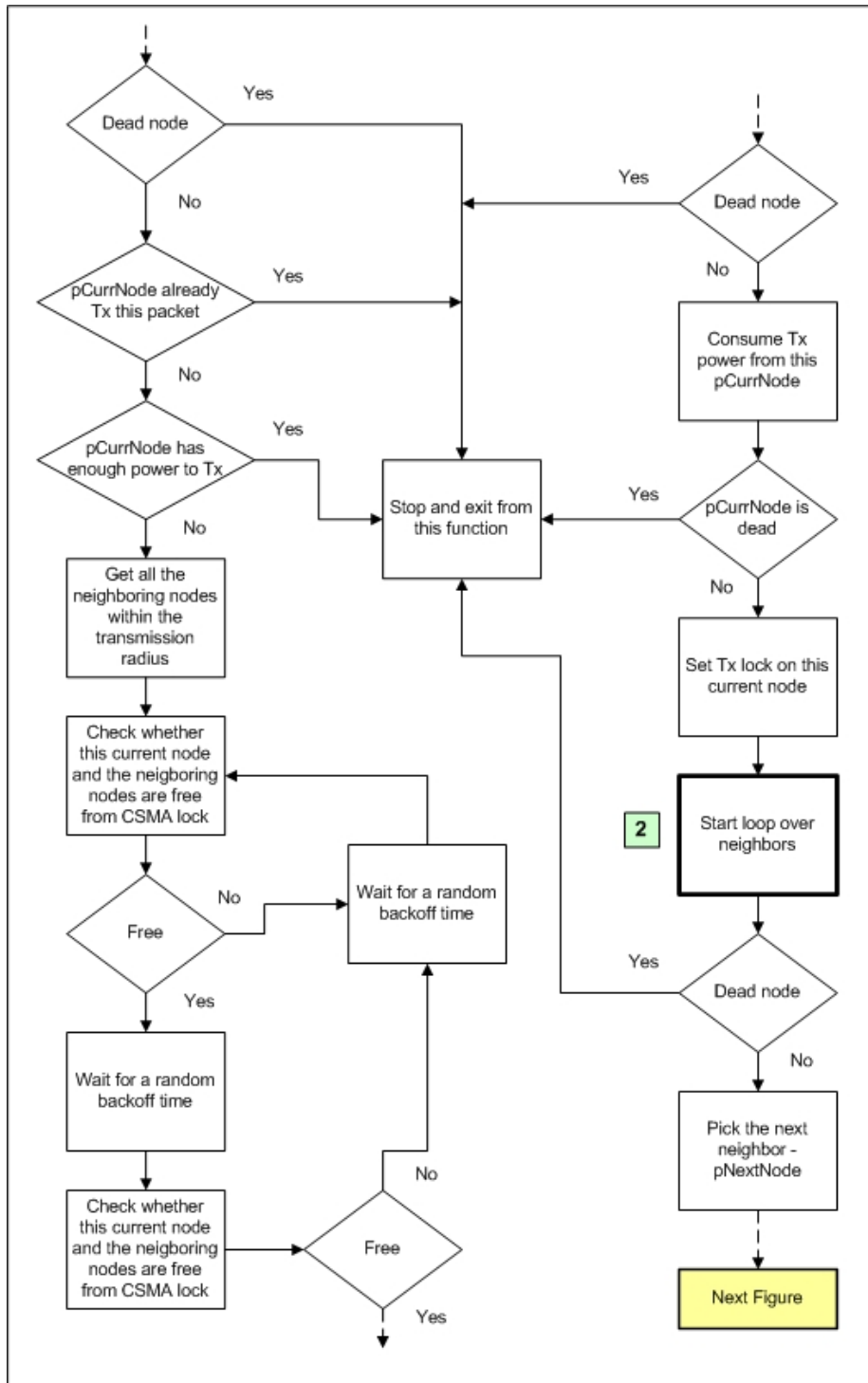


Figure 49: A flowchart of a threading method with packet processing in the simulation.

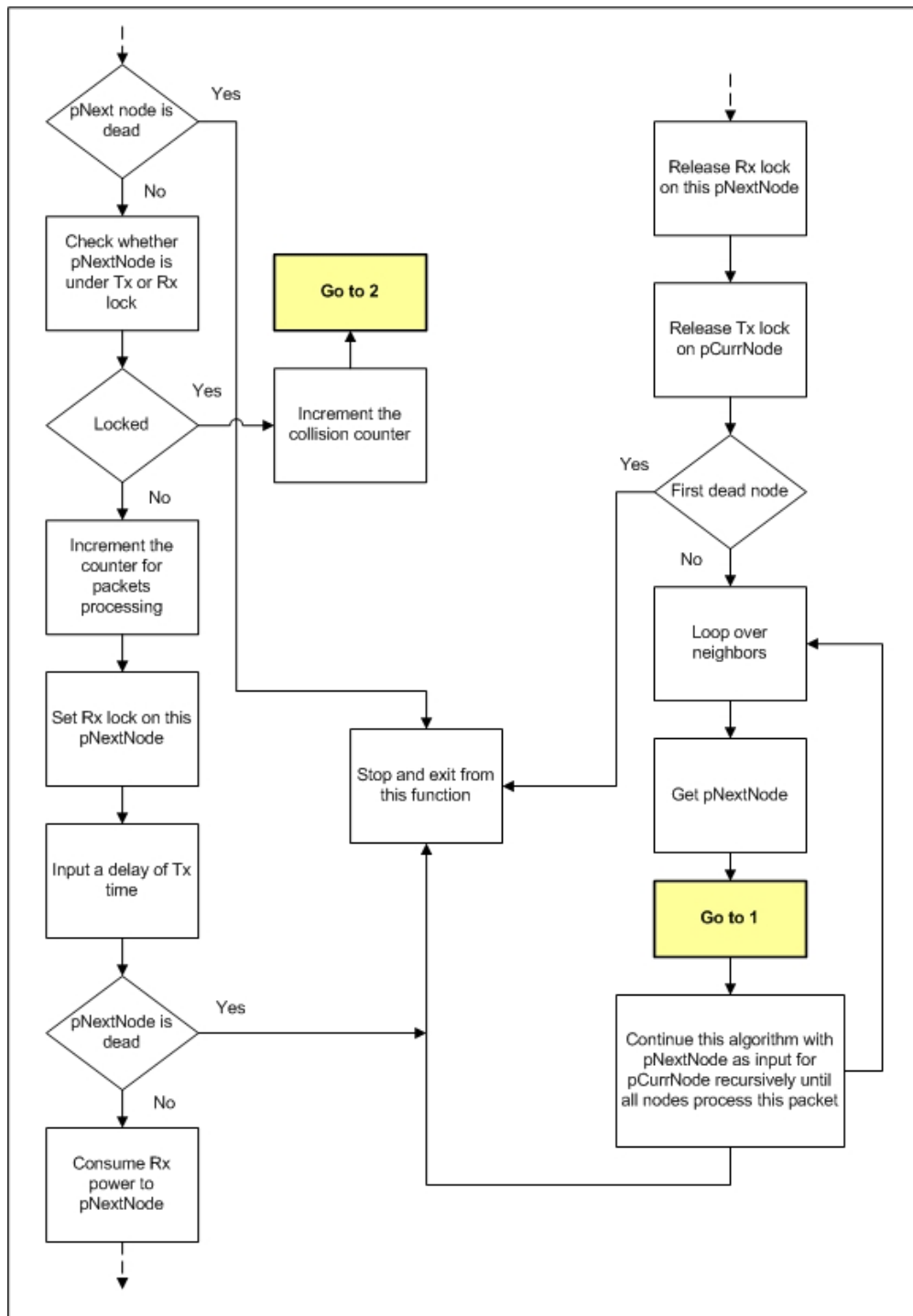


Figure 50: A flowchart of a threading method with packet processing in the simulation (Continue).

7.2 TOPOLOGY

Physical topologies of wireless sensor networks vary with their applications. As examples, the shape of bridges requires rectangular grid networks, and road monitoring applications need lattice topologies. Therefore, network topology plays an important role in designing protocols such as GSP because each topology may require a unique gossip sleep probability (p). As a result, GSP performance varies over topologies. To evaluate GSP performance, GSP performs on different sizes of various topologies, such as square grids, rectangular grids, random grids, lattice topology and star topology to measure the network lifetime.

7.2.1 Square Grids

Square grids are the most common topologies to study network lifetime. GSP was tested on three different network sizes, i.e., 100, 400, and 900 nodes with a sink at the center of the grid, to measure the network lifetime. First, the simulation evaluates the highest probability of the sleeping node, called gossip sleep probability (p) that creates a connected network for different network sizes. By doing so, the simulation was conducted to find the average path length in hops and average number of disconnected nodes for varying sleep probabilities.

7.2.1.1 Transmission Power/Radius d in the Square Grids

The energy consumption model and network parameters used for transmission power/radius d came from the measurement of the TinyOS Mica2 motes [15] shown in Table 8. The data rate is 19.2 kbps, and the packet size is 21 bytes or 168 bits [17]. To improve the network lifetime analysis, the simulation used five times larger initial energy store than the one in chapter 5, which is 50 Joules. Figures 16 and 17 demonstrate the gossip sleep probability (p) that create a connected network. The simulation suggests $p = 0.3$ for all network sizes of square grids topologies when using transmission power/radius d .

Table 8: Simulation parameters and energy consumption model when using transmission power/radius d .

<i>Data rate</i>	19.2 kbps
<i>Packet size</i>	21 bytes
<i>MAC</i>	CSMA/CA
<i>Initial energy stored</i>	50 Joules
<i>Transmit</i>	3.07 μ Joules/bit
<i>Receive</i>	2.21 μ Joules/bit
<i>Idle/Listening</i>	2.21 μ Joules/bit
<i>Sleep</i>	0.87 μ Joules/bit

Figure 51 shows the average number of gossip periods for GSP and Non-GSP networks. The simulation assumes the shortest gossip period (G_p) equal to 30 seconds. Also, the simulation tested GSP with the longer gossip period to observe the effects of energy consumption on the idle/listening states, which is equal to 360 seconds. GSP provides the higher average number of gossip periods on both 30 and 360 second cases. Figure 52 represents the change in network lifetime when using GSP compared to Non-GSP. GSP with the 360 gossip period results in a larger change in network lifetime compared to GSP with the 30 seconds gossip period for all network sizes. The largest change occurs for the small network on both $G_p = 30$ and 360 seconds. However, as networks increase in size, the change decreases.

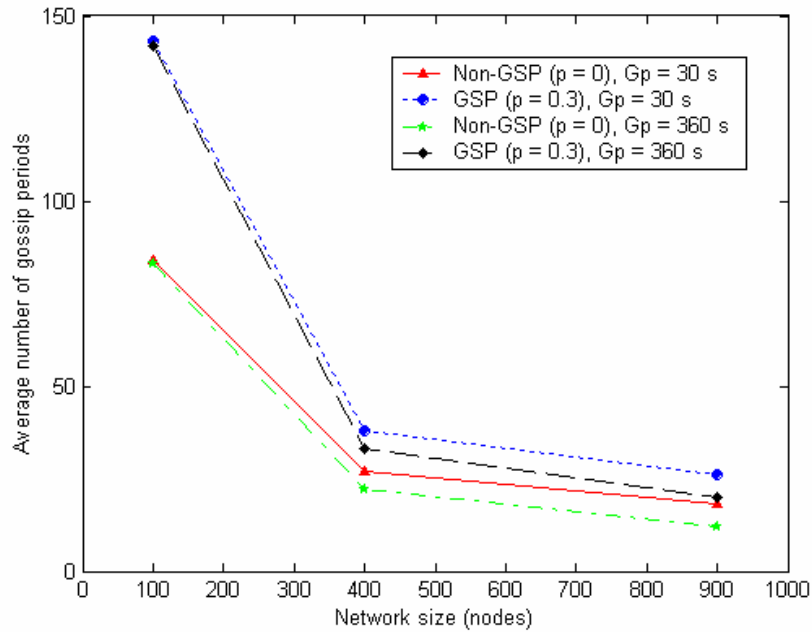


Figure 51: Average number of gossip periods vs. network size for the square grids with transmission power/distance d , $G_p = 30$ and 360 seconds.

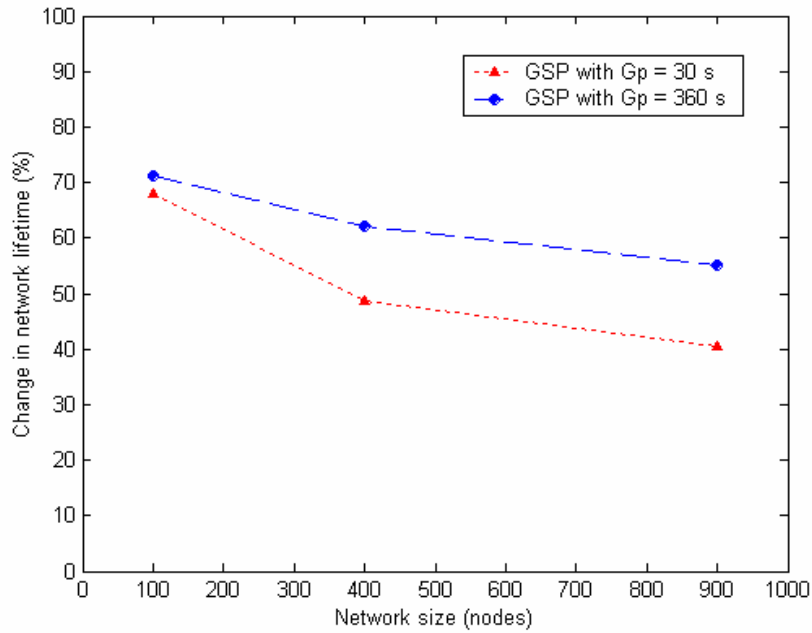


Figure 52: The changes in network lifetime on the different sizes of the square grids with transmission power/radius d when using GSP with $p = 0.3$ compared to Non-GSP, $G_p = 30$ and 360 seconds.

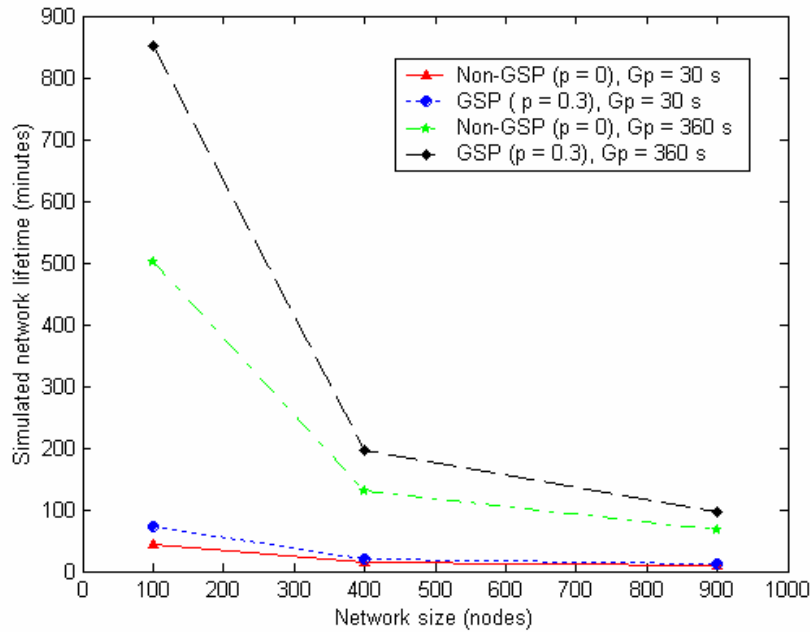


Figure 53: Simulated network lifetime vs. network size for the square grids with transmission power/radius d , $G_p = 30$ and 360 seconds.

Figure 53 presents the simulated network lifetime when using transmission power/radius d on both 30 and 360 seconds gossip period. The longest lifetime occurs for small GSP network with 360 second gossip period. When the network size increases, the network lifetime decreases because of the high traffic load in the large network.

Figure 54 plots Average Energy Remaining (ARE) per node after discovering the first depleted node averaged over 30 runs. The results show GSP achieves higher ARE for all network sizes. Moreover, the ARE increases with GSP when the network size increases. On the other hand, as networks increase in size, Non-GSP shows the decreasing in the ARE. AREs are useful for the networks that consider network lifetime as the multiple dead nodes or the cluster-based networks can continue using the energy after rotating the cluster-heads. However, Figure 54 presents a small decrease in ARE per node when using the longer gossip periods ($G_p = 360$ second) on both GSP and Non-GSP networks. The longer period consumes more energy in the idle/listening states.

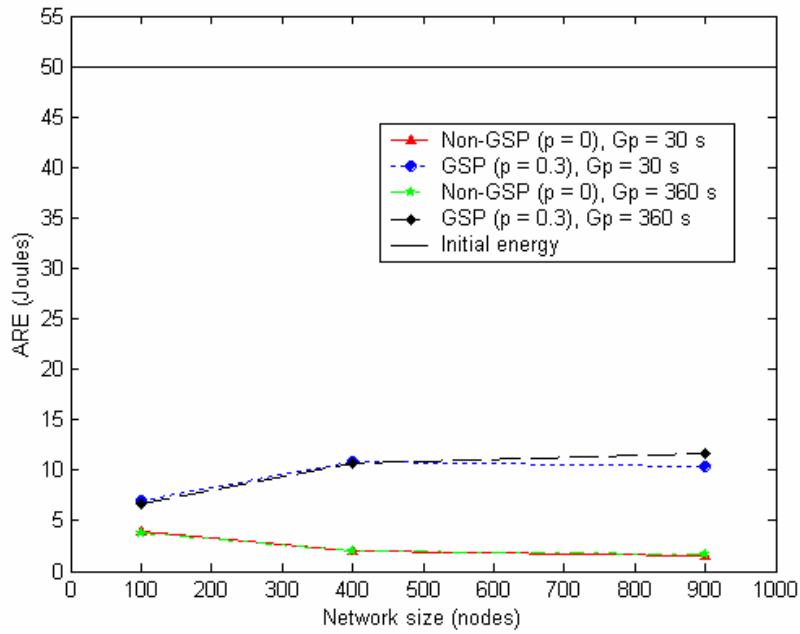


Figure 54: Average remaining energy (ARE) vs. network size for the square grids with transmission power/radius d , $G_p = 30$ and 360 seconds.

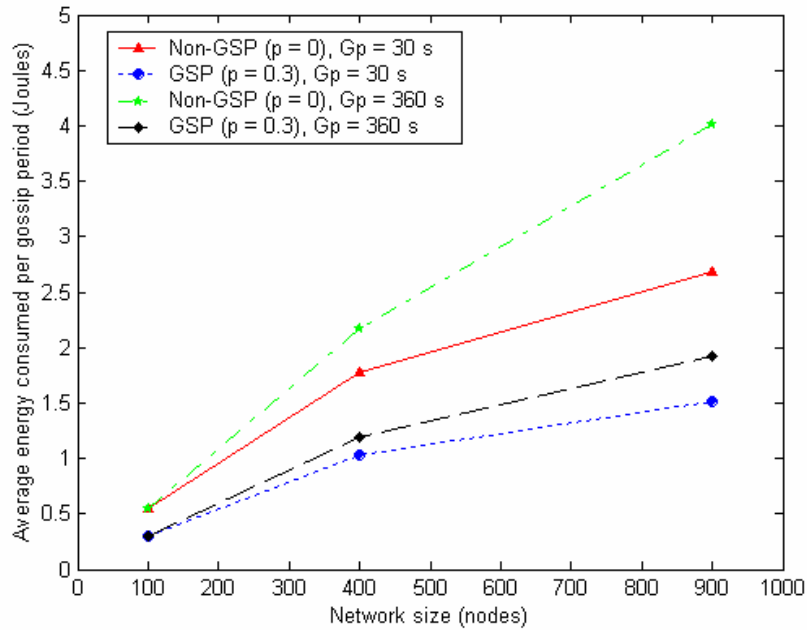


Figure 55: Average energy consumed per gossip period vs. network sizes for the square grids with transmission power/radius d , $G_p = 30$ and 360 seconds.

Figure 55 shows that GSP networks consume less energy per gossip period compared to Non-GSP network for all network sizes. Because of the high traffic load in large networks, energy consumption per gossip period increases when networks increase in size.

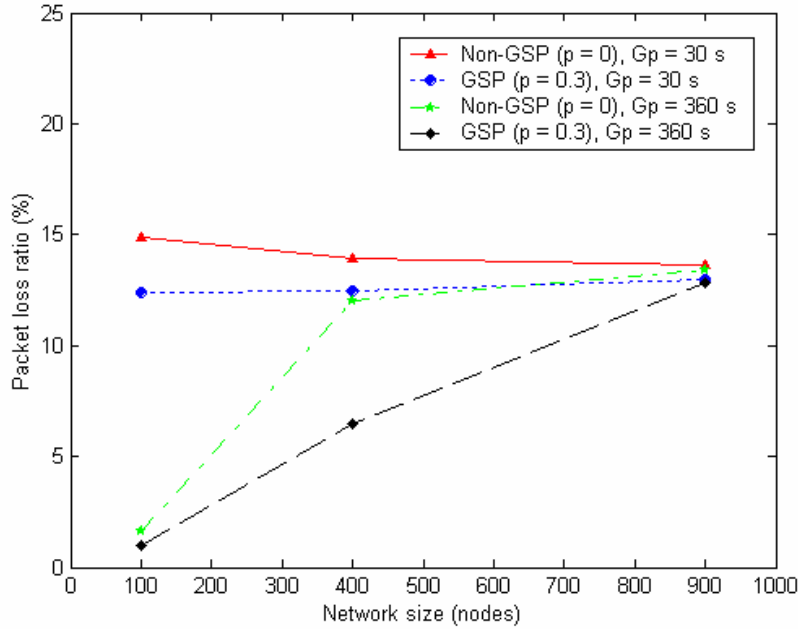


Figure 56: Packet loss ratio vs. network size for the square grids with transmission power/radius d , $G_p = 30$ and 360.

Figure 56 presents the packet loss ratio in percentage, which is the ratio of the number of packets dropped due to collisions over the total number of transmitted/relayed packets. Also, GSP network considers the number of dropped packets when changing the topology between the gossip periods. Network employing GSP shows smaller packet loss ratio compared to Non-GSP in the 30 seconds gossip period. Also, results show that the longer gossip period results in a smaller packet loss ratio. The smallest ratio happens with the small network with the 360 seconds gossip period on both GSP and Non-GSP because a smaller network has a lower offered traffic load resulting in fewer collisions. However, when the network employs the short gossip period time ($G_p = 30$ seconds), the small network shows approximately the same packet loss ratio as the medium and the large networks.

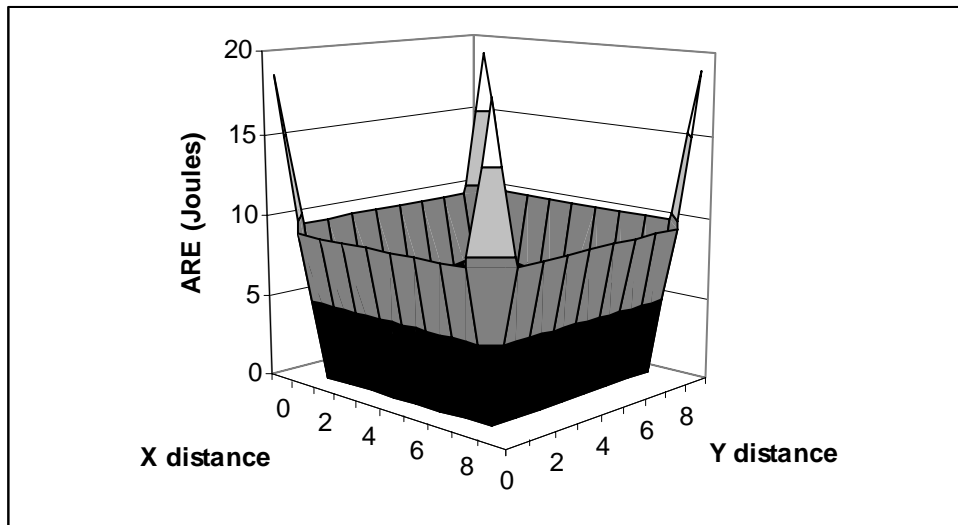


Figure 57: ARE for 10x10 (100 nodes) square grid Non-GSP network ($p = 0$) with transmission power/radius d .

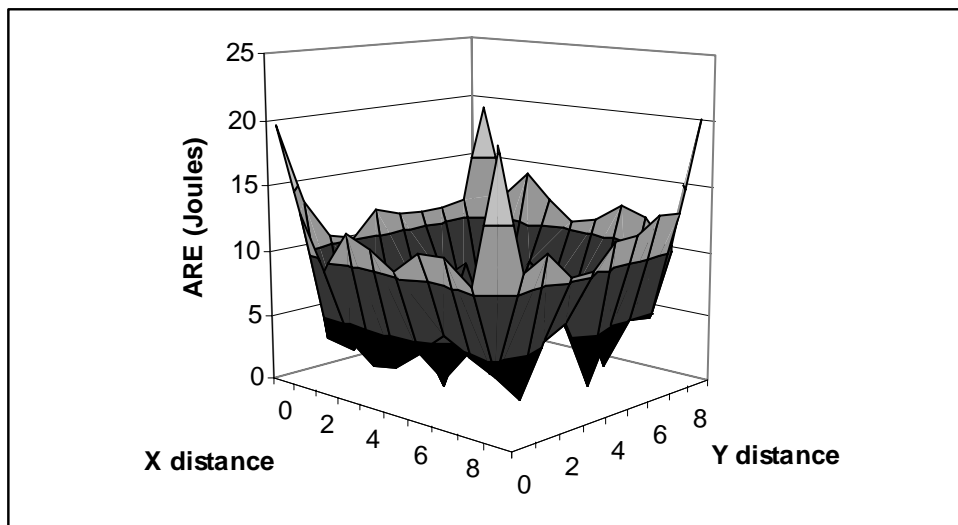


Figure 58: ARE for 10x10 (100 nodes) square grid GSP network ($p = 0.3$) with transmission power/radius d .

Figures 57 and 58 plot the AREs in 10x10 (100 node) square grids on both GSP and Non-GSP networks. The X and Y distances represent locations of the nodes in the grids. ARE surface plots for $G_p = 30$ and 360 seconds are similarly shaped. Therefore, in this chapter, all plots of AREs are for $G_p = 30$ seconds. Nodes in the Non-GSP network quickly consume energy throughout the network and reach 0 Joules. On the other hand, when using gossip sleep probability 0.3, ARE increases from 3.89 to 7.03 Joules (80%) in 100 nodes network. Because of random sleeping nodes, there is no average energy remaining per node reaching 0 Joules in GSP network. Moreover, Figures 59 and 60 show the higher ARE in larger GSP network size (900 nodes), which is increased from 1.6 to 10.4 Joules (550%). The largest change is presented in the large network size because in the larger network ARE increases with GSP and decreases with Non-GSP.

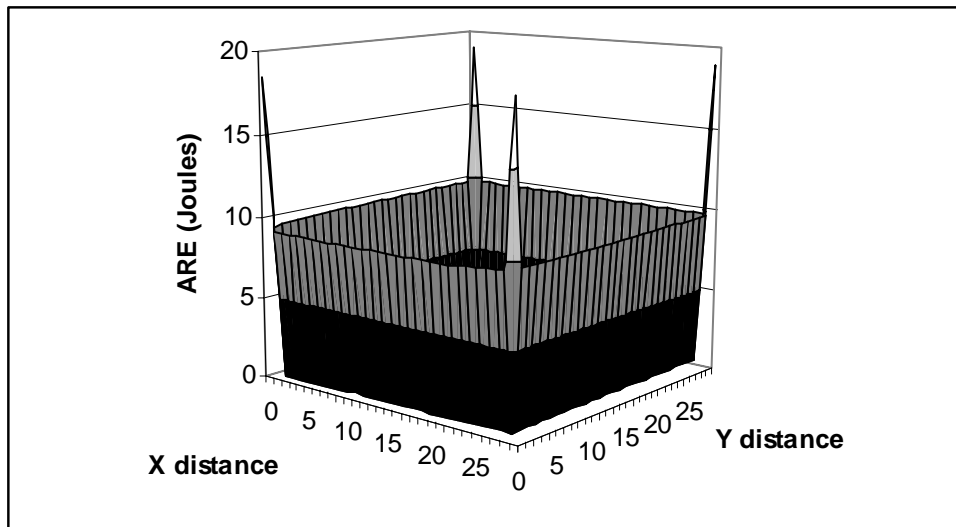


Figure 59: ARE for 30x30 (900 nodes) square grid Non-GSP network ($p = 0$) with transmission power/radius d .

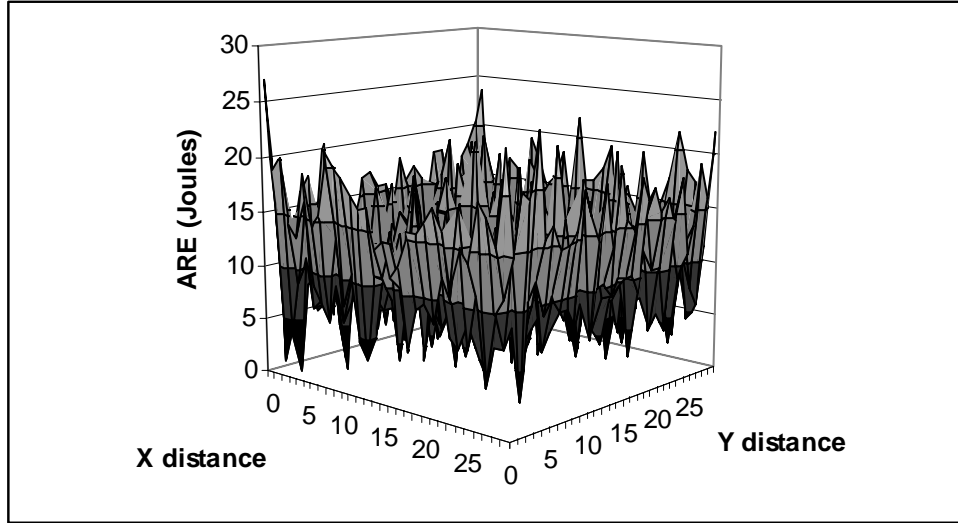


Figure 60: ARE for 30x30 (900 nodes) square grid GSP network ($p = 0.3$) with transmission power/radius d .

7.2.1.2 Transmission Power/Radius $2d$ in the Square Grids

Table 9 shows the simulation parameters and energy consumption model used in transmission power/radius $2d$ analysis. With the increased transmission power, the simulation allows more sleeping nodes in each gossip period. Figures 42 and 43 evaluate the gossip sleep probability (p) that creates a connected network. The plots suggest $p = 0.6$ as the gossip sleep probability for all GSP network sizes when using $2d$ transmission power/radius.

Table 9: Simulation parameters and energy consumption model when using transmission power/radius $2d$.

<i>Data rate</i>	19.2 kbps
<i>Packet size</i>	21 bytes
<i>MAC</i>	CSMA/CA
<i>Initial energy stored</i>	50 Joules

<i>Transmit</i>	4.28 μ Joules/bit
<i>Receive</i>	2.36 μ Joules/bit
<i>Idle/Listening</i>	2.36 μ Joules/bit
<i>Sleep</i>	0.9 μ Joules/bit

Figure 61 presents the network lifetime in term of the average number of gossip periods when using $p = 0$ in the Non-GSP and $p = 0.6$ in the GSP network. The results show that the highest average number of gossip periods occurs for the small GSP network (150 periods). Because of the high traffic load, when networks increase in size, the average number of gossip periods reduces on both GSP and Non-GSP. Since the longer gossip period consumes more energy in the idle/listening states, when using $G_p = 360$ seconds with $2d$ transmission power/radius, the average number of gossip period decreases.

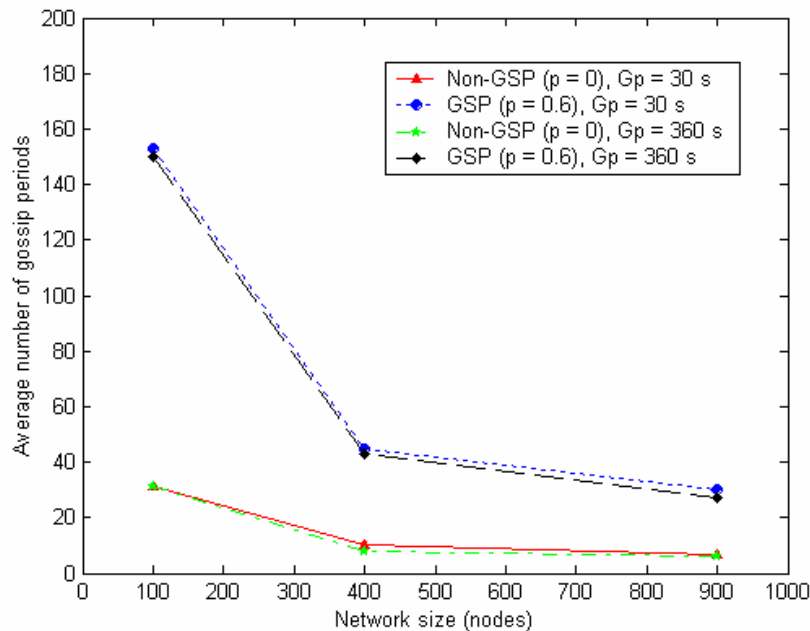


Figure 61: Average number of gossip periods vs. network size for the square grids with transmission power/distance $2d$, $G_p = 30$ and 360 seconds.

Figure 62 demonstrates the change in network lifetime when using GSP_{2d} compared to Non- GSP_{2d} . Since, in Non- GSP_{2d} , nodes transmit with high transmission power without sleeping nodes in the network, energy is consumed faster than Non- GSP_d . The largest change occurs for the small network with the 360 seconds gossip period, which the changes tend to decrease when the networks increase in size.

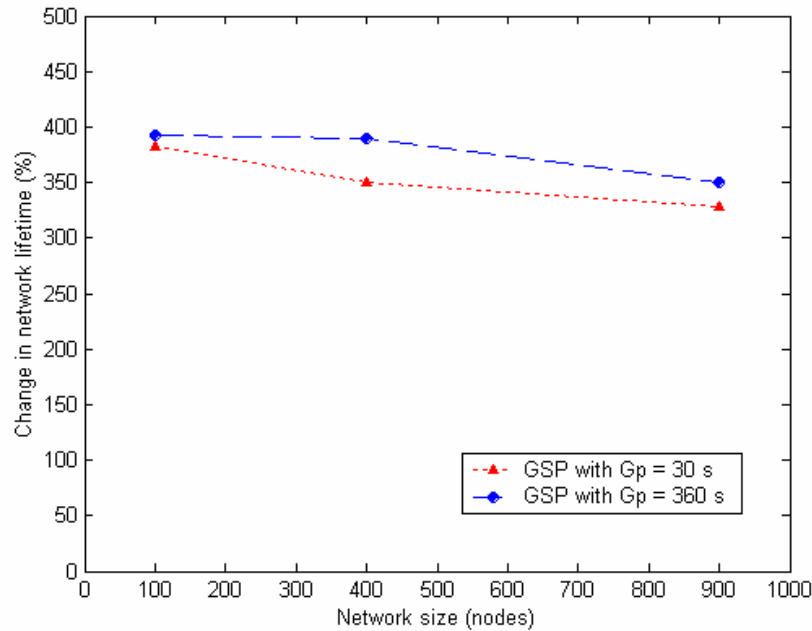


Figure 62: The changes in network lifetime on the different sizes of the square grids with transmission power/radius $2d$ when using GSP with $p = 0.6$ compared to Non-GSP, $G_p = 30$ and 360 seconds.

Figure 63 presents the simulated network lifetime when using the transmission power $2d$ in three sizes of square grids. The longest network lifetime occurs for the small GSP network with the 360 second gossip period. Figure 64 plots the ARE per node varying on different network sizes. The ARE improves when the network size increases in GSP network. On the other hand, ARE shows a decrease for the large network size in Non-GSP network.

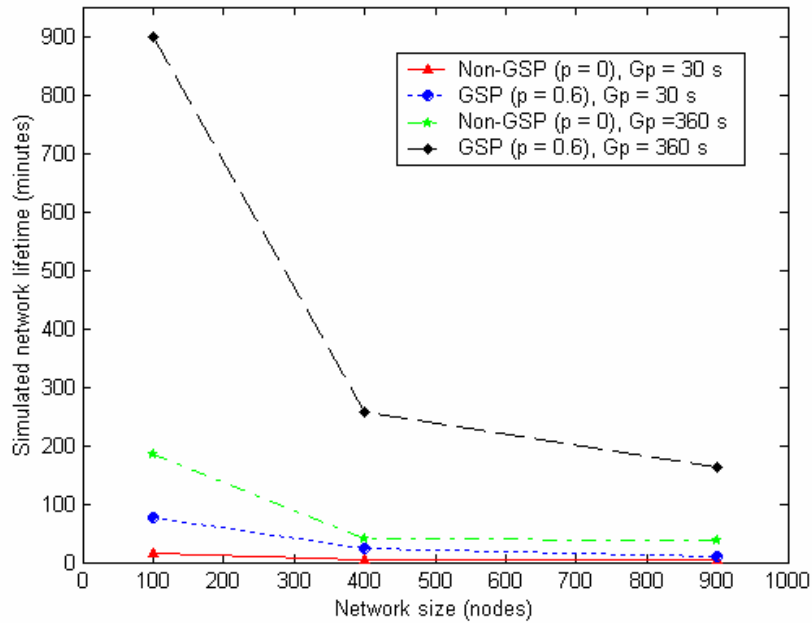


Figure 63: Simulated network lifetime vs. network size for the square grids with transmission power/distance $2d$, $G_p = 30$ and 360 seconds.

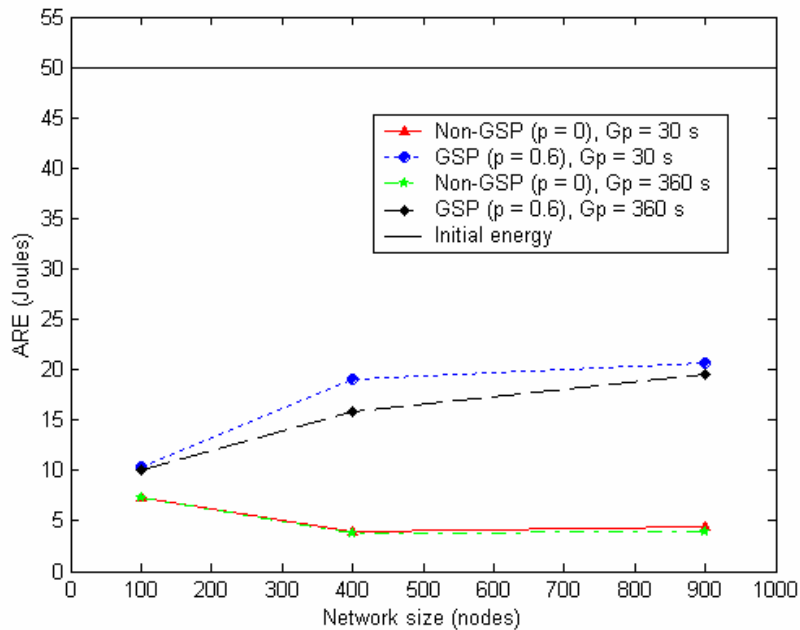


Figure 64: Average remaining energy (ARE) vs. network size for the square grids with transmission power/radius $2d$, $G_p = 30$ and 360 seconds.

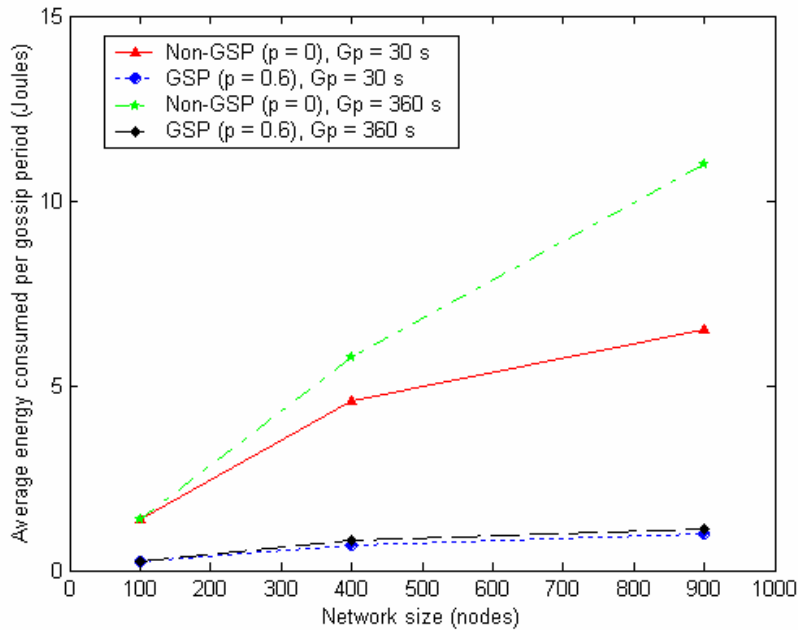


Figure 65: Average energy consumed per gossip period vs. network size for the square grids with transmission power/radius $2d$, $G_p = 30$ and 360 seconds.

Figure 65 represents the average energy consumed per gossip period for both GSP and non-GSP networks. GSP network shows lower energy consumption in a node per gossip period for all network sizes compared to Non-GSP. Figure 66 shows the packet loss ratio on both GSP and Non-GSP networks when using transmission power/radius $2d$. The GSP packet loss ratio drops under 10% in the 30 seconds gossip period, which improves from the ones with the transmission power/radius d . However, GSP network presents the higher packet loss ratio compared to Non-GSP network in the $2d$ case. The observation is that GSP has high number of sleeping nodes (60%), which presents less traffic as forward/relay packet. Thus, when presenting the ratio of the total number of dropped packets divided by the total number of transmitted/relayed packets, the GSP results show the higher packet loss rate in $2d$ case. The results show a decreased packet loss ratio for only the small GSP and Non-GSP networks in the 360 seconds gossip period, which is increased when the network size increases.

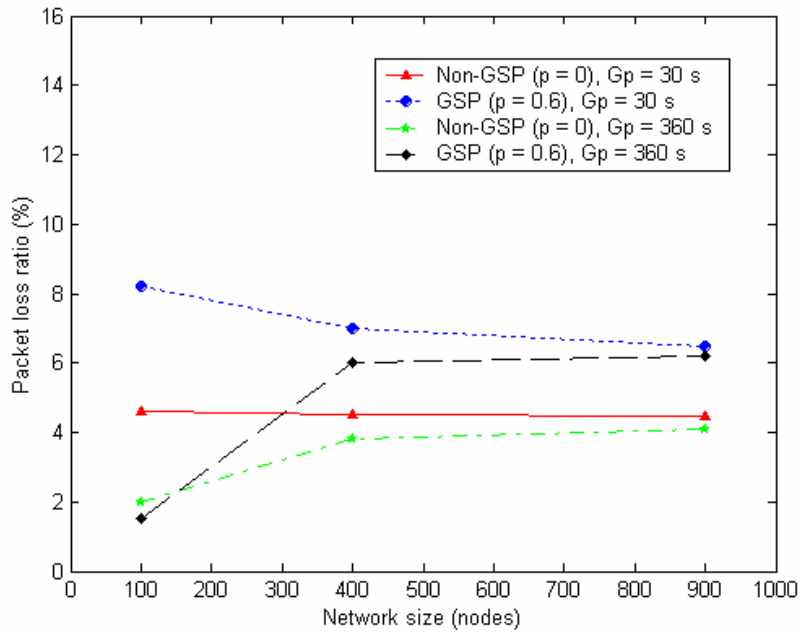


Figure 66: Packet loss ratio vs. network size for the square grids with transmission power/radius $2d$, $G_p = 30$ and 360 seconds.

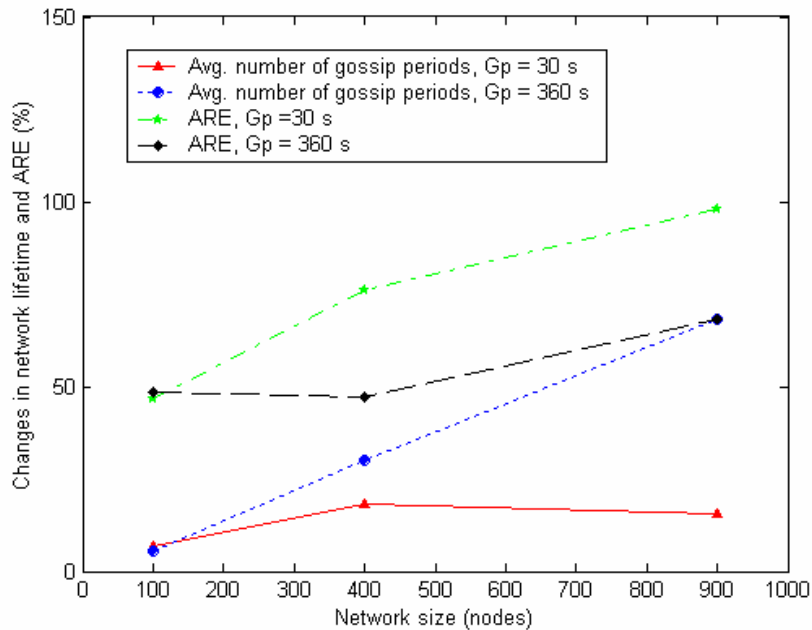


Figure 67: The changes of the average number of gossip periods and AREs in the square grids when using GSP_{2d} compared to GSP_d with $G_p = 30$ and 360 seconds.

Figure 67 demonstrates the changes in percentage of the average number of gossip periods and AREs when using transmission power/radius $2d$ compared to d in the GSP network on both $G_p = 30$ and 360 seconds in the square grids. Even though GSP_{2d} employs a higher transmission power than GSP_d , with higher p GSP_{2d} shows increasing network lifetime compared to GSP_d . When the network size increases, the network lifetime improvement in GSP_{2d} increases. Also, the results show that the networks employing GSP_{2d} improve on the ARE. The largest change occurs for the ARE with the shorter gossip period ($G_p = 30$ seconds), which the ARE improvement increases when the network size increases. Employing GSP_{2d} over GSP_d in the small network (100 nodes) shows small improvements on both network lifetime and ARE.

Figures 68 and 69 represent the plots on ARE in the 100 nodes square grid with transmission power/radius $2d$ on both Non-GSP and GSP respectively. In the Non-GSP network, all nodes rapidly deplete their energy stores. Networks employing GSP show the increasing in ARE from the average of 7.32 to 10.3 Joules (40%). As networks increase in size, ARE increases, which is from the average of 4.48 to 20.64 Joules (360%) as shown in Figures 70 and 71.

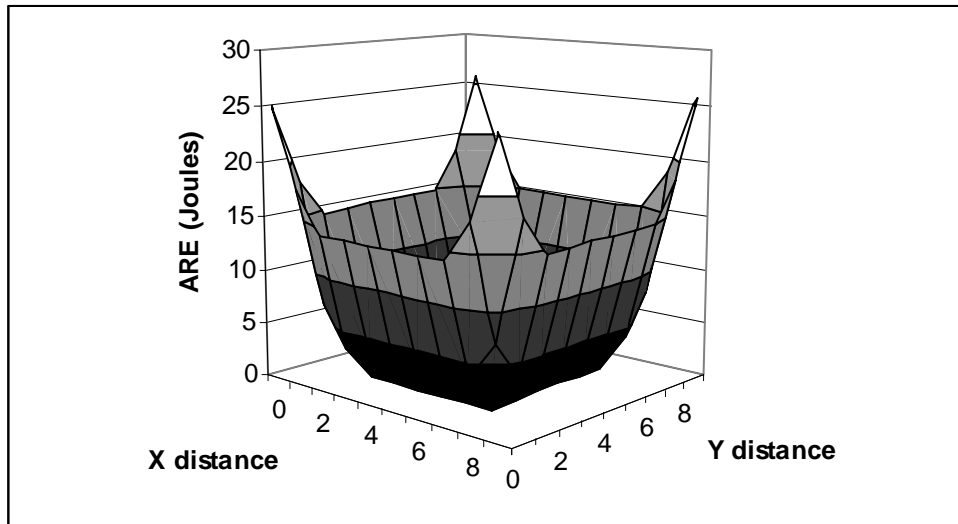


Figure 68: ARE for 10x10 (100 nodes) square grid Non-GSP network ($p = 0$) with transmission power/radius $2d$.

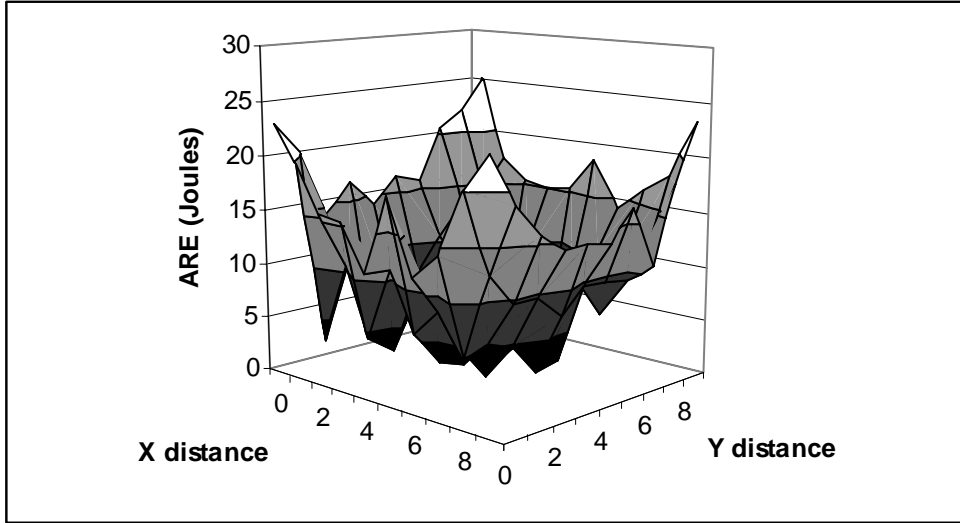


Figure 69: ARE for 10x10 (100 nodes) square grid GSP network ($p = 0.6$) with transmission power/radius $2d$.

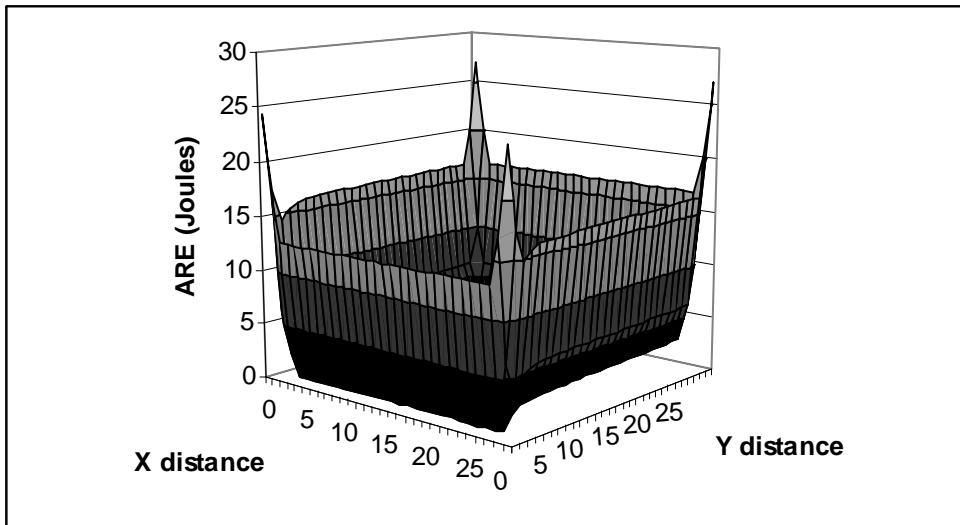


Figure 70: ARE for 30x30 (900 nodes) square grid Non-GSP network ($p = 0$) with transmission power/radius $2d$.

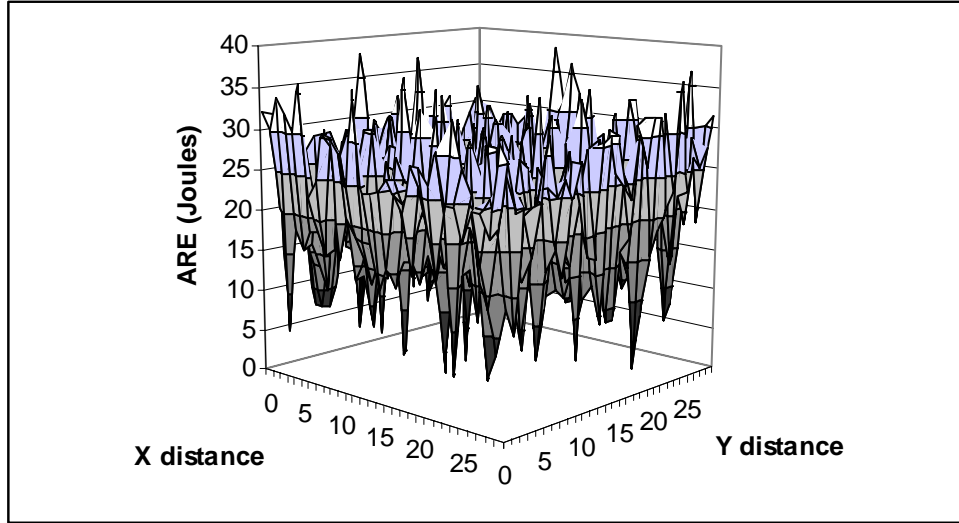


Figure 71: ARE for 30x30 (900 nodes) square grid GSP network ($p = 0.6$) with transmission power/radius $2d$.

This subsection has shown GSP network lifetime analysis performing on various sizes of square grids when using transmission power d and $2d$. Simulation results show that by allowing some sensor nodes into sleep states, such as GSP network, we can extend the square grids network lifetime and improve network energy remaining for all network sizes. When the networks use d transmission power, GSP_d presents the largest network lifetime improvement (70%) in the small network size (100 nodes) for both 30 and 360 seconds gossip period. However, the improvement drops to 40% in the medium and large networks. The networks employing GSP increase in ARE when the network size increases. Unlike the Non- GSP_d , as networks increase in size, the ARE decreases. As a result, the largest ARE improvement occurs for the large network (900 nodes), which is the average of 8.8 to 10 Joules. GSP_d shows smaller packet loss ratio by approximately 1-2 % for all network size on the 30 seconds gossip period. Since the small network presents less traffic, the smallest packet loss ratio occurs for the small network size (100 nodes) with the 360 seconds gossip period. When networks use the longer gossip period, a node has more time to transmit packets because the simulation applies lower transmission rate. However, the packet loss ratio increases as same as the 30 seconds gossip period in the medium and large network sizes.

When the networks employ GSP_{2d} compared to $Non-GSP_{2d}$, the network lifetime is extended by 3 – 4 lifetimes and the ARE increases by 2 – 16 Joules ranged from small to large network sizes. However, the packet loss ratio in GSP is higher than Non-GSP by approximately 2 – 4%. Even though the simulation applied the same generated traffic between GSP and Non-GSP networks, GSP still has less forward/relay traffic resulted by the sleeping nodes. Thus, when presenting the ratio of the total number of packet collisions divided by the total number of transmitted/relayed packets, the GSP results show higher packet loss rate in $2d$ case.

When using GSP_{2d} over GSP_d , the network lifetime is increased by 7 – 16% in the 30 seconds gossip period and 6 – 68% in the 360 seconds gossip period ranging from small to large networks. Moreover, the ARE increases approximately 50 – 100% when using GSP_{2d} over GSP_d .

7.2.2 Rectangular Grids

Rectangular grids are the common topologies employed in the environments such as bridges, roads, and airport runways monitoring. GSP performs on three rectangular grid sizes, 5×20 , 5×100 , and 5×200 , which are 100, 500, and 1000 node networks respectively.

7.2.2.1 Transmission Power/Radius d in the Rectangular Grids

To perform GSP on various rectangular grid sizes with the d transmission power/radius, the simulation employed the energy consumption model as shown in Table 8. Since the gossip sleep probability (p) varies over topologies, the simulation finds the average path length and the average number of disconnected nodes to evaluate the highest sleep probability that create a connected network called gossip sleep probability (p). Figures 72 and 73 represents the average path length in hops and ratio of nodes disconnected performing on various sleep probabilities. The plots recommend the gossip sleep probabilities (p) for 5×20 , 5×100 , and 5×200 node networks equal to 0.25, 0.15, and 0.15 respectively.

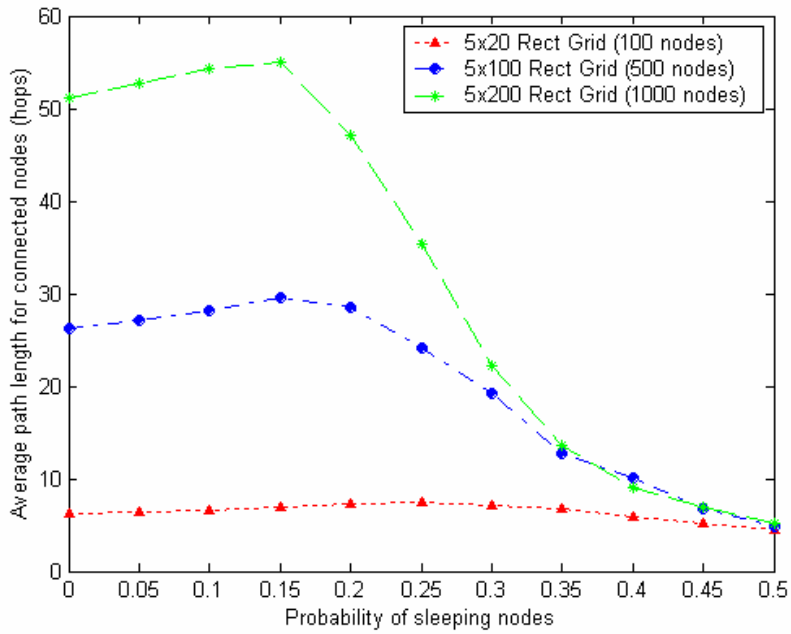


Figure 72: Probability of sleeping nodes vs. average path length for connected nodes in rectangular grids.

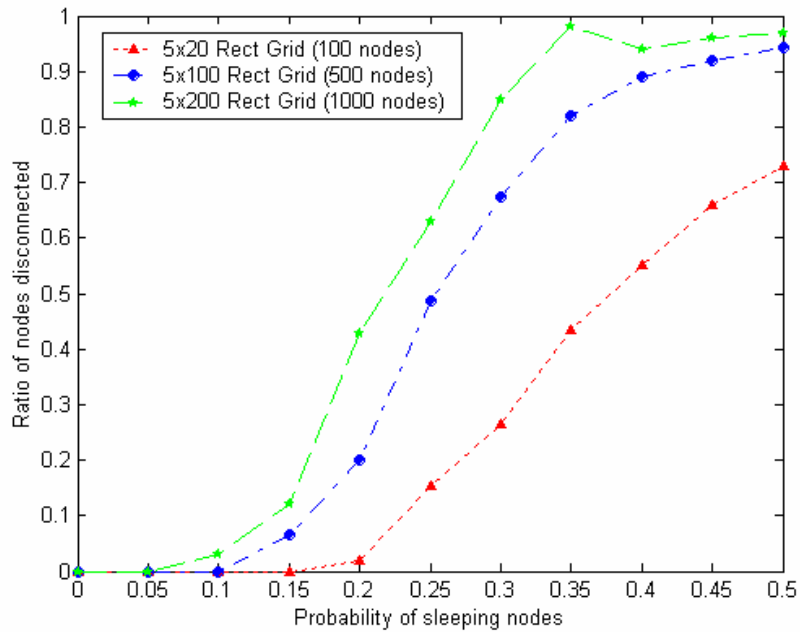


Figure 73: Probability of sleeping nodes vs. ratio of nodes disconnected in rectangular grids.

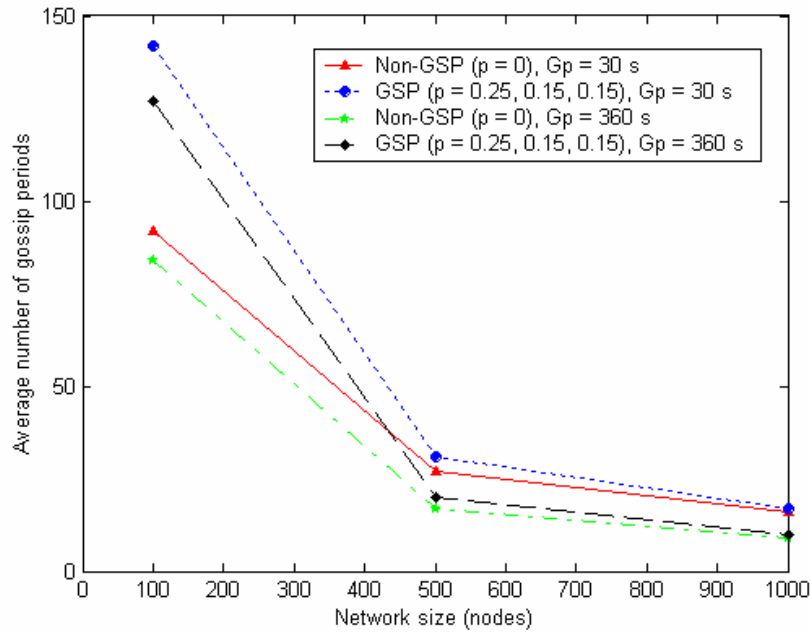


Figure 74: Average number of gossip periods vs. network size for the rectangular grids with transmission power/distance d , $G_p = 30$ and 360 seconds.

Figure 74 shows a plot on average number of gossip periods that represents the network lifetime on GSP and Non-GSP network in the rectangular grids when using transmission power/radius d . The highest average number of gossip periods occurs for the 100 node network. Since GSP used the small gossip sleep probability ($p = 0.15$) in the 1000 node network, the average number of gossip periods shows a small increase. Also,

Figure 75 presents the change in the network lifetime when using GSP over Non-GSP network. When the networks increase in size, the changes tend to decrease on both $G_p = 30$ and 360 seconds.

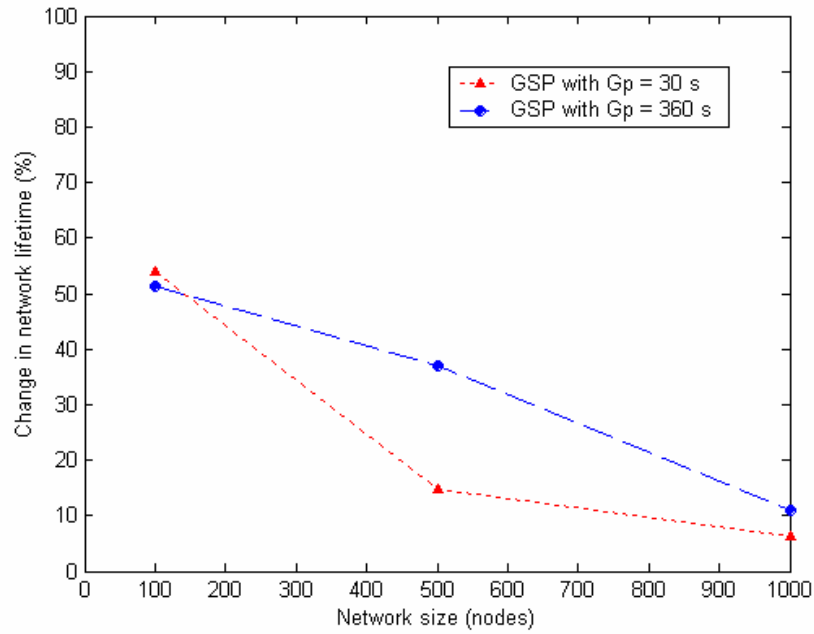


Figure 75: The changes in network lifetime on the different sizes of the rectangular grids with transmission power/radius d when using GSP compared to Non-GSP, $G_p = 30$ and 360 seconds.

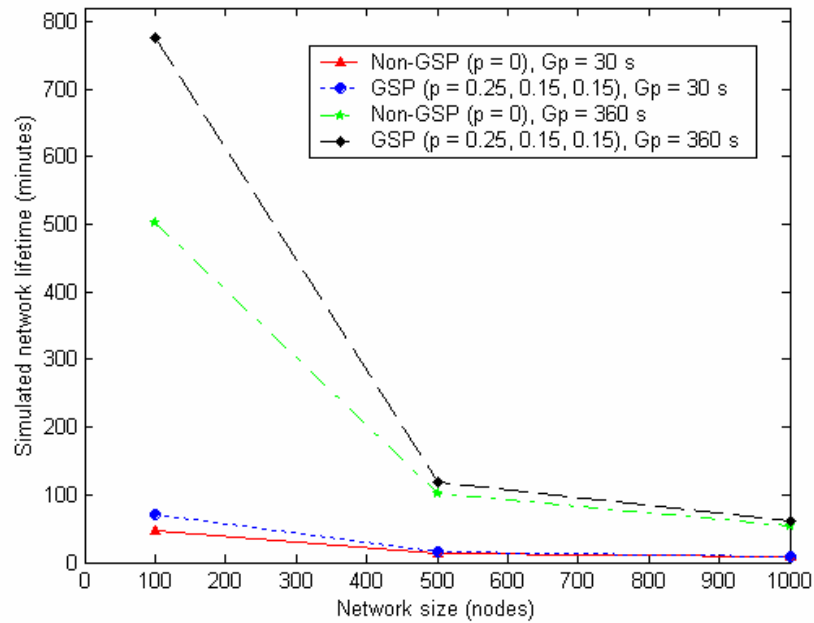


Figure 76: Simulated network lifetime vs. network size for the rectangular grids with transmission power/distance d , $G_p = 30$ and 360 seconds.

Figure 76 presents the simulated network lifetime. The longest network lifetime occurs for the small GSP network with the 360 seconds gossip period. Figure 77 plots the ARE per node performed on the rectangular grids when using transmission power/radius d . Networks employing GSP shows higher ARE compared to Non-GSP for all network sizes on both 30 and 360 seconds gossip periods. ARE increases with GSP network and decreases with Non-GSP network when the network increases in size.

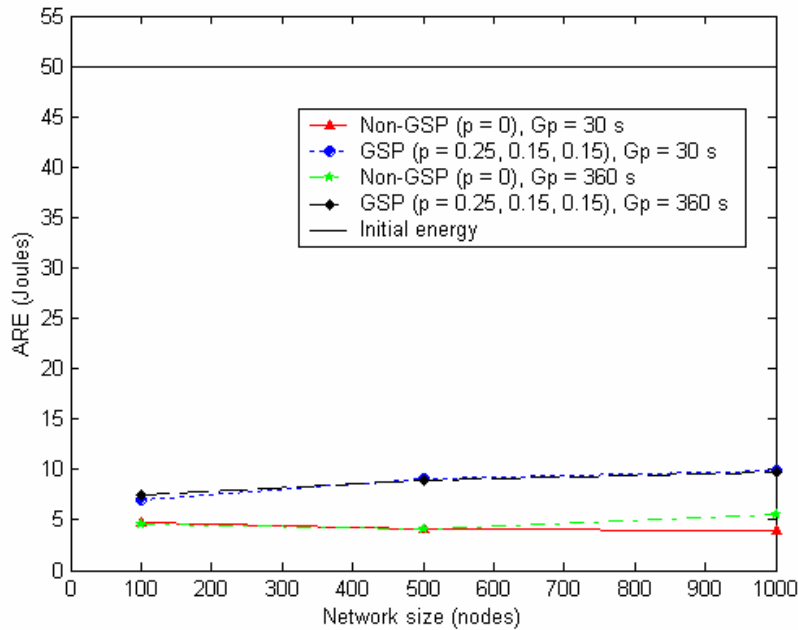


Figure 77: Average remaining energy (ARE) vs. network size for the rectangular grids with transmission power/radius d , $G_p = 30$ and 360 seconds.

Figure 78 shows the average energy consumed per gossip period for both GSP and Non-GSP networks. The GSP network consumes lower energy compared to Non-GSP for both 30 and 360 second gossip periods. However, the longer gossip period time shows higher energy consumption compared to the shorter one.

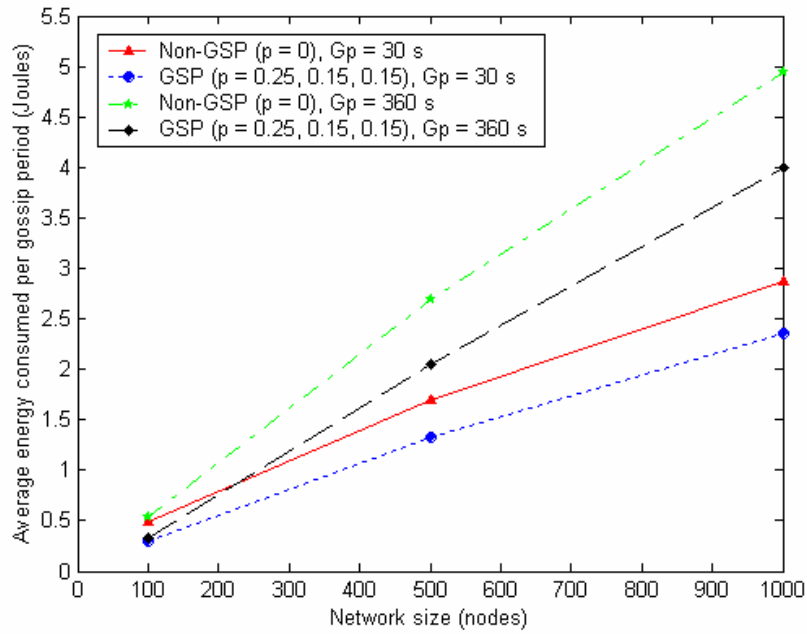


Figure 78: Average energy consumed per gossip period vs. network size for the rectangular grids with transmission power/distance d , $G_p = 30$ and 360 seconds.

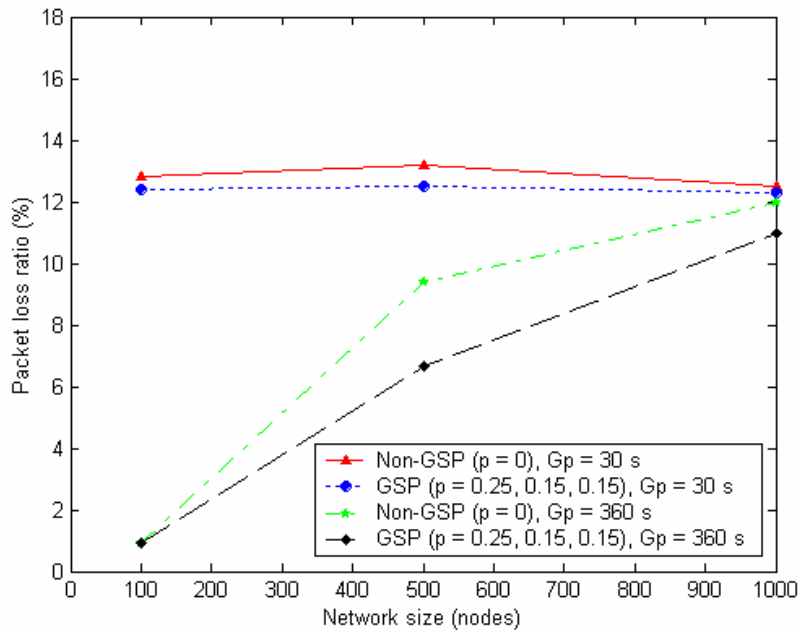


Figure 79: Packet loss ratio vs. network size for the rectangular grids with transmission power/radius d , $G_p = 30$ and 360 seconds.

Figure 79 illustrates the packet loss ratio in the rectangular grids, which GSP shows smaller ratios compared to Non-GSP on both 30 and 360 seconds gossip period. The small network with the longer gossip period ($G_p = 360$ seconds) presents a smaller ratio, which increases as the network increases in size.

Figures 80 and 81 plot the ARE per node in the 5x20 (100 nodes) network when using transmission power/radius d with the 30 seconds gossip period (G_p). All nodes quickly deplete their energy stores in Non-GSP network. With a certain gossip sleep probability, GSP can increase the ARE by 45% in the 100 node network. Moreover, Figures 82 and 83 present the ARE plots on the 5x200 (1000 nodes) rectangular grids. The result shows that ARE has increased by 140% in the large GSP network (1000 nodes).

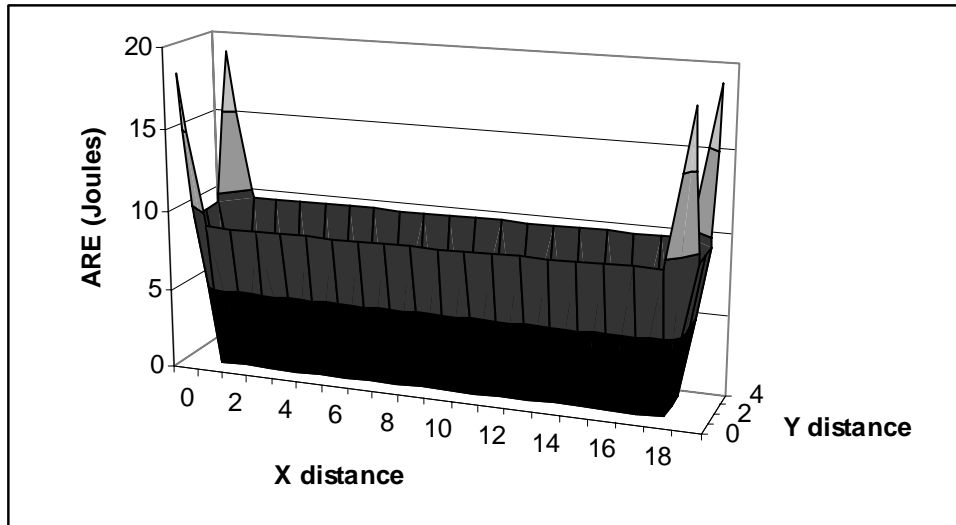


Figure 80: ARE for 5x20 (100 nodes) rectangular grid Non-GSP network ($p = 0$) with transmission power/radius d .

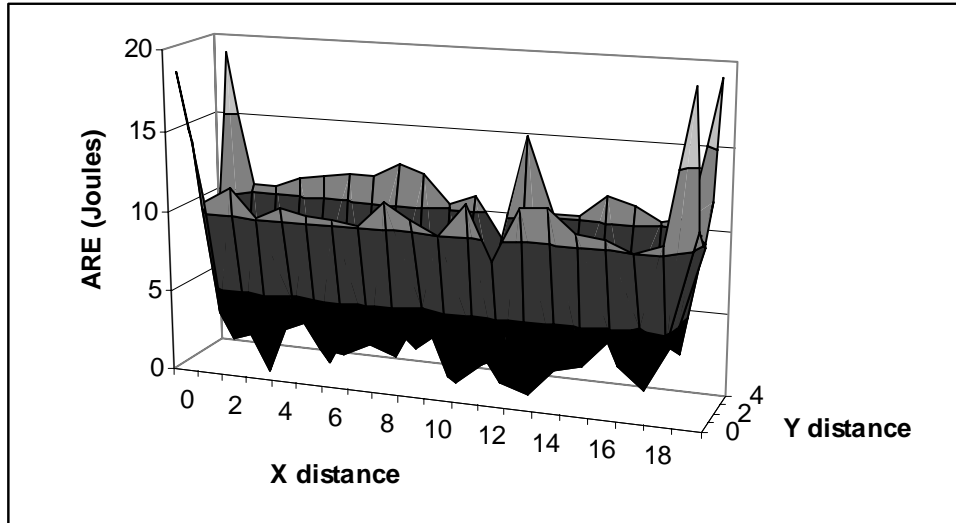


Figure 81: ARE for 5x20 (100 nodes) rectangular grid GSP network ($p = 0.25$) with transmission power/radius d .

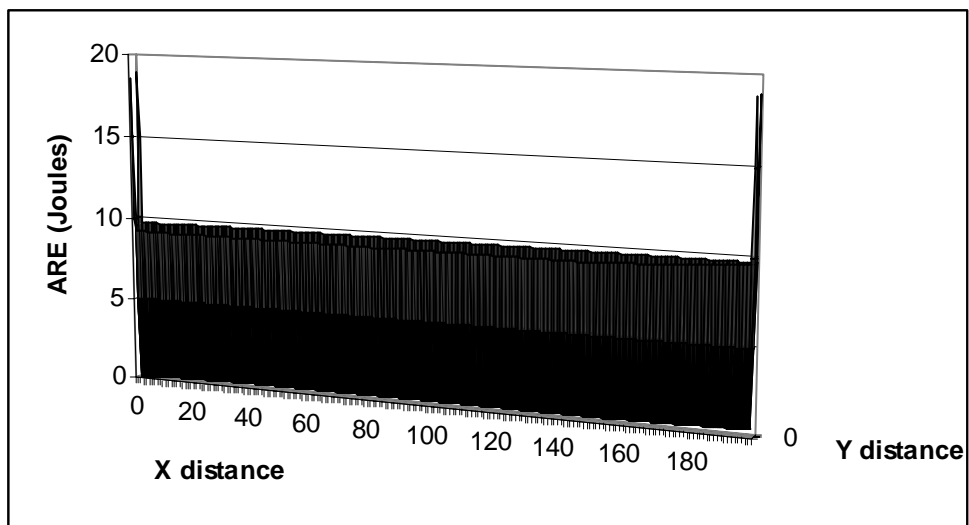


Figure 82: ARE for 5x200 (1000 nodes) rectangular grid Non-GSP network ($p = 0$) with transmission power/radius d .

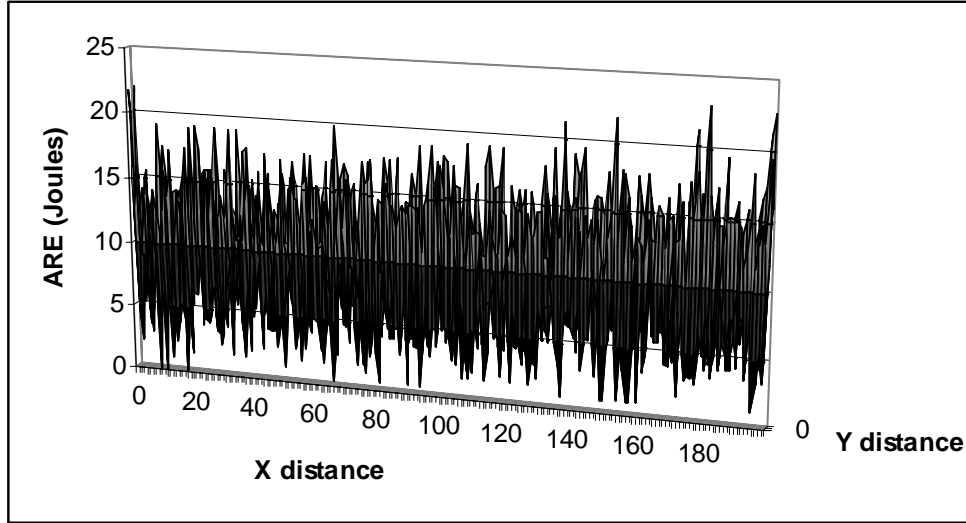


Figure 83: ARE for 5x200 (1000 nodes) rectangular grid GSP network ($p = 0.15$) with transmission power/radius d .

7.2.2.2 Transmission Power/Radius $2d$ in the Rectangular Grids

When networks increase the transmission power/radius in the rectangular grids, the simulation applied the energy consumption model in Table 9, which nodes use 5 dBm as transmission power. The subsection analyses the network lifetime of the rectangular grids, 5x20, 5x100, 5x200, which has 100, 500, and 1000 nodes when using higher transmission power/radius. First, the simulation evaluates the average path length and the ratio of nodes disconnected on various sleep probabilities. With higher transmission power/radius, Figures 84 and 85 recommend the gossip sleep probability (p) equal to 0.55, 0.45, and 0.4 for the 100, 500 and 1000 node networks respectively. These probabilities are the highest sleep probabilities that create connected networks.

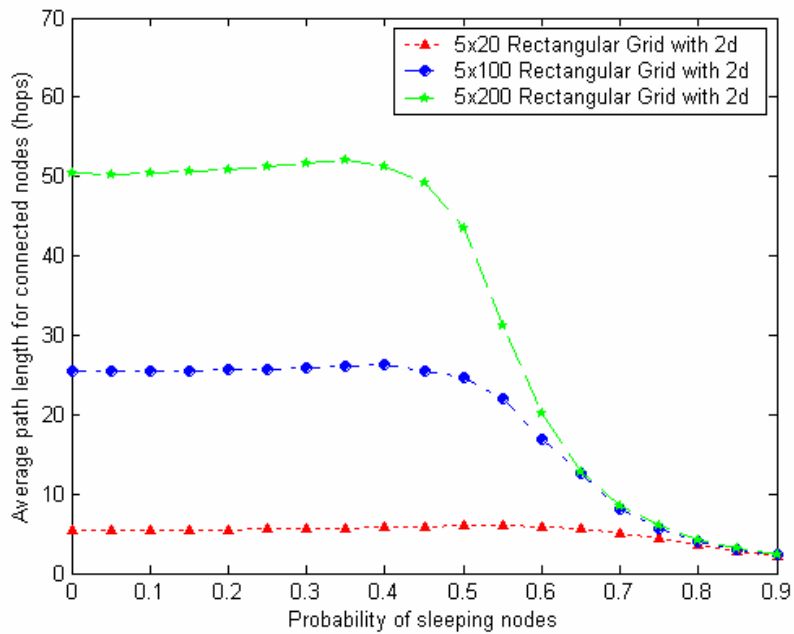


Figure 84: Probability of sleeping nodes vs. average path length for connected nodes in rectangular grids with $2d$ transmission power/radius.

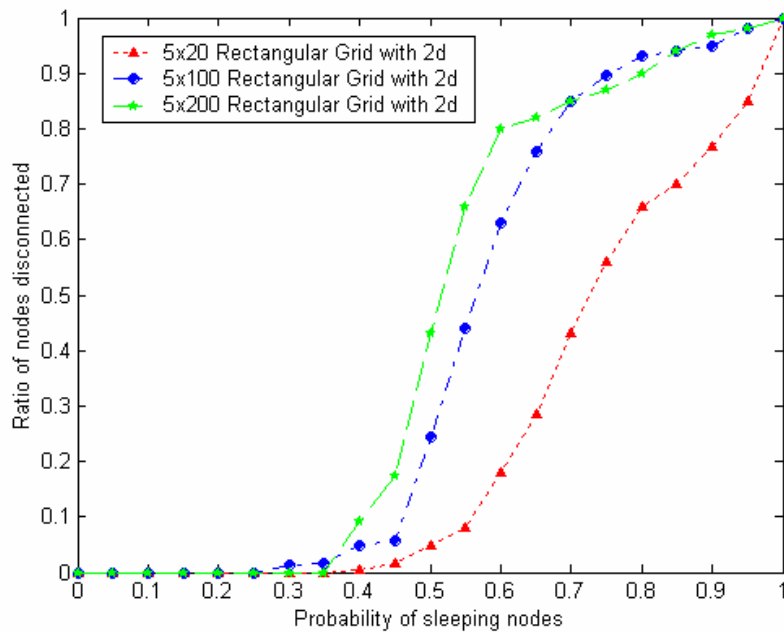


Figure 85: Probability of sleeping nodes vs. ratio of nodes disconnected in rectangular grids with $2d$ transmission power/radius.

Figure 86 presents the average number of gossip periods in the rectangular grids when using

transmission power/radius $2d$. The average number of gossip periods increases when employing GSP for all network sizes. However, as the networks increase in size, the average number of gossip periods decrease.

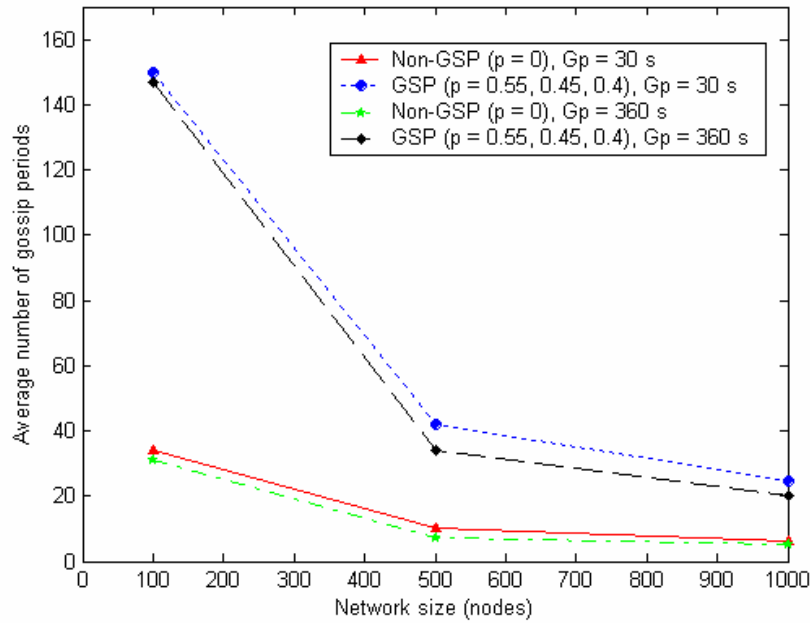


Figure 86: Average number of gossip periods vs. network size for the rectangular grids with transmission power/distance $2d$, $G_p = 30$ and 360 seconds.

Figure 87 demonstrates the changes in network lifetime when using transmission power/radius $2d$ in the GSP network compared to the Non-GSP network. The huge change is due to the fact that Non-GSP network with transmission power/radius $2d$ consumes high energy in transmission without sleeping nodes in the network. The largest change occurs for the medium network with the 360 gossip period. The plots shows non-straight lines due to the different in gossip sleep probabilities (p) using for the different network sizes. Also, when the network increases in size, the rectangular grid topology is changed, which affects the changes in network lifetime.

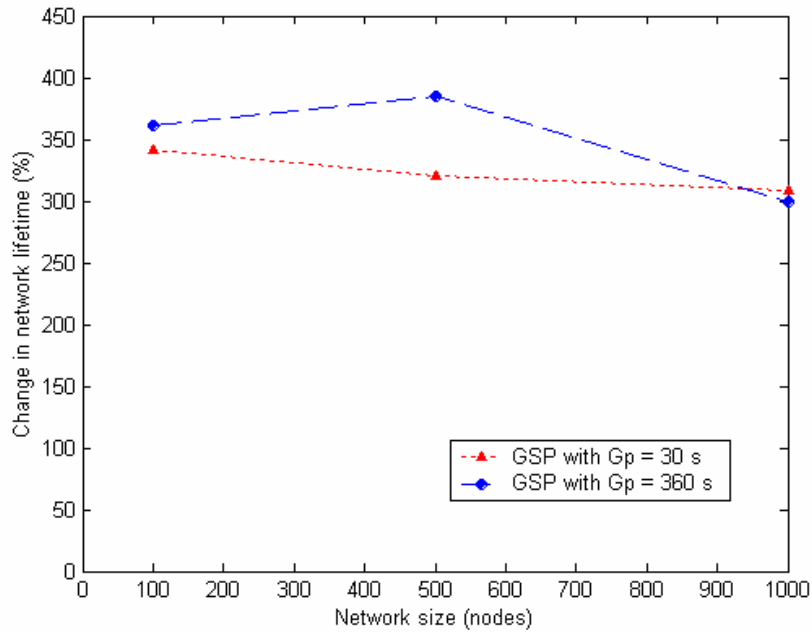


Figure 87: The changes in network lifetime on the different sizes of the rectangular grids with transmission power/radius $2d$ when using GSP compared to Non-GSP, $G_p = 30$ and 360 seconds.

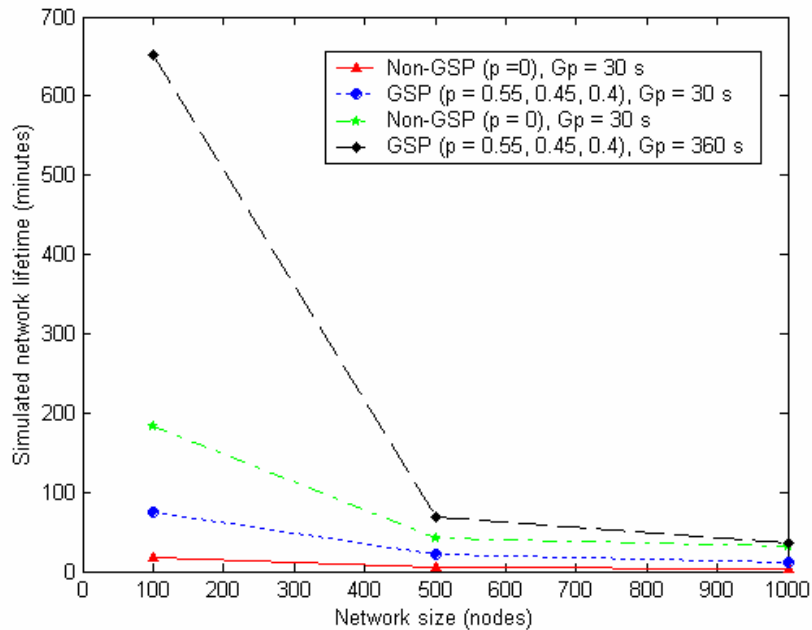


Figure 88: Simulated network lifetime vs. network size for the rectangular grid topologies with transmission power/distance $2d$, $G_p = 30$ and 360 seconds.

Figure 88 illustrates the simulated network lifetime performed on three sizes of rectangular grids. The longest network lifetime is presented in the small GSP network with the 360 seconds gossip period. Figure 89 plots the ARE per node in rectangular grids when using transmission power/radius $2d$. GSP shows higher AREs for all network sizes. Moreover, ARE increases when the GSP network size increases. The longer gossip period ($G_p = 360$ seconds) presents a small decrease in the ARE compared to the shorter one ($G_p = 30$ seconds).

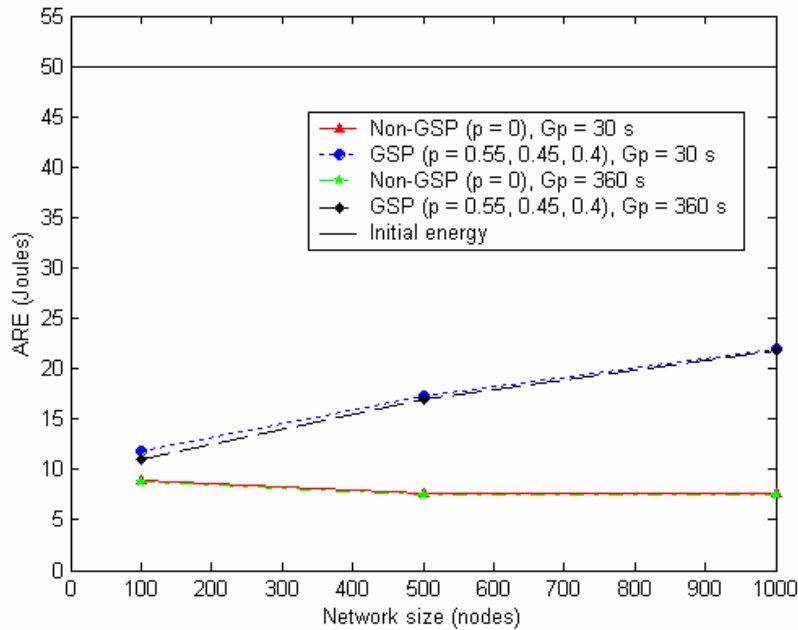


Figure 89: Average remaining energy (ARE) vs. network size for the rectangular grids with transmission power/radius $2d$, $G_p = 30$ and 360 seconds.

Figure 90 shows that the average energy consumed per gossip period varies over different network sizes for both GSP and Non-GSP networks. However, GSP networks consume less energy compared to Non-GSP for all network sizes.

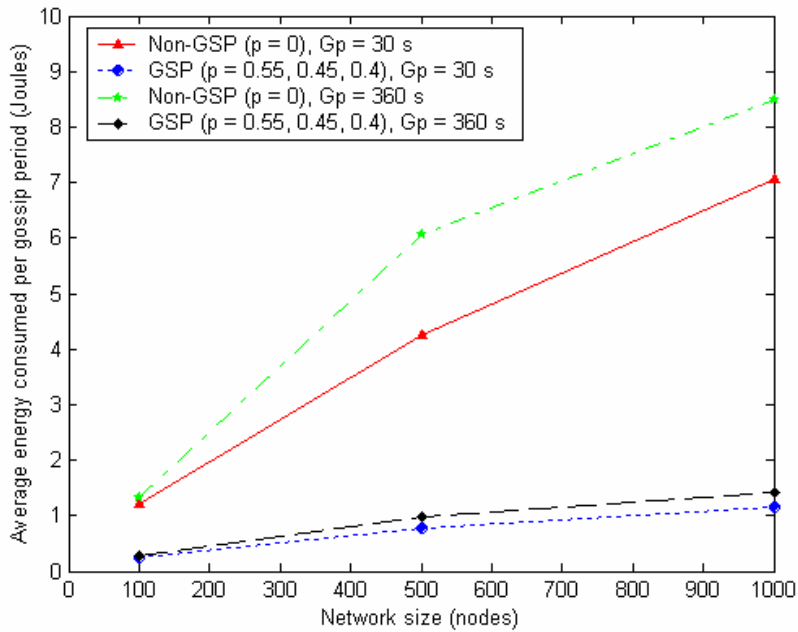


Figure 90: Average energy consumed per gossip period vs. network size for the rectangular grids with transmission power/distance $2d$, $G_p = 30$ and 360 seconds.

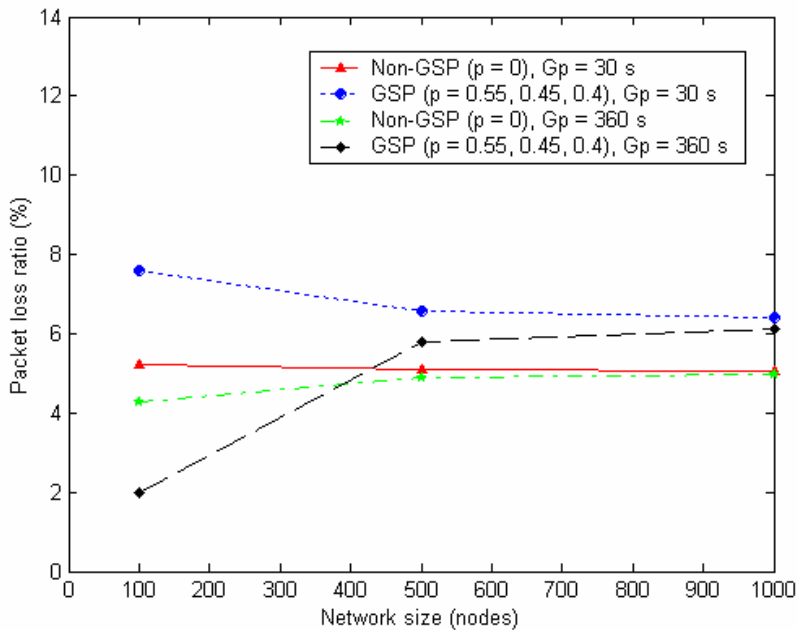


Figure 91: Packet loss ratio vs. network size for the rectangular grids with transmission power/radius $2d$, $G_p = 30$ and 360 seconds.

Figure 91 represents the packet loss ratio in the rectangular grids with transmission power/radius $2d$. Networks employing GSP show the higher packet loss ratio compared to the Non-GSP network in the $2d$ case. GSP network offers less relay/forward traffic resulted by sleeping nodes. Thus, the ratio of the total number of dropped packets over the total number of transmitted/relayed packets in the GSP network can be higher than in the Non-GSP network. However, the smallest packet loss ratio occurs for the small GSP network with the 360 seconds gossip period. Figure 92 demonstrates the changes in percentage of average number of gossip periods and the AREs when using transmission power/radius $2d$ compared to d in the GSP network performed on the rectangular grids with both $G_p = 30$ and 360 seconds. The results show that GSP network presents improvements on both network lifetime and ARE when increasing transmission power/radius from d to $2d$. The change increases when the network size increases. The largest change occurs for the ARE in large network (122%).

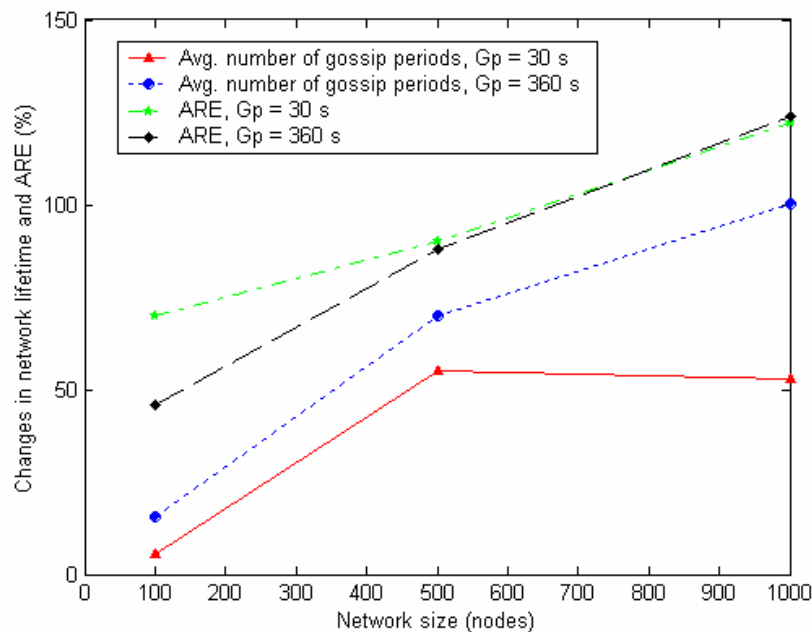


Figure 92: The changes of the average number of gossip periods and AREs in the rectangular grids when using GSP_{2d} compared to GSP_d with $G_p = 30$ and 360 seconds.

Figures 93 and 94 plot ARE in the 100 node rectangular grid for Non-GSP and GSP networks respectively. By employing GSP, the ARE increases by 33% in the 30 seconds gossip period and 37.5% in the 360 seconds gossip periods.

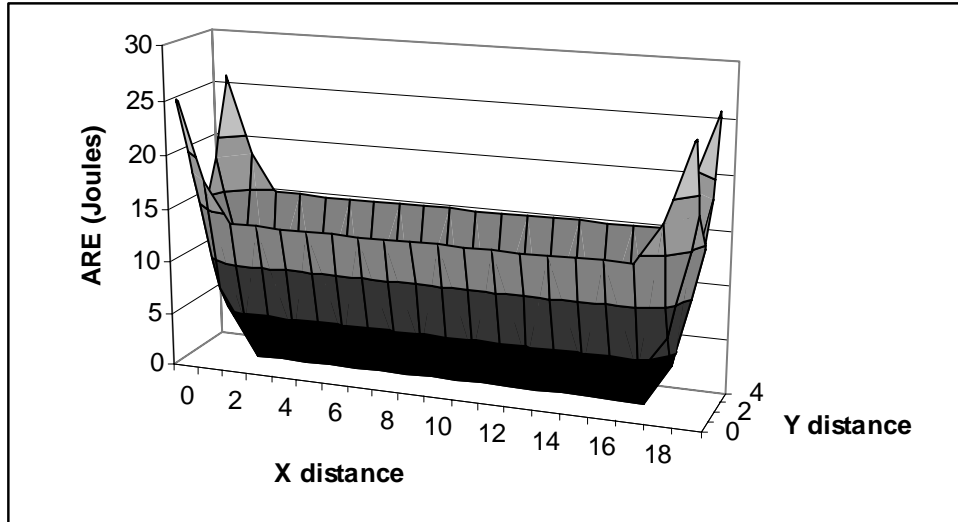


Figure 93: ARE for 5x20 (100 nodes) rectangular grid Non-GSP network ($p = 0$) with transmission power/radius $2d$.

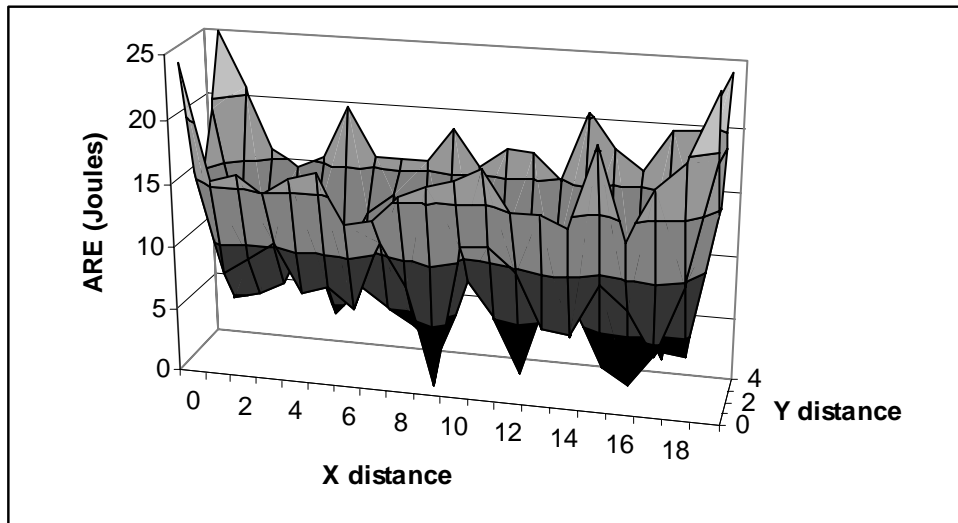


Figure 94: ARE for 5x20 (100 nodes) rectangular grid GSP network ($p = 0.55$) with transmission power/radius $2d$.

Figures 95 and 96 present the ARE plots in 5x200 (1000 nodes) for the Non-GSP and GSP networks respectively. The results show the huge increasing in ARE for the 1000 node network, which is 185% in the 30 seconds gossip period and 191% in the 360 seconds gossip period.

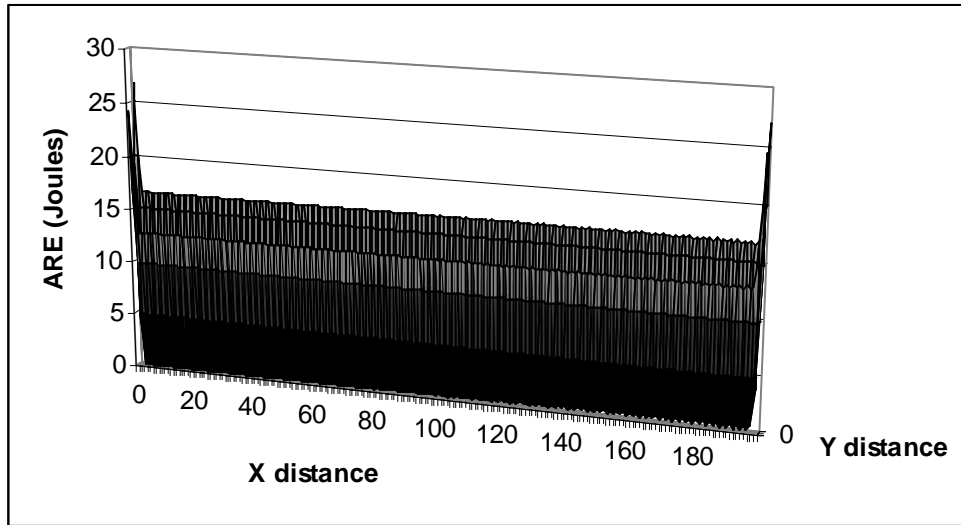


Figure 95: ARE for 5x200 (1000 nodes) rectangular grid Non-GSP network ($p = 0$) with transmission power/radius $2d$.

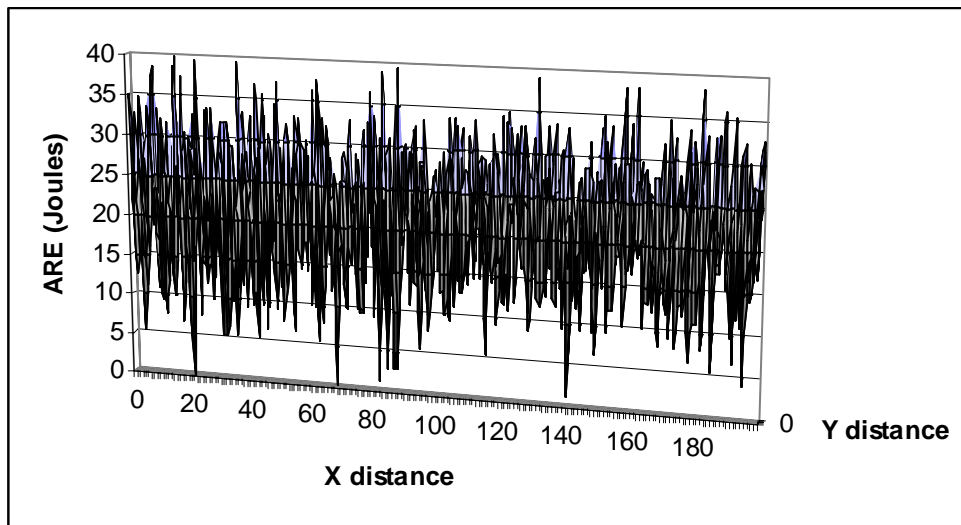


Figure 96: ARE for 5x200 (1000 nodes) rectangular grid GSP network ($p = 0.4$) with transmission power/radius $2d$.

By using GSP in the rectangular grids with transmission power/radius d , the network lifetime is increased by approximately 55% in the small and 10% in the large network. The small increasing in the rectangular grid network lifetime is the result of the smaller optimal value of the gossip sleep probability (p) that was figured and used by the simulation. In addition, the ARE is improved by 2-5 Joules ranged from small to large network sizes. GSP_d shows smaller packet loss ratio compared to Non-GSP_d, which the smallest ratio occurs for the small network (100 nodes). However, the packet loss ratio increases when the network size increases.

Networks employing GSP_{2d} extend the network lifetime approximately by 3 – 4 lifetimes. Moreover, the ARE is improved by 3 – 14 Joules ranging from small to large network. GSP shows higher packet loss ratio compared to Non-GSP_{2d} except the small 5x20 (100 node) network with the 360 seconds gossip period. Using GSP_{2d} over GSP_d extends the network lifetime approximately by 5 – 53% in the 30 seconds gossip period and 15 – 100% in the 360 seconds gossip period ranging from small to large network size. In addition, ARE is increased by 45 – 125%.

Since one of the research goals is to study the GSP performance on various network topologies. Therefore, in the next subsections, the simulation will perform GSP network lifetime analysis on the random grid, lattice topology, and star topology.

7.2.3 Random Grid Topology

The deployment of sensor nodes in the physical environment may take several forms. However, one of the most practical network deployments is to place the sensor nodes randomly. Nodes are normally spread out to observe the ongoing activities in the environment, which may be employed randomly, e.g., by dropping from the aircraft or throwing to the inaccessible environment. However, to the best analysis in this research, the simulation randomly assigns nodes into grids to ensure that the entire area will be properly covered. Thus, to observe the energy efficiency in the networks, GSP performs on the different sizes of random grid topologies.

7.2.3.1 Transmission Power/Radius d in the Random Grid Topology

The simulation tests GSP with the d transmission power/radius, which allows node to transmit a packet to the neighbors within one hop away. To evaluate GSP performance, the simulation selected topologies that can provide the best analysis in comparison to Non-GSP network. The following three selected random grid topologies demonstrate how the simulation randomly assigns the nodes into $d \times d$ grids.

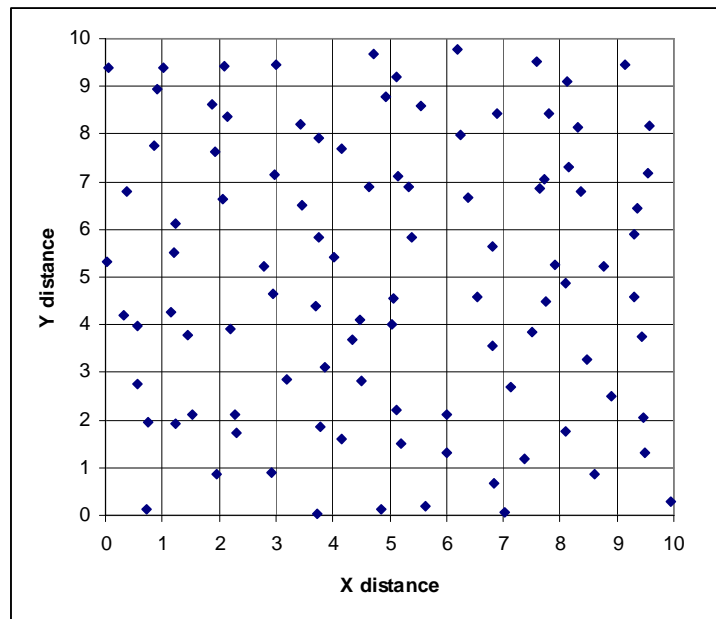


Figure 97: A random $10d \times 10d$ grid topology with one node in a $d \times d$ grid.

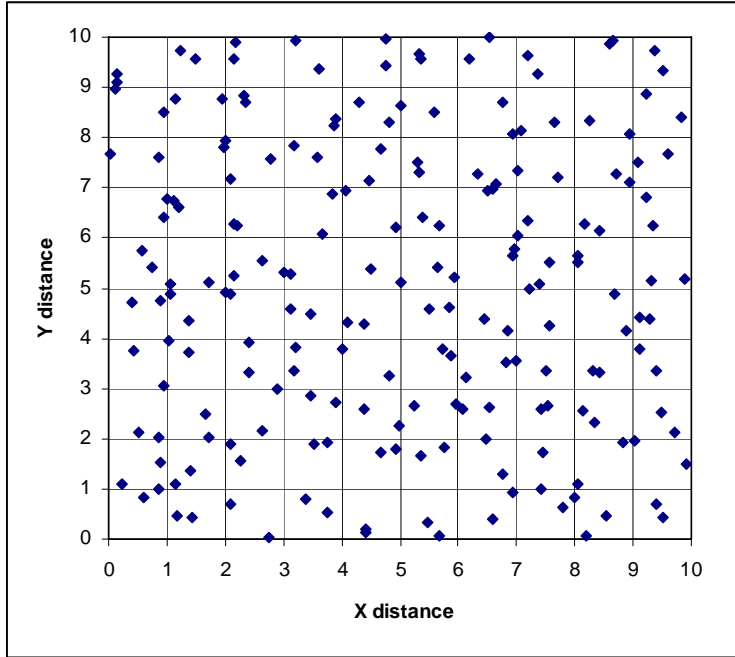


Figure 98: A random $10d \times 10d$ grid topology with two nodes in a $d \times d$ grid.

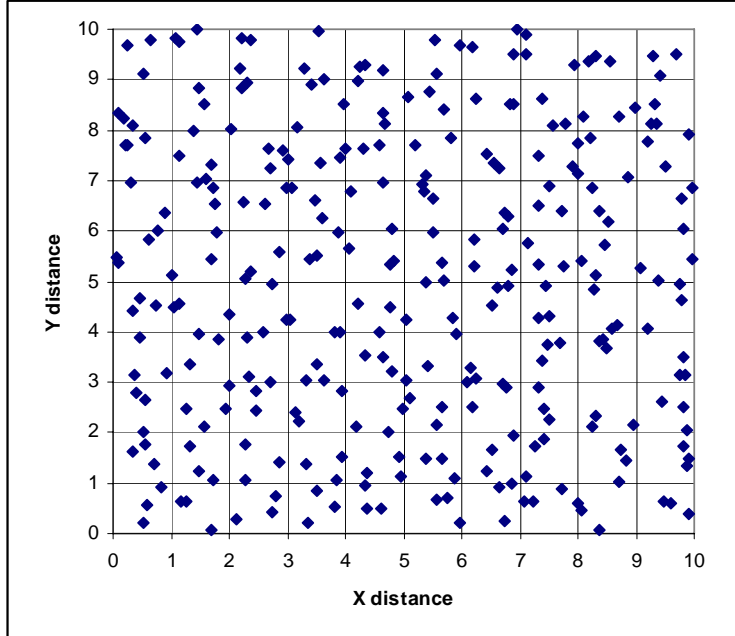


Figure 99: A random $10d \times 10d$ grid topology with three nodes in a $d \times d$ grid.

By placing nodes in a sensor network application, the simulation divided the area into grids to allow nodes spreading out to cover the area properly. The simulation conducted three types of topologies in $10d \times 10d$ grid to evaluate the density and connectivity of the random grid network. A small square grid is $d \times d$, which grid lines are distance d apart and a sink is always placed at the center of the grid. The simulation presents three types of random grid topologies as the following.

- *A node in a grid*: The simulation placed a node into a $d \times d$ grid in the total of 100 nodes, which each node position is randomly selected and placed in each $d \times d$ grid (see Figure 97). Within d transmission power/radius, the results show high number of disconnected nodes as shown in Figure 100, which presents the average of 85 disconnected nodes out of 100 in the Non-GSP network ($p = 0$). Since the research requires all nodes in Non-GSP network can reach the sink by single hop or multi-hops, the simulation increased the number of nodes in the network as the following.
- *Two nodes in a grid*: Figure 98 demonstrates an example of two nodes in a $d \times d$ grid, which has the total of 200 nodes in the network. The results in Figure 100 present no disconnected nodes in the Non-GSP network and some numbers of disconnected nodes when employing GSP.
- *Three nodes in a grid*: Figure 99 shows how the simulation places three nodes in a $d \times d$ grid. The network carries 300 nodes in the $10d \times 10d$ network. The results present small number of disconnected nodes even when using GSP. The three nodes in a grid present high network density, which may not be suitable for the network lifetime analysis.

After evaluating three types of random grid networks, our network lifetime analysis recommends to use the two nodes in a $d \times d$ grid throughout the analysis because it presents no disconnected nodes in the Non-GSP network and reasonable disconnected nodes in the GSP network. The two nodes in a $d \times d$ grid is applied to the larger network sizes as 20×20 and 25×25 random grids, which has the total of 800 and 1250 nodes respectively. The locations of the nodes are randomly selected and then placed into the grids, there are cases that simulation finds numbers of disconnected nodes in the two nodes in a grid case. However, in this research, simulation properly selected random grid topologies that allow all nodes reaching the sink in the Non-GSP network.

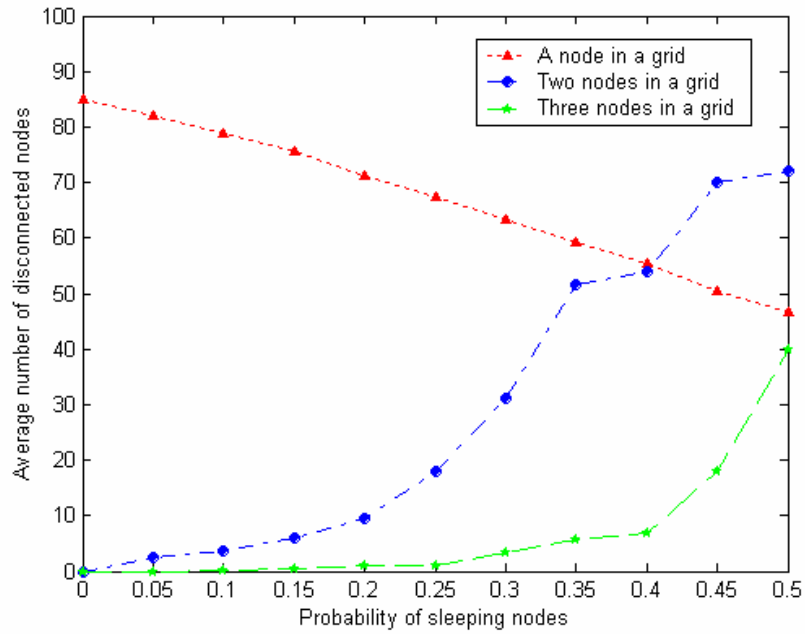


Figure 100: A plot to represent average number of disconnected nodes when a node, two nodes, and three nodes placed in a $d \times d$ grid with d transmission power/radius.

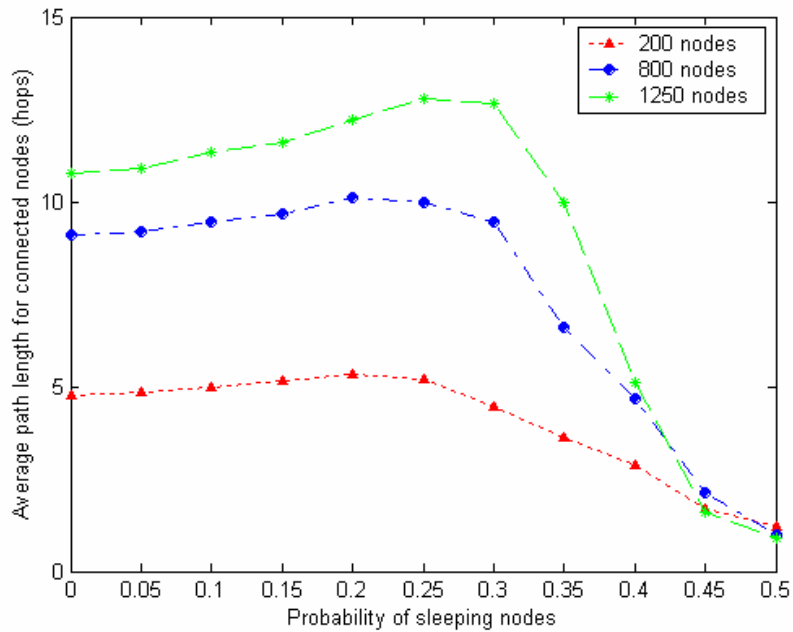


Figure 101: Probability of sleeping nodes vs. average path length for connected nodes in the selected random grids with transmission power/radius d .

Figures 101 and 102 show the average path length and the ratio of nodes disconnected in the 10x10, 20x20, and 25x25 random grids, which have 200, 800, and 1250 nodes and a sink placed in the center. Figures recommend the gossip sleep probability (p) equal to 0.2, 0.2, and 0.25 for the 10x10, 20x20, and 25x25 random grids correspondingly. These three probabilities will be used to evaluate the GSP performance in the d transmission power/radius analysis.

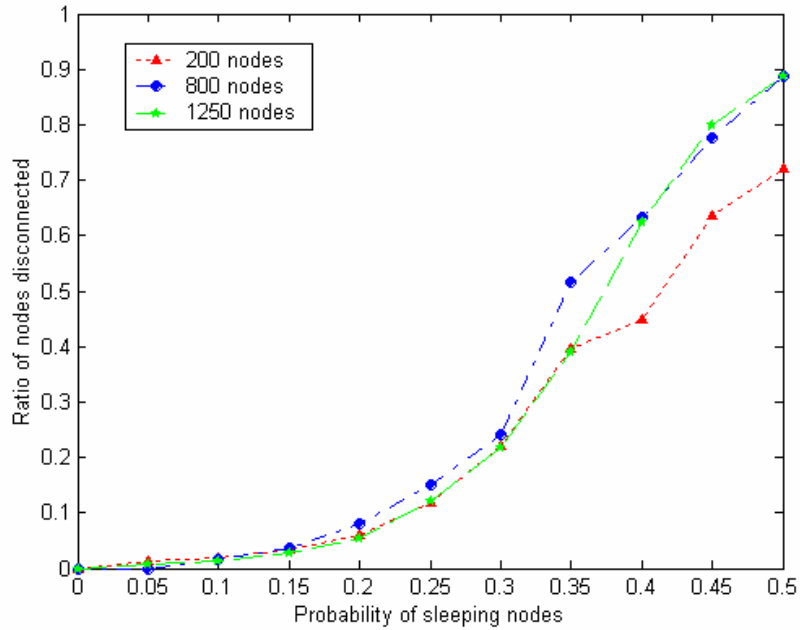


Figure 102: Probability of sleeping nodes vs. ratio of nodes disconnected in the selected random grids with transmission power/radius d .

Figures 103 and 104 represent selected 20x20 (800 nodes) and 25x25 (1250 nodes) random grid topologies used in the analysis for the medium and large networks respectively.

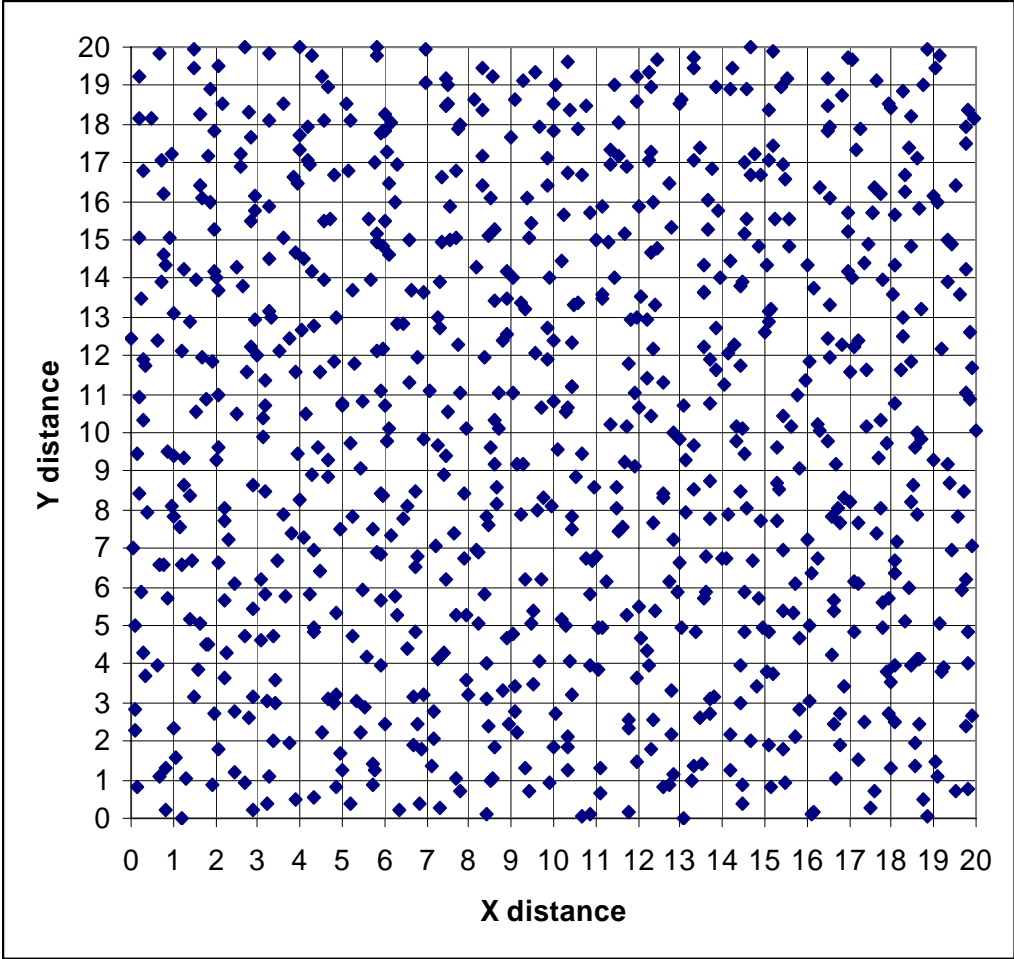


Figure 103: A selected 20x20 random grid topology (800 nodes) using in the network lifetime analysis.

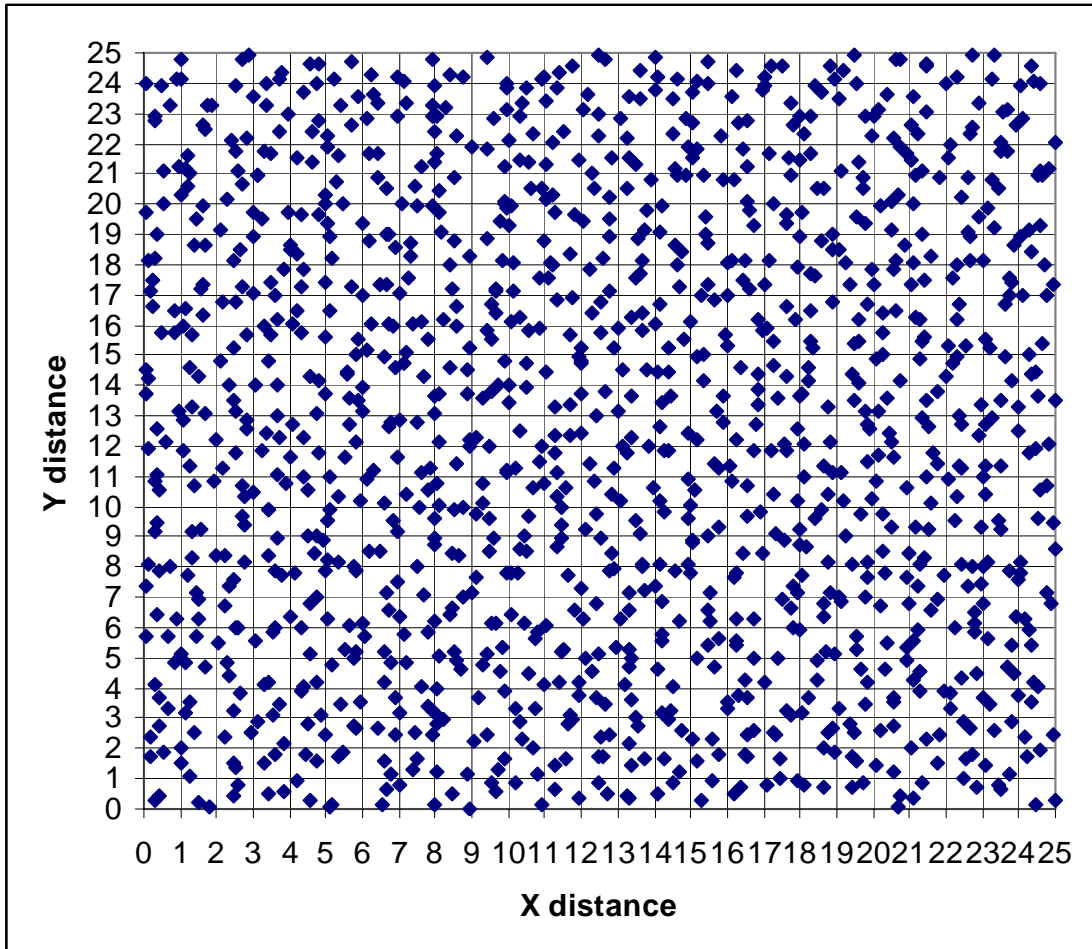


Figure 104: A selected 25x25 random grid topology (1250 nodes) using in the network lifetime analysis.

Figure 105 shows the plot on average number of gossip periods, which represents the network lifetime. GSP achieves the higher number of gossip periods compared to the Non-GSP network. The longer gossip period (360 seconds) shows the decreasing in the average number of gossip periods on both GSP and Non-GSP networks. Figure 106 demonstrates the change in network lifetime by using GSP_d over $Non-GSP_d$ network. The network lifetime is changed by roughly 52% and 40% in the small network size with the 360 and 30 seconds gossip periods. The changes decrease when the network size increases. The changes in the network lifetime for 1250 node network are about 26% and 14% in the 360 and 30 seconds gossip periods respectively.

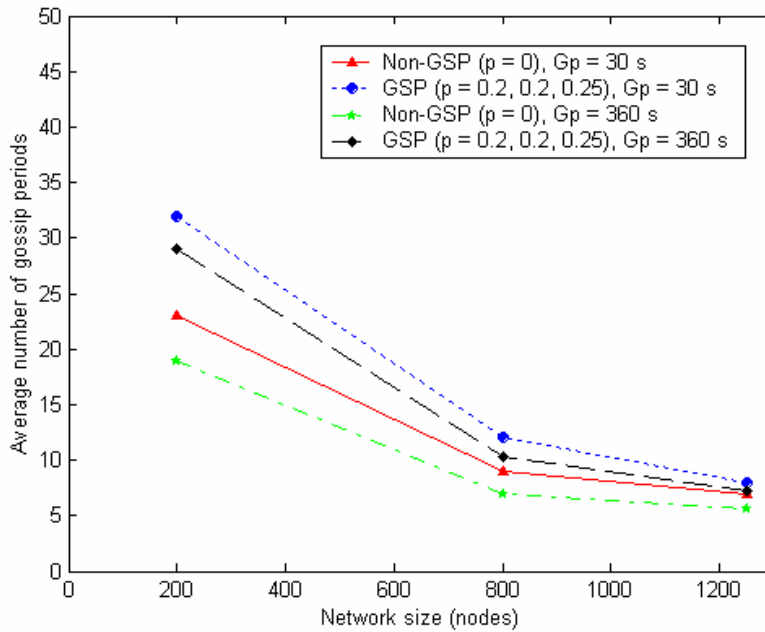


Figure 105: Average number of gossip period vs. network size for the random grids with transmission power/radius d , $G_p = 30$ and 360 seconds.

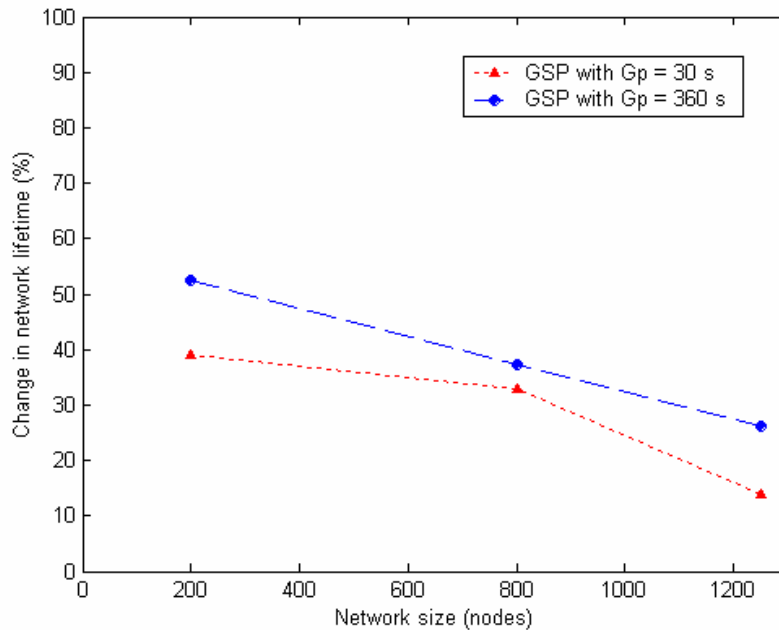


Figure 106: The changes in network lifetime on the different sizes of the random grids with transmission power/radius d when using GSP compared to Non-GSP, $G_p = 30$ and 360 seconds.

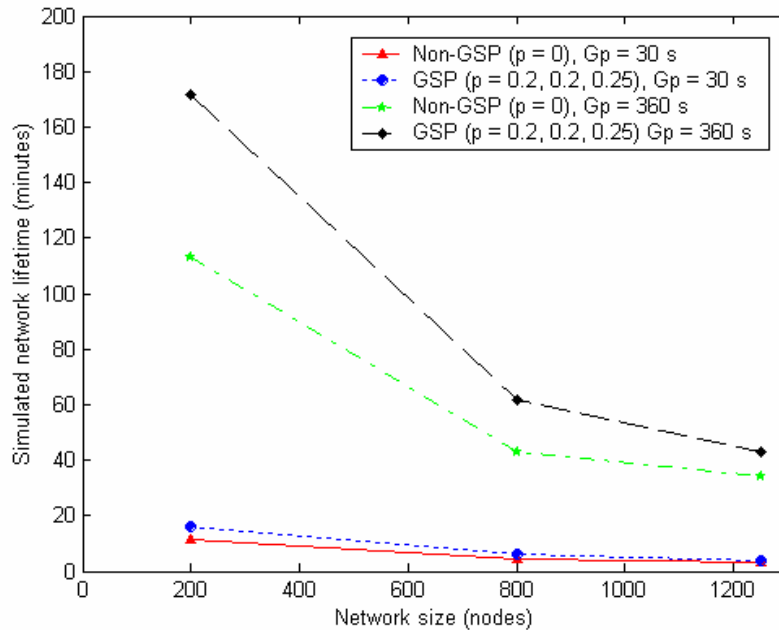


Figure 107: Simulated network lifetime vs. network size for the random grids with transmission power/radius d , $G_p = 30$ and 360 seconds.

Figure 107 illustrates the simulated network lifetime performed on three sizes of random grids. Figure 108 is presented to evaluate the GSP performance on the ARE per node after simulation discovered a dead node. GSP network shows a small increase in Average Remaining Energy (ARE) compared to Non-GSP for all network sizes. Previous analysis in the square and rectangular grids shows an ARE increases in GSP networks when the networks increase in size. However, the random grid results show it differently. Since all three random grid sizes have unique topologies and gossip sleep probabilities (p), they create different ARE results than the previous analysis. However, the result in Figure 108 shows that the highest ARE occurs for the GSP networks with the 30 seconds gossip period.

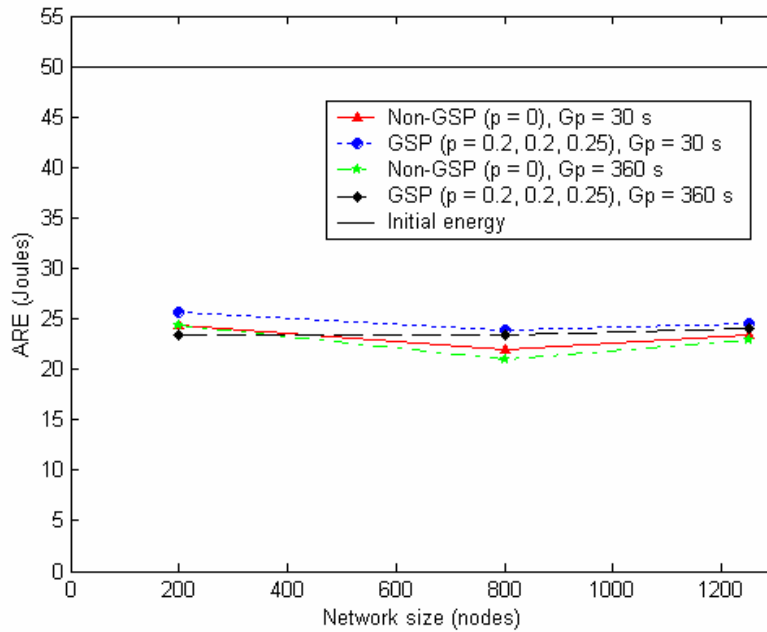


Figure 108: Average remaining energy (ARE) vs. network size for the random grids with transmission power/radius d , $G_p = 30$ and 360 seconds.

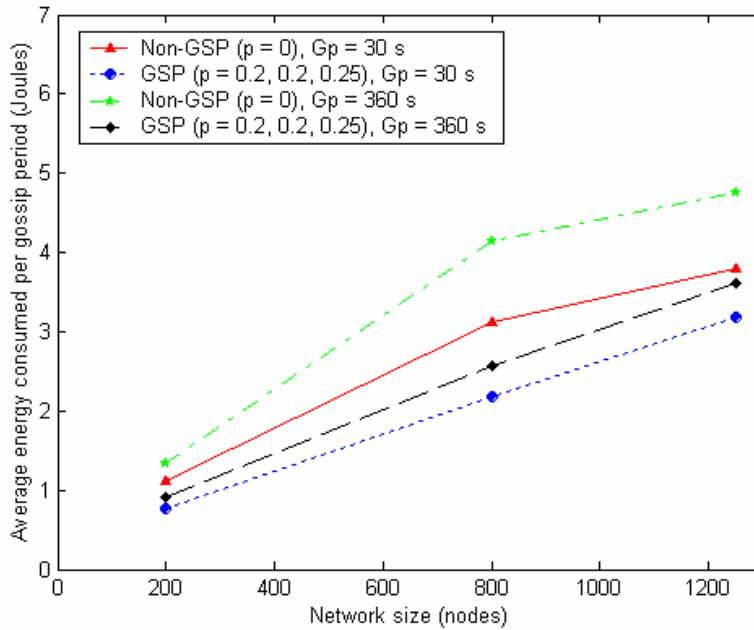


Figure 109: Average energy consumed per gossip period vs. network size for the random grids with transmission power/radius d , $G_p = 30$ and 360 seconds.

Figure 109 shows the average energy consumed per gossip period on both GSP and Non-GSP in random grids. The GSP networks consume less energy compared to Non-GSP networks for all sizes, where the smallest energy consumption per period occurs for GSP with the 30 seconds gossip period.

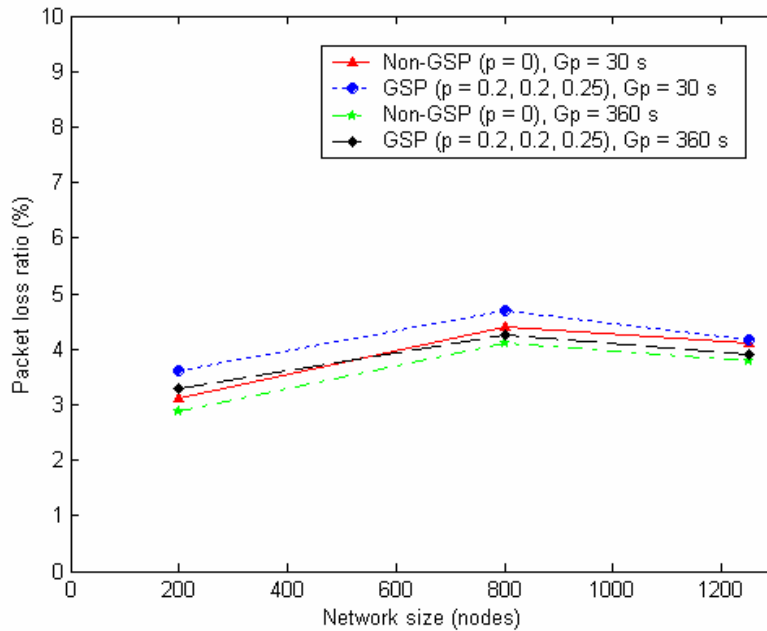


Figure 110: Packet loss ratio vs. network size for the random grids with transmission power/radius d , $G_p = 30$ and 360 seconds.

Figure 110 represents the packet loss ratio resulted by the packet collisions in the random grid networks when using transmission power/radius d . GSP shows higher packet loss ratio for all network sizes. The plots show the non-straight lines because the different topologies employed different values of p using for the different random grid network sizes. Since the random grid network is a random topology in which a node can possibly have any number of neighboring nodes that are located within the transmission range, the small network presents the lowest increase when using the longer gossip period ($G_p = 360$ seconds) compared to the previous analysis on the square and rectangular grids.

7.2.3.2 Transmission Power/Radius $2d$ in the Random Grid Topology

The subsection discusses the network lifetime analysis by increasing transmission power from distance d to $2d$ in random grids. By increasing transmission power/radius, the simulation allows more nodes entering sleep states without losing network connectivity. Thus, simulation investigated a highest sleep probability that creates a connected network by plotting the average path length and the ratio of nodes disconnected as shown in Figures 111 and 112 respectively. These two figures recommend 0.7 gossip sleep probability (p) for all three random grid network sizes.

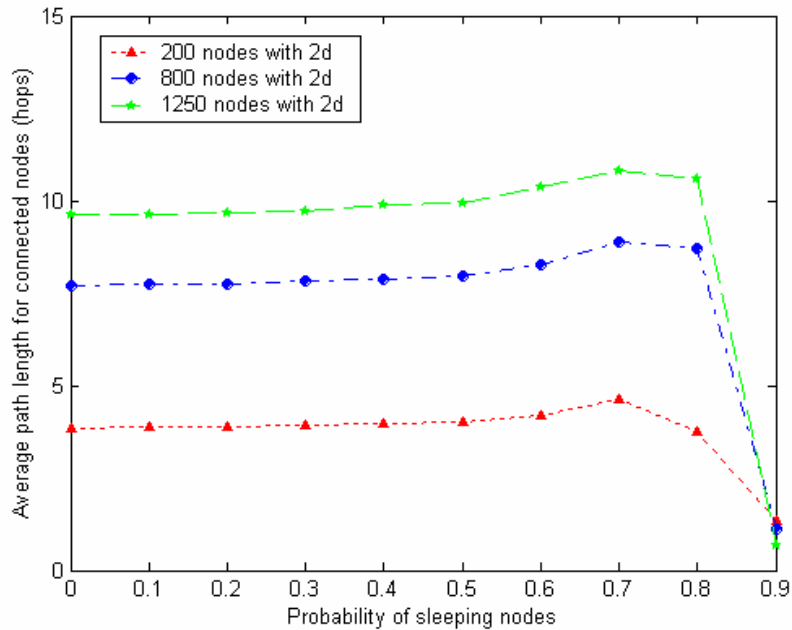


Figure 111: Probability of sleeping nodes vs. average path length for connected nodes in the selected random grids with transmission power/radius $2d$.

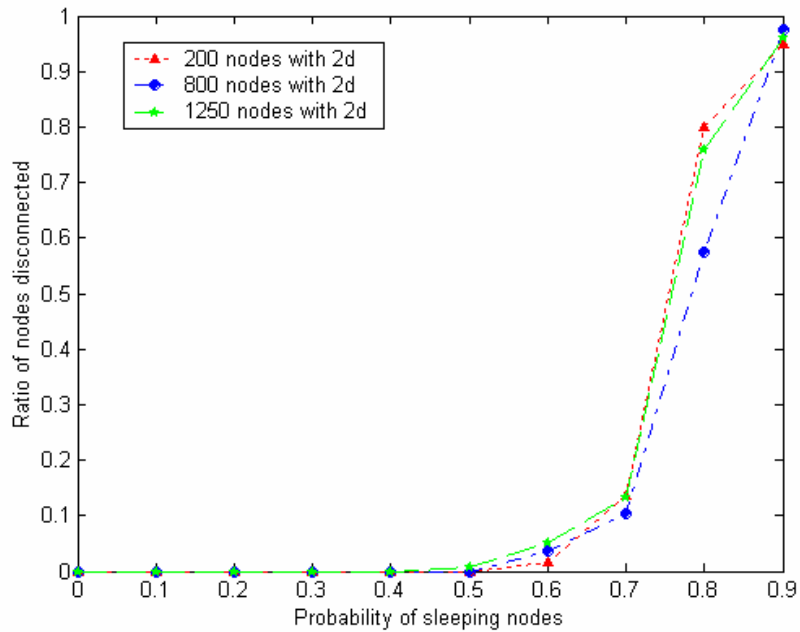


Figure 112: Probability of sleeping nodes vs. ratio of nodes disconnected in the selected random grids with transmission power/radius $2d$.

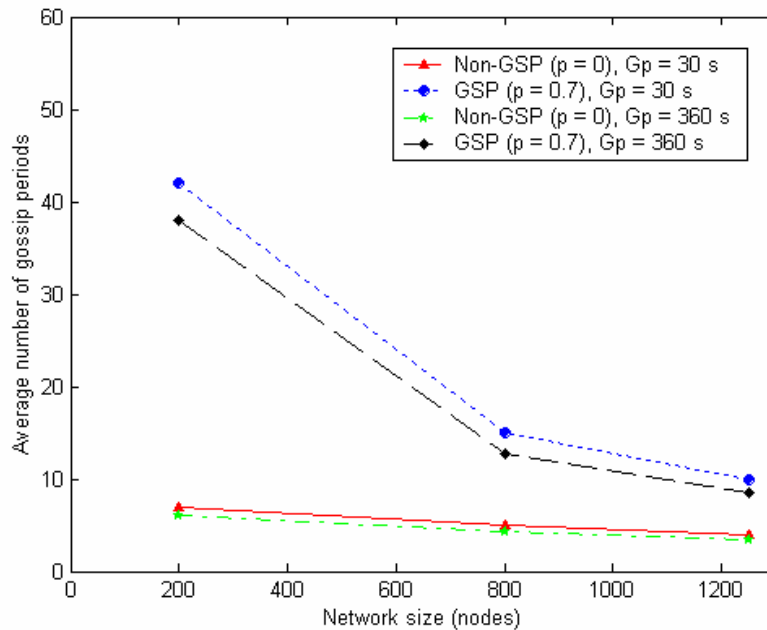


Figure 113: Average number of gossip periods vs. network size for the random grids with transmission power/radius $2d$, $G_p = 30$ and 360 seconds.

Figure 113 illustrates the average number of gossip periods on both GSP and Non-GSP networks when using $2d$ transmission power/radius. By allowing sleeping nodes as in the GSP network, GSP achieves higher average number of gossip periods for all network sizes. However, as networks increase in size, the average number of gossip periods decrease. Figure 114 presents the changes in network lifetime when using GSP compared to Non-GSP. With the $2d$ transmission power/radius, GSP network presents huge changes over Non-GSP network, which is approximately 500% to 150% ranged from small to large network size. However, as the networks increase in size, the changes decrease on both 30 and 360 seconds gossip period.

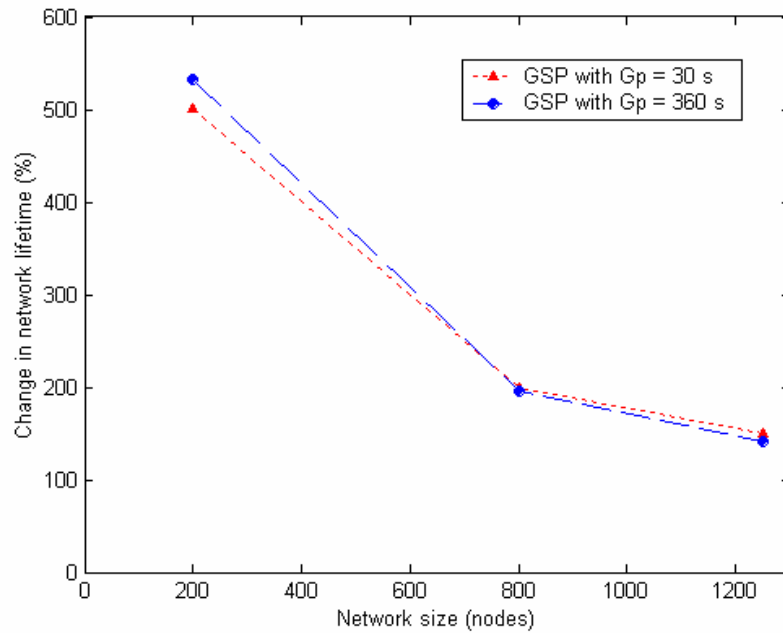


Figure 114: The changes in network lifetime on the different sizes of the random grids with transmission power/radius $2d$ when using GSP compared to Non-GSP, $G_p = 30$ and 360 seconds.

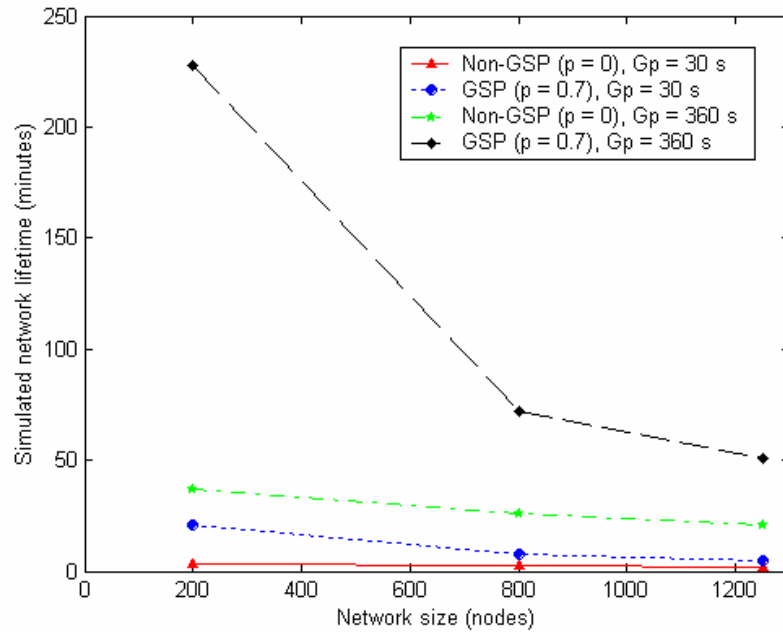


Figure 115: Simulated network lifetime vs. network size for the random grids with transmission power/radius $2d$, $G_p = 30$ and 360 seconds.

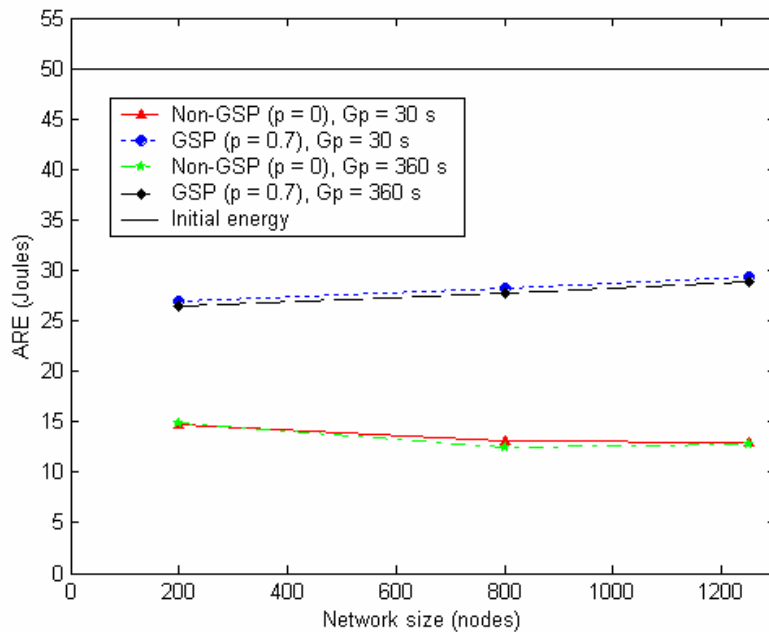


Figure 116: Average remaining energy (ARE) vs. network size for the random grids with transmission power/radius $2d$, $G_p = 30$ and 360 seconds.

Figure 115 shows the simulated network lifetime performed on three sizes of random grid topologies. The longest network lifetime is presented at the small GSP network with the 360 seconds gossip period. Figure 116 plots the ARE per node in various sizes of random grid topologies when using $2d$ transmission power/radius analysis. The results show that by using GSP network the ARE increases approximately 12-16 Joules ranged from small to large network size.

Figure 117 shows the average energy consumption per gossip period in random grids with $2d$ transmission power/radius. The GSP networks consume less energy compared to Non-GSP networks for all sizes, where the smallest energy consumption per period occurs for GSP with the 30 seconds gossip period.

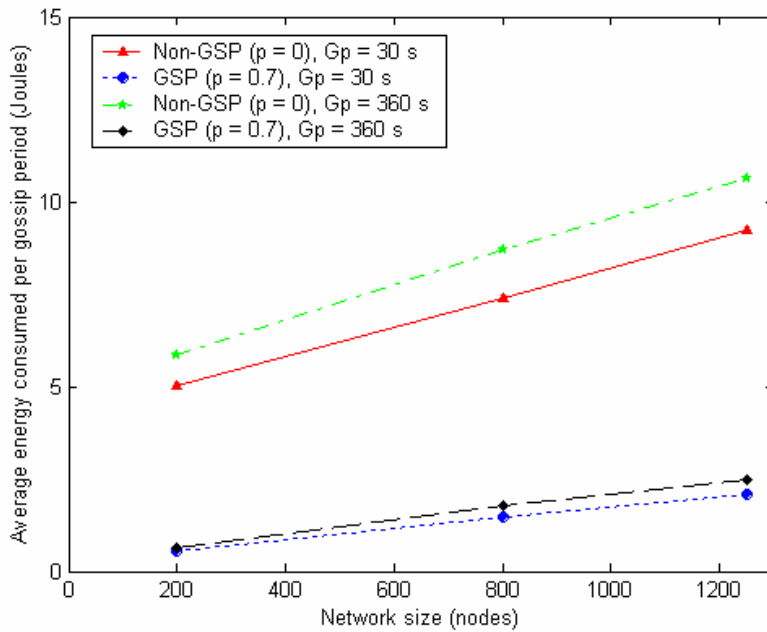


Figure 117: Average energy consumed per gossip period vs. network size for the random grids with transmission power/radius $2d$, $G_p = 30$ and 360 seconds.

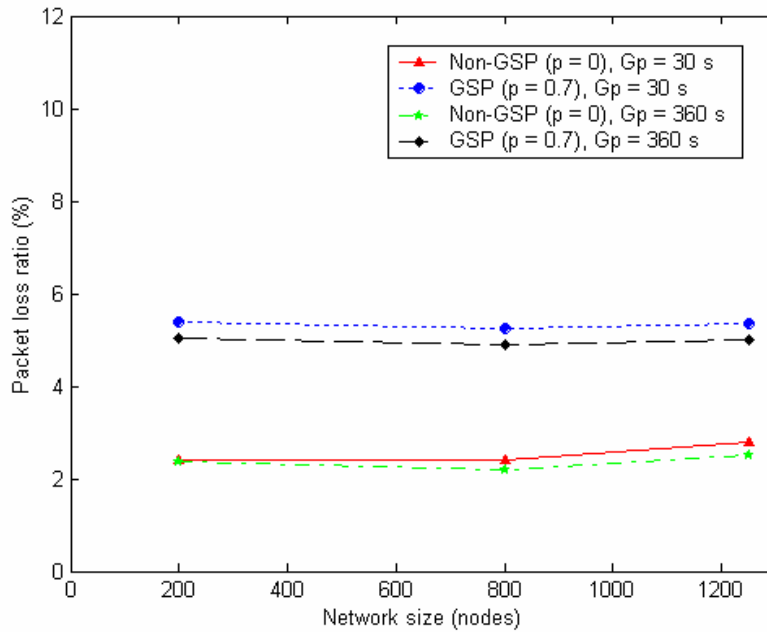


Figure 118: Packet loss ratio vs. network size for the random grids with transmission power/radius $2d$, $G_p = 30$ and 360 seconds.

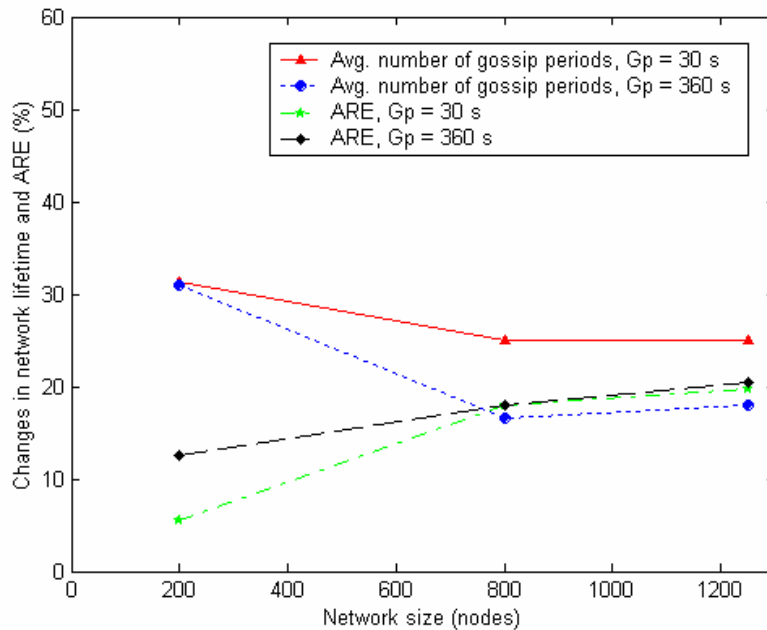


Figure 119: The changes of the average number of gossip periods and AREs in the random grids when using GSP_{2d} compared to GSP_d with $G_p = 30$ and 360 seconds.

Figure 118 presents the packet loss ratio on three network sizes of random grid topologies. GSP_{2d} shows approximately 3% higher packet loss ratio than Non- GSP_{2d} for all network sizes. Due to the random topologies, networks employing GSP_{2d} show 1-2% increase in packet loss ratio compared to GSP_d , which is different than the square and rectangular grids which exhibited smaller packet loss ratio when increasing the transmission power/radius. Less traffic load in $2d$ case can possibly offer the higher packet loss ratio since the ratio presents the total of packet collisions over total number of transmitted/relayed packets. Moreover, the results show that the longer gossip period can decrease the packet loss ratio. Figure 119 shows the changes in network lifetime and ARE for the random grid topologies when using GSP_{2d} compared to GSP_d . By increasing transmission power/radius, the network lifetime is increased by 30% in the small and 18 - 25% in the large network, which the changes decrease when the network size increases. On the other hand, when using GSP_{2d} over GSP_d , ARE increases when the network size increases, which is approximately 5 - 10% in the small and up to 20% in the large network size.

7.2.4 Lattice Topology

The subsection studies GSP performance on three sizes of lattice topologies, 240, 656, and 1136 nodes. These topologies present the idea how sensors can be located along the roads, which a sink is placed at the center of each topology.

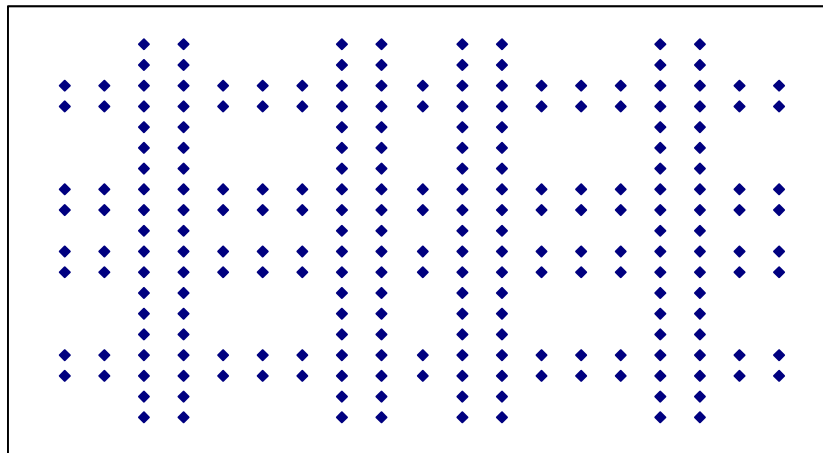


Figure 120: A small lattice topology with 240 nodes.

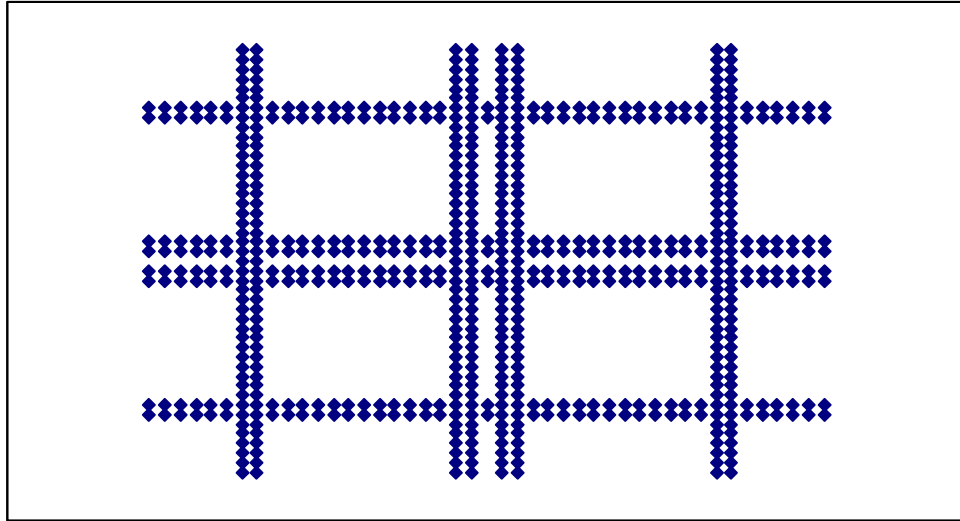


Figure 121: A medium lattice topology with 656 nodes.

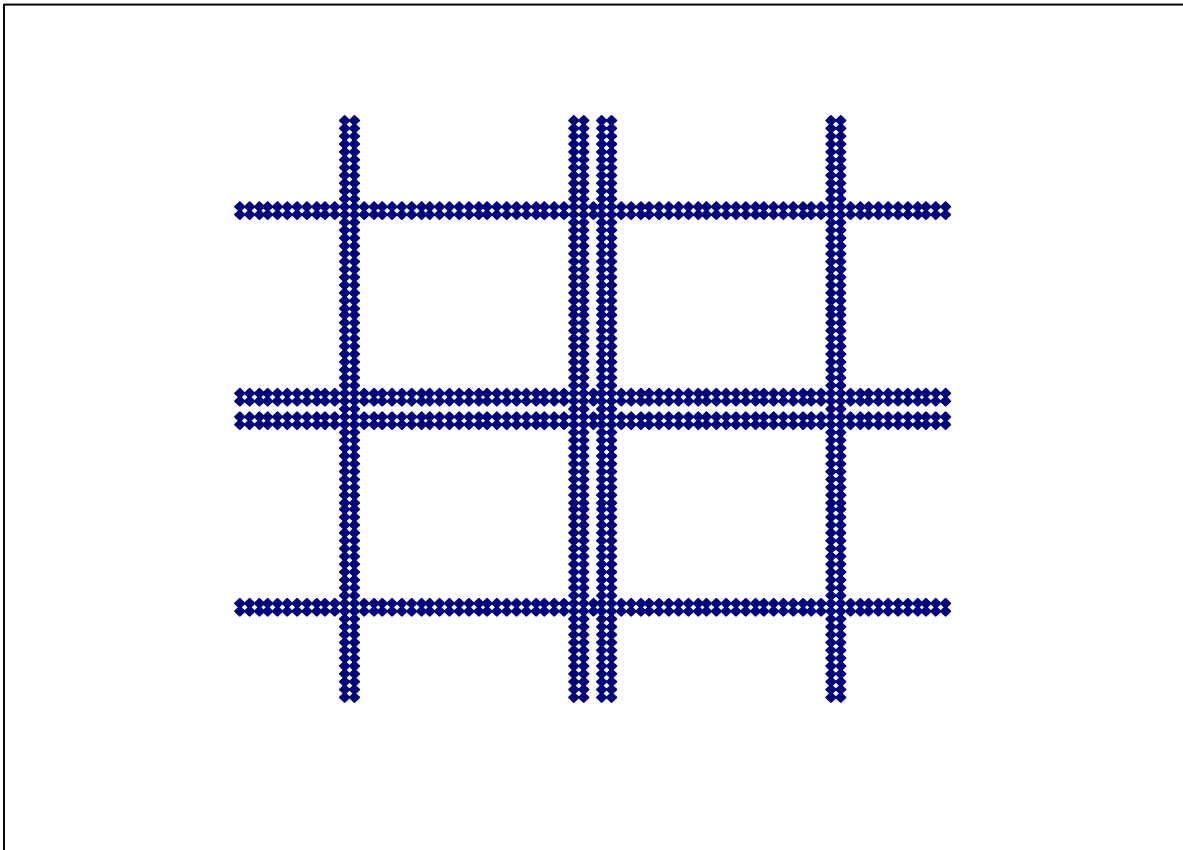


Figure 122: A large lattice topology with 1136 nodes.

7.2.4.1 Transmission Power/Radius d in the Lattice Topology

Figures 120, 121, and, 122 are examples of small, medium, and large lattice topologies using in the network lifetime analysis. First, the simulation evaluates the highest sleep probability that creates a connected network called gossip sleep probability (p). The simulation results in Figures 123 and 124 recommend 0.2, 0.15, and 0.1 for the 240, 656, and 1136 node networks respectively. These numbers are lower than the numbers suggested for the previous topologies because the lattice topologies are low density networks, which the node locations are more vulnerable in connectivity.

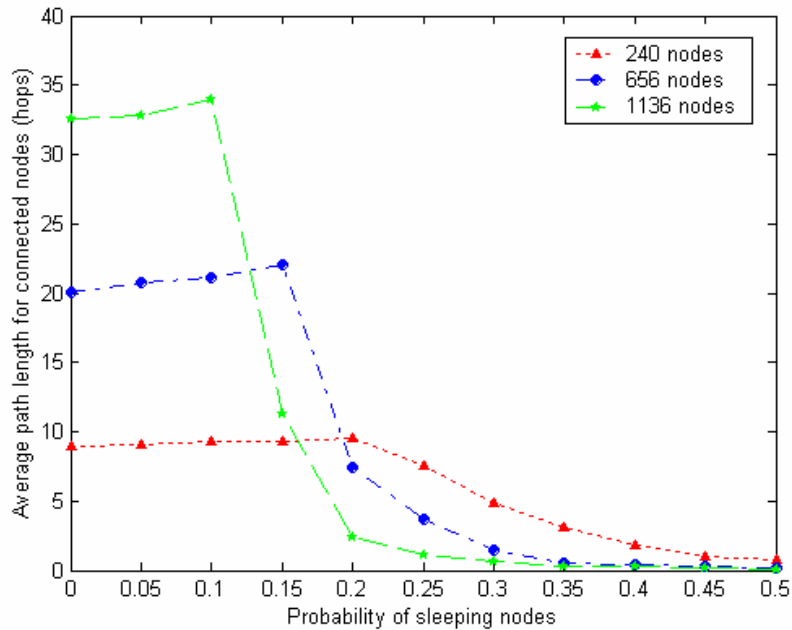


Figure 123: Probability of sleeping nodes vs. average path length for connected nodes in lattice topologies with transmission power/radius d .

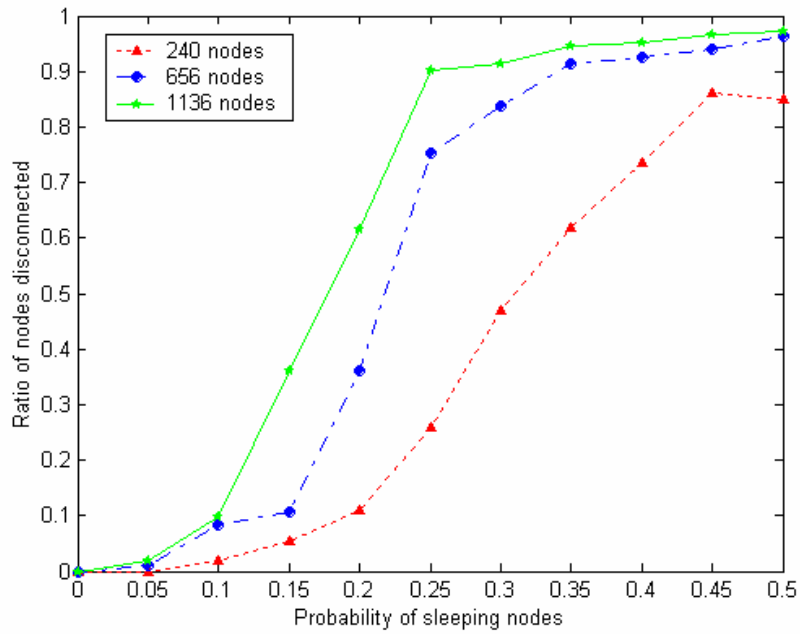


Figure 124: Probability of sleeping nodes vs. ratio of nodes disconnected in lattice topologies with transmission power/radius d .

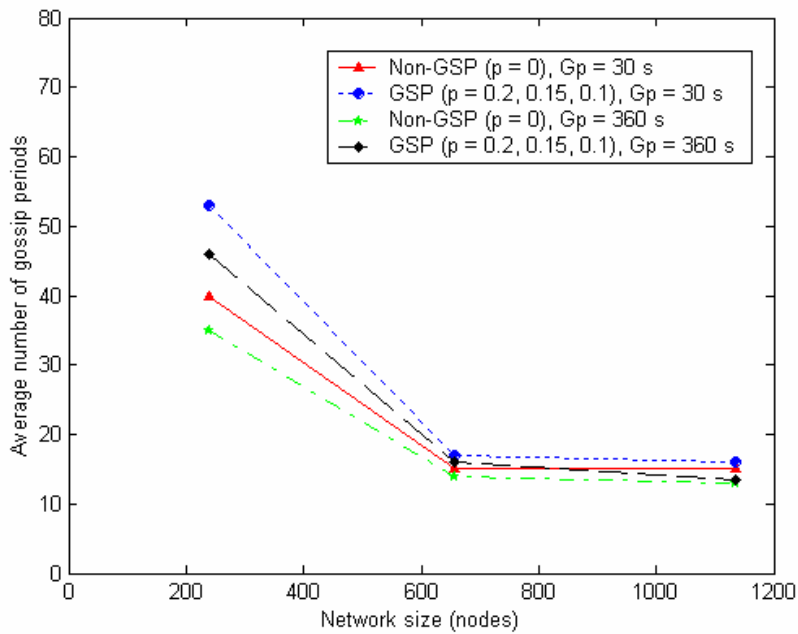


Figure 125: Average number of gossip periods vs. network size for the lattice topologies with transmission power/radius d , $G_p = 30$ and 360 seconds.

Figure 125 shows the average number of gossip periods when using GSP compared to Non-GSP with transmission power/radius d . The idle/listening energy consumption for the 360 seconds gossip period results in fewer average number of gossip periods on both GSP and Non-GSP. Since the large network size presents higher traffic load, the average number of gossip periods decrease when the network size increases. Figure 126 demonstrates the changes in the network lifetime when using GSP on both 30 and 360 seconds gossip period. The largest change occurs for the small network size, and the change is decreased when the network size increases.

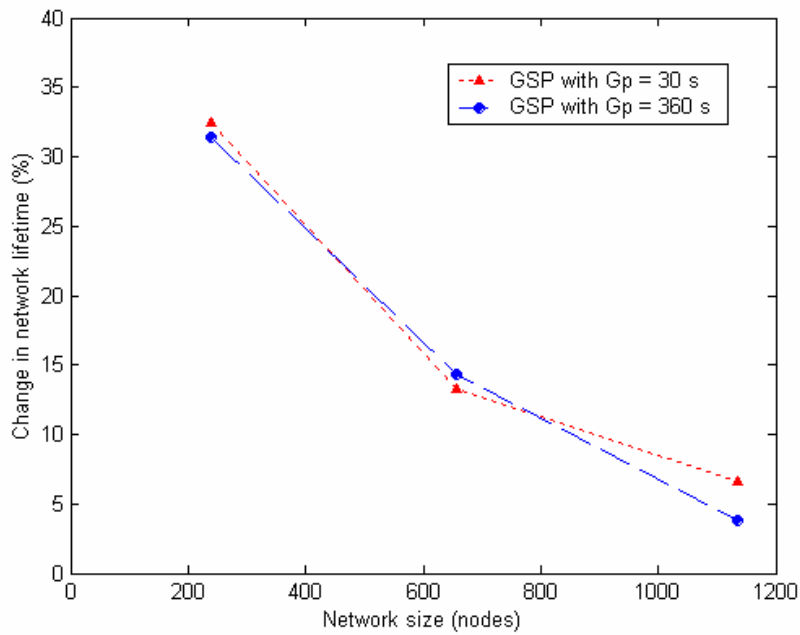


Figure 126: The changes in network lifetime on the different sizes of the lattice topologies with transmission power/radius d when using GSP compared to Non-GSP, $G_p = 30$ and 360 seconds.

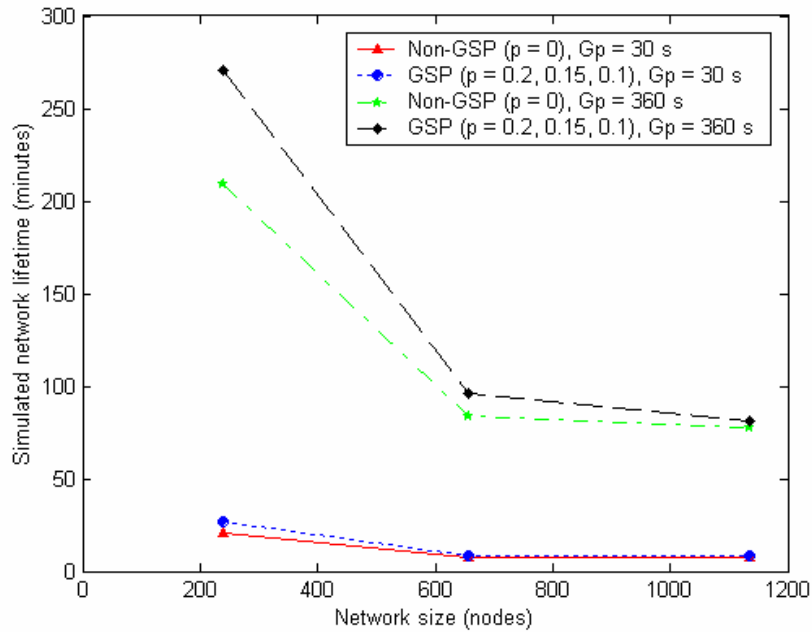


Figure 127: Simulated network lifetime vs. network size for the lattice topologies with transmission power/radius d , $G_p = 30$ and 360 seconds.

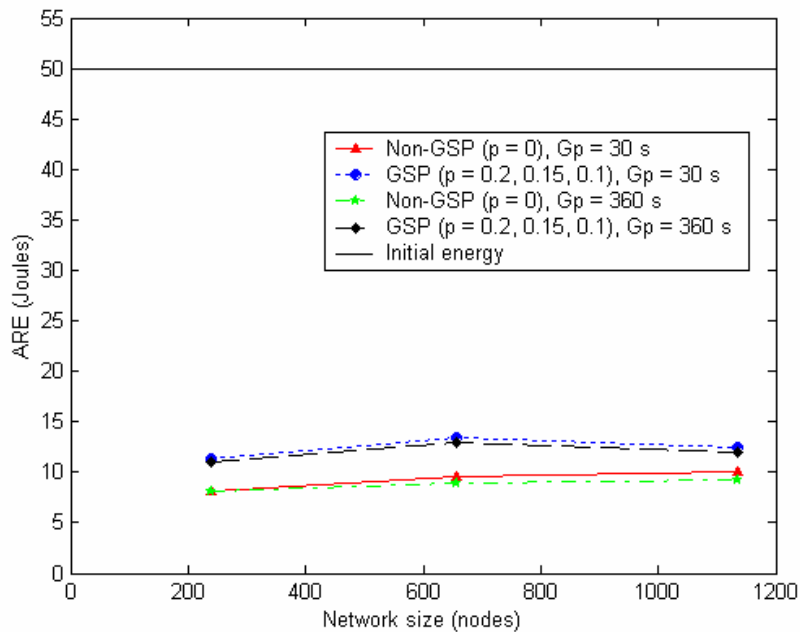


Figure 128: Average remaining energy (ARE) vs. network size for the lattice topologies with transmission power/radius d , $G_p = 30$ and 360 seconds.

Figure 127 presents the simulated network lifetime in minutes on both GSP and Non-GSP network with the 30 and 360 seconds gossip periods. The longest lifetime occurs for the 240 node network with the 360 seconds gossip period. When the network grows larger, the network lifetime decreases. GSP shows small increase in network lifetime because of the small values of gossip sleep probabilities (p) using in the simulation. Figure 128 plots the ARE per node for the GSP and Non-GSP networks. GSP network shows approximately 3-4 Joules higher AREs than the Non-GSP network for all three network sizes. A longer gossip period presents lower a ARE compared to a short one on both GSP and Non-GSP network. The lattice topologies result in straight lines for both GSP and Non-GSP, which is different than the analysis in square and rectangular grids, which show that ARE increases when the network size increases in GSP and decreases when the network size increases in Non-GSP.

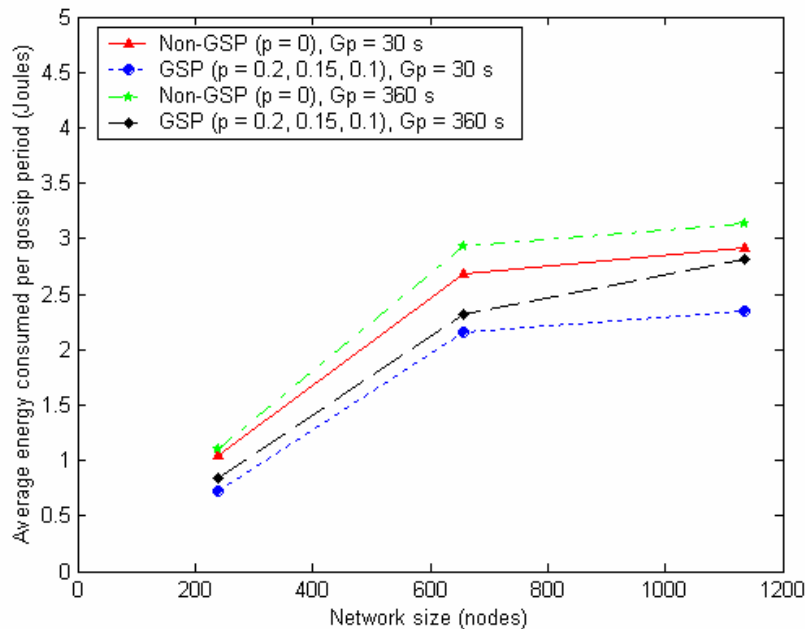


Figure 129: Average energy consumed per gossip period vs. network size for lattice topologies with transmission power/radius d , $G_p = 30$ and 360 seconds.

Figure 129 shows the energy consumption per gossip period in lattice topology with d transmission power/radius. The GSP networks consume less energy compared to Non-GSP. When networks increase in size, the average energy consumed per gossip period decreases.

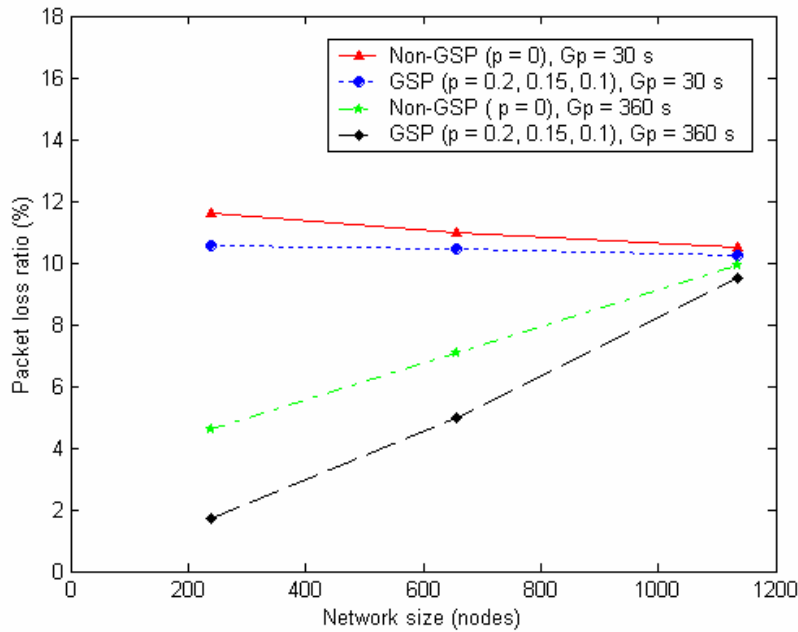


Figure 130: Packet loss ratio vs. network size for the lattice topologies with transmission power/radius d , $G_p = 30$ and 360 seconds.

Figure 130 shows the packet loss ratio on GSP and Non-GSP networks when using transmission power/radius d . The longer gossip period provides smaller packet loss ratio in which the minimum ratio occurs for the small GSP network with the 360 seconds gossip period. However, as the networks increase in size, the packet loss ratio increases for the 360 seconds gossip period. On the other hand, GSP and Non-GSP networks using 30 seconds gossip periods present approximately the same ratios for all network sizes.

7.2.4.2 Transmission Power/Radius $2d$ in the Lattice Topology

To evaluate the gossip sleep probabilities for all three networks, the simulation is conducted to plot the average path length and the ratio of nodes disconnected from the sink. Figures 131 and 132 recommend $p = 0.55$, 0.4, and 0.35 for 240, 656, and 1136 node networks respectively. These probabilities are lower than the previous topologies because the weak network connectivity in lattice topologies when using a $2d$ transmission power/radius.

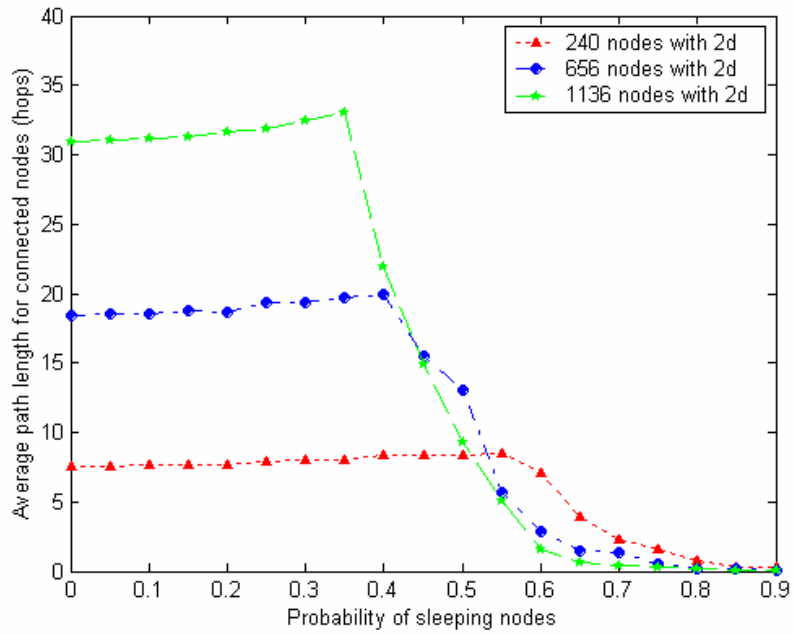


Figure 131: Probability of sleeping nodes vs. average path length for connected nodes in lattice topologies with transmission power/radius $2d$.

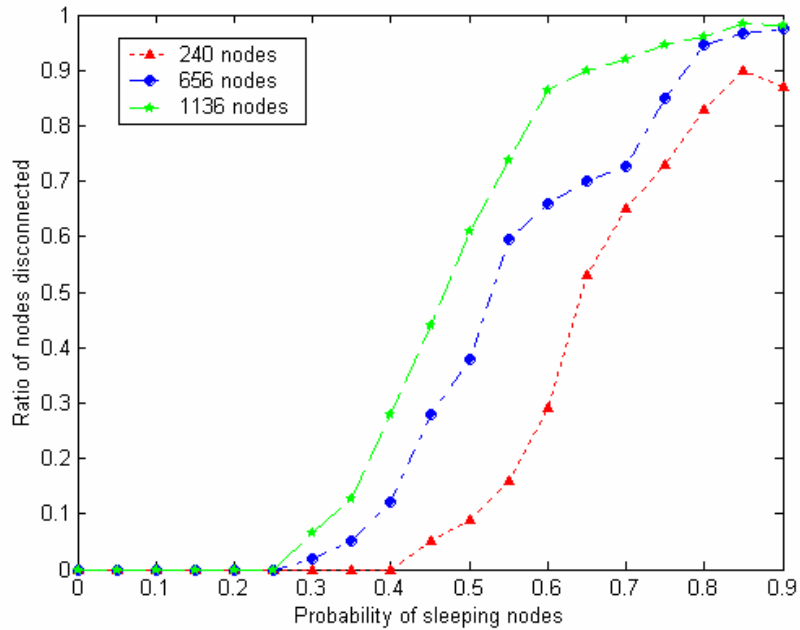


Figure 132: Probability of sleeping nodes vs. ratio of nodes disconnected in lattice topologies with transmission power/radius $2d$.

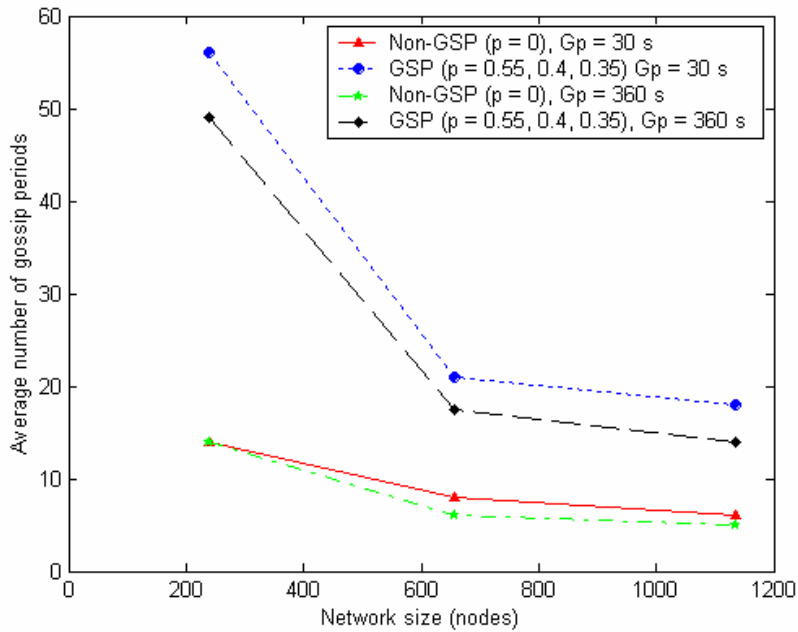


Figure 133: Average number of gossip periods vs. network size for lattice topologies with transmission power/radius $2d$, $G_p = 30$ and 360 seconds.

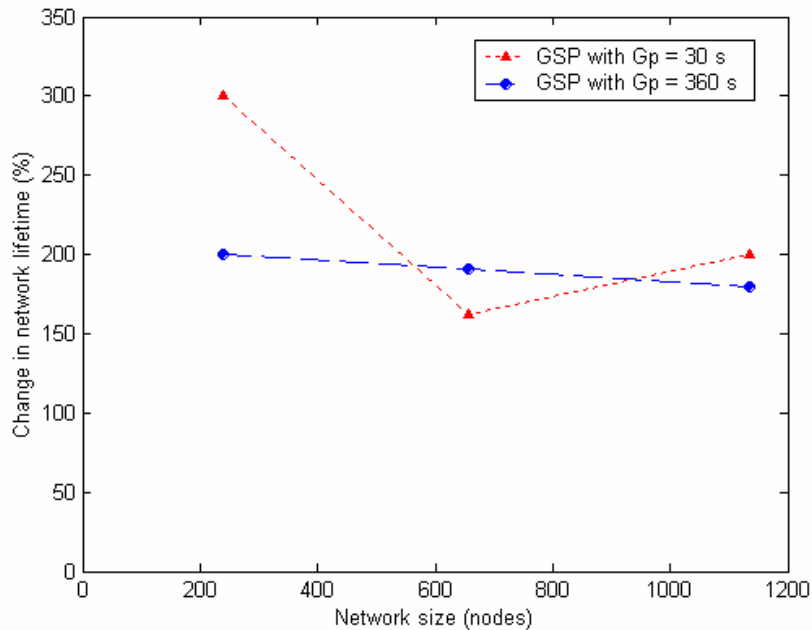


Figure 134: The changes in network lifetime on the different sizes of lattice topologies with transmission power/radius $2d$ when using GSP compared to Non-GSP, $G_p = 30$ and 360 seconds.

Figure 133 shows the average number of gossip periods on both GSP and Non-GSP when using transmission power/radius $2d$. Networks employing GSP presents the higher average number of gossip periods compared to Non-GSP for all three network sizes. However, because of the higher traffic load in the large network, the change decreases when the network size increases. Figure 134 illustrates the changes in the network lifetime when using GSP_{2d} over Non-GSP_{2d} networks. The largest change occurs for the 240 node network. The plots show non-straight up and down lines because of the different in network topologies employ different gossip sleep probabilities (p).

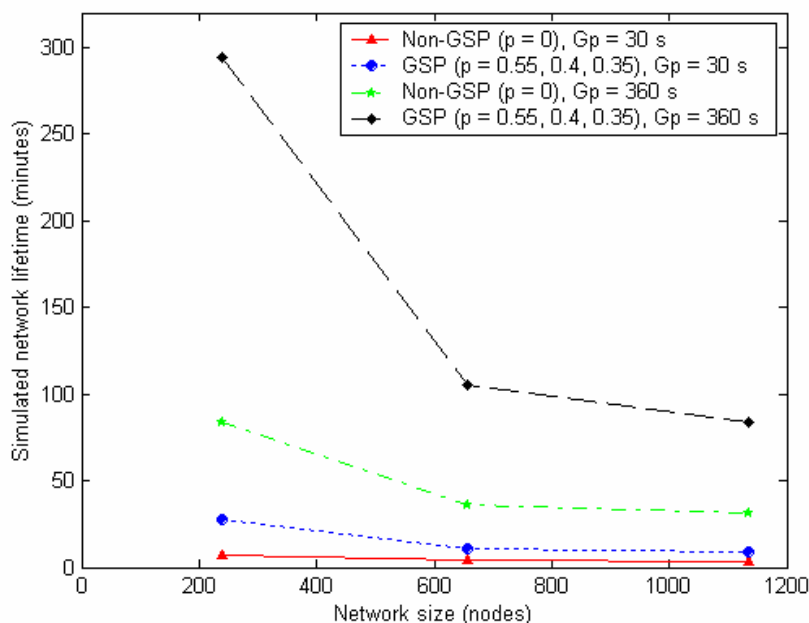


Figure 135: Simulated network lifetime vs. network size for lattice topologies with transmission power/radius $2d$, $G_p = 30$ and 360 seconds.

Figure 135 compares the simulated network lifetime between GSP_{2d} and Non-GSP_{2d} networks with 30 and 360 seconds gossip period. The longest simulated network lifetime occurs for the 240 node network with the 360 seconds gossip period. Figure 136 plots the ARE per node for all three lattice network sizes. ARE increases when the network size increases on both GSP and Non-GSP networks. Because of the higher energy consumption in the idle/listening periods, a 360 seconds gossip period shows a small decrease in an ARE compared to a 30 seconds gossip period.

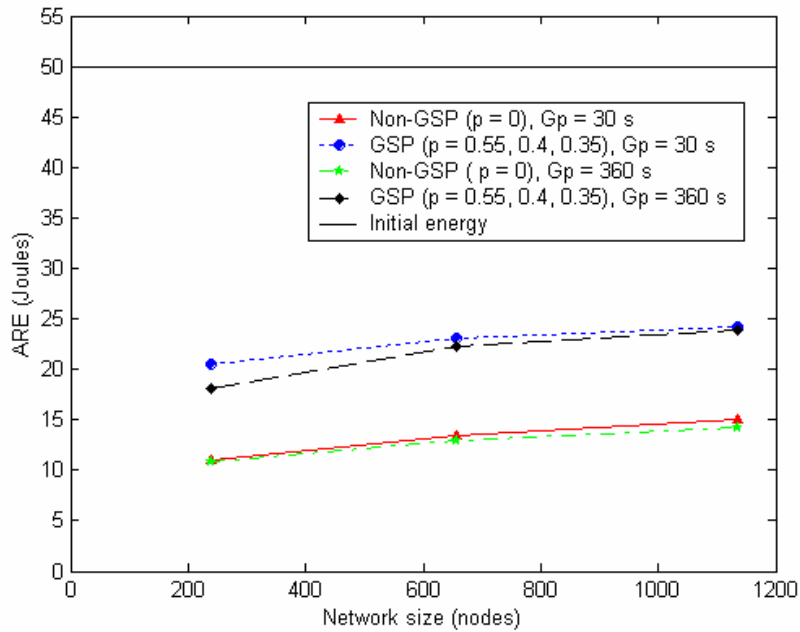


Figure 136: Average remaining energy (ARE) vs. network sizes for lattice topologies with transmission power/radius $2d$, $G_p = 30$ and 360 seconds.

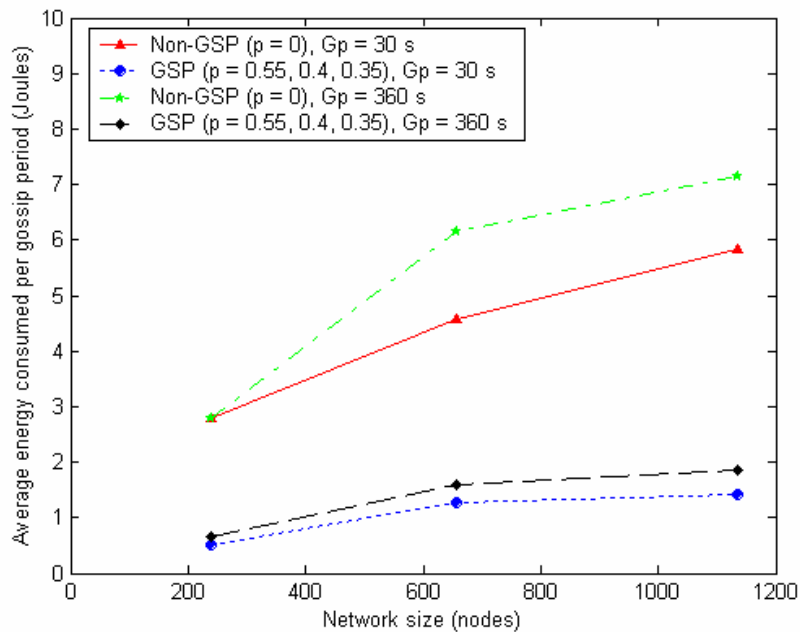


Figure 137: Average energy consumed per gossip period vs. network size for the lattice topologies with transmission power/radius $2d$, $G_p = 30$ and 360 seconds.

Figure 137 shows the average energy consumed per gossip period in lattice topology with $2d$ transmission power/radius. Non-GSP with 360 gossip period has the highest energy consumption per period. On the other hand, the smallest energy consumed per node per gossip period occurs for the GSP with 30 seconds gossip period.

Figure 138 represents the packet loss ratio on both GSP and Non-GSP networks when using transmission power/radius $2d$. The smallest packet loss ratio occurs for the small network with the 360 seconds gossip period. On the other hand, the highest ratio is presented at the small GSP network with the 30 seconds gossip period. As the networks increase in size, the ratios are approximately the same.

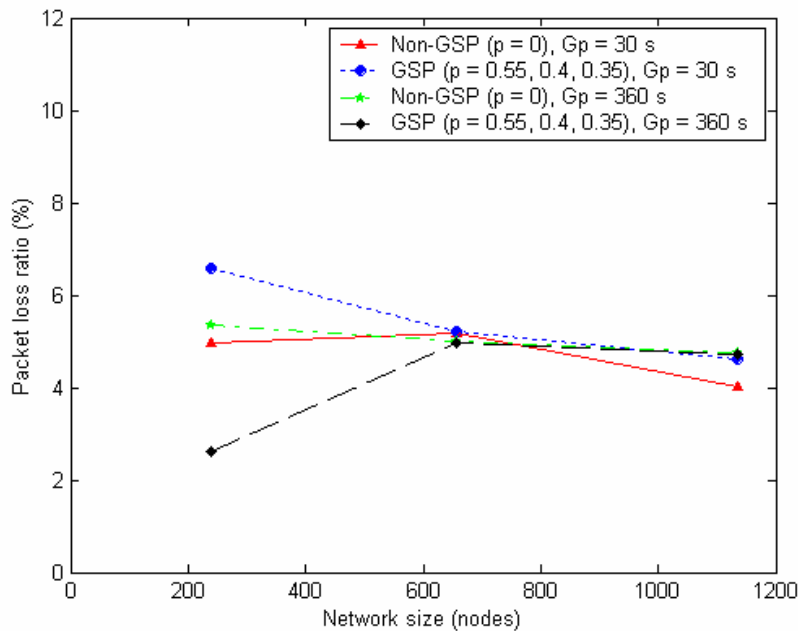


Figure 138: Packet loss ratio vs. network size for lattice topologies with transmission power/radius $2d$, $G_p = 30$ and 360 seconds.

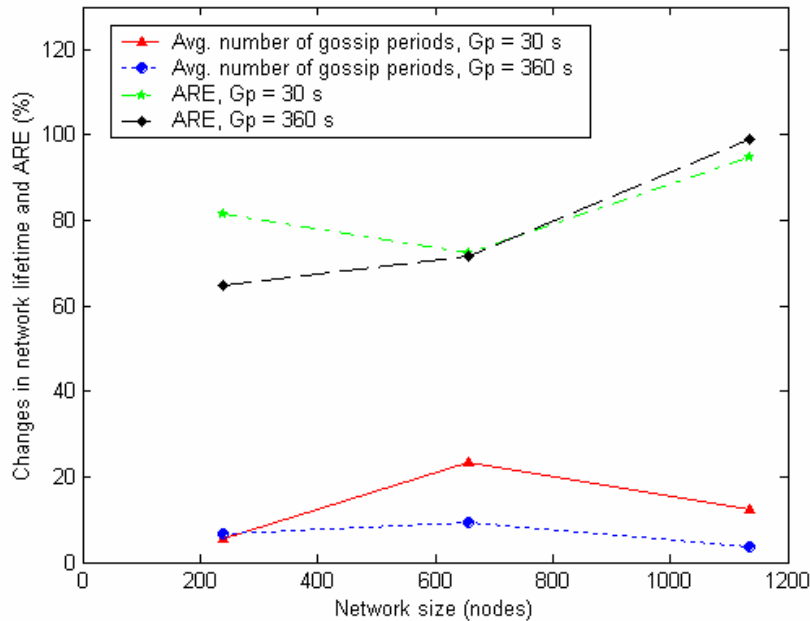


Figure 139: The changes of the average number of gossip periods and AREs in lattice topologies when using GSP_{2d} compared to GSP_d with $G_p = 30$ and 360 seconds.

Figure 139 illustrates the changes in network lifetime and AREs in lattice topologies when using transmission power/radius $2d$ compared to d in the GSP network. By increasing transmission power/radius, the network lifetime is increased by approximately 6% in small and up to 23% in the medium network size. When using a GSP_{2d} over a GSP_d , AREs are increased approximately 65 - 80% in the small and up to 100% in the large lattice network.

7.2.5 Star Topology

The subsection discusses the three different sizes of the star topologies. An example of a star topology with 5 nodes in each line for the total of 6 lines network is shown in Figure 140. To generate the different network sizes, the simulation used ratio of five. For instance, a 320 node network contains 8 nodes and 40 lines, $40/8 = 5$. In cases of 720 and 1280 node networks, the simulation employed 60/12 and 80/16 ratios respectively. The simulation assumes a sink always located at the center. Figures 141, 142, and 143 represent the actual three sizes of the star topologies using in this network lifetime analysis.

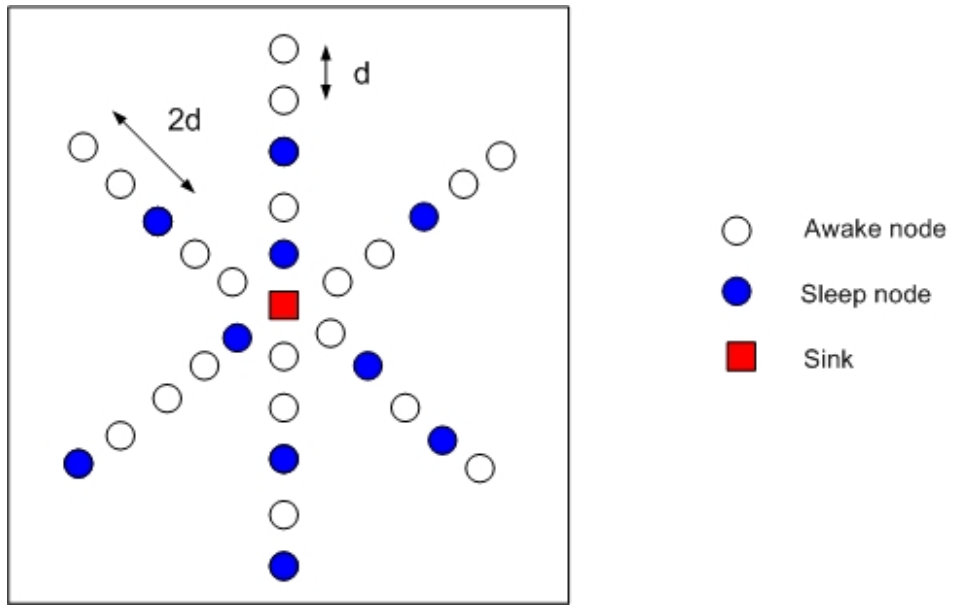


Figure 140: An example of 5 nodes and 6 lines star topology with a sink at the center.

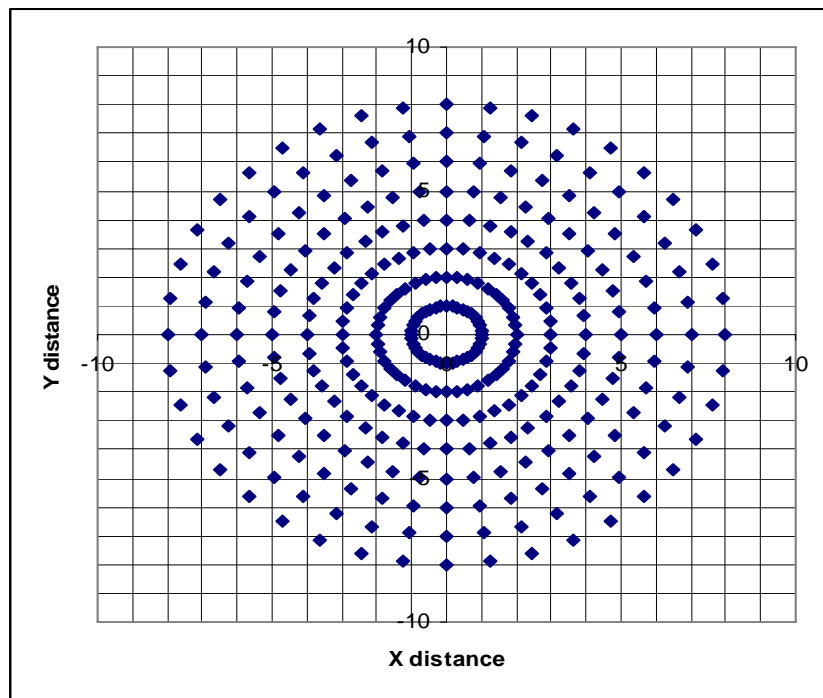


Figure 141: A small star topology with 320 nodes.

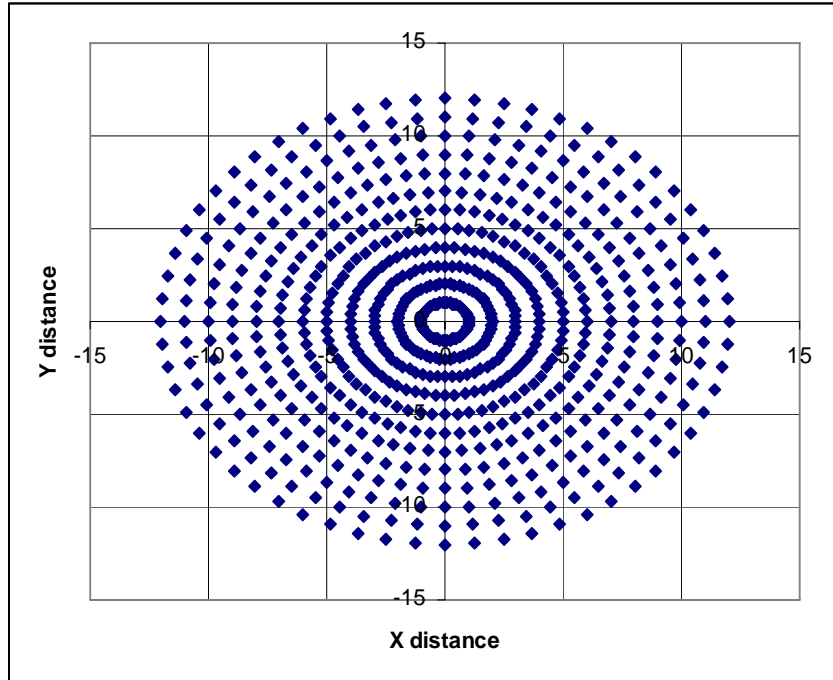


Figure 142: A medium star topology with 720 nodes.

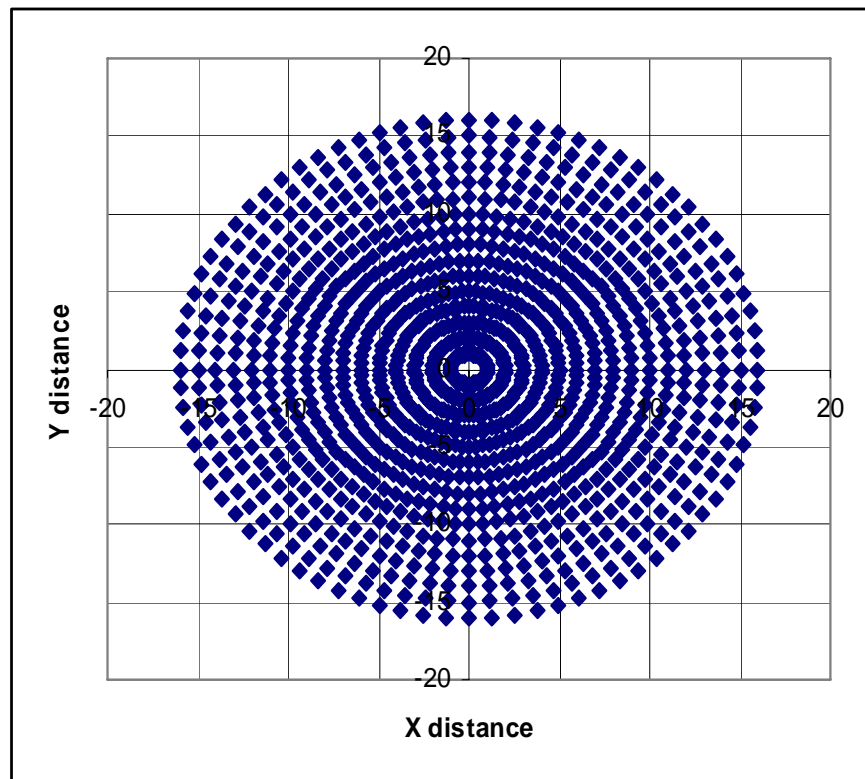


Figure 143: A large star topology with 1280 nodes.

7.2.5.1 Transmission Power/Radius d in the Star Topology

The simulation calculates the gossip sleep probability, which is the highest sleep probability that creates a connected network. With transmission power/distance d , Figures 144 and 145 plot the average path length and the ratio of nodes disconnected that recommend 0.3, 0.25, and 0.25 for the 320, 720, and 1280 node star networks respectively.

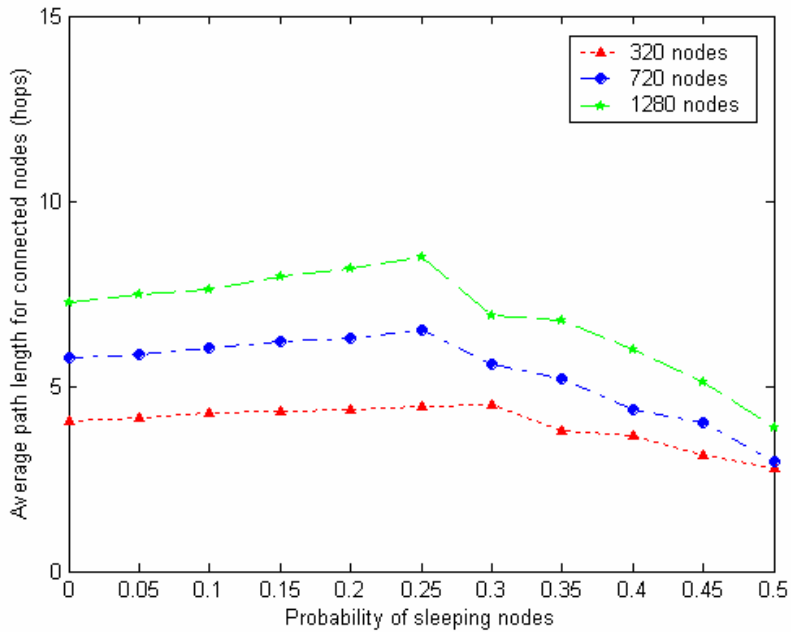


Figure 144: Probability of sleeping nodes vs. average path length for connected nodes in star topologies with transmission power/radius d .

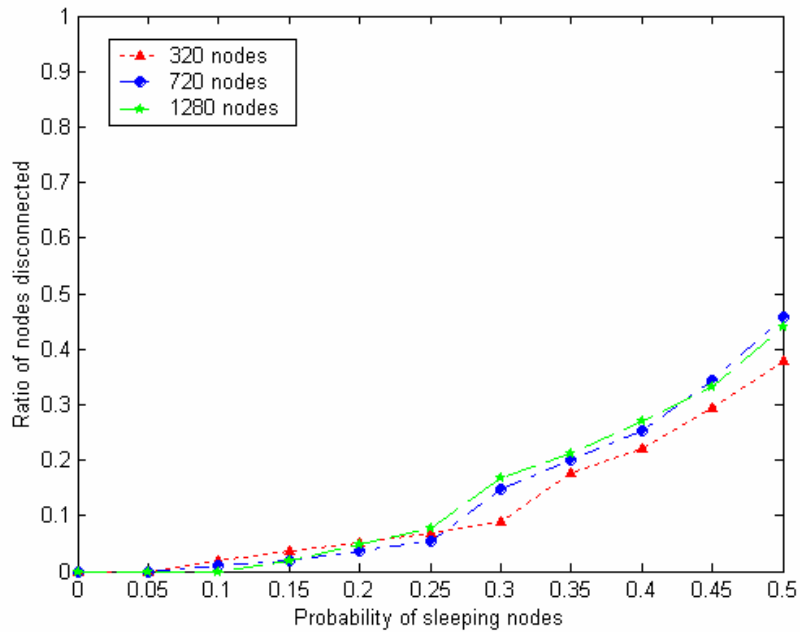


Figure 145: Probability of sleeping nodes vs. ratio of nodes disconnected in star topologies with transmission power/radius d .

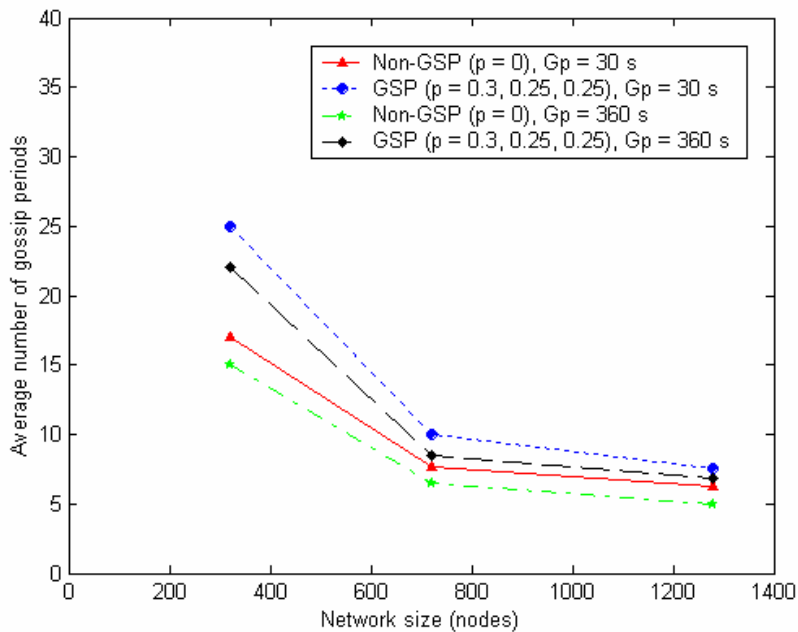


Figure 146: Average number of gossip periods vs. network size for star topologies with transmission power/radius d , $G_p = 30$ and 360 seconds.

Figure 146 shows the average number of gossip periods on three network sizes with the 30 and 360 seconds gossip periods. The highest number of gossip period occurs for the small 320 node GSP network with the 30 seconds gossip period. As the network increases in size, the average number of gossip periods decrease. The 360 seconds gossip period presents smaller average number of gossip periods than the 30 seconds gossip period for all network sizes on both GSP_d and Non-GSP_d. This is because a longer gossip period consumed more energy in the idle/listening states than a shorter gossip period.

Figure 147 shows the changes in network lifetime in term of average number of gossip periods on the different sizes of the star topologies when using GSP_d compared to Non-GSP_d. The largest change occurs for the small network (320 nodes). However, the changes decrease when the networks increase in size.

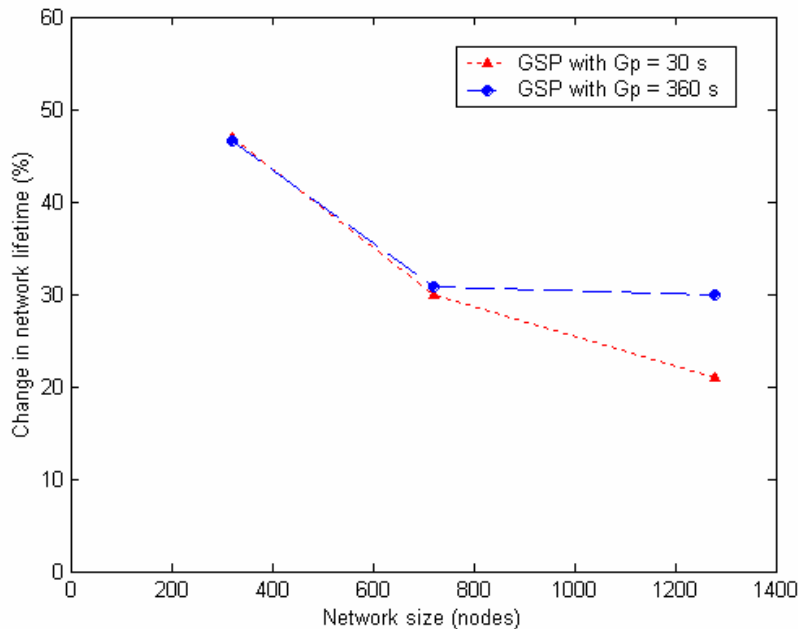


Figure 147: The changes in network lifetime on the different sizes of the star topologies with transmission power/radius d when using GSP compared to Non-GSP, $G_p = 30$ and 360 seconds.

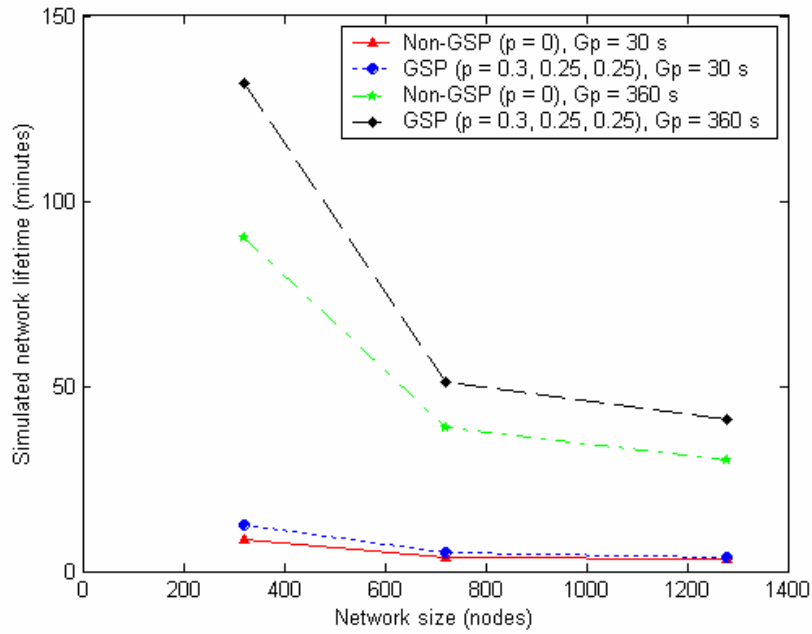


Figure 148: Simulated network lifetime vs. network size for star topologies with transmission power/radius d , $G_p = 30$ and 360 seconds.

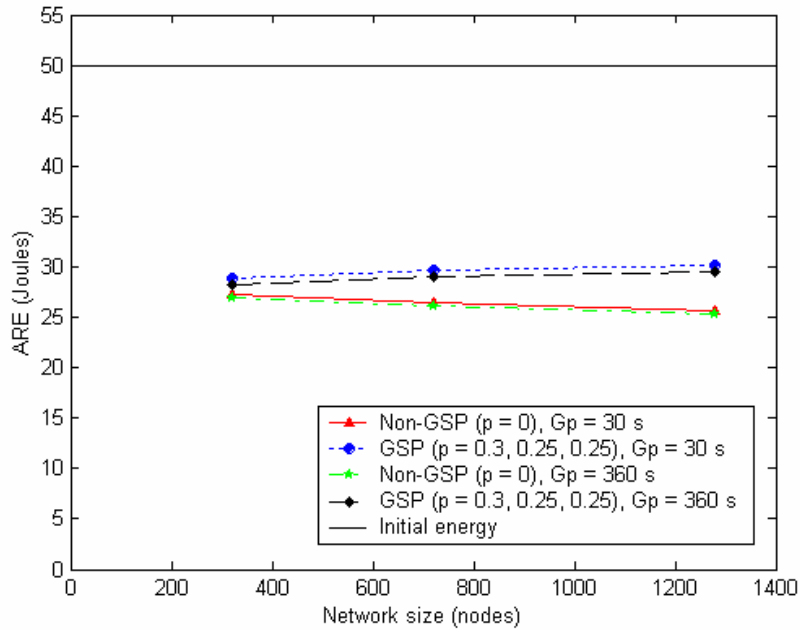


Figure 149: Average remaining energy (ARE) vs. network size for star topologies with transmission power/radius d , $G_p = 30$ and 360 seconds.

Figure 148 illustrates the simulated network lifetime. The longest network lifetime is presented at the 320 node GSP network with the 360 seconds gossip period. Since the large network presents higher traffic load, the simulated network lifetime decreases when the network size increases. Figure 149 plots the ARE per node for the star topologies with d transmission power/radius. The networks using the 360 seconds gossip period shows smaller ARE than the 30 seconds gossip period for all network sizes. As the networks increase in size, the ARE increases for the GSP. On the other hand, ARE shows small decreasing when the network size increases in the Non-GSP network.

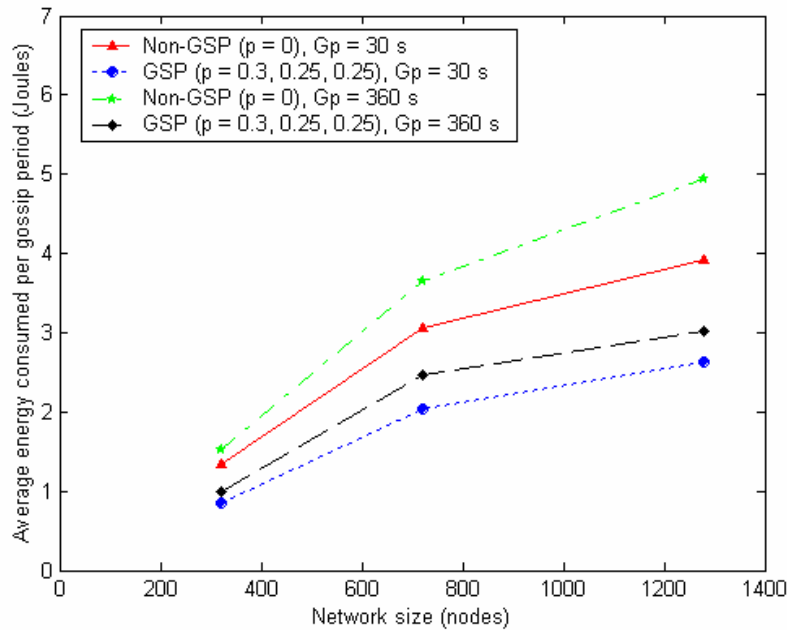


Figure 150: Average energy consumed per gossip period vs. network size for star topologies with transmission power/radius d , $G_p = 30$ and 360 seconds.

Figure 150 shows the average energy consumed per gossip period in star topologies with d transmission power/radius. The lowest energy consumed per gossip period occurs for the GSP network with the 30 second gossip period.

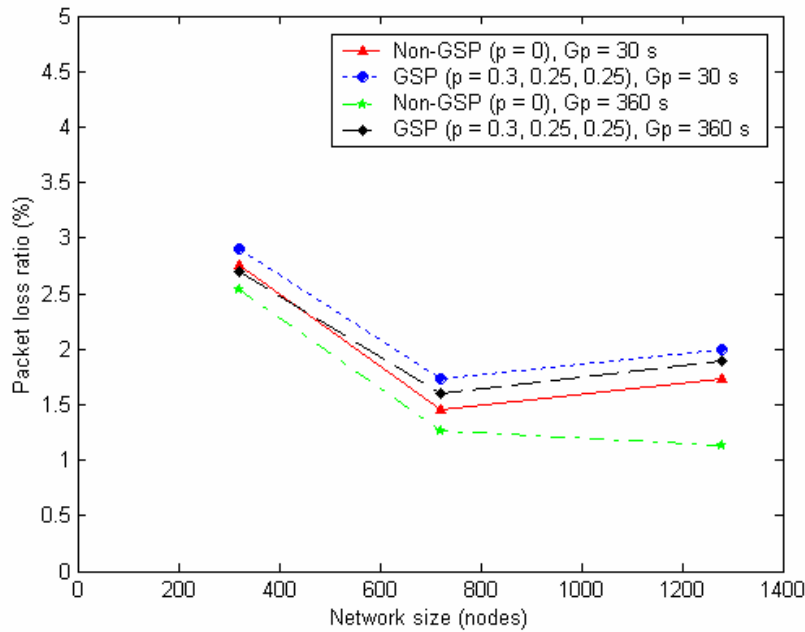


Figure 151: Packet loss ratio vs. network size for star topologies with transmission power/radius d , $G_p = 30$ and 360 seconds.

Figure 151 shows the packet loss ratio in the star topologies when using d transmission power/radius. The largest ratio occurs for the small 320 node network. The plots show non-straight lines because of the different topologies employed different gossip sleep probabilities (p) for different network sizes. Networks employing GSP present larger ratio compared to Non-GSP for both 30 and 360 seconds gossip periods.

7.2.5.2 Transmission Power/Radius $2d$ in the Star Topology

The purpose of the increasing transmission power/radius is to allow more sleeping nodes in the network. However, the analysis requires the network connectivity. Therefore, the simulation finds the gossip sleep probabilities (p) for different star network sizes. When using $2d$ transmission power/radius, Figures 152 and 153 plot the average path length and the ratio of nodes disconnected from the sink that suggest $p = 0.6$ for all three star network sizes

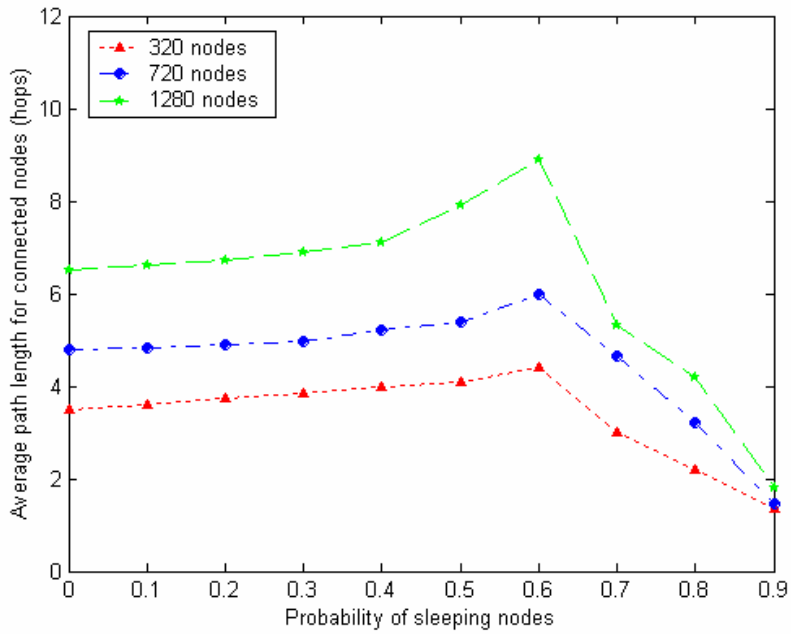


Figure 152: Probability of sleeping nodes vs. average path length for connected nodes in star topologies with transmission power/radius $2d$.

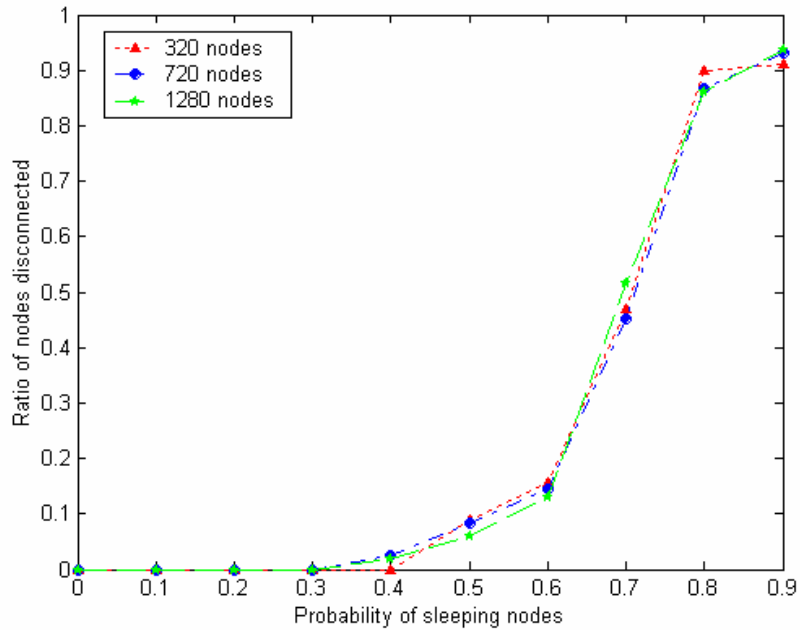


Figure 153: Probability of sleeping nodes vs. ratio of nodes disconnected in star topologies with transmission power/radius $2d$.

Figure 154 shows the average number of gossip periods that represents the network lifetime when using $2d$ transmission power/radius on the three sizes of the star topologies. GSP network with 320 nodes presents the highest average number of gossip periods. As networks increase in size, the average number of gossip periods decrease. The network with 30 seconds gossip period shows higher average number of gossip periods than the one with the 360 seconds for all network sizes. This is because a long gossip period consumes more energy in the idle/listening states than a short gossip period.

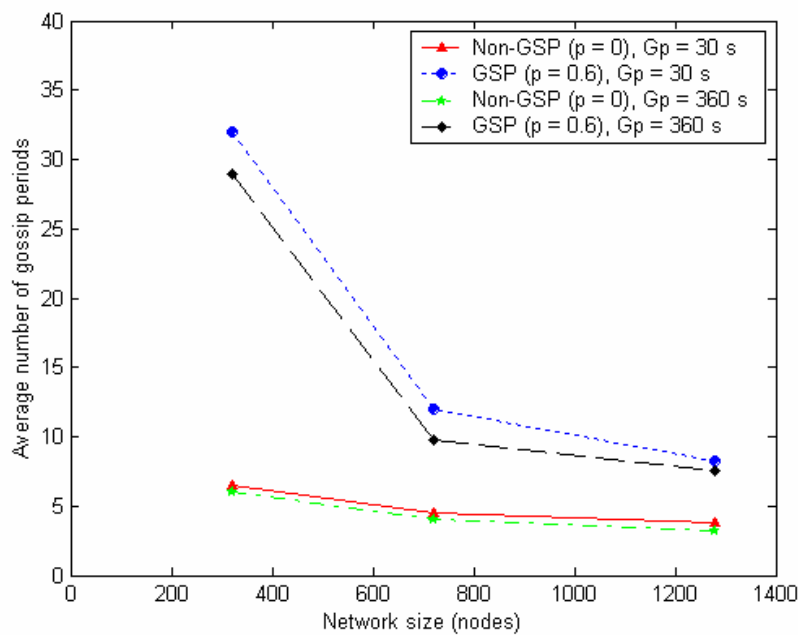


Figure 154: Average number of gossip periods vs. network size for star topologies with transmission power/radius $2d$, $G_p = 30$ and 360 seconds.

Figure 155 demonstrates the changes in the network lifetime in term of average number of gossip periods on the different sizes of the star topologies when using GSP_{2d} compared to $Non-GSP_{2d}$. The largest change occurs for the small network (320 nodes), which the changes decrease when the network size increases. Figure 156 presents the simulated network lifetime in minutes. The longest simulated network lifetime occurs for the small 320 node GSP network with the 360 seconds gossip period.

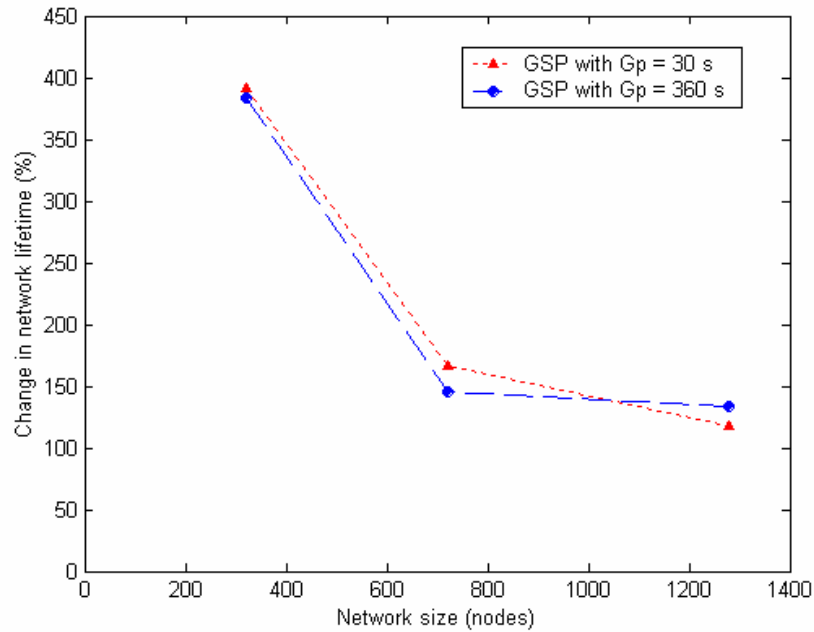


Figure 155: The changes in network lifetime on the different sizes of the star topologies with transmission power/radius $2d$ when using GSP compared to Non-GSP, $G_p = 30$ and 360 seconds.

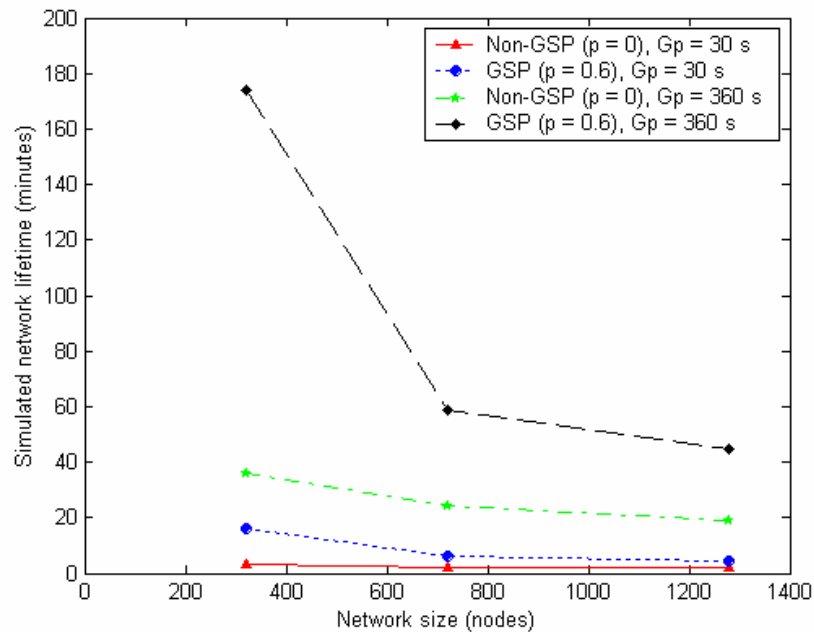


Figure 156: Simulated network lifetime vs. network size for star topologies with transmission power/radius $2d$, $G_p = 30$ and 360 seconds.

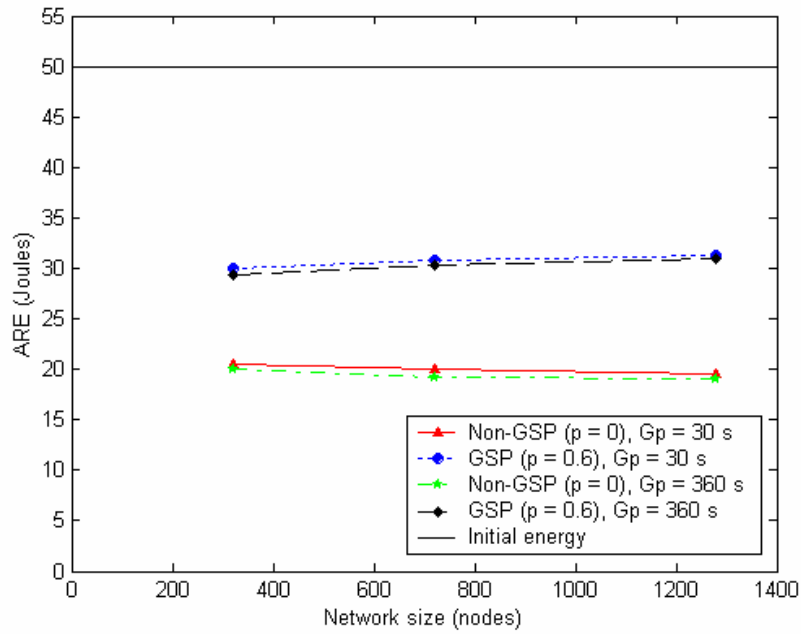


Figure 157: Average remaining energy (ARE) vs. network size for star topologies with transmission power/radius $2d$, $G_p = 30$ and 360 seconds.

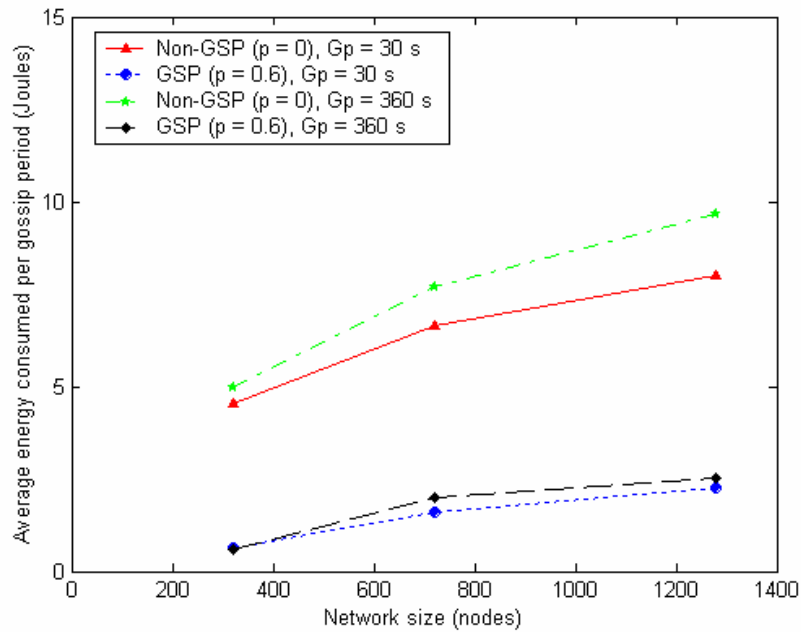


Figure 158: Average energy consumed per gossip period vs. network size for star topologies with transmission power/radius $2d$, $G_p = 30$ and 360 seconds.

Figure 157 plots the ARE per node for the star topologies when using $2d$ transmission power/radius. Networks employing GSP present approximately 10 Joules higher ARE than Non-GSP for all network sizes. ARE increases when the network size increases for GSP. On the other hand, ARE shows the decreasing when the network size increases for Non-GSP. Figure 158 shows the average energy consumed per gossip period in star topology when using $2d$ transmission power/radius. GSP shows smaller energy consumption per period compared to Non-GSP for all network sizes, which the smallest energy consumed per gossip period occurs for GSP with 30 seconds gossip period.

Figure 159 illustrates the packet loss ratios for the star topology when increasing transmission power/radius to $2d$. The smallest ratio occurs for the small 320 node Non-GSP network. The ratio tends to increase when the network size increases for Non-GSP network. On the other hand, as networks increase in size, the packet loss ratio decreases for GSP network. The network with the 360 seconds gossip period presents smaller packet loss ratio than the one with the 30 seconds gossip period for all cases.

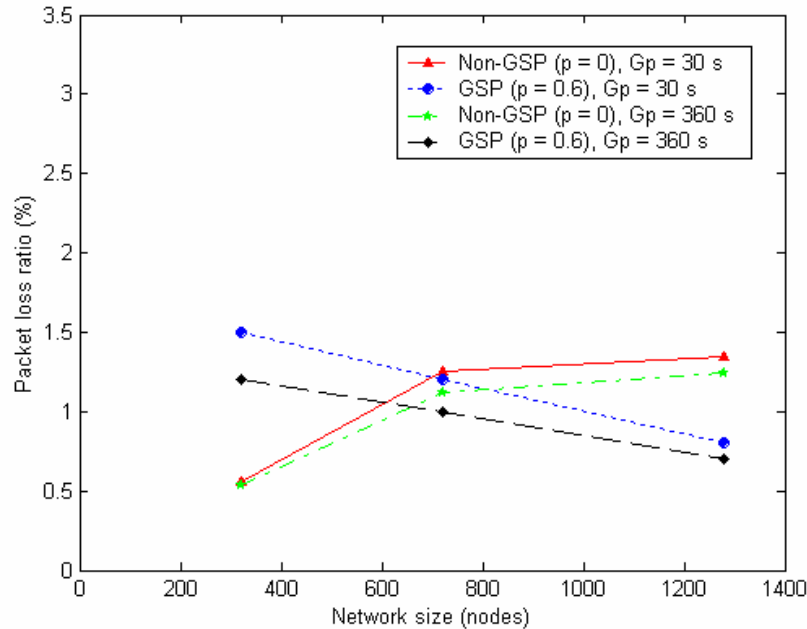


Figure 159: Packet loss ratio vs. network size for star topologies with transmission power/radius $2d$, $G_p = 30$ and 360 seconds.

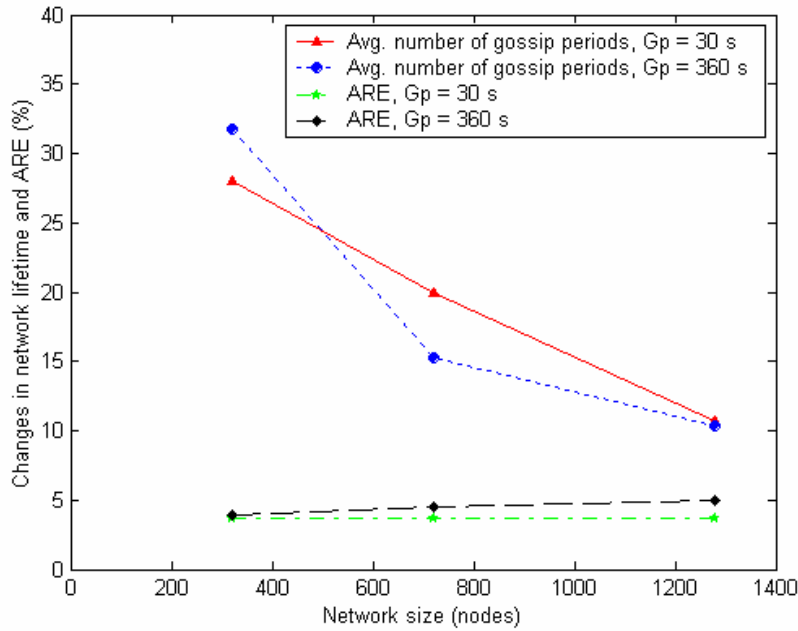


Figure 160: The changes of the average number of gossip periods and AREs in star topologies when using GSP_{2d} compared to GSP_d with $G_p = 30$ and 360 seconds.

Figure 160 illustrates the changes in network lifetime and AREs for the star topologies when using GSP_{2d} compared to GSP_d . By increasing transmission power/radius, network lifetime is extended by approximately 30% in the small and 10% in the large network. However, as network increases in size, the improvement decreases. On the other hand, when network employs GSP_{2d} over GSP_d , the ARE show small increasing when the network increases in size, which is approximately 3% in the small and up to 5% in the large network.

8.0 CONCLUSIONS AND FUTURE WORK

The research objective is to develop a cross layer scheme to target at the network layer issues, e.g. routing schemes, in wireless sensor networks. The dissertation discussed the use of GSP as a low complexity protocol to reduce the energy cost for each node. The objectives and contributions in developing GSP were:

- *Simplicity*: Sensor nodes require efficient use of the computational resources. GSP achieves the simplicity because GSP requires only a local timer to turn sensor nodes on and off. Moreover, it requires no information, even from immediate neighbors.
- *Scalability*: unlike conventional ad-hoc networks, a sensor network could be composed of a very great number of nodes. GSP does not require a sensor node to maintain the state of the other nodes.
- *Connectivity*: With a certain value of gossip sleep probability (p) and under certain topology density constraints, the network remains connected. To conserve more energy, the results in chapter 6 show that network can stay connected when it has more sleeping nodes by increasing of transmission power/radius.
- *Energy efficiency*: The major objective of GSP is to achieve energy efficiency by making some nodes enter sleep mode. Nodes awake in idle periods results in more energy consumption in the network. The preliminary results in chapter 4 show that energy efficiency can be achieved because the energy saved in sleeping by GSP is larger than the extra energy consumed by non-optimal paths.

The initial analysis of GSP shows that it can achieve energy efficiency. However, additional research was needed to better understand the performance of GSP. Specifically chapters 5 - 7 tested GSP to determine network lifetime as a function of the transmission power and physical topology of the network.

Network lifetime: In chapter 4, the results were based on closed-form expressions to estimate the GSP network lifetime by assuming evenly distributed energy consumption, which may not be accurate since the sleep and active nodes are fully random based on gossip sleep probability (p). Therefore, results were checked against a time-based simulation to estimate the network lifetime as shown in chapter 7. The results show that GSP can extend the network lifetime for all sizes in five selected network topologies. Also, GSP results in higher average energy remaining (ARE) per node. Based on the network topologies studied in this dissertation, the high node density networks such as random grids and star topologies present shorter network lifetime compared to the square grids, rectangular grids, and lattice topologies. This is because a node possibly has a large number of neighboring nodes who frequently consume energy in transmitting and receiving the packets. However, by using GSP, network lifetime can be extended. The results in chapter 7 show that the smaller networks always have longer network lifetimes, which decrease as the networks increase in size. The result emerges the larger networks needing to relay more traffic, which consumes a large amount of energy and presents the shorter network lifetime for all network topologies.

A more detailed radio model: Initial research assumed an idle receiver consumes $E_{idle} = 40 \text{ nJ}$ in the period of transmitting or receiving a bit and that a sleep node does not dissipate any energy. The classic energy consumption model was replaced with a measurement model using in the simulation [15], [65]. The measurement-based model resulted in different outcomes than the classic radio model when using a Mica2 mote sensor network. As a result, the simulation applied this measurement model in the analysis as shown in chapters 5 - 7.

Increased transmission power: Chapter 6 discussed the potential improvement on GSP network lifetime by increasing the transmission power/radius. The network lifetime as a function of transmission power was determined through simulations and analytical models. Increasing the

transmission power/radius, results extended network lifetime for all sizes of the network topologies. GSP_{2d} shows a large improvement in network lifetime when comparing to the Non-GSP_{2d} network. When increasing nodes' transmission power, Non-GSP_{2d} networks can be considered as a higher density network, which the results show a shorter network lifetime compared to Non-GSP_d. By using higher p as in GSP_{2d}, networks allow more nodes to sleep, which therefore improve the network lifetimes and AREs. Moreover, increasing nodes' transmission powers can reduce the packet loss ratios on both GSP and Non-GSP networks, which Non-GSP_{2d} shows small ratio than GSP_{2d}.

Critical nodes: Critical nodes occur in an energy constrained network due to patterns in traffic flow, a node consumes energy more rapidly than the average. Energy balancing methods in section 3.2 evaluates the network lifetime as the first node to die around the sink node. Chapter 5 shows the surface plots for the Known Path (KP) scheme that present the energy consumption of critical nodes around the sink area, which consumed energy faster than the other nodes. However, when GSP was used, the network lifetime was extended. This is because GSP distributes energy consumption over the entire network. Nodes go to sleep in a fully random fashion and the traffic forwarding continuously via the same path can be avoided. The star topology presents high density nodes especially around the sink area. As a result, the star network lifetime is shorter than the others because these critical nodes were used to carry huge traffic before forwarding to the sink.

Gossip period: The research used two gossip period times, one represents a short gossip period ($G_p = 30$ seconds), and the other represents a long gossip period ($G_p = 360$ seconds). The short period time may be best suited in applications that require frequent samplings, e.g., monitoring patient vital signs. On the other hand, the longer gossip period can be used in application such environment monitoring, e.g., buildings, bridges, and airport runways monitoring. The analysis used the 360 seconds gossip period to study the impacts of energy consumption when nodes are listening in the idle states for a longer time. As expected, the results show that the longer period shows less average number of gossip periods, AREs, and packet loss ratios. However, it provides longer simulated network lifetime in minutes. On the contrary, networks with the shorter gossip period presents the higher average number of gossip periods, AREs, and packet loss ratio but the

shorter simulated network lifetime in minutes.

Topologies: To estimate the network lifetime, GSP was tested on the selected five physical topologies, which are square grid, rectangular grid, random grid, lattice topology, and star topology. Some applications place sensor nodes randomly or in patterns as they are employed along the roads, bridges, or airport runways. The results show that the different physical topologies present different system lifetimes. The square and rectangular grids present the longest network lifetime compared to the other topologies when using GSP_d and GSP_{2d} . Also, the AREs are increased as the networks increase in size. On the other hand, Non- GSP_d and Non- GSP_{2d} show decreasing in AREs when the network size increases. Within a transmission range d or $2d$, a node in the high density networks such as a random grid and a star topology may have large number of neighboring nodes, which consume energy frequently to transmit and receive a packet. Therefore, the random grid and star topology show shorter network lifetimes compared to the square and rectangular grids. However, when networks employ GSP_d and GSP_{2d} , the network lifetime and ARE are increased. The simulation recommended a small optimal value of the gossip sleep probabilities (p) using for the lattice topologies due to the vulnerable in connectivity of the networks. Networks employing GSP achieve the energy efficiency and improve on both network lifetime and ARE.

Application of GSP: GSP is a tool used to investigate improvements in network lifetime employing zero overhead. As application currently exists it is not suitable for network operations because it requires finding the gossip sleep probability (p), which we found to be sensitive to local topology. With a given network density, as in square grids, e.g., the same average number of a node's neighbors, the gossip sleep probabilities (p) are the same for all network sizes. However, other topologies such as rectangular grids, random grids, lattice topologies, and star topologies, require different values of p .

Future Work:

The dissertation proposed the Gossip-based Sleep Protocol (GSP) as an energy-efficient protocol for wireless sensor networks which there are rooms of improvements. Since a sensor node can

store its energy up to 5000 Joules, the simulation can use higher nodes' initial energy to improve the network lifetime. Also, the research applied a traditional CSMA/CA MAC protocol, which the integration with an energy efficient MAC protocol may improve energy efficiency. The system lifetime is estimated as a network discovering a dead node. However, to extend the analysis and continue using the energy remaining, the simulation may consider the network lifetime as multiple dead nodes, or network partitioning. The research always used the optimal gossip sleep probability (p), which is the highest sleep probability resulting in a connected network and an optimal network lifetime. However, network designers can tradeoff the shorter network lifetime with e.g., the less disconnected nodes.

The study of physical topologies are important because the networks are not necessary deployed as a random. As an air traffic control officer who is dealing at all types of the airports in Thailand, the study of the pattern topologies will be useful when the sensor networks are installed along the airport runways and taxiways. The tool was developed along this dissertation to generate any types of physical topologies and then put it in the main program to estimate the network lifetime based on the network parameters. We expect that this tool will be helpful in designing any types of physical topologies for wireless sensor networks as a function of network lifetime.

BIBLIOGRAPHY

- [1] 21 ideas for the 21st century. *Business Week*, pages 78-167, August 30, 1999.
- [2] C. Chong and P. Kumar. Sensor networks: evolution, opportunities, and challenges. In *Proceedings of the IEEE*, 91(8): 1247-1256, August 2003.
- [3] J. N. Al-Karaki and A. E. Kamal. Routing techniques in wireless sensor networks: a survey. *IEEE Wireless Communications*, 11(60): 6-28, 2004.
- [4] K. Romer and F. Mattern. The design space of wireless sensor networks. *IEEE Wireless Communications*, 11(6): 54-61, 2004.
- [5] S. Rhee, D. Seetharam and S. Liu. Techniques for Minimizing Power Consumption in Low-Data Rate Wireless Sensor Networks. *IEEE Wireless Communications and Networking Conference (WCNC)*, March 2004.
- [6] M. Tubaishat and S. Madria. Sensor networks: an overview. *Potentials*, 22(2): 20-23, 2003.
- [7] L. Wang and Y. Xiao. A survey of energy saving mechanisms in sensor networks. In *Proceedings of the IEEE Broadnets*, October 2005.
- [8] Y. Ma and J. H. Aylor. System lifetime optimization for heterogeneous sensor networks with a hub-spoke topology. *IEEE Transactions on Mobile Computing*, 3(3), 2004.
- [9] X. Hou, D. Tipper, D. Yupho, and J. Kabara. GSP: gossip-based sleep protocol for energy efficient routing in wireless sensor networks. In *Proceedings of the 16th International Conference on Wireless Communications*, Calgary, Alberta, Canada, 2004.
- [10] G. J. Pottie and W. J. Kaiser. Wireless integrated network sensors. *Communication of the ACM*, 43: 51-58, 2000.
- [11] S. Vardhan, M. Wilczynski, G. J. Pottie, and W. J. Kaiser. Wireless integrated network sensors (WINS): distributed in situ sensing for mission and flight systems. In *Proceedings of Aerospace Conference*, 7: 459-463, 2000.
- [12] W. R. Heinzelman, A. Chandrakasan, and H. Balakrishnan. Energy-efficient communication protocol for wireless microsensor networks. In *Proceedings of the 33rd*

International Conference on System Sciences (HICSS), 2000.

- [13] E. Shin, S. H. Cho, N. Ickes, R. Min, A. Sinha, A. Wang, and A. Chandrakasan. Physical layer driven protocol and algorithm design for energy-efficient wireless sensor networks. *ACM SIGMOBILE Conference on Mobile Computing and Networking*, Rome, Italy, July 2001.
- [14] T. Wayne. *Electronic Communications Systems*. Prentice Hall, Upper Saddle River, NJ, 2001.
- [15] M. Calle and J. Kabara. Measuring energy consumption in wireless sensor networks using GSP In *Proceedings of the 17th annual IEEE International Symposium on Personal Indoor and Mobile Radio Communications (PIMRC)*, Helsinki, Finland, 2006.
- [16] B. Sklar. *Digital communications fundamentals and applications*. Prentice Hall PTR, 2001.
- [17] Crossbow Technology Inc. Wireless Sensor Networks: MOTE – VIEW 1.2 User’s Manual,” October 2005, Online: http://www.xbow.com/Support/Support_pdf_files/MOTE-VIEW_Users_Manual_.pdf.
- [18] A. Y. Wang, S. Cho, C. G. Sodini, and A. P. Chandrakasan. Energy efficient modulation and MAC for asymmetric RF microsensor systems. In *Proceedings of the 2001 international symposium on Low power electronics and design*, pages 106-111, Huntington Beach, California, 2001.
- [19] I. F. Akyildiz, W. Su, Y. Sankarasubramaniam, and E. Cayirci. A survey on sensor networks. *IEEE Communication Magazine*, 40(8): 102-114, 2002.
- [20] H. Karl. A short survey of wireless sensor networks. Telecommunication Networks Group, Technische Universität Berlin, Technical Report TKN-03-018, October 2003.
- [21] C. Chien, I. Elgorriaga, and C. McConaghy. Low-power direct-sequence spread-spectrum, modem architecture for distributed wireless sensor networks. In *Proceedings of the 2001 International Symposium on Low Power Electronics and Design*, pages 251-254, Huntington Beach, California, 2001.
- [22] A. Chandrakasan and A. Sinha. Dynamic power management in wireless sensor networks. *Design and Test of Computers*, 18(2): 62-74, 2001.
- [23] M. A. Youssef, M. F. Younis, and K. A. Arisha. A constrained shortest-path energy-aware routing algorithm for wireless sensor networks. *Wireless Communications and Networking Conference (WCNC)*, 2: 794 -799, 2002.
- [24] M. Ilyas. *Ad hoc wireless network*. CRC Press LLC, Florida, 2003.
- [25] D. J. Goodman. *Wireless Personal Communications Systems*. Addison Wesley Longman,

Inc., MA, 1997.

- [26] A. Woo and D. E. Culler. A transmission control scheme for media access in sensor networks. In *Proceedings of ACM Mobicom*, pages 221-235, Rome, Italy, July 2001.
- [27] K. Sohrabi, J. Gao, V. Ailawadhi, and G. J. Pottie. Protocols for self-organization of a wireless sensor network. *Personal Communications*, 7(5): 16-27, October 2000.
- [28] B. Krishnamachari, D. Estrin, and S. Wicker. The impact of data aggregation in wireless sensor networks. In *Proceedings of the 22nd International Conference Distributed Computing Systems Workshops*, pages 575-578, July 2002.
- [29] W. R. Heinzelman, J. Kulik, and H. Balakrishnan. Adaptive protocols for information dissemination in wireless sensor networks. In *Proceedings of the 5th ACM/IEEE Mobicom Conference*, Seattle, WA, August 1999.
- [30] F. Ye, A. Chen, S. Lu, and L. Zhang. A scalable solution to minimum cost forwarding in large sensor networks. In *Proceedings of the 10th International Conference of the Computer Communications and Networks*, pages 304-309, October 2001.
- [31] M. Haenggi. Twelve reasons not to route over many short hops. *IEEE Vehicular Technology Conference (VTC)*, pages 3130-3134, Los Angeles, CA, September 2004.
- [32] M. Haenggi. Energy-balancing strategies for wireless sensor networks. In *IEEE International Symposium on Circuits and Systems (ISCAS'03)*, Bangkok, Thailand, May 2003.
- [33] M. Haenggi. On Routing in Random Rayleigh Fading Networks. *IEEE Transactions on Wireless Communications*, 4: 1553-1562, 2005.
- [34] A. Manjeshwar and D. P. Agrawal. TEEN: A Routing Protocol for Enhanced Efficient in Wireless Sensor Networks. In *Proceedings of the 15th International, Parallel and Distributed Processing Symposium*, pages 2009-2015, April 2001.
- [35] A. Manjeshwar and D. P. Agrawal. APTEEN: A hybrid protocol for efficient routing and comprehensive information retrieval in wireless sensor networks. In *Proceedings of the Parallel and Distributed Processing Symposium, International, (IPDPS)*, pages 195-202, April 2002.
- [36] S. Lindsey and C. S. Raghavendra. PEGASIS: Power-efficient gathering in sensor information systems. In *Proceedings of the Aerospace Conference*, 3: 1125–1130, 2002.
- [37] F. Ye, H. Luo, J. Cheng, S. Lu, and L. Zhang. A two-tier data dissemination model for large-scale wireless sensor networks. In *Proceedings of the 8th International Conference on Mobile Computing and Networking*, pages 148-159, Atlanta, Georgia, 2002.

- [38] I. Carreras, I. Chlamtac, H. Woesner, and H. Zhang. Nomadic Sensor Networks. *The 2nd European Workshop on Wireless Sensor Networks (EWSN)*, Istanbul, Turkey, January 2005.
- [39] C. Intanagonwiwat, R. Govindan, D. Estrin, J. Heidemann, and F. Silva. Directed diffusion for wireless sensor networking. *Networking, IEEE/ACM Transactions*, 11(1): 2-16, 2003.
- [40] J. Kulik, W. Heinzelman, and H. Balakrishnan. Negotiation-based protocols for disseminating information in wireless sensor networks. *Wireless Networks*, 8(2/3): 169-185, 2002.
- [41] R. C. Shah and J. M. Rabaey. Energy aware routing for low energy ad hoc sensor networks. *Wireless Communications and Networking Conference*, 1: 350-355, 2002.
- [42] S. D. Servetto and G. Barrenechea. Constrained random walks on random graphs: routing algorithms for large scale wireless sensor networks. In *Proceedings of the 1st ACM International Workshop, Wireless Sensor Networks and Applications*, pages 12-21, Atlanta, GA, 2002.
- [43] D. Braginsky and D. Estrin. Rumor routing algorithm for sensor networks. In *Proceedings of the 1st Workshop Sensor Networks and Applications*, Atlanta, GA, October 2002.
- [44] Y. Xu, J. Heidemann, and D. Estrin. Geography-informed energy conservation for ad-hoc routing. In *Proceedings of the 7th Annual ACM/IEEE International Conference Mobile Comp. and Net.*, pages 70-84, 2001.
- [45] R. RAjaraman. Topology control and routing in ad hoc networks. *AMC SIGACT News*, 33(2): 60-73, 2002.
- [46] J. Diaz, M. D. Penrose, J. Petit, and M. Serna. Convergence theorems for some layout measures on random lattice and random geometric graphs. *Combinatorics, Probability, and Computing*, pages 489-511, 2000.
- [47] C. Bettstetter. On the minimum node degree and connectivity of a wireless multihop network. In *Proceedings of the 3rd ACM International Symposium on Mobile Ad Hoc Networking and Computing (MobiHoc)*, Lausanne, Switzerland, 2002.
- [48] M. D. Penrose. On k -connectivity for a geometric random graph. *Wiley Random Structures and Algorithms*, 15(2): 145-164, 1999.
- [49] X. Y. Li, P. J. Wan, Y. Wang, and C. W. Yi. Fault tolerant deployment and topology control in wireless networks. In *Proceedings of the 4th ACM International Symposium on Mobile Ad Hoc Networking and Computing (MobiHoc)*, Annapolis, MD, 2003.
- [50] F. Xue and P. R. Kumar. The number of neighbors needed for connectivity of wireless networks. *Wireless Networks*, 10(2): 169-181, 2004.

- [51] S. Basagni, I. Chlamtac, and A. Farago. A generalized clustering algorithm for peer-to-peer networks. In *Proceedings of the Workshop on Algorithmic Aspects of communications (Satellite workshop of ICALP)*, Bologna, Italy, July 1997.
- [52] H. Karl and A. Willig. *Protocols and architectures for wireless sensor networks*. John Wiley & Sons, Ltd, Hoboken, NJ, 2005.
- [53] I. Chlamtac and A. Farago. A new approach to the design and analysis of peer-to-peer mobile networks. *Wireless Networks*, 5(3): 149-156, 1999.
- [54] L. Bao and J. J. Garcia-Luna-Aceves. Topology management in ad hoc networks. In *Proceedings of the 4th ACM International Symposium on Mobile Ad Hoc Networking and computing (MobiHoc)*, Annapolis, MD, 2003.
- [55] M. Chatterjee, S. Das, and D. Turgut. WCA: A weighted clustering algorithm for mobile ad hoc networks. *Cluster Computing Journal*, 5: 193-204, 2002.
- [56] D. Tian and N. D. Georganas. A coverage-preserving node scheduling scheme for large wireless sensor networks. In *Proceedings of the First ACM international Workshop on Wireless Sensor Networks and Applications (WSNA)*, pages 32-41, Atlanta, GA, 2002.
- [57] S. Hedetniemi, S. Hedetniemi, and A. Liestman. A survey of gossiping and broadcasting in communication networks. *IEEE Networks*, 18: 319-349, 1988.
- [58] C. M. Okino and M. G. Corr. Best afford adaptive routing in statistically accurate sensor networks neural networks. In *Proceeding of IJCNN*, 2002.
- [59] B. Chen, K. Jamieson, H. Balakrishnan, and R. Morris. Span: An energy-efficient coordination algorithm for topology maintenance in ad hoc wireless networks. *Wireless Networks*, 8: 481-494, 2002.
- [60] V. Raghunathan, C. Schurgers, S. Park, and M. B. Srivastava. Energy-aware wireless microsensor networks. *IEEE Signal Processing Magazine*, March 2002.
- [61] J. L. Jabs, C. H. Chang, and R. Tingley. Performance of a very low power wireless protocol In *Proceedings of IEEE Golbal Conference on Communications*, 2001.
- [62] Z. J. Haas, J.Y. Helpern, and L. Li. Gossip-based ad hoc routing. In *Proceedings of the IEEE INFOCOM*, 2002.
- [63] R. Meester and R. Roy. *Continuum Percolation*. Cambridge University Press, 1996.
- [64] G. Grimmett. *Percolation*. Springer-Verlag, 1989.
- [65] M. Calle. Energy Consumption in Wireless Sensor Networks Using GSP. M.S. Thesis, Department of Information Science & Telecommunications, University of Pittsburgh,

Pittsburgh, PA, USA, 2006.

- [66] X. Hou and D. Tipper. Gossip-based sleep protocol (GSP) for energy efficient routing in wireless ad hoc networks. *Wireless Communications and Networking (WCNC)*, 3: 21-25, March 2004.
- [67] L. M. Feeney and M. Nilsson. Investigating the energy consumption of a wireless network interface in an ad hoc networking environment. In *Proceedings of IEEE INFOCOM*, 2001.
- [68] D. Yupho, M. Calle, and J. Kabara. Longer network lifetime when using energy efficient GSP for wireless sensor networks. In *Proceedings of the Workshop on Ad Hoc, Sensor, and P2P Networks (AHSP)*, Sedona, AZ, March 2007.
- [69] D. Yupho and J. Kabara. Continuous vs. event driven routing protocol for WSNs in healthcare environment. In *Proceedings of the Workshop on Security and Privacy in Mobile Health Care (PMHCS)*, Innsbruck, Austria, November 2006.